
**REDUCING SIMULATION PERFORMANCE GAP FROM HEMPCRETE USING
MULTI OBJECTIVE OPTIMISATION**

BY

ATAITIYA PATERSON BANA

**SUBMITTED TO THE UNIVERSITY OF HERTFORDSHIRE IN PARTIAL
FULFILMENT OF THE REQUIREMENTS OF THE DEGREE OF PHD.**

NOVEMBER 2021

ABSTRACT

The impacts of climate change in the built environment is undeniably overwhelming, which highlights the need for a sustainable reduction of carbon from buildings and the built environment. While carbon reduction from the built environment seems ideal for mitigating climate change issues, there are necessary actions to be taken. Especially a shift from the use of conventional construction materials and methods, to using sustainable materials and methods to increase the resilience of buildings to climate change. The technological advancement of the world and built environment has made it possible and necessary to design and simulate buildings for sustainable construction. In this regard, hempcrete is a sustainable construction material increasingly used in the built environment as it provides stable temperature and relative humidity conditions in buildings. In addition to its thermal qualities and low energy operations, it is carbon negative as it possesses carbon sequestration properties. Buildings built from hempcrete also possess negative embodied carbon, which is absorbed into the hemp plant material. However, Hempcrete is hard to represent in design and simulation because standard dynamic simulation tools do not have a built-in capability to accurately simulate it. This is due to hempcrete's specific material structure and combined heat and moisture transfer, causing a considerable performance gap.

This study investigates the appropriate specification of key parameters to be used in simulation of hempcrete, for reducing simulation performance gap from hempcrete buildings, using multi-objective optimisation, to facilitate hempcrete simulation. To this end, this study uses experimental research method with secondary method of data collection by obtaining monitored data of hempcrete buildings from Zero Carbon Lab. The monitored hempcrete buildings will be simulated and RMSE between the monitored and simulated values will be calculated. The simulation of monitored hempcrete buildings is carried out in IES Virtual Environment and the RMSE is calculated using Microsoft Excel. The results of RMSE between monitored and simulated hempcrete building is the performance gap, which is then investigated in EnergyPlus using the HAMT Simulations coupled into jEPlus+EA for multi-objective optimisation to reduce the performance gap. This study is carried out within simulation tools and the results show a significant reduction in performance gap of temperature and relative humidity, while identifying the accurate parameters to be used for hempcrete simulation. The identified parameters for hempcrete simulation, facilitate the modelling of heat and moisture transfer in hempcrete for optimised simulation.

KEY WORDS

- I. Building Performance Evaluation.
- II. Building Simulation.
- III. Building Optimization.
- IV. Energy Efficiency.
- V. EnergyPlus simulation.
- VI. Evolutionary Algorithm.
- VII. Experimental Simulation.
- VIII. Genetic Algorithm.
- IX. Heat and Moisture Transfer.
- X. Hempcrete.
- XI. Input Data File.
- XII. Integrated Environment Solutions Virtual Environment.
- XIII. Monitored Building.
- XIV. Non – Sorting Genetic Algorithm II.
- XV. Root Mean Square Error.
- XVI. Simulation Performance Gap.

ABBREVIATIONS

AEC	Architecture Engineering and Construction
BPE	Building Performance Evaluation
CIBSE	Chartered Institution of Building Services Engineers
EA	Evolutionary Algorithm
GA	Genetic Algorithm
HAMT	Heat and Moisture Transfer
IDF	Input Data File
IESVE	Integrated Environment Solutions Virtual Environment
NSGA II	Non – Sorting Genetic Algorithm II
PAM	Performance Assessment Method
POE	Post Occupancy Evaluation
RMSE	Root Mean Square Error
WMO	World Metrological Organizations

TABLE OF CONTENTS

	Pages
Chapter One – Introduction	
1.1	Research Context.....18
1.2	Research Rationale.....20
1.3	Novelty.....22
1.4	Research Questions.....22
1.5	Research Aim and Objectives23
1.6	Overall objectives and Methodology.....23
1.7	Scope and Limitation.....28
1.8	Research Outcome.....28
Chapter Two – Literature Review	
2.1	Hempcrete as a Construction Material.....30
2.2	Simulation Performance Gap.....34
2.3	Simulation Performance Gap in Hempcrete Buildings.....38
2.4	Simulation of hempcrete for Buildings.....41
2.5	Multi objective Optimisation.....45
2.6	Coupling Simulation with Multi Objective Optimisation.....54
Chapter Three – Methodology	
3.1	Research Methodology.....63
3.2	Data Used in The Study.....70
3.3	Experimental Simulation.....73
3.3.1	Reasoning.....75
3.3.2	Simulation Experiment in IES Virtual Environment.....78
3.3.3	Calibration of Experimental Simulation outputs.....79
3.3.4	Heat and Moisture Transfer (HAMT) Simulation in EnergyPlus.....83
3.3.5	Multi objective optimisation.....91
3.4	Analysis.....100
3.5	Validation.....102

Chapter Four - Experimentation

4.1	Simulation of Experimental Hempcrete Buildings.....	104
4.2	Simulation Experiments in IES Virtual Environment.....	104
4.2.1	Simulation with conventional and natural materials.....	105
4.2.2	Simulation to investigate properties of a created hempcrete material.....	106
4.3	RMSE Calculation with Simulation Experiment Outputs.....	107
4.4	EnergyPlus Heat and Moisture Transfer (HAMT) Simulation.....	107
4.5	Multi Objective Optimisation in jEPlus+EA.....	113

Chapter Five – Analysis

5.1	Monitored and Simulated Data Analysis.....	127
5.1.1	Base case simulation analysis for Hempod.....	129
5.1.2	Base case simulation analysis for the residential building.....	130
5.2	Root Mean Square Error (RMSE) Calculation.....	131
5.3	Multi Objective Optimisation using jEPlus+EA.....	148

Chapter Six – Results and Discussion

6.1	Results.....	155
6.1.1	Validation of Results with Hempod.....	157
6.1.2	Validation of Results with Residential Building.....	159
6.2	Discussion.....	166

Chapter Seven – Conclusion

7.1	Research Conclusion.....	171
7.1.1	Research Outcome.....	173
7.1.2	Contribution to Knowledge.....	174
7.1.3	Future Work.....	174
7.2	Recommendation.....	175

List of References.....	176
--------------------------------	------------

Appendices

Appendix A	EnergyPlus Heat and Moisture Transfer Simulation.....	196
------------	---	-----

Appendix B	Multi Objective Optimisation in jEPlus+EA.....	201
Appendix C	Validation of Results with Hempod.....	213
Appendix D	Validation of Results with Residential Building	218
Appendix T.....		223

LIST OF FIGURES

	Pages
Figure 1:	Hempcrete from a plant to a construction material.....31
Figure 2:	An example of simulation performance gap in a hempcrete building39
Figure 3:	Performance gap in hempcrete40
Figure 4:	General Process of the building energy efficient design optimization.....50
Figure 5:	Basic workflow of coupling building energy with optimisation.....55
Figure 6:	Flow chart of the experimental research methodology69
Figure 7:	Hempod.....70
Figure 8:	Hempod 3D Geometry.....70
Figure 9:	IES Virtual Environment, 3D Geometry of the residential building.....72
Figure 10:	Phases of the simulation experiment.....77
Figure 11:	An example of the IES Virtual Environment simulation experiment method...78
Figure 12:	An example of the IES Virtual Environment simulation experiment with hempcrete material.....79
Figure 13:	IES model of Hempod.....81
Figure 14:	IES model of Hempod imported into Design Builder.....81
Figure 15:	IES model of the residential building.....82
Figure 16:	IES model of the residential building imported into Design Builder.....82
Figure 17:	A cross-section of hempcrete wall surface made up of 5 material layers split into cells a-j.....87
Figure 18:	Showing the HAMT model parameters.....90
Figure 19:	Example of a jEPlus project file.....93
Figure 20:	rvi file.....94
Figure 21:	rvx file.....95
Figure 22:	jEPlus interface, showing parameter tree and Parameter item.....97
Figure 23:	A folder ready for multi objective optimisation in jEPlus+EA.....98
Figure 24:	CalcRMSE.py file.....100
Figure 25:	An example of the IES Virtual Environment simulation experiment method.105
Figure 26:	An example of the IES simulation experiment with hempcrete material of 75mm layers thickness.....106
Figure 27:	Combined Heat and Moisture Finite Element.....108

Figure 28:	Site location setting for HAMT simulations.....	108
Figure 29:	Run Period of HAMT Simulation.....	109
Figure 30:	A jEPlus project.....	113
Figure 31:	Showing Hemcretewall8, Hemcretewall7 and Hemcretewall6.....	114
Figure 32:	Showing Hemcretewall5, Hemcretewall4, Hemcretewall3, Hemcretewall2 and Hemcretewall1.....	115
Figure 33:	Showing the wall optimisation parameter specification.....	116
Figure 34:	jEPlus+EA Optimisation folder.....	120
Figure 35:	jEPlus+EA interface showing loaded jEPlus project with parameters ready For optimisation.....	120
Figure 36:	Scatterplot from the multi objective optimisation.....	121
Figure 37:	EnergyPlus simulation output for the optimisation results from Figure 36....	121
Figure 38:	Building parameter for HAMT Simulations.....	122
Figure 39:	Showing the wall optimisation parameter specification.....	124
Figure 40:	jEPlus+EA interface showing loaded jEPlus project with parameters ready for optimisation.....	125
Figure 41:	Monitored external Temperature Values.....	127
Figure 42:	Monitored external Rel. humidity Values.....	127
Figure 43:	Hempod simulated temperature.....	128
Figure 44:	Hempod simulated rel. humidity.....	128
Figure 45:	Monitored external Temperature Values.....	128
Figure 46:	Monitored external Rel. humidity values.....	128
Figure 47:	Simulated weather for temperature.....	129
Figure 48:	Simulated weather for rel. humidity.....	129
Figure 49:	Monitored Temperature Values.....	129
Figure 50:	Monitored Rel. humidity values.....	129
Figure 51:	Hempod simulated temperature.....	129
Figure 52:	Hempod simulated rel. humidity	129
Figure 53:	Hempod monitored and simulated temperature values	130

Figure 54:	Hempod monitored and simulated relative humidity values	130
Figure 55:	Hempod monitored and simulated weather values for temperature	130
Figure 56:	Hempod monitored and simulated weather values for rel. humidity	130
Figure 57:	Monitored and simulated weather values for temperature.	131
Figure 58:	Monitored and simulated weather values for relative humidity.....	131
Figure 59:	218mm wall experiment with rammed earth and chipboard.....	132
Figure 60:	243mm wall experiment with rammed earth and chipboard.....	132
Figure 61:	268mm wall experiment with rammed earth and chipboard.....	133
Figure 62:	318mm wall experiment with rammed earth and chipboard.....	133
Figure 63:	318mm wall experiment with rammed earth and chipboard.....	133
Figure 64:	418mm wall experiment with rammed earth and chipboard.....	133
Figure 65:	Hempod Experiment1 and Experiment2 showing the temperature values...	147
Figure 66:	Hempod Experiment1 and Experiment2 showing the relative humidity values...	147
Figure 67:	Hempod 201 and Hempod monitored temperature values.....	148
Figure 68:	Hempod 201 and Hempod monitored Rel. humidity.....	148
Figure 69:	Scatter plot showing all the optimization outputs and the Pareto.....	149
Figure 70:	Scatter plot showing all the optimisation outputs and the Pareto.....	150
Figure 71:	Showing a solution chosen from the Pareto front	151
Figure 72:	Showing a solution chosen from the Pareto front.....	151
Figure 73:	Showing a solution chosen from the Pareto front.....	152
Figure 74:	Showing the optimum solution chosen from the Pareto front.....	152
Figure 75:	Simulation to confirm eight layers of hempcrete is the same as 400mm of hempcrete.....	153
Figure 76:	EnergyPlus simulation interface to confirm “hempcretewall8” is the same 400mm of hempcrete.....	154

Figure 77:	Showing the optimum solution chosen from the Pareto front.....	156
Figure 78:	Optimised and monitored temperature	159
Figure 79:	Optimised and monitored Relative humidity.....	159
Figure 80:	Heat balance algorithm for HAMT Simulation.....	160
Figure 81:	Showing the selected site location for the residential building HAMT simulation	161
Figure 82:	Showing the specified run period for the residential building HAMT Simulation.....	161
Figure 83:	Simulated and monitored living room temperature	164
Figure 84:	Simulated and monitored living room relative humidity.....	164
Figure 85:	Simulated and monitored kitchen temperature.....	165
Figure 86:	Simulated and monitored kitchen relative humidity.....	165
Figure 87:	Simulated and monitored bedroom temperature.....	165
Figure 88:	Simulated and monitored bedroom relative humidity.....	165

APPENDIX A: ENERGYPLUS HEAT AND MOISTURE TRANSFER SIMULATION

Figure A1:	The created Hempcrete material property for simulation.....	196
Figure A2:	Material property heat and moisture transfer: settings.....	196
Figure A3:	Material property heat and moisture transfer: sorption isotherm.....	197
Figure A4:	Material property heat and moisture transfer: suction.....	197
Figure A5:	Material property heat and moisture transfer: Redistribution.....	198
Figure A6:	Material property heat and moisture transfer: Diffusion.....	198
Figure A7:	Material property heat and moisture transfer: thermal conductivity.....	199
Figure A8:	Construction component of hempod showing the wall layers.....	199
Figure A9:	Building surface detailed for Heat and Moisture transfer simulation.....	200
Figure A10:	Output variables for Heat and Moisture transfer simulation.....	200

APPENDIX B: MULTI OBJECTIVE OPTIMISATION IN jEPlus+EA

Figure B1:	Showing the thermal conductivity optimisation parameter specification.....	201
Figure B2:	Showing the Density optimisation parameter specification.....	201
Figure B3:	Showing specific heat capacity optimisation parameter specification.....	202
Figure B4:	Showing the porosity optimisation parameter specification.....	202
Figure B5:	Showing initial water content ratio optimisation parameter.....	203
Figure B6:	Showing moisture content optimisation parameter - sorption isotherm.....	203
Figure B7:	Showing relative humidity fraction optimisation parameter – sorption isotherm	204
Figure B8:	Showing moisture content optimisation parameter – suction.....	204
Figure B9:	Showing the liquid transport coefficient optimisation parameter – suction..	205
Figure B10:	Showing the liquid transport coefficient optimisation parameter – redistribution.....	205
Figure B11:	Showing moisture content optimisation parameter – redistribution.....	206
Figure B12:	Showing relative humidity fraction optimisation parameter – diffusion.....	206
Figure B13:	Showing water vapour diffusion resistance factor optimisation parameter – diffusion.....	207
Figure B14:	Showing the orientation optimisation parameter	207
Figure B15:	Showing the temperature convergence tolerance value optimisation parameter	208
Figure B16:	Showing the porosity optimisation parameter specification.....	208
Figure B17:	Showing the Initial water content ratio optimisation parameter specification.....	209
Figure B18:	Showing the investigated field for Material property class list.....	209
Figure B19:	Showing the thermal conductivity optimisation parameter specification.....	210
Figure B20:	Showing the density optimisation parameter.....	210
Figure B21:	Showing specific heat capacity optimisation parameter specification.....	211

- Figure B22:** Showing thermal absorptance optimisation parameter – material property...211
- Figure B23:** Showing visible absorptance optimisation parameter – material property...212
- Figure B24:** Showing solar absorptance optimisation parameter – material property.....212

APPENDIX C: VALIDATION OF RESULTS WITH HEMPOD

- Figure C1:** Showing material property for hempcrete simulation.....213
- Figure C2:** Showing HAMT- setting for hempcrete porosity and initial water content ratio.....213
- Figure C3:** Showing HAMT – sorption isotherm for hempcrete relative humidity fraction and moisture content.....214
- Figure C4:** Showing HAMT – suction for hempcrete liquid transport coefficient and moisture content.....214
- Figure C5:** Showing HAMT – redistribution for hempcrete liquid transport coefficient and moisture content..... 215
- Figure C6:** Showing HAMT – diffusion for hempcrete relative humidity fraction and water vapor diffusion215
- Figure C7:** Showing HAMT – for hempcrete thermal conductivity and moisture content216
- Figure C8:** Showing Construction layers of hempcrete wall.....216
- Figure C9:** Showing Building surface detailed for Hempod wall construction..... 217

APPENDIX D: VALIDATION OF RESULTS WITH RESIDENTIAL BUILDING

- Figure D1:** Showing the material property for hempcrete simulation applied to the residential building model..... 218
- Figure D2:** Showing HAMT- settings for hempcrete porosity and initial water content ratio.....218
- Figure D3:** Showing HAMT – sorption isotherm for hempcrete relative humidity fraction and moisture content.....219

Figure D4:	Showing HAMT – suction for hempcrete liquid transport coefficient and moisture content.....	219
Figure D5:	Showing HAMT – redistribution for hempcrete liquid transport coefficient and moisture content.....	220
Figure D6:	Showing HAMT – diffusion for hempcrete relative humidity fraction and water vapor diffusion.....	220
Figure D7:	Showing HAMT – for hempcrete thermal conductivity and moisture content	221
Figure D8:	Showing Construction layers of hempcrete wall applied to the residential building model.....	221
Figure D9:	Showing the building model zone for HAMT Simulations of the residential building.....	222
Figure D10:	Showing Building surface detailed for the hempcrete wall construction applied to the living room, kitchen and bedroom of the residential building.....	222

LIST OF TABLES

	Pages
Table 1: Hempod wall construction.....	70
Table 2: Hempod floor construction.....	71
Table 3: Hempod roof construction.....	71
Table 4: Wall construction of the residential building.....	72
Table 5: Floor construction of the residential building.....	72
Table 6: Roof construction of the residential building.....	72
Table 7: Hempcrete carbon sequestration of 1m ³ wall.....	76
Table 8: Hempod simulation experiment with conventional and natural materials....	135
Table 9: Hempod simulation with hempcrete material	146
Table 10 Representation of hempcrete for reduced simulation performance gap.....	156
Table T1: Residential building simulation experiment of combining conventional and natural material.....	223
Table T2: Residential building simulation experiment with hempcrete material.....	239

ACKNOWLEDGEMENT

I would like to express my gratitude to my supervisor's; Prof. Ljubomir Jankovic and Dr. Silvio Carta for their academic supervision through the course of this research project, to the completion of this dissertation. I acknowledge the school of creative arts, department of architecture in the University of Hertfordshire, where this study was successfully completed. Thank you to the Zero Carbon Lab for providing me with the data of the monitored Hempcrete buildings, used in this research project. I appreciate the IT support rendered to me, by Dr. Yi Zhang, the director of jEPlus+EA and Energy Simulation Solutions Ltd. through the period of my simulation and optimisation with jEPlus+EA software for this study.

My special appreciation goes to Arc. And Mrs Paterson Bana for being the best parents and for the unreserved emotional, financial and psychological support they offered to me throughout this research study. My sincere appreciation to Helti, Papa'a, Akacha and Usaku Bana for their immense care, support and encouragement throughout the period of this project. I am grateful to my good friend, Hadiza Ahmed for her support through this study. My unreserved gratitude goes to Ken Blackhurst for his impactful academic and professional advice, which has improved my intellectual competence and been helpful in guiding me through this study and my career advancement.

The relevance and contribution of International Building Performance Simulation Association (IBPSA) enabled me to exchange quality knowledge by writing and publishing a research paper, which increased my knowledge of building performance simulation. Thank you to Ty Mawr for the opportunity they provided for me to get to understand the production process of Hempcrete from a plant to a construction material (hemp plaster), through the introduction to hemp and lime plaster course, which I participated in, at the early stage of this research study.

DEDICATION

I dedicate this research project to God almighty and my family.

CHAPTER ONE

INTRODUCTION

Chapter one is the introduction to this research study. It describes the background to the study as research context in section 1.1. And section 1.2 explains the rationale for the overall study, section 1.3 explains the novelty of the research study and section 1.4 states the research questions. The aim and objectives of the study is explained in section 1.5 respectively. Section 1.6 contains the overall objectives and methodology for this research, further highlighting the justification for the chosen research methods. Section 1.7 includes the scope and limitation of this study while section 1.8 explains the research outcome.

1.1 RESEARCH CONTEXT

Currently, sustainability and sustainable development is under close scrutiny by many nations in the world; one of the major challenges for the built environment is climate change (Global sustainable development report, 2019). Meaning, climate change is not to be anticipated, as it has already started and its impacts are currently being experienced, such as the extreme weather conditions - increasing temperatures, rising sea levels, diminishing arctic sea ice and modified rainfall patterns (GOV.UK, 2019). The increased incidence and severity of heat waves has implications for building design (Chalmers, 2014). Climate change is projected to have profound impacts on the built environment, although the precise extent of these impact is uncertain. These potentially implies there's a need to move away from current architectural designs with conventional construction materials and embrace sustainable and innovative approaches for the built environment (Cimato and Mullan, 2010).

The built environment refers to the human-made surroundings that provide the basic setting for human activities such as; buildings, parks, road side infrastructure, and energy networks. It is “the human-made space where people live, work, and recreate on a daily basis” (Environmental Protection Agency, 2013; Moffatt and Kohler, 2008). Buildings and facilities not only provide basic shelter, but it is where the majority of individuals do their work, spend time with family and friends, and also accomplish various daily activities. Buildings are an integral part of the built environment and are vulnerable to the effects of climate change and

global warming such as overheating, due to extreme temperature rise and increased precipitation (Riffat, Powell and Aydin, 2016).

However, designing for climate change can be a positive influence in architecture and the built environment, with buildings responding to it accordingly rather than excluding the climate. Cutting down the vulnerability of the built environment to climate change requires utilising adaptive strategies such as constructing resilient buildings and infrastructure (Carter et al., 2015). Resilient building design considers the impacts of extreme weather, while protecting against them by controlling the indoor climate, through strengthening existing buildings. And using energy efficient construction materials to improve the fabric of new builds (Chalmers, 2014). Natural building materials such as hempcrete has been identified as a sustainable and energy efficient material (Geiger, 2011), enabling innovative construction of buildings.

Hempcrete as a construction material contributes to the resilience of buildings and mitigates the effects of climate change in the built environment; 1m³ of hempcrete absorbs 130kg CO₂ of carbon (Abbott, 2014). It possesses negative embodied CO₂, absorbed into the hemp plant material while improving the thermal performance of buildings (Jami and Kumar, 2017). It increases the quality of living for the inhabitants of the buildings, by providing a clean breathable environment, with stable internal environmental conditions. Hempcrete provides stable internal temperatures and relative humidity, characterized with low diffusivity and high thermal inertia in buildings (Walker and Pavia, 2014). It warms up easily in a short time and once heated, it slowly releases the heat to its surrounding when the temperature drops (Evrard, 2008). Hempcrete is a building material made from cannabis sativa, the male of hemp plant which has a very low tetrahydrocannabinol (THC) chemical when compared to the female hemp (cannabis Indiana also called Indian hemp), which is popularly known to be consumed for its mind-altering properties (Peev, 2012).

Hempcrete is an example of a vapor permeable and “breathable” building material that utilizes a combination of thermal and hygroscopic attributes to enable good thermal performance (Walker and Pavia, 2014; Shea, Lawrence and Walker, 2012). Hempcrete is hygroscopic as it is able to create healthy buildings, due to its ability to absorb and release moisture vapour from the interior air and exterior of the building. The hygroscopicity of hempcrete enables it to passively regulate internal humidity, which prevents condensation and damp as it is vapour permeable (Building with Hempcrete - UK Hempcrete, 2020). This increases the longevity of the material while maximising the thermal performance, of the building’s fabric

(Ducoulombier and Lafhaj, 2017). Given the characteristics and thermal properties of hempcrete, it could easily be deduced that, hempcrete is the answer to the current climate change related problems in the built environment. However, the breathability and excellent thermal properties of hempcrete are not been able to be accurately demonstrated in design and simulation models, which causes simulation performance gap. Simulation performance gap is a discrepancy between the performance of a simulation model and the constructed building; a degree of inaccuracy which is contained in a simulation model when it is eventually built (Monfet et al., 2009).

1.2 RESEARCH RATIONALE

The built environment's development in the field of computation, has made it possible to use digital environment for building energy design and estimating building energy consumptions. As well as to imitate the real-life behaviour of buildings through design simulations, for improving building construction (Hong, Langevin and Sun, 2018). As the world is evolving, the construction sector is experiencing technological advancements where design of buildings is carried out using digital environment through computers to save time and cost (Wright, 2016). Building performance simulation is the use of computational models to represent physics properties, expected or actual operation, and physical characteristics, of a building to improve its performance (Hong, Langevin and Sun, 2018). The importance of building performance cannot be over emphasized, as it is a significant facet of building design and construction, specifically concerned with the design and operation of energy efficient buildings. It can facilitate future innovation and technological progress in the field of building construction while reducing the negative impact that buildings could have on the built environment (Hensen and Lamberts, 2011). Effective building performance simulation can provide a conducive interior environment by improving indoor air quality, which potentially increase the productivity of people in the buildings (Hong, Langevin and Sun, 2018).

Hempcrete is increasingly used for construction as it has zero carbon emission with low embodied energy (Boutin et.al., 2006). It is considered to be more sustainable than other conventional building materials such as concrete, because hempcrete is mostly used with timber frame (Sutton and Black, 2011). Although it is lightweight, hempcrete has a unique property of being able to quickly store energy (heat or cool) and release it at a slow rate to stabilise day/night fluctuations of temperature. Hempcrete is breathable (Abbott, 2014);

breathability in materials is majorly about the exchange and movement of water in a gas or liquid form inside the building, outside the building, and through the walls, floors and roof. Materials possessing the capacity to absorb and release water as vapour (known as hygroscopicity), absorb and release water as liquid (known as capillarity) are breathable (Groves, 2018; Napier, 2015). Hygrothermal properties of hempcrete enables it to stabilize the indoor temperature while preventing possible condensation and dampness on walls (Tran le. et.al., 2010). This is as a result of its thermal behavior which reduces variations in the air temperature and the surface heat of the material, while improving thermal comfort. Hence, it is an excellent passive regulator for indoor temperature, which decreases the building's energy requirement (Gourlay et. al., 2017). It also regulates relative humidity in the envelope due to constant water vapor exchange between indoor and outdoor environments; as a result, it modulates any changes in temperature (Amziane and Arnaud, 2014). Hempcrete is a natural building material, which means identifying and addressing its performance gap is imperative towards curbing climate change problems from buildings. Hence, this study focuses on reducing the simulation performance gap from hempcrete buildings, to facilitate hempcrete simulation, design and construction.

Jankovic (2016) conducted a research for eliminating simulation performance gap from hempcrete buildings. The research was conducted experimentally outside of the simulation tools using the Fast Fourier Transform (Heckbert, 1995) to develop transfer functions that enable accurate representation of hempcrete to enhance simulation results. The research concluded by contributing to the confidence of designers with regards to the selection of plant size, and the scale of possible energy consumption and carbon emission savings. As the research was carried out outside of the simulation tools, it also highlights a need to represent hempcrete within simulation tools to facilitate simulation. Further giving room for more research to be carried out towards reducing simulation performance gap from hempcrete within simulation tools.

Evrard & De Herde (2010) studied the hygrothermal properties of hempcrete walls and performed simulations in WUFI, a computer programme that simulates heat and moisture transport in building material. They concluded that hempcrete appears to have rapid moisture transport in combination with high vapour permeability and high moisture retention. Accurate simulations of changes in moisture levels inside an LHC wall, caused by rain exposure and/or

changes in temperature, would allow studies to be made on different climate scenarios (de Bruijn, 2012).

The performance gap in hempcrete presents a challenge to the built environment, because the operational energy demand in hempcrete buildings is considerably low, as a result of the material possessing and exhibiting high thermal performance in real-life operation (Ingrao et.al., 2015; Jankovic, 2016). This is due to its specific material structure with combined heat and moisture transfer, causing a discrepancy between the performance of the simulation model and the actual performance of the building. More so, simulation of hempcrete is hindered by its specific structure and simultaneous occurrence of heat and moisture transfer, coupled with the absence of accurate design tools. Standard dynamic simulation software, such as Design Builder (DesignBuilder, 2018), IES Virtual Environment (IESVE, 2018), EnergyPlus (EnergyPlus, 2016) and other tools do not have a built-in capability to accurately simulate the effect of hempcrete. Therefore, to investigate into solving this simulation performance gap problem in hempcrete, exploring ways to reduce the simulation performance gap is a panacea. In this study, multi objective optimisation will be used to reduce the simulation performance gap from hempcrete within simulation tools. And calibration of measured against simulated data will be carried out, as applicable.

1.3 NOVELTY

The technique used in this study of reducing simulation performance gap from hempcrete using multi objective optimization, seeks to establish appropriate specification of key parameters to be used in simulation tools to reduce performance gap. The detailed simulation of heat and moisture transfer provides new and relevant information from optimization results, aiding to improve the quality of reliability in designing and constructing buildings with hempcrete. This simulation technique is tested for different climates, providing climate-independent results as well as establishing the essence of the physics behavior of this material. The results increase the understanding of hempcrete behaviour and facilitate increased confidence in building design simulations, leading to a wider use of this material in the built environment.

1.4 RESEARCH QUESTIONS

1. To what extent can multi-objective optimisation reduce the simulation performance gap from hempcrete?

- 1a. To what extent can identifying the appropriate parameters for hempcrete simulation reduce the simulation performance gap?
- 1b. How can the heat and moisture transfer in hempcrete be modelled for optimised simulation?

1.5 RESEARCH AIM AND OBJECTIVES

This study aims at investigating how to reduce the simulation performance gap from hempcrete using multi objective optimisation, by identifying the appropriate specification of key parameters for facilitating hempcrete simulation.

The research objectives will be addressed through experimentation and quantitative analysis. The objectives are:

- I. Analyzing the obtained monitored data in Microsoft excel;
- II. Moderating the IES Virtual Environment model with its original construction materials for conducting simulation;
- III. Establishing a base case model for the experiments with the simulation outputs;
- IV. Calculating the error between monitoring and simulation output, towards reducing simulation performance gap;
- V. Conducting Experimental simulation to investigate the construction component for hempcrete simulation;
- VI. Developing parametric simulations with transfer functions;
- VII. Investigating the simulation models of the buildings, using EnergyPlus heat and moisture transfer principles;
- VIII. Creating a wide range of parameters for the parametric simulations, for obtaining the accurate representation of parameters towards reducing the performance gap;
- IX. Carrying out multi objective optimisation, to identify the optimum representation of hempcrete from the simulation experiments;
- X. Establish hempcrete construction system that reduces the simulation performance gap and increase confidence in hempcrete simulation.

1.6 OVERALL OBJECTIVES AND METHODOLOGY

Given the overall objectives of this study, experimental research method has been adopted to conduct this study. The experimental research integrates secondary method of data collection with quantitative analysis to answer the research questions, achieve the aim and address the

objectives as applicable. Experimental research involves a procedure with specific plans, which requires collection, manipulation and interpretation of data (Liu, Sun, Wei and Lu, 2018). In order to conduct this study, the design of this experimental research is a combination of several steps as will be explained below;

- i Data was obtained from Zero Carbon Lab to conduct this research. The data is from the monitoring of two hempcrete buildings– Hempod (an experimental test cell) formerly located in Bath, UK and a residential building located in Diss-Norfolk, UK. The monitored hempcrete buildings are the experimental buildings to be modelled and simulated. The experimental simulation output will be collated alongside the monitored data towards calculating the performance gap reduction as applicable.

- ii Simulation experiments – Experimental simulations are carried out with a number of tools. First, using IES Virtual Environment (IESVE, 2018), hempcrete will be represented with a combination of conventional and natural construction materials for simulation experiments. The second set of the experiment will involve creating a material called hempcrete within simulation tools for experimental simulations. This will be followed by performing the heat and moisture transfer simulations in EnergyPlus (EnergyPlus, 2016) with the model that produced the best output from the simulation experiment in IES Virtual Environment. The input data file (.idf) from the EnergyPlus HAMT simulation will be coupled into jEPlus+EA (jEPlus, 2018) for the optimization. IES Virtual Environment (IESVE, 2018), is a standard tool for dynamic simulations, with a good capacity to create a complete 3D model of any building while conducting thermal simulations of the same building. However, it does not possess the capability to perform heat and moisture transfer simulations of a building model to demonstrate heat and moisture movement through walls and building envelope.

EnergyPlus on the other hand, has the built-in capabilities for performing advanced simulations of building such as, combined heat and moisture transfer, conduction transfer functions, and many other notable features (EnergyPlus, 2016). However, EnergyPlus (EnergyPlus, 2016) does not have the capacity to design or create geometry of a building model for simulation on its own. This is why it was reformed in 2008 and updated with features to enable its integration with other software's as a plug in such

as Design Builder (DesignBuilder, 2018) and Open studio (OpenStudio, 2020). The plug-in software's are for 3D designs while enabling a smooth transfer of modelled building geometry into EnergyPlus as an idf for simulations as applicable. EnergyPlus is a console-based program and it operates by reading input and writing output to text files. It enables a number of utilities including input data file (IDF) editor. An idf is a file format for text files containing data, which describes the building and HVAC system for simulation while creating input files using a spreadsheet-like interface (EnergyPlus, 2016).

- iii Calibration of simulation outputs - The simulation outputs are calculated against the monitored data, using the root mean square error metric to analyse the performance gap; the lower the Root Mean Square Error, the more performance gap is reduced.

- iv Multi-objective optimisation - Multi objective optimisation in this study uses jEPlus+EA (jEPlus, 2018) as the tool, to perform the optimisation towards finding out the accurate representation for hempcrete. The idf model template obtained from EnergyPlus HAMT simulations will be coupled in to jEPlus and jEplus+EA (jEPlus, 2018) for the optimisation. The optimization uses the non-dominated sorting genetic algorithm (NSGA II) in the background as an evolutionary process (Deb et al. 2002). Evolutionary Algorithms (EA) are the most used multi objective optimisation choice for construction-based problems because of their efficient rigorous technique and “robustness”. Meaning, a correctly implemented EA tends to solve the problem, no matter what kind of problem it is (jEPlus, 2018). Multi- objective optimisation is a decision-making method for selecting an appropriate set of design variables to enable adequate building design solutions (Panagiotidou and Aye, 2018). For this reason, multi-objective optimisation with NSGA II is used to perform the optimisation, as will be demonstrated further below.

- v Analysis - The analysis of optimisation results will be carried out using a visual representation of the Pareto front and the set of solutions produced on the Pareto front. Any point on this front is considered “Pareto optimal”. Technically, Pareto optimality means there is no mathematical “best” point along the Pareto front. Therefore, the

overall objective of the study will be used to figure out how to balance the priorities and identify the optimal solution from the set of solutions on the Pareto front. The optimal solution will now be selected and further evaluated for validation.

- vi Validation - The validation of the analysis will be carried out by using the identified hempcrete parameters of the optimal solution realised from the multi objective optimisation in new simulations to be carried out and comparing the root mean square error results from the optimisation with the corresponding values from the validation simulation.

Some researchers have challenged the ability of designers to estimate energy performance of a building using simulation due to uncertainty and sensitivity associated with the current tools and methods used (Ahmad and Culp, 2006). Similarly, the variability of modelling results produced by different software packages has been criticised (Raslan and Davies, 2010). However, methods to evaluate uncertainty of deterministic models in decision support from simulation for buildings have been developed (Uusitalo, 2015). More so, building design simulation has been of great help in the design and construction of buildings, especially in the estimation of energy use in buildings. It contributes to saving time by designing faster with software's and carrying out thermal modelling and simulations of buildings (Rotimi et. al., 2017).

The real-life operation of hempcrete buildings has been monitored and obtained, it will be analysed through simulation, to understand the behaviour of hempcrete material for simulation. Consequently, simulation experiments will be used to investigate the behaviour of the hempcrete buildings when modelled, in order to produce new and useful information for facilitating its simulation. The overall objectives of this study firstly, require the use of a 3D geometry of the experimental hempcrete buildings, to enable a detailed process of assigning the construction materials for the simulation experiments. The model is now transferred into EnergyPlus (EnergyPlus, 2016) for conducting the HAMT simulations, from which the idf is obtained for performing multi objective optimisation. Researchers have studied multi objective optimisation problems from different viewpoints; hence, there exist different solution philosophies and goals when setting and solving multi objective problems (Deb, 2001). For instance, the goal may be to find a representative set of Pareto optimal solutions, quantify the trade-offs in satisfying the different objectives, and/or find a single solution that satisfies the subjective preferences of a designer (Chang, 2015). In this study, the goal of the multi objective

optimisation is to identify the appropriate specification for hempcrete simulation while reducing performance gap. This will be achieved through specifying root mean square error for air temperature and relative humidity, as the optimisation objectives. The model with the accurate representation for hempcrete simulation, will be the model with the lowest root mean error from the set of solutions provided on the Pareto front.

Hwang and Masud (1979) and Miettinen (1998) presented suggestions on how the designer / decision maker articulates their preferences for optimisation solutions: no-preference method, a priori method, interactive method and a posteriori method. In the no-preference method, the preferences of the designer are not taken into consideration because the solution obtained is presented to the designer to accept or reject it. In a priori preference method, the hopes and opinions of the designer are taken into consideration before the solution process and it requires that the designer knows beforehand the priority of each objective function, transforming the multi-objective function into a single objective function where the problem to be optimized is a combination of objective functions. In the interactive preference method, the designer's preferences are continuously used during the search process and are subsequently adjusted as the search continues. In the posteriori preference method, no preferences of the designer are considered. After the Pareto set has been generated, the designer chooses a favourable solution from the set of solution alternatives as the optimum solution (Augusto, Fouad and Caro, 2012). This study proposes the posteriori preference method to identify and investigate the most energy efficient and favorable design parameter from the simulation experiments, which will create a hempcrete construction system to reduce simulation performance gap. In the posteriori preference method, no preferences of the designer are considered. This is because, after the Pareto set has been generated, the designer chooses a favorable solution from the set of solution alternatives as the optimum solution. The basic idea of the Pareto approach is that, instead of transforming a multi-objective problem into a single-objective problem and then solving it by using a single-objective search method, it uses a multi-objective algorithm to solve the original multi-objective problems which is logical. It adapts the algorithm to the problem being solved, rather than the other way around. The Pareto approach consists of finding many non-dominated solutions as possible and returning the set of non-dominated solutions to the user (Deb, 2001). Research shows that NSGA-II has proven to be efficient and is the most widely applied for optimizing design parameters (Yusoff, Ngadiman and Zain, 2011). Hence, this study uses the NSGA II in the background of the optimisation method, to identify the simulation design

parameter for hempcrete. The interest of this study is to increase confidence in designing and constructing buildings with hempcrete. Firstly, by reducing the simulation performance gap existing between hempcrete buildings and its corresponding simulated designs and then identify the simulation design parameter of hempcrete.

1.7 SCOPE AND LIMITATION

This study focuses on hempcrete as a construction material and facilitating hempcrete simulation technique to reduce simulation performance gap, through experimental simulation and multi objective optimisation. Hempcrete is not a conventional building material and there are also not many available hempcrete buildings that have been monitored for a considerable period of time. Hence, this research uses secondary method of data collection, by obtaining data from Zero Carbon Lab. The data was from two hempcrete buildings (Hempod and a residential building), differently monitored for a period of time. The run period of the experimental simulations performed, were limited to the period that the hempcrete buildings were monitored for. This was necessary to maintain a meticulous order and obtain accurate results as applicable. Hempod was monitored from 12th March to 05th April, therefore the simulation run period for Hempod experiments was limited to run from 12th March to 05th April and the multi-objective optimisation was set to run for the same period. Also, the residential building was monitored for one year from 1st January to 31st December and for that reason, the simulation experiments were limited to run for one year. The validation simulation carried out with the residential building was also limited and set to run from 1st January to 31st December as applicable. Though, there is a limitation from data collection and simulation run period, the simulation experiments provided ample opportunity without much limitation towards investigating the hempcrete material for accurate simulation representation. The research also used quantitative data analysis with the experimental research simulation.

1.8 RESEARCH OUTCOME

The results from the simulation experiments and multi objective optimisation, identify the accurate representation of parameters for hempcrete simulation. The results provide readily available specification within simulation tools, to represent hempcrete which in turn, will save time and increase confidence in hempcrete simulation. Additionally, in order to construct and build hempcrete buildings, it must be designed by architects and simulated by architects or building engineers (Attia, Hensen, Beltran and De Herde, 2012). The output of this research

inform architects through increasing hempcrete design accuracy, for construction drawings specifically in section drawings.

Since the multi objective optimisation identifies the accurate parameters for hempcrete material simulation and construction, the outcome will be helpful to design and construction professionals. This means that architects will be more confident in designing hempcrete buildings with accurate representation of this materials. Building engineers will also be able to simulate this material with increased confidence. More so, given the thermal and environmental benefits of hempcrete, the outcome of this research will be beneficial to researchers, by facilitating an increase in understanding of its performance. The reduced simulation performance gap from hempcrete is beneficial to the built environment because hempcrete increases energy efficiency in the operations of buildings, thereby developing resilience of the built environment to climate change. The review of literature on hempcrete, its simulation and optimisation further explain its benefits as a construction material and elaborates on the simulation performance gap in hempcrete.

CHAPTER TWO

LITERATURE REVIEW

Chapter two is the literature review for this study. Section 2.1 explains the characteristics of hempcrete as a construction material while reviewing current literatures which includes its pros and cons for construction. This is followed by Simulation Performance gap in section 2.2; where explanations of simulation performance gap in the built environment was carried out. Section 2.3 contains explanation of the simulation performance gap in hempcrete buildings and describing it as the focus of this study. Section 2.4 focuses on simulation of hempcrete for buildings and contains literature on simulation of hempcrete for construction. It further identifies that there is indeed a simulation performance gap in hempcrete that needs to be reduced and how this research will address this reduction. Section 2.5 is multi objective optimisation for construction, which describes the technique this study uses for analysis and decision-making, and for identifying the appropriate specification of hempcrete to facilitate its simulation. Section 2.6 contains literature synthesis in the field by combining simulation with multi objective optimisation for improving building performance. It introduces this as the concept adopted for carrying out this study through simulation experiments.

2.1 HEMPCRETE AS A CONSTRUCTION MATERIAL

Hempcrete was first introduced as a construction material for buildings in France, in the beginning of the 1990s to lighten concrete mixes (Evrard, de Herde and Minet, 2006). From there, the use of hemp in combination with lime has evolved into a more mainstream material that is marketed by several companies, mainly in France and the United Kingdom (Hemp uses, information facts - Hemp Basics, 2020; Cazacu et al., 2016). It is a plant-based construction material and the shiv is mixed with building limes as a binder, to create a building material that provides good thermal and acoustic insulation (Evrard, 2003).

Additionally, it provides a method that allows simplification and reduction of the number of layers and processes involved in timber-frame construction (Woolley, 2006); a construction method much used with hempcrete. Figure 1 below, shows the stages of hempcrete from a plant in to construction material.



Figure 1: Hempcrete from a plant to a construction material: (a) hemp plant (Cordis, 2019) (b) hemp shiv (Gle, Gourdon and Arnaud, 2011) (c) hempcrete blocks (UK Hempcrete.com) (d) hempcrete constructed building (UK Hempcrete.com).

Hemp is a particularly promising plant material that grows up to 4m in 4 months, without much fertilizer and irrigation demand. The woody core, a by-product after harvesting of seeds, fibres and stems, can be used as aggregate in a composite formulation (Walker and Pavía, 2014). Hempcrete consist of a mixture of hemp stalks (shiv), a binder/lime-based binder and water (Bevan and Woolley, 2008). Hemp shiv (also called hurds) are the woody core parts of the hemp stalk. For construction purposes, it is mostly used in lining or filling to form a construction element due to its good thermal and sound insulation properties (Walker and Pavía, 2014). Hempcrete is a lightweight composite insulation material, characterised with a dry density ranging from 200 to 800kgm³ and its low density contributes to its good thermal properties. Its dry thermal conductivity is between 0.04 and 0.2WmK, depending on the mix formulations (Amziane and Arnaud, 2014). Hempcrete compressive strength is often less than 1MPa which is relatively low, compared to other conventional building materials. It is also characterized by an important mechanical ductility, with a compressive strain higher than 10% (Arnaud and Gourlay, 2011). This suggests that the high absorption capacity of lignocellulosic aggregates, which is sometimes greater than 300% by mass, is one of the main causes of hempcrete's low mechanical performances (Nozahic et.al, 2012).

Additionally, hempcrete has a porous structure, which contributes to its low mechanical strength and low rigidity of the material after curing, making it unable to be used as a load bearing material in construction (Hirst et.al., 2010). Amziane and Sonebi (2016) carried out an overview on bio-based building materials made with plant aggregates and they established that hempcrete has multitude of useful properties. It exhibits a degree of porosity which is high and increases its ability to absorb sound while enhancing its hygrothermal transfer ability, resulting in its capacity to deform. These characteristics are essentially what differentiates hempcretes from other conventional materials such as concretes for which the granulates are considered to be non-deformable (Amziane and Sonebi 2016). More so, the life-cycle analysis

of hempcrete explains that, 1.8 tons of CO₂ are sequestered for every ton of hempcrete, which means 180kg of CO₂ is locked in 1m³ of hempcrete (Prétot, Collet and Garnier, 2013; Pervaiz and Sain, 2003; Bevan and Woolley, 2008). When hempcrete is used for constructing buildings, it captures and ‘locks up’ carbon throughout the life span of the building. According to the study published by Boutin et.al., (2006), the hempcrete wall interestingly absorbs carbon for a duration of at least 100 years, as it stores more CO₂, than it emits through its life-cycle (Amziane and Arnaud, 2014; Boutin et.al., 2006). The hygrothermal properties of hempcrete enables it to stabilize the indoor temperature while preventing possible condensation and dampness on walls (Tran Le et al., 2010). This is as a result of its thermal behavior, which reduces variations in the air temperature and the surface heat of the material, while improving thermal comfort. It also regulates relative humidity in the envelope due to constant water vapor exchange between indoor and outdoor environments, which modulates any changes in temperature. Hence, it is an excellent passive regulator for indoor temperature, which is advantageous towards decreasing the building’s energy requirement (Gourlay et al., 2017).

Pochwała et al., (2020) conducted a study on the heat conductivity properties of hemp–lime composite material, used in single-family buildings. The study aimed to calculate the heat conductivity of three experimental hemp–lime composites used for structural construction purposes, with an experimental stand, inside two compartments. The heat transfers co-efficient, fire resistance, and bulk density properties of hempcrete were compared to those of other conventional construction materials. The results from the research, established a thermal conductivity for hempcrete ranging from 0.038 W/m²K – 0.20 W/m²K for walls. This value obtained from the study, makes it possible to erect hempcrete walls without needing any additional insulation. It further demonstrated that, together with supporting structures such as beams and columns made with biodegradable materials, hempcrete is a sustainable potential replacement for commonly used conventional building materials (Pochwała et al., 2020).

Hempcrete is often directly implemented on the construction site, or manually set into forms or by projection processes, and these methods of implementation do not allow it to reach a sufficiently high compactness (Elfordy et.al., 2008). However, previous work has shown that the compaction of hempcrete at fresh state is responsible for the increase of its mechanical performances (Nguyen et. al., 2009; Nguyen at al., 2010).

Hempcrete has been used to construct and build a number of buildings, which has demonstrated its excellent thermal performance in real life. For example, the English beer brewery Adnams,

built a distribution centre/warehouse near Southwold in 2006, and hempcrete blocks were used to construct diaphragm walls. The diaphragm walls had cavity that was filled with substantial hemp and lime, giving a U-value of 0.18 W/mK (Lane, 2006). The thermal insulation of this building envelope itself proved to be sufficient, so that no mechanical cooling was needed to achieve the desired storage temperature (Lane, 2006). Although, hempcrete cannot provide enough structural integrity to be used as a load-bearing material, it can, however, make up for its mechanical drawbacks through functionality and environmental benefits. For instance, it exhibits a low thermal conductivity, that not only regulates the temperature and relative humidity levels within a dwelling, but also enables high acoustic performance when compared to traditional concretes, and an exceptional resistance to fire without the need for fire-preventative measures (Arizzi et al, 2015).

In as much as hempcrete appears to be the ideal natural material for sustainable construction of buildings, the literature related to hempcrete composites as seen above, established some important properties of this material, such as the compressive strength, porosity, acoustic properties, density and thermal conductivity. The repeatability in research results of its density and other mechanical strengths from different hempcrete research experiment, highlights the consistency of its properties. Despite the established efficient construction properties and ever-growing popularity of hempcrete, the actual material properties have not been confirmed yet, as they are mostly provided within a range. Hence, it is imperative to investigate the properties of the materials to facilitate, a wider use of this material with increased confidence, for design and simulation purposes as applicable.

The Architect Ralph Carpenter, of Modece Architects designed and built houses situated in Haverhill, Suffolk. The project consists of four terrace houses; two hempcrete houses and two masonry houses. The hempcrete houses were compared to the masonry houses by the Building Research Establishment (BRE, 2002). Some of the important findings were that, the structural qualities and durability of the hempcrete houses were at least equal to those of the masonry houses. However, “the external walls of the Hempcrete Homes appear to retain more heat than those of the masonry houses” (BRE, 2002). Another finding was that even though both forms of construction offer equal protection against water penetration, the hempcrete houses generated less condensation inside the construction. The report concluded that the hempcrete houses performed as well as, or in some cases even better than, the masonry houses when it comes to energy efficiency, acoustic insulation, water permeability and thermal stability (BRE,

2002). These examples are a few examples of buildings constructed using hempcrete as the building material. While hempcrete does have some drawbacks in its mechanical performance, as a natural and practical building material it remains a resource that can be used to lower carbon emissions. It also reasonably reduces any other harmful impact the construction sector has on the built environment in relation to climate change (Yates, 2003).

Furthermore, Benfratello et. al. (2013) carried out an experimental study on the thermal and structural properties of a hempcrete bio composite. The study involved analysis of the thermal and structural behaviour of a bio composite concrete, constituting of lime as the binder with the addition of hemp. The analysis from the experiment carried out shows that hemp can be used both for the realization of insulation panel (hemp fibres alone) and as a construction material (hemp bast and concrete mix) (Benfratello et. al., 2013). These examples demonstrate the thermal and structural properties of hempcrete when used for construction. They also create more research opportunities and encourage the incorporation of hempcrete into construction of buildings and other structures in the built environment. Especially as the above literature explains, hempcrete is capable of absolutely transforming the built environment while providing healthy internal environmental conditions in buildings. Given the characteristics and thermal properties of this hempcrete material, it could easily be deduced that, hempcrete is one of the answers to current problems of climate change in the built environment. However, it still performs differently when simulated and more efficiently in real life operation of the building. This means that, demystifying hempcrete simulation through reducing its performance gap, will be helpful to the building design and simulation community for facilitating design and simulation of buildings constructed from this material (Bana and Jankovic, 2019). Hempcrete's performance gap is not a myth but an existing fact in design and construction of hempcrete buildings. Hence, this study identifies that there is a simulation performance gap in hempcrete buildings and develops a method to specify adequate parameters to reduce this performance gap within simulation tools.

2.2 SIMULATION PERFORMANCE GAP

Simulation performance gap is a discrepancy between the performance of a simulation model and the constructed building; a degree of inaccuracy which is contained in a simulation model when it is eventually built (Monfet et al., 2009). De Wilde, (2017) suggested a logical definition for performance gap, by conducting a literature review articulating building performance as a

concept that describes in a quantifiable way, how well a building and its systems operate while providing the tasks and functions expected of that building. Essentially, performance gap may stem from three main views: an engineering view of buildings as an object, a process views of buildings as a construction activity, and an arts view where performance involves the integration of form and appreciation (De Wilde, 2017). This study towards reducing simulation performance gap appreciates the three views from De Wilde (2017) definition and combines them into a single concept as ‘performance gap’. For instance, engineering view of buildings as an object includes the design and simulation of the building. A process views of buildings as a construction activity which is the construction of the designed and simulated buildings and an arts view where performance involves the integration of form (design) and the constructed building. CIBSE (2013) evaluated that there are two main reasons for performance gap in a building. The first is that, the method of calculating energy use during the building design stage for the purposes of compliance, does not take into account all the energy uses in a building while the second reason, is related to construction and site practice. They further produced a standard methodology for Evaluating Operational Energy Performance of Buildings at the Design Stage in order to assist designers with addressing the issue of performance gap in buildings (Cibse.org, 2013).

Shi et.al., (2019) conducted a systematic review towards addressing performance gap in buildings. They focused on the five fundamental questions usually arising from performance gap in buildings; the definition, magnitude, causes, determination, and bridging solutions. In the review, they identified that a variety of factors could cause a building to deviate from its designed and intended performance, stating that the root causes of the performance gap can occur in design as often as they do in the construction and operation stages. This demonstrates that bridging the performance gap of buildings requires a collective effort from all professionals involved in a building project (Shi et al., 2019). Reasonably bridging the performance gap in hempcrete buildings is essential, as it will provide a sustainable solution for professionals actively involved in construction, including architects and engineers responsible for design and simulation, builders responsible for the construction, clients and facility managers responsible for the building use and operations.

Allard, Olofsson and Nair (2018) conducted a research on Energy evaluation of residential buildings, focusing on Performance gap analysis and uncertainties in the evaluation methods.

The research proposed that performance gap in buildings can be analysed by calibrating the simulation model against the measured data, as it is imperative for identifying any deviations from the intended design or flaws in the finished building (Allard, Olofsson and Nair, 2018). While calibrating the simulation model to its measured data for identifying any performance gap is understandable, calibrating simulation outputs and measured data is essential, and is made valid by adhering to a consistent method of calibration (Fabrizio and Monetti, 2015). As will be demonstrated in this study, the metric of root mean square error will be used as applicable, to calibrate the simulation output against the measured data of the experimental buildings. Hence, calibration of simulation models to match and address the measured energy use may therefore be an underdetermined mathematical problem with multiple non-unique solutions (Coakley et al. 2014).

IEA Annex 21 (2016) presented performance gap in buildings by developing the concept of a Performance Assessment Method (PAM). A PAM is a roadmap for assessing building performance through building energy simulation. It requires the establishment of a representation of a base case design, model calibration, the evaluation of boundary conditions, integrated simulation, an expression of multivariate building performance, including an identification of problem areas, generation and testing of solutions to any problems, and a testing of the robustness of the performance analysis by running different weather files. Additionally, Preiser and Vischer (2005) contributed a seminal book on Post Occupancy Evaluation (POE) in the wider sense, which they label Building Performance Evaluation (BPE). Interestingly the book does not really connect to building performance simulation approaches, but it explores performance during strategic planning, briefing, design, construction, occupancy, reuse and recycling. It also includes case studies which is very important in understanding performance gap from post occupancy evaluation and building performance itself.

Augenbroe (2011) provides a deep discussion on the role of building performance and its simulation in building design. It explains building simulation as a virtual experiment that is needed to quantify how well a technological solution meets user requirements. It emphasizes the need for a stakeholder dialogue about performance requirements, and about how the building meets its requirements. The discussion was followed by deep observations, which include comments on the need to balance the complexity of simulations with the information needed to make an informed design choice, including the need to account for the uncertainties

that underlie simulations, especially in early design stages, and the importance of the fact that simulation is based on a range of assumptions. Meaning, it never fully matches reality, leading to the issue of the ‘performance gap’. The contribution of Augenbroe (2011) on the role of simulation in performance of buildings, addresses some fundamental issues, limited to simulation and design rooted in a pure view of decision making. Building performance is an important facet of building and construction efficiency (van Dronkelaar et al., 2016). Simulation on the other hand, helps in analysing and establishing the parameters of the building, related to its performance (Hong, Langevin and Sun, 2018). Simulation in this study is used in creating this composite construction system which will be a part of decision making through optimisation. Moreover, there also is a mismatch between the needs of the building community, experimental measurement, and simulation approaches, which clearly leads to a range of work that addresses what is, and what has been established as “the performance gap”. Yet in reality, there are many such gaps existing in the built environment in different building types, at different levels and different construction techniques with different materials including sustainable buildings with natural building materials such as hempcrete.

Researchers such as De Wilde (2014), Jones et al. (2015) and Burman et al. (2012) have suggested ways to bridge and reduce performance gap from the building design stage, construction stage and operational stage. In the design stage, design guidance and corresponding reports have been suggested to inform clients and design teams, to ensure adequate communication of design intent and responsibilities, leaving no room for error during the building construction. In the construction stage, improving the quality of construction delivery process through increase in care was suggested (Tofield 2012). With the operational stage, adopting accurate data collection and monitoring techniques, to reduce any uncertainty in operational data was the key suggestion. In order to bridge the simulation performance gap and performance gap caused by misalignment of different roles in a building construction process, there is a need to develop efficient integrated methods of building design, construction and operation. The reason is, such methods have the potential to improve accuracy in building design, through to the building life cycle (Hong, Langevin and Sun, 2018).

Additionally, De Wilde (2014) carried out a pilot study to investigate, while carrying out a literature review on the performance gap of buildings. The review concluded with a worthy point to note that, the only way to bridge the building performance gap is to adopt an explicit and coordinated approach, such as to combine model validation and verification, improved

data collection for predictions, better forecasting, and change of industry practice. The study identified some critical issues regarding performance gap and suggested future study to be adequately addressed. Generally, performance gap could be described as a problem from the design stage of buildings coupled with unrealistic expectations from the design, which cannot be achieved by the building when constructed. Meaning, current predictions tend to be unrealistically low while its corresponding actual energy demand, is typically unnecessarily high (van Dronkelaar et al., 2016).

While all the above reviewed literature provides a contextual explanation on simulation performance gap in buildings with substantial discussion of various aspects of building performance. The key concept of performance drawn from the literature reviewed is that, performance gap is based on building operation and exists due to user requirements, influenced by the behaviour of technical solutions. These concept captures how well the intended design solutions meet the actual operational demands of the building. There is no doubt that building performance is complex due to a number of characteristics of buildings and the built environment. However, a full review and critical analysis of most contributions in the field of building thermal performance and simulation performance gap will be outside of the scope of this study.

Most of the literature reviewed above, explain that performance gap has a lot to do in early design stage and construction of buildings. This study seeks to address hempcrete's performance gap, in order to develop a solution for increased accuracy at the early design stage of hempcrete building design, specifically the early design simulation stages of hempcrete buildings.

2.3 SIMULATION PERFORMANCE GAP IN HEMPCRETE BUILDINGS

The overall objective of building performance simulation is to analyse the performance of the model in relation to the design, construction, operation and control of buildings (De Wilde, 2018). Building performance simulation involves the replication of a building, using simulation model created based on fundamental physics properties of its physical principles and engineering to assess its performance (Favoino et al., 2018). While dynamic simulation enables accurate comparison between different design options, it is less accurate in the

simulation, designing and prediction of actual performance of hempcrete buildings (Jankovic, 2016). As seen from the above literatures in Section 2.1, hempcrete is a high-performance building material with great potential to be environmentally and economically beneficial, as it reduces embodied carbon emissions and the in-use energy demands from buildings. More so, vapor permeability and Nordtest result has validated hempcrete’s capability to maintain its hygroscopic and moisture buffer ability in any state, even after hydrophobic treatment of the aggregate (Shea, Lawrence and Walker, 2012). Given the excellent thermal and hygroscopic properties of hempcrete in its real-life performance, the properties cannot be accurately represented in simulation tools for design and simulation (Bana and Jankovic, 2019). This in turn, affects the simulation outputs of hempcrete making the real-life performance of hempcrete and hempcrete buildings better than the performance of the simulated hempcrete material.

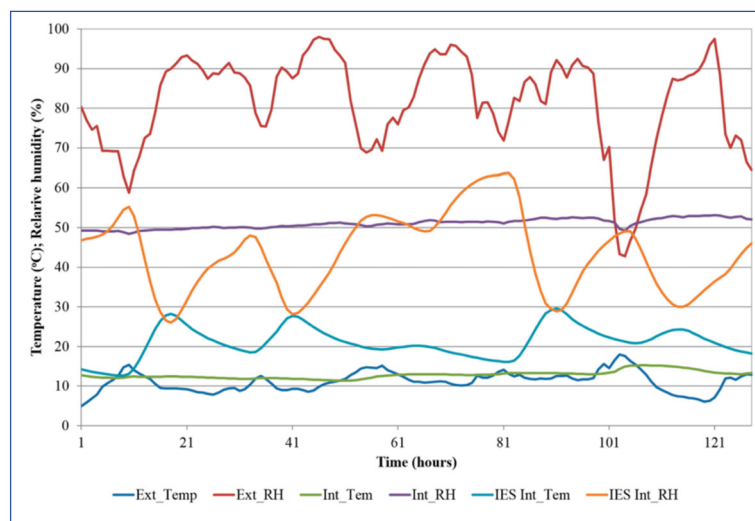


Figure 2: An example of simulation performance gap in a hempcrete building (Jankovic, 2016)

Figure 2 above, is a comparison between measured and simulated internal conditions in an experimental lime-bonded hemp building (Jankovic, 2016). As seen from Figure 2 above, the measured/monitored internal temperature and internal relative humidity seem stable. While the IES Int_Tem and IES Int_RH which are the simulated internal temperature and internal relative humidity outputs are different from the monitored value. The comparison between the monitored internal temperature and relative humidity with the simulated temperature and relative humidity show an obvious gap, which is the performance gap. This performance gap also shows that the monitored values which represents the real-life performance of the hempcrete building, has a better and stable performance than the simulated.

Simulation performance gap in hempcrete is due to the fact that performance of actual hempcrete buildings is better than the performance of the simulated hempcrete buildings. Making it a reverse case scenario of the conventional performance gap in the built environment, caused by underperformance of the actual building compared to the simulated (Bana and Jankovic, 2019).

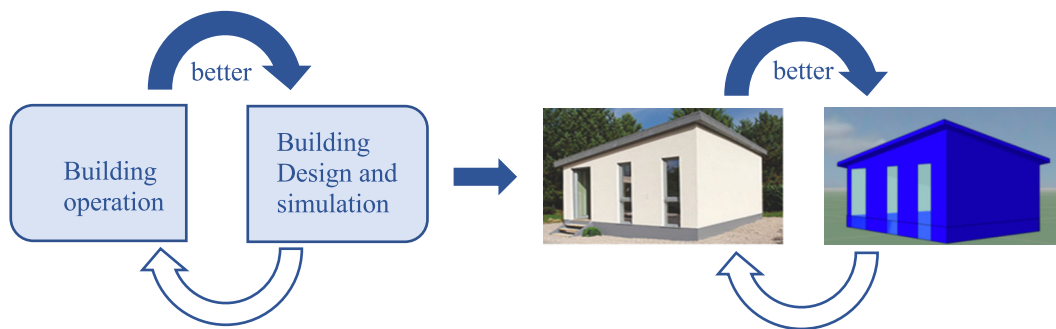


Figure 3: Performance gap in hempcrete

Figure 3 above, describes the performance gap issue in Hempcrete buildings. Simulation performance gap in hempcrete is still a challenge and if successfully reduced to a reasonable extent, can increase the accuracy of simulating hempcrete for construction.

Evrard (2008) performed material property tests on hempcrete and introduced the resultant material data in WUFI Pro 4.0 for simulations. Results from the simulations were compared with measurements and they were found to differ from the measured data, which clearly demonstrated a performance gap. However, Evrard (2008) ascribed these differences to a retarded sorption effect, whereby it takes time before equilibrium water content in sorption tests is achieved, and in the simulations this equilibrium was assumed to occur instantly. Similarly, Arnaud (2009) studied the hygrothermal behaviour of hempcrete, using a cell of exchange, which consisted of a 30 cm thick wall element placed between a climate box and the laboratory. The temperature and relative humidity were changed inside the climate box and then, test results on temperature and relative humidity fluctuations inside the wall element were compared with simulations made in COMSOL Multiphysics. COMSOL Multiphysics is a simulation software that enables modelling and simulation of physics-based systems. And from studying a change in temperature, Arnaud (2009) found significant differences between simulated and measured data. He ascribed these differences to coupled heat and mass transfer inside the material, establishing it as indications that phase change occurs inside the hempcrete material. These clearly demonstrate that the coupled heat and mass transfer inside hempcrete

material affect the accuracy of simulation results and causes simulation performance gap. These are indications that the heat and moisture transfer properties of hempcrete need to be investigated to reduce the simulation performance gap, as will be carried out in this study.

The literature reviewed above on hempcrete and its simulation performance gap demonstrate that, hempcrete's performance in real life is better than the simulated, and it critically highlight the importance of improving hempcrete simulations to increase confidence for designers. This research is focused on improving the performance of simulated hempcrete buildings to match and level up to the performance of the constructed buildings, by reducing the simulation performance gap. Hence, this study involves a detailed investigation through simulation, to address the simulation performance gap from hempcrete buildings.

2.4 SIMULATION OF HEMPCRETE FOR BUILDINGS

Simulations for building design was explained by Spitler (2006); "Building performance simulation; the now and the not yet" (Spitler, 2006). He described that simulations of building thermal performance using digital computers, has been an active facet of investigation since the 1960s (Spitler, 2006). As time went on, the simulation domain grew richer and more coupled, with available tools integrating simulation of heat and moisture transfer in the building fabric, including airflow in and through the building, daylighting, and a vast array of system types and components (Clarke and Hensen, 2015). Building simulation is an acceptable technique for investigating and assessing the dynamic interactions between building envelope, its corresponding energy consumption, as well as its external climates (Coakley, Raftery and Keane, 2014).

Burman et. al. (2012) carried out a research focused on performance gap and thermal modelling, to compare simulation results and actual energy performance of a building, towards reducing simulation performance gap, to identify how the thermal modelling process could be enhanced. The results from their research demonstrate that, if correct and up to date information is used, dynamic simulation method is very capable of producing realistic results to relate and reflect the actual energy performance of buildings significantly, with a reasonable accuracy. The research further highlighted that, improving simulation method is one of the important factors that could help reduce performance gap between simulations and actual performance of a building.

While dynamic simulation as a building design tool enables accurate comparison between different design options. It is, however, less accurate in designing and predicting actual performance of hempcrete buildings (Jankovic, 2016). Kinnane, et.al (2015) performed an experiment to investigate the thermal inertia properties and dynamic thermal responsiveness in hempcrete walls. The results from their experiment demonstrates that hempcrete exhibits high thermal inertia, enabling the characteristics to compensate for any limitations in the thermal resistance of the hempcrete material. When viewed critically, the thermal resistance and mass characteristics of hemp-lime are appropriate to maintain comfortable thermal indoor conditions with low energy operation (Yates, 2003).

Hempcrete possess some distinct advantages in its properties, including low thermal conductivity, effective moisture buffering, and high sound absorption, while having a high carbon sequestration (Shea, Lawrence and Walker, 2012). Dhakal et al., (2017) conducted an experimental study to investigate the hygrothermal performance of hempcrete for buildings in Canada. The study concluded with results from their experiment demonstrating that when using hempcrete in the Canadian climate, a rain screen wall system is more suitable than a mass wall (Dhakal et al., 2017). It is therefore essential, to adopt an efficient system of building with hempcrete to suit each climate and sustainably address climate change through efficient building design and construction. Specifically, with this study, reducing the simulation performance gap will necessitate the identification of the accurate representation of hempcrete for increased simulation accuracy.

Latif et al., (2015), experimentally investigated the moisture buffer potential of wall assemblies incorporating formulated hemp-lime. They reasonably concluded that the moisture buffering capacity of hemp-lime is under-utilised or unutilised in their experimental assembly incorporating plasterboards and wood wool boards because of hempcrete material's inherent moisture buffer capacity (Latif et al., 2015). More so, assessment of hempcrete's thermal performance through evaluation of its resistance to thermal transfer alone, underestimates its true thermal quality (Kinnane, et.al, 2015). Moisture buffering can directly and indirectly reduce the energy consumption of buildings (Osanyintola and Simonson, 2006). Hempcrete's moisture buffer capability contributes to its overall excellent thermal performance, which is why it is essential to reduce the simulation performance gap from hempcrete buildings. Piot et al., (2017), studied a hempcrete wall exposed to outdoor climate, with an objective to analyse the behaviour of the wall in realistic conditions. The study further highlighted that regarding

the numerical model, some improvement was suggested to make it more accurate, especially in short term dynamic simulation. (Piot et al., 2017). Bejat et. al (2015) conducted a study of two hemp concrete walls in real weather conditions, to examine the hygrothermal behaviour of a real hemp concrete wall. Their results demonstrated a good agreement between measured and simulated data, the reproducibility of the measured results by the simulation showed room for further improvement on the numerical model. Technically, this means improving numerical/thermal model of buildings are important. However, thermal modelling plays a pivotal role under current building regulations and is used extensively to ensure buildings meet the energy efficiency standards and carbon emissions targets set out by national regulations (Rotimi et. al., 2017).

Hussain et. al., (2019) experimentally researched into hygrothermal and mechanical characterisation of novel hemp shiv based thermal insulation composites. The study focused on the development of advanced water-resistant bio-based hempcrete composites with enhanced hygrothermal performance for building applications. The highly porous structure of hemp shiv is responsible for low thermal conductivity and allows the material to adapt to varying humidity conditions providing comfortable indoor environment. However, the pore network and the hydrophilic nature of these hemp shiv affects the compatibility and durability of the material in presence of excess moisture conditions. In their work, they created hemp shiv composites in starch based and silica-based matrix, characterised for their hygroscopic, thermal and mechanical properties. It was realised that the hemp shiv-based composites were resistant to water yet permeable to vapour and showed excellent moisture buffering capacity when compared to conventional hemp-lime composites (Hussain et.al., 2019).

Gourlay et.al., (2017) examined the effect of water content on the acoustical and thermal properties of hempcrete as a multifunctional ecological material used in buildings. Due to its high porosity (ranging from 60 to 90%), it presents an “atypical” mechanical behaviour and its hygrothermal and acoustical properties are particularly interesting. The paper focused on influence of the water content of hempcretes on their acoustical and thermal properties, four mixtures of hempcrete were manufactured using a binder and two shives under two distinct stresses of compaction. It is shown that water content does not affect significantly the acoustical properties of hempcretes although a swelling effect can be detected by an increase of resistivity and a decrease of porosity. Finally, that study confirms that thermal conductivity

rises almost linearly with water content while evolutions of thermal diffusivity and specific heat capacity are different depending on the hempcrete mixture.

Collet and Pretot (2014), carried out a study on Experimental highlight of hygrothermal phenomena in hemp concrete wall. The study investigates the hygrothermal behaviour of a timber-framed hemp concrete wall made of precast blocks. Measurements are performed on an uncoated wall as well as on a coated wall. The experimental device consists in two airconditioned rooms where ambient conditions are selected to induce temperature and/or vapour pressure gradient between the two sides of the wall. The monitoring deals with temperature and relative humidity within the wall. Kinetics of temperature and of vapour pressure are given. Profiles are drawn at several times of the transient phase. In the regular part of the wall, several kinds of hygric behaviours are highlighted such as homogeneous vapour diffusion and huge vapour pressure variations due to evaporation, condensation and/or sorption-desorption phenomena. The results in the line of frame show that the frame doesn't induce disturbances in the hygrothermal behaviour of the wall. It is also shown that the coating reduces and delays vapour diffusion.

Niyigena et.al., (2015) researched into the Variability of the mechanical properties of hempcrete. Focusing on the statistical analysis to determine the variability for material density, compressive strength and Young's modulus. The analysis was carried out with respect to four main parameters: the testing laboratory equipment and procedure, the hemp shiv type, the batch elaboration and finally the specimen size. From the study, the results obtained show low variability for compressive strength and dry density; which is not the case for Young's modulus. Three probability distributions, namely: normal, log-normal and Weibull, have been proposed to fit the experimental results.

The literature reviewed above on hempcrete, its simulation and its investigation for construction, demonstrate that effort has been made to reduce this simulation performance gap from hempcrete, outside simulation tools and some, within simulation tools. However, there is still a gap causing a discrepancy between operation and simulation of this material. Simulation is very important and beneficial to architects and other construction professionals (Hong, Langevin and Sun, 2018), thus getting to reduce the simulation performance gap from hempcrete buildings will be of great benefit to the construction field. It will not only increase confidence in the simulation of hempcrete but will increase the construction of high-performance buildings, more specifically, the buildings that are climate change resilient

(Hensen and Lamberts, 2011). The core of simulation experiment and physical experiment utilises the idea that the effect of a process in a system can be identified through manipulating the process and holding others as constant. And, quantifying the effect of the process, requires a point of reference as a control (Tomandl et al., 2015). Building simulation tools will be used to experimentally investigate hempcrete in this study through coupling simulation and multi objective optimisation as applicable.

2.5 MULTI OBJECTIVE OPTIMISATION

Investigating the appropriate specification of key parameters to be used for simulation of hempcrete is imperative in this study, and it involves using jEPlus+EA (jeplus, 2018) as the tool for multi objective optimisation to identify these parameters. Multi objective optimization involves more than one objective being optimized simultaneously for an optimization problem (NEOS, 2019). Optimizing building elements such as fabric design or optimizing building energy design, essentially means finding the values of some design variables, related to the building element characteristics, such as finding design variables related to the thermal characteristics of the material that minimize (or maximize) one or more objective functions as applicable (Sariyildiz, Bittermann and Ciftcioglu, 2015). Depending on the objectives, the optimisation procedure generally requires the specific exploration of a wide domain of considerable options (Augusto, Bennis and Caro, 2012). Multi objective genetic algorithm is a method which focuses on design objective functions to provide results as a constructive means to any building design (Sariyildiz, Bittermann and Ciftcioglu, 2015). Algorithms are finite processes that if followed will solve a problem, they are solutions (Mitchell, 1998). Also, genetic algorithms (single and multi-objective) are a class of algorithms that include objectives and fitness functions but are not necessarily related to building design. Genetic Algorithms are applied to many fields to study evolution and emergence, even outside of the Architecture, Engineering and Construction (AEC) industry (Li, Liu and Peng, 2020).

Deb et al. (2002) developed the non-sorting genetic algorithm (NSGA II) as the second version of the NSGA. Recently, the NSGA II has been increasingly used in research for efficiently optimizing design parameters (Deb et al., 2002). The parameter space contains the values of the design parameters, which forms a 'genetic string' analogous to DNA in a biological system. It uniquely represents each design option in the population (Chiandussi et. al., 2012). The

NSGA II method follows a sequence of generations, where the best design option in the population (i.e., those having low objective function values, in case of minimization) are considered to be the most successful and are allowed to survive and reproduce. The algorithm simulates the evolutionary process by employing the mathematical analogy of processes such as natural selection, breeding, and mutation (Mijwel, 2016). Mitchell (1998) explained genetic algorithms by combining the basics and implementation, in problem solving and scientific modelling. Both as computational models of natural systems and as algorithmic techniques for problem-solving (Mitchell, 1998).

The genetic algorithm established by Goldberg (1989) is an algorithm inspired by Darwin's theory of evolution, which states that the survival of species is influenced and maintained through reproduction, mutation and crossover. These have been developed using computational algorithm and applied towards finding solutions to problems in a natural way. It uses the computational genetic algorithm to perform optimization process, in order to get an optimal solution from a set of possible solutions as applicable. Technically, a representation generated through genetic algorithm is called a chromosome and a collection of these chromosomes represents a population. A gene is a constituent component that forms a chromosome and these genes could be a numeric, binary, symbol or a character value that depends on the problem to be solved, and generally correspond to a numerical value of a building design parameter, for instance air tightness. The chromosomes are therefore assembled from a representation of several building design parameters (genes), whose effect on building performance needs to be investigated. These chromosomes are evaluated through the success rate of finding solutions to the problem that needs to be solved (objective function). The process of chromosome selection is based on the previously mentioned concept of Darwin's evolutionary genetic algorithm, where the dominance of a chromosome value will increase the chances of the chromosome being selected (Mijwel, 2016).

The objective functions in this study is applied as root mean square error (RMSE) of air temperature and relative humidity between the measured and simulated performance of a hempcrete building. The simulated hempcrete building is represented with the simulation template from EnergyPlus, which is coupled as a parameter for optimisation and will contain search strings used as placeholders for inserting different numerical values of performance parameters, such as wall construction type etc. The optimisation focuses on design objectives to provide results, as the optimum means to identify appropriate design parameters for hempcrete simulation and building design. It explores potential hempcrete construction

composition, by replacing the search strings with numerical representations of different construction types. Evolutionary algorithms seem particularly suitable to solve multi-objective optimisation problems because they deal simultaneously with a set of possible solutions. This allows for a multitude of the Pareto optimal points resulting from a single run of the algorithm, instead of having to perform a series of separate runs as in the case of the traditional mathematical programming techniques (Coello, Veldhuizen and Lamont, 2013). However, the main disadvantage is the computational cost that is in general very high. This is due to the operational process of the method itself (Chiandussi et.al. 2012). More so, one significant advantage of multi objective optimisation with the genetic algorithm in this study, is its ability to solve multiple problems simultaneously as objectives and produce optimal solutions which efficiently saves time.

Torres-Rivas et al., (2018) conducted an investigative study on a bio-based thermal insulation material in building envelope, with multi objective optimisation to analyse condensation risks. The moisture transfer and the energy consumption for seven bio-based materials and polyurethane for a building-like cubicle were used. The performance was evaluated using EnergyPlus software for simulation and jEPlus for optimization, to model the cubicle and optimize its performance. The aim of their study was to optimise the insulation type and thickness, verifying the condensation risk and preventing the deterioration of the materials. From the study, hempcrete offered the most balanced solution with results showing how cost and environmental impact can be reduced if bio-based materials are used instead of conventional ones, in any climate (Torres-Rivas et al., 2018). The outcome of their study demonstrates the level of detailed information obtained from performing multi objective optimisation. It also highlights the general efficiency of hempcrete as a construction material. In this study, detailed information of heat and moisture transfer properties of hempcrete will be obtained from the optimal solution identified, from the multi objective optimisation performed.

Hamdy, Palonen and Hasan (2012) carried out a research for implementation of Pareto-archive NSGA II algorithm to a nearly zero energy building optimisation problem. The aim of their research was to test the NSGA II algorithm, rather than to answer particular questions about building design. The performance of three multi -objective elitist non-dominating sorting algorithms (original NSGA II, pNSGA II, and aNSGA) was tested for finding the optimal

solutions for a cost-optimal and nZEB design problem. The results indicated that aNSGA II (NSGA II with active archive) has a better repeatability in finding optimal solutions with high convergence than the original NSGA II with a passive archive strategy (pNSGA II). A main advantage of aNSGA-II is that, it produces high-quality solutions close to the true Pareto front using a low number of evaluations. On the other hand, with a larger number of evaluations, it is found that aNSGA-II achieved better convergence than the two other algorithms. These features of aNSGA-II were also confirmed when testing it with two benchmark test problems (ZDT2 and ZDT3) (Hamdy, Palonen and Hasan 2012). Based on their findings; simulation-based optimization can be effectively used to find solutions, as optimal solutions to problems. The multi objective optimisation in this study, is a combination of qualitative and quantitative data that yields an automated process. It is entirely based on numerical simulation and mathematical optimisation to identify the optimum construction component for hempcrete as a solution, for efficient design and construction of hempcrete buildings.

Gunantara (2018), conducted a review of multi-objective optimisation methods with its applications. The study established that, there are two methods of multi objective optimisation that do not require complicated mathematical equations; the Pareto and scalarization method. Based on the review, the Pareto method consists of a dominated solution and a non-dominated solution obtained by a continuously updated evolutionary algorithm. Whereas, the scalarization method creates multi-objective functions into a single solution using weights - there are three types of weights in scalarization which are equal weights, rank order centroid weights, and rank-sum weights. The solution using the Pareto method is a performance indicators component that forms multi objective optimisation separately and produces a compromise solution that can be displayed in the form of Pareto optimal front, while the solution using the scalarization method is a performance indicators component that forms a scalar function which is incorporated in the fitness function. From this review, it is evident that the Pareto method has the potential to produce viable and efficient results.

Nikjoofar and Zargami (2013) shared a view on the problems with multi objective optimisation, stating that the multi objective optimisation problems has more than one objective function. Even though there is a striking difference between single-objective and multi objective optimisation, they are solved as single-objective problems so that all of the objective functions are considered to find an optimised solution. They ascribed the technique to lack of appropriate method for solving these multi objective optimisation problems in

multiples. However, in multi objective optimisation, the objective functions and the usual decision variable spaces consists of multi-dimensional space and in single objective optimization, the decision to accept or reject the solution is based on the value of the objective function (Akbari, et al., 2014).

In building performance modelling, optimization has a different meaning to different researchers. For instance, it is either treated as a technique to find a global optimum to a defined problem through sensitive and qualitative analysis alone. Or it is performed by implementing a numerical simulation and mathematical optimisation to derive the optimal solution to an objective problem (Nguyen and Reiter, 2015). In this study, it is performed as a numerical simulation using mathematical optimisation to derive the optimal solution to multi objective problems as ‘simulation-based optimisation’. This is because the optimisation routine integrates EnergyPlus simulation model into the jEPlus optimisation as part of the parameters, to be executed as will be demonstrated in the next chapter.

Mitra & Gopinath (2004) conducted a research and explored on adapting NSGA-II for optimising the industrial grinding operation of a lead-zinc ore beneficiation. Part of the study considered two objective functions; maximizing grinding product throughout and maximizing percentage passing of midsize. Additionally, three process parameters were optimised, the solid ore flowrate, primary water flowrate and secondary water flowrate. They further compared the spread of Pareto front found from NSGA-II optimisation technique and SOOP (single objective optimisation problem) formulation for MOOP (Multi-objective optimisation problem) using weighted average approach / constraint-based approach. The study concluded that the quality of Pareto front by NSGA-II is better than the other techniques explored (Mitra & Gopinath, 2004).

Kodali et al. (2008) used NSGA-II to solve problems involving two objectives, four constraints and ten decision variables of the grinding machining operation. The Pareto-optimal front obtained was compared with earlier reported results of quadratic programming (QP), GA, PSO, scatter search (SS), ACO, differential evolution (DE), and it showed that NSGA-II outperformed others. Also, Jianling (2009) proposed an improved NSGA-II in order to deal with multiple constraints in milling operation. Minimal machining time and minimal elapsed tool life were considered, by extending the non-dominance concept to constraint space of NSGA-II. The optimization process become more approximate to application, more

economical and effective in searching the Pareto front. This previous research demonstrates the efficiency of multi objective optimisation with NSGA-II, in finding an optimum solution for a defined problem or set of defined problems. As it is in this study, the defined problem is simulation performance gap in hempcrete buildings, represented with root mean square as the objectives. It employs NSGA-II, in the background for multi objective optimisation to calculate the root mean square error as applicable. Multi objective optimisation is a technique observed to be efficient, substantial, and more likely to find the optimal or near-optimal design solution for a given set of problems (Chiandussi, 2012). The Postprocessing methods in optimisation such as the Pareto front, is mostly used to identify the optimal or near-optimal design solutions (Carlucci et. al., 2015). Building and energy efficient design optimisation for buildings, is evidently a technique actively being researched on. The technique focuses on optimisation algorithms to generate new points and ideas of designs, based on simulation results and the user-defined design objectives (Shi et al., 2016).

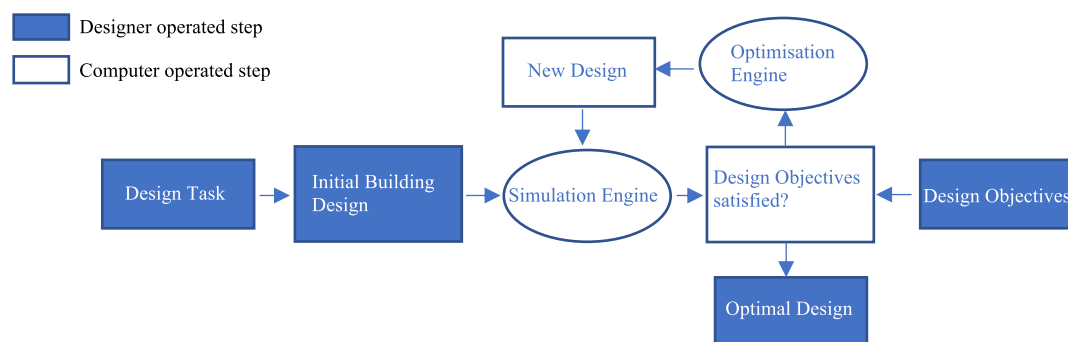


Figure 4: General Process of the building energy efficient design optimization (Chen et al., 2016).

As seen in Figure 3 above, building optimisation typically follow a similar general procedure of optimisation consisting of multiple steps. The design and optimisation process start with a design task which is based on an initial design, developed by the designer. The initial design is then imported into the simulation software /engine to calculate the building energy consumption or other energy related variables. The designer needs to define a single design objective or multiple design objectives. The computer compares the energy simulation results with the design objectives defined. If the design objectives are satisfied, the design process will be terminated, and the optimal design will be determined. Otherwise, the design process calls for the optimisation engine to generate a new design and the above steps are iterated. An emphasis is placed on the optimisation technique, through iteration while achieving the goal of energy efficient design optimisation, further addressing particular design needs (Chen et al.,

2016). This study uses EnergyPlus and jEPlus as the engines for conducting the simulation, optimisation and iterative optimisation to obtain the required optimum solution for accurate hempcrete construction.

Xu et al., (2018) carried out Optimization of Performance Parameter Design and Energy use Prediction for Nearly Zero Energy Buildings. The key performance parameters in the design were optimised based on nZEB energy requirements, and the building demonstrates a high thermal inertia, which further reduces the energy consumption induced by the requirement for heating in the climate. The research concluded by establishing that in the future, thermal comfort of the nZEBs will be considered for design, highlighting multi objective optimisation will be carried out for air temperature, mean radiant temperature, relative humidity, air velocity, dressing style, human activity. (Xu et al., (2018). The suggestion by Xu et al., indicates that multi objective optimisation is gaining momentum for enabling increased efficiency in most sectors of life. More importantly, obtaining the optimum hempcrete construction composition from this study will be an absolute transformation in the construction industry, giving confidence to designers when designing and constructing hempcrete buildings.

Bre et al. (2016) optimised three design variables type of external walls, windows infiltration rate, and solar azimuth for minimum energy consumption and thermal discomfort using Distributed Evolutionary Algorithms in Python (DEAP) and EnergyPlus. Delgarm et al. (2016) presented an EnergyPlus and MATLAB coupling-based multi objective optimisation method to optimize the following parameters for reducing building energy consumption and improving thermal comfort: building rotation, window length and height, glazing solar and visible transmittance, glazing conductivity, wall thermal absorptance, solar absorptance, visible absorptance, wall conductivity, and heating and cooling setpoint temperatures. Their case studies in four different climates resulted in improved thermal comfort levels and increased total energy consumption levels. In addition, the comparisons of single-objective and double-objective optimisation approaches clearly show that multi objective optimisation methods yield more appropriate results respect to the single ones. This is mainly because of the lower deviation index value from the ideal solution (Delgarm et al., 2016). This highlights the reliability and efficiency of multi objective optimisation in design decision making. Thus, using multi objective optimisation in this study to address the objectives towards reducing

simulation performance gap from hempcrete is efficient and capable of investigating the physics behaviour of hempcrete.

Polson et al., (2017) investigated into optimum design options for the early design stage of a reduced construction capital cost. The results from their research, show that the benefits of applying design optimisation to a project potentially outweighs the additional engineering design input required. Apparently, applying optimisation as a design tool is most beneficial during early design development stages where project specific objectives and constraints can inform design decisions and propagate through the design process. This is because the optimisation results successfully provided a solution with lower capital cost whilst sustaining a comparable energy performance against the base reference solution. The research further demonstrated that although an improved building fabric performance achieves minimum energy consumption, a more average building fabric can be more cost effective providing a similar saving in energy. The optimisation module enables the designer and user to run multiple combinations of design objectives as options that in common engineering practice, would be very time consuming and commercially unsustainable.

From this computational study, it can be deduced that an optimisation run is best performed at an early stage of the design process to influence the major parameters affecting energy efficiency and capital cost. The optimum solutions identified can then be further interrogated if they are feasible to be applied in the building design. This optimisation process offers greater assurance from early stage design that the best solution is implemented. Similarly, this research employs multi objective optimisation as a means to determine the construction component for hempcrete and hempcrete building fabric at an early stage of design for simulation. For example, a building is first designed before it is built (Dumas II, 2016). Identifying the accurate parameter for hempcrete design and construction, will be helpful towards creating an efficient hempcrete construction composition. To reduce simulation performance gap, from the early stage of a hempcrete building construction project, which is the design and simulation stage.

It could be argued that research on multi objective optimisation for public buildings has been relatively comprehensive. Negendahl (2015) proposed the office building performance optimisation design method, considering such factors as building energy use, capital cost, daylight distribution, and indoor thermal environments. In 2017, using school building in the cold zones of china as research subjects, Zhang et al., (2017) explored the use of simulation

based multi objective optimisation tools to balance multiple objectives, including minimal energy use for heating and lighting, minimal summer discomfort time, and maximal thermal and daylighting performance. For residential buildings, performance objectives have not been fully considered and mainly focus on certain aspects. Dubrow (2010) adopted the simulation optimisation tool coupled with genetic algorithm to minimize energy use and life cycle costs for residential buildings (Dubrow, 2010). Yassin et. al., (2017), focused on the energy consumption and daylighting optimisation of multi-storey residential buildings (Yassin et. al., 2017).

Many real-world problems, no matter whether they are in the domain of engineering, finance, business, or science, can be formulated into different forms of optimization problems. These problems are characterized by the requirement of finding the best possible solution that fulfils certain criteria under certain constraints (Leung and Lau, 2018). Most of the real-world optimization problems normally involve multiple objectives rather than one single objective, in which some objectives conflict with others. Solving this kind of problems is never an easy task because objectives of such problems are often found to be no commensurable and conflicting (Chang, 2015). Very often, there is no single best solution to the multi objectives optimization problems, but rather a set of optimal solutions that exists among the objectives. However, using simulation modelling alone cannot provide us with optimal solutions to these optimization problems. Therefore, an optimization algorithm is needed to guide the search process to the optimal solutions (Leung and Lau, 2018).

It is essential to study the optimisation of objectives related to building performance in the designing of residential buildings in severely cold regions, just as it is essential to study the same for severely hot regions (Han, Yu and Sun, 2017). A significant part of this study is focused on multi objective optimisation with jEPlus+EA using NSGA- II in the background. It uses the concept of Pareto approach for obtaining the optimum hempcrete component for simulation with increased confidence. Detailed simulations of heat and moisture transfer will be conducted, which will provide new information from optimisation results, aiding to improve the quality of reliability in designing and constructing with hempcrete. Since the results are climate-independent, it establishes the essence of the physics behaviour of this hempcrete material. The Pareto approach consists of finding many non-dominated solutions as possible and returning the set of these solutions to the user (Freitas, 2004). The basic idea of the Pareto approach is that, instead of transforming a multi-objective problem into a single-objective

problem and then solving it by using a single-objective search method, it uses a multi-objective evolutionary algorithm to solve the original multi-objective problems which makes it an efficient technique. The reason is, it adapts the algorithm to the problem being solved, rather than the other way around (Freitas, 2004). As deduced from the above literatures, an integral aspect of obtaining optimum solutions from performing multi objective optimisation, is linked with the defined objective functions. Similarly, the values of the objective functions in this study are assessed to achieve optimum outcomes for hempcrete building design. To this end, building thermal performance simulation tools, such as IES Virtual Environment is used to carry out dynamic simulation and EnergyPlus (EnergyPlus, 2016) is used for advanced simulation. Certainly, not all hempcrete design scenarios can be investigated by means of simulation and exhaustive solution search, because this would require prohibitive computational burden. However, the optimisation will be conducted to investigate a wide range of possibilities for accurate hempcrete properties.

2.6 COUPLING SIMULATION WITH MULTI OBJECTIVE OPTIMIZATION

Building performance simulation coupled with building performance optimization is an effective method for evaluating design options and obtaining the optimal design solutions for a given objective or set of objectives. Optimisation and simulation virtually push each other to run concurrently and find an acceptable solution which is considered the optimal solution (Bandara, 2012). The technique automatically conducts energy simulation and optimisation until the optimal solution is found based on the pre-defined design criteria. Technically, based on the original baseline model and proposed energy efficient measures, the optimisation engine is able to generate a new optimal design parameter. The energy simulation engine also calculates the energy performance of the new design, then the optimisation engine evaluates whether the pre-defined design criteria are met. However, if the design criteria are not met, the simulation and optimisation process will be reiterated until the design criteria are met, or until the optimal design has been achieved (Tian et. al., 2017). Coupling building energy simulation with optimisation follows a general workflow, as seen from Figure 5 below.

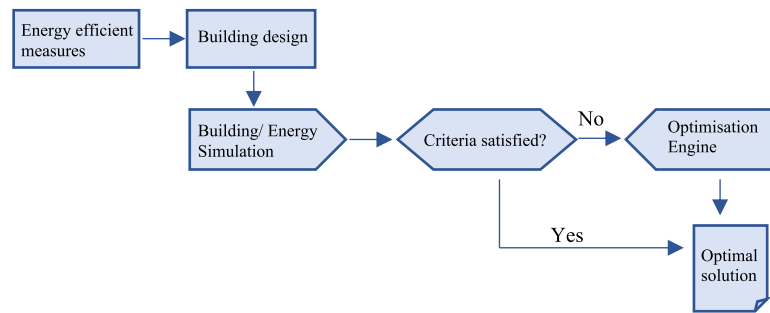


Figure 5: Basic workflow of coupling building energy with optimisation (Tian et. al., 2017).

Schwartz et. al., (2017) studied on Integrated Building Performance Optimisation: Coupling Parametric Thermal Simulation Optimisation and Generative Spatial Design Programming. The study investigated the potential of coupling computational design algorithm with a parametric simulation and genetic algorithm optimisation. The method explicitly demonstrated it can enable decision makers to explore a wide range of possible solutions while offering design teams an optimally efficient design. The outcome of the study is a set of early-stage results showing that the methodology of coupling thermal simulation is attainable. The study concluded by establishing that further work to implement this method for addressing complex optimisation problems such as building performance issues should be considered, including, geometrical arrangement on conflicting objective functions, energy performance and daylight factor, or for determining the more favourable solution when examining design options (Schwartz et. al., 2017).

Building design is quite a rigorous task, because buildings are complex systems with various antagonistic parameters to counterbalance, and in turn are subject to various constraints. Due to this complexity at various levels, performance simulation tools are employed, and as a consequence, optimization methods are further used, mainly as a decision aid (Seltman, 2018). In this study, using multi objective optimisation to reduce the simulation performance gap from hemcrete buildings, involves the coupling of simulation model into the optimization engine. The basic framework for the simulation based multi objective optimisation adopted, consists of two components; the simulation model and the multi objective optimisation algorithm. The problem to be optimised is the difference between monitored and simulated output, which is represented by a RMSE formula, specified in the optimisation algorithm. The simulation model template from EnergyPlus takes the inputs produced from the process workflow framework, such as the search strings. Based on these inputs, the simulation is then executed with the

various parameter settings as will be explained in the methodology chapter, in detail. Integrating the simulation model as a template for the optimisation parameters, aids in the decision making of specifying the appropriate specification and identifying the optimum design option for hempcrete simulation.

Optimizations apply mathematical techniques for modelling real-world problems and to solve problems based on specific objectives to produce actionable recommendations (Kibira et. al., 2015). Building Energy Simulation and Optimization is an innovative technique which helps to identify the needs, benefits, and hindrances of applying sustainable building design. Recent progress in computer science and stringent requirements of “sustainable” building designs, puts forward the research and applications of simulation-based optimization methods in the building and construction sector (Si et al., 2018). Brady and Yelling (2005) proposed two approaches for integrating simulation with optimization. The first one, is to construct an external optimization framework around the simulation model. The second one, is an internal approach to investigate the relationships and interactions among system variables within the simulation model, so that the tracking features within the tools can be used for the purpose. The latter approach is the technique used in this study, because EnergyPlus is used to further investigate the experimental simulation output IES Virtual Environment. This is after it has been transferred into input data file (.idf) format for advanced building simulation into the heat and moisture transfer properties of the hempcrete material. It will then be coupled in jEPlus alongside the weather file, report variable input (rvi) file, and search strings as the parameters necessary for running an optimisation in jEPlus. EnergyPlus, is an Energy simulation software accounting for the whole building energy parameters as an input, driving more focused integrated system design.

In a study on Coupling of whole-building energy simulation and multi-dimensional numerical optimization for minimizing the life cycle costs of office buildings, Karaguzel, Zhang and Poh Lam (2013) researched on the minimization of life cycle costs for building materials and operational energy consumption of a reference commercial office building. The model is achieved through the optimization of envelope design parameters by the use of integrated energy simulation and multi-dimensional numerical optimization techniques. This algorithm resulted in a 36.2% reduction in the computational effort to converge to the global minimum point with a very high degree of accuracy compared to the full enumeration technique. The

results further indicate that the annual total site energy consumption of the optimized building model is reduced by 33.3% with respect to the initial baseline case. The optimized envelope parameters yielded 28.7% life cycle cost reduction over a 25 years life span with a simple pay-back period of 4.2 years (Karaguzel, Zhang and Poh Lam, 2013). It is evident from the research carried out by Karaguzel, Zhang and Poh Lam (2013) that coupling of simulation and optimization is an efficient way of achieving sustainable results. While the study focuses on minimizing life cycle cost of a building, it emphasizes coupling simulation and optimization to enhance efficiency in design.

Recent progress in computer science and stringent requirements of the design of “greener” buildings puts forward the research and applications of simulation-based optimisation methods in the building sector. Ammeri, (2014) describes the development of a process simulation model and integration of the genetic algorithms with the model as optimisation techniques, using a case study of lot sizing problem in make-to-order (MTO) supply chain solved by a combined simulation and genetic algorithm optimisation model. The simulation model is performed using ARENA software. Genetic algorithms were implemented into the model using visual basic for application (VBA) language because it ensures exchanges between ARENA software and MS Excel. The case study’s objective was to determine the optimal solution to further find out the fixed lot size for each manufacturing product type that will ensure order in mean flow time target. The comparative results with Opt Quest software, which is used as a global search method, illustrate the efficiency and effectiveness of the proposed approach (Ammeri et. al., 2014).

Delgarm et. al., (2016) offered an efficient methodology for simulation-based multi-objective optimization problems, which addresses important limitations for the optimization of building energy performance. In the study, a mono and multi-objective particle swarm optimization algorithm was coupled with EnergyPlus building energy simulation software, to find a set of non-dominated solutions to enhance the building energy performance. The optimisation involved, mono-criterion and multi-criteria optimization analyses of the annual cooling, heating, and lighting electricity consumption. They were examined to understand interactions between the objective functions, and to minimize the annual total building energy demand. The achieved optimum solutions from the multi-objective optimisation process were realised as Pareto optimal fronts. The results of the multi-criteria minimization were compared with the non-criterion ones. The proposed optimization method shows a powerful and useful tool that

can save time while searching for the optimal solutions with conflicting objective functions. thereby, facilitating decision making in early phases of a building design in order to enhance its energy efficiency (Delgarm et. al., 2016).

Nguyen, Reiter and Rigo, (2014) provide an overview on applications of simulation-based optimisation methods, with the aim of clarifying recent advances and outlining potential challenges and obstacles in building design optimisation. They focused on handling discontinuous multi-modal building optimisation problems, including the performance and selection of optimisation algorithms, multi-objective optimisation, the application of surrogate models, optimisation under uncertainty and the propagation of optimisation techniques into real-world design challenges. The review indicates that future researches should be oriented towards improving the efficiency of search techniques and approximation methods (surrogate models) for large-scale building optimisation problems; and reducing time and effort for such activities. Further effort is also required to quantify the robustness in optimal solutions so as to improve building performance stability (Nguyen, Reiter and Rigo, 2014). The technique of coupling simulation and optimization is developed and applied to optimize building shape and building envelope features in a research study Dubrow and Krarti, (2010). The simulation–optimization tool couples a genetic algorithm to a building energy simulation engine to select optimal values of a comprehensive list of parameters associated with the envelope to minimize energy use for residential buildings. Different building shapes were investigated as part of the envelope optimization, including rectangle, L, T, cross, U, H, and trapezoid. However, building envelope features were considered in the optimization analysis including wall and roof constructions, foundation types, insulation levels, and window types and areas. The results of the optimization indicate rectangular and trapezoidal shaped buildings consistently have the best performance in terms of lowest life-cycle cost, across five different climates. It was also found that rectangle and trapezoid exhibit the least variability from best to worst within the shape (Dubrow and Krarti, 2010). Potentially, this level of detailed information will be obtained as optimum results from coupling simulation and multi objective optimisation in this study, for solving the defined problem as applicable.

Additionally, Gossard, Lartigue and Thellier, (2013) presented a method of coupling simulation with optimisation to optimise the equivalent thermophysical properties of the external walls (thermal conductivity and volumetric specific heat capacity) of a dwelling in

order to improve its thermal efficiency. This is because classical optimisation involves several dynamic yearly thermal simulations, which will be time consuming. To reduce the computational requirements, they adopted a methodology that coupled an artificial neural network and the genetic algorithm NSGA-II. The energy performance of the dwelling was characterised with two criteria, which were the optimisation objectives: the annual energy consumption QTOT and the summer comfort degree issue. The optimal solutions were compared to those from mono-objective optimization by using an aggregative method and a constraint problem in GenOpt. The comparison clearly showed the importance of performing multi objective optimization, because the results from multi objective optimisation was more efficient, especially as it was coupled with simulation, which increased the results efficiency (Gossard, Lartigue and Thellier, 2013). Several conflicting criteria exist in building design optimisation, especially energy consumption and thermal performance of indoor environment. Yu et. al., (2015) presented a novel multi-objective optimisation model that could assist designers in sustainable building design. They incorporated the Pareto solution to obtain a set of optimal solutions for building design with an improved multi-objective genetic algorithm (NSGA-II) as a theoretical basis for the building design. Based on the simulation data on energy consumption and indoor thermal comfort, their study also used a simulation-based improved back-propagation (BP) network which is optimized by a genetic algorithm (GA) to characterize building behaviour, and to establish a GA–BP network model for rapidly predicting the energy consumption and indoor thermal comfort status of residential buildings; Third, the building design multi objective optimization model was established by using the GA–BP network as a fitness function of the multi-objective Genetic Algorithm (NSGA-II). Finally, a case study was presented with the aid of the multi-objective approach in which dozens of potential designs are revealed for a typical building design in China, with a wide range of trade-offs between thermal comfort and energy consumption (Yu et. Al., 2015).

Similarly, Tian et. al., (2017) conducted a study towards the adoption of building energy simulation and optimisation for passive building design. The study involved a survey and a review to identify the needs, benefits, and hindrances of applying simulation and optimisation to sustainable passive building design. A two-part survey was carried out, and a significant amount of attention was dedicated to analysing the opinions of the early adopters. Out of nine potential hindrances of the simulation and optimisation technique; long calculation time, lack of adequate advertisement, and lack of a standard method or procedure were the most

identified. Simulation and optimisation coupling technique was then applied to investigate the passive building design components which covered building forms, opaque envelopes, fenestrations, shadings, natural ventilation, and thermal mass materials. It was realised from the review that the three-phase optimization method was the most widely used method. Currently, compared to other passive design methods, building energy simulation and optimisation proved to be a more efficient method for helping professionals in the construction industry especially architects, to design and explore various design territories where applicable (Tian et. al., 2017).

Furthermore, Bana and Jankovic (2019) conducted an experimental study to reduce simulation performance gap from hempcrete using multi objective optimisation. The study used IES Virtual for simulation experiments and integrated the experimental simulation model as a template for multi objective optimisation in jEPlus+EA. The study experimented using cast concrete and a created hempcrete material for simulation experiments and also used hempcrete with different thickness for the simulation experiments. Results of the experimental simulations from the RMSE calculation of the simulation outputs show that, the simulation model where hempcrete was used had the lowest root mean square error. However, the results were not as expected, which highlights energy efficiency and high thermal performance of hempcrete in real life construction projects. More so, the method proved to be efficient and provided a baseline method for reducing simulation performance gap using simulation coupled with multi objective optimisation. The study concluded by stating that, further work is required to actually reduce the performance gap from hempcrete using multi objective optimisation. It also suggests that the properties of the hempcrete material itself needs to be investigated to analyse the heat and moisture transfer properties within the material. Including the adequate material thickness and other properties, to demonstrate how it can be represented in simulation tools. Hence, this study will further conduct experimental simulations as applicable.

From the literature reviewed so far in this study; climate change is obviously a threatening issue in the built environment especially to every living thing. When there is an unfavourable weather condition, buildings serve as shelter. Also, buildings have been responsible for contributing to climate change by increasing carbon emissions into the atmosphere through the building material manufacturing stages, buildings and construction stages, as well as the operational stages. The panacea is constructing buildings with highly sustainable and natural

building materials. Hempcrete as a construction material is environmentally friendly and capable of providing a sustainable solution towards combating the effects of climate change in the built environment because of its carbon sequestration qualities. However, using hempcrete for construction will involve designing and simulation of the building before construction.

Literature demonstrates how hempcrete contains excellent thermal properties suited for constructing sustainable buildings. Including how it is advantageous to the inhabitants of the buildings, as well as to the built environment. In the same vein, hempcrete possess its drawbacks as a sustainable construction material, especially with its mechanical properties when simulated for design and construction. Evidently, the drawbacks have challenged the accurate simulation of hempcrete and reduced the confidence in simulation results of hempcrete due to the performance gap. This performance gap is a challenge posing a barrier in adequate construction of hempcrete buildings by affecting the accuracy in its design and simulation. The energy performance in buildings is a complex function of the building form and structure, systems (heating and cooling), occupancy pattern, operating schedules, internal environmental conditions and the building's external climatic conditions. Simulations help in analysing and establishing the dynamic interactions of these parameters in a building. Therefore, accurate representation of building parameters during simulation is important for detailed simulation process with a realistic and reliable output for increased thermal efficiency in buildings and the built environment.

These have informed a pathway for this study, requiring a focus on detailed parametric simulations to enable investigation into the heat and moisture transfer of this hempcrete material. These also necessitates the utilisation of some construction methods to be integrated in the investigation process, such as wall thickness as experiment scenarios for hempcrete wall. The experiments will also be performed, with other natural building materials, conventional building materials and other composite wall systems created to replace hempcrete for simulation. Given the objectives of this study, measured data will be used from two monitored hempcrete buildings. The monitored buildings will be modelled and simulated to collect the simulation output, which will then be calibrated with reference to the measured data with an aim of reducing the performance gap.

Additionally, from the above literature, multi objective optimisation evidently has the potential to efficiently investigate the appropriate parameter sets for hempcrete simulation while reducing the simulation performance gap. The technical complexity of coupling simulation with multi objective

optimisation has also been acknowledged. This technique of coupling multi objective optimisation and simulation will also be employed and explained in the next chapter and subsequently, through the research process. including how it is used to achieve the optimal solution towards achieving the overall aim of this study, specifically, to identify the appropriate specification of key parameters to reduce performance gap and facilitate hempcrete simulation. For this simulation based multi objective optimization study, Root Mean Square Error is used as a performance metric to examine the quality of the set of solutions based on optimality as applicable. As mentioned earlier, experimental research will be used and potential hempcrete simulation parameters will be applied using search strings in the multi objective optimisation as will be explained in the next chapter.

CHAPTER THREE

METHODOLOGY

Chapter three is the methodology chapter of this research study. Section 3.1 explains the research method adopted to carry out this study as experimental research with quantitative analysis. Section 3.2 explains the data used to carry out this study. Section 3.3 is the experimental research simulation section, which elaborates on the type of experiments conducted as simulation experiments. Section 3.3.1 is the reasoning section and it explains the thought process of the research study. Section 3.3.2 explains the simulation experiments carried out in IES Virtual Environment. Section 3.3.3 explains the calibration of experimental simulation outputs and Section 3.3.4 explains the EnergyPlus heat and moisture transfer simulation. Section 3.3.5 explains the multi objective optimisation carried out in jEPlus+EA. Section 3.4 explains the quantitative analysis process carried out and Section 3.5 explains the validation of the research method and confirmation of results as applicable.

3.1 RESEARCH METHODOLOGY

Given the aim of this research identified in section 1.5 of Chapter 1, the methodologies considered to conduct this study are mixed research methodology and quantitative research methodology. Qualitative research methodology was not considered to be feasible for carrying out this study, because it involves collecting and analysing non-numerical data (e.g., text, video, or audio) (Mack et al., 2005). It is also subjective, centred around quality of data and focused on understanding concepts, opinions, and experiences (Austin and Sutton, 2014). The obtained data for this research is numerical and requires building simulation and statistical analysis. The research questions in this study as explained in section 1.4 of chapter 1, require detailed building performance simulation with the numerical data obtained from the monitored hempcrete buildings. Hence, qualitative research methodology does not provide the ample opportunity to achieve the aim of this study or answer the research questions as applicable.

The rationale for considering mixed research and quantitative research methodologies for this study, is as explained below:

1. Mixed research methodology integrates qualitative and quantitative research to efficiently solve research problems (Almalki, 2016; Wisdom and Creswell, 2013). Mixed research methodology is feasible when neither quantitative nor qualitative

method is sufficient by itself for a particular study (Plano, Clark and Creswell, 2008). It involves collecting, analysing, and “mixing” both quantitative and qualitative data within a single study. The mixing could be concurrently or sequentially, with an aim to gain a better understanding of the research problem (Creswell, 2009; Tashakkori and Teddlie 2003). Quantitative data is hard data in numbers and figures. It consists of values that can be measured objectively and analysed mathematically, such as height, width, length, temperature, humidity, area and volume (Seltman, 2018; Afonja, 2001; Anyanwu, 2002). It is usually subjected to statistical procedures, such as calculating the mean or average number of times an event or behaviour occurs (per day, month, year). For instance, the quantitative data obtained for this research is the monitored air temperature and relative humidity values from hempcrete buildings. Since numbers are “hard data” and not interpretation, they can give definitive, or nearly definitive answers to different questions (Seltman, 2018). Whereas, qualitative data is soft data mainly in words, sounds or Images. It deals with characteristics and descriptors that can't be easily measured, but can be observed subjectively—such as smells, tastes, textures, attractiveness, and colour (Ratner, 2002). The qualitative data obtained for this research includes pictures, alongside construction information of the hempcrete buildings.

Essentially, mixed research method has the potential to produce answers to research questions with evidence, because qualitative data supports the quantitative data analysis results and vice-versa (Daniel, 2016). The reason for considering mixed research method as a potential methodology for conducting this study, is because of the obtained data. While the monitored values are quantitative, the pictures are qualitative, and the construction information are a mixture of hard and soft data. Having considered the overall aim of this study, it is evident that the picture of the monitored hempcrete building and material names obtained as part of data to be used for this study are not substantial qualitative data for mixed research methodology. This is because the construction information obtained are a mixture of values and material names. Hence, mixed research methodology is not feasible to successfully achieve the aim and answer the research questions required to conduct this study.

2. Quantitative methodology quantifies the research problem. It is the process of objectively collecting and analysing numerical data to describe, predict and control variables for a research (Apuke, 2017). Quantitative research seeks to determine relationship between an independent variable and a dependent variable, to test causal relationships between variables within a population (Adedoyin, 2020). It is empirical in nature and involves a systematic investigation based on precise measurement, replicable, controlled and used to predict events (Goundar, 2012). Quantitative research deals in an objective stance, which is focused on the generation of ideas towards solving the research problem in a free-flowing manner, giving room for investigation and systemic data manipulation (MacDonald and Headlam, 2019). It is inherently concerned with allowing flexibility in the treatment of data while determining the truth-value of propositions (Goundar, 2012). In quantitative research, reliability and validity are determined more objectively. This is because comparative analysis and statistical analysis are allowed in order to verify reliability as applicable (MacDonald and Headlam, 2019). The types of quantitative research designs explored to conduct this study are descriptive research design, correlational research and experimental research design.
 - a. Descriptive research uses quantifiable information for statistical analysis of variables or a population sample (Haradhan, 2020). It is a type of quantitative research that describes a population, situation, or phenomenon being studied and it is characterised as the attempt to describe, determine or identify what is (Kabir, 2016). Descriptive research design was considered for this study because it allows for comparative analysis, which seemed suitable for comparing the monitored and simulated hempcrete data respectively. It investigates the characteristics of a variable and identify problems that exist within a unit, an organization, or a population (Stangor and Wallings, 2014). The purpose of descriptive studies is to describe individuals, events, or conditions by studying them as they are (Houser, 2008). It focuses more on exploring variables, where the researcher does not manipulate any of the variables but rather, only describe the variables (Stangor and Wallings, 2014). Saunders et al. and Miller explain descriptive research as an accurate technique for detailed explanation of a phenomena (Jilcha and Sileyew, 2019; Saunders et al., 2009). The descriptive research does not control or

manipulate any of the variables, but observes, measures and describe them as they are because it is not open to change behaviour or conditions of any phenomena (Bhattacharjee, 2012; Ethridge 2004). Although a descriptive study explores multiple variables, it is the only design that can also explore a single variable (Stangor and Wallings, 2014). It offers an opportunity for detailed explanation of the research data and can describe the building physics of hempcrete buildings to investigate what performance gap is. However, descriptive research was considered not suitable for conducting this study, because it does not provide substantial opportunity to investigate the reduction of simulation performance gap in hempcrete, to adequately achieve this research aim. The research questions and research aim require an in-depth investigation of the obtained monitored data to reduce the simulation performance gap which descriptive method does not provide.

- b. Correlational research design is a type of quantitative research in which the statistical relationship between two or more variables are measured and assessed with little or no effort to control extraneous variables (Kabir, 2016). It involves observing two variables in order to establish a statistically corresponding relationship between them. Correlational research aims to identify variables that have some sort of relationship where a change in one, creates some change in the other variable (Howe, 2016). The relationships are assessed without manipulating independent variables or assigning participants to different conditions (Manca, 2018). This means that correlational research has the potential to assess the relationship between the monitored hempcrete data as the independent variable and the simulated data as the dependent variable. However, it does not have the capacity to allow for rigorous investigation into reducing the simulation performance gap which is the aim of this study. This is because the defining feature of correlational research is that the two variables are measured and neither one is manipulated, regardless of whether the variables are quantitative or categorical (Pace, 2019). Therefore, correlational research methodology was considered not viable to effectively conduct this study. More so, it is perceived not ideal for a statistical research focused on causal investigation and cannot be used to draw inferences about the causal relationships between and among the variables as applicable (Pace, 2019; Johnson 2000).

- c. Experimental research design is undertaken to determine cause-effect relationships between defined variables. Experiments have been established as a valid approach for obtaining information about causal relationships, allowing researchers to assess the relationship between one variable and another (Robson, 1993). A principal factor of this design is that, one element is manipulated by the researcher to see whether it has any impact on the other variable (Chiang, Jhangiani and Price, 2015). Experimental research is the process of conducting research that is highly based on causal validity. Causal validity in experimental research is concerned with theories and accuracy of cause-effect relationships (Lazar, Feng and Hochheiser, 2017). This study focuses on cause-effect relationship of hempcrete's performance gap by examining the behaviour of real life hempcrete buildings and the cause of the simulation performance gap. The reason why experimental research was considered viable for conducting this study is because experimental research allows for detailed investigation without much limitation (Winsberg, 2019). Since experimental research allows for data manipulation and discovering causal relationships among variables, it has the potential to logically and unambiguously address the simulation performance gap issue in this study. Experimenters try to control all variables except the one being manipulated, which is the independent variable. The effects of the independent variable on the dependent variable are then collected and analysed for a subjective relationship, as applicable (Tierney, 2008). For instance, in this study, the obtained monitored air temperature and relative humidity values from the experimental hempcrete buildings are the independent variables. While the air temperature and relative humidity outputs from the simulation experiments are the dependent variables. These simulation outputs as the dependent variables, will be statistically analysed through investigating the effect of the monitored values (independent variable) on the simulated values (dependent variable). Therefore, experimental research can be explored effectively, to address the research problem and reduce simulation performance gap towards achieving the research aim in this study as applicable.

Due to the complexity of real-world problems and the limitations of human intelligence models, simulation is able to provide a virtual world. A virtual world where the decision makers can better understand the nature of the problem, by conducting experiments in a more controllable and low-cost environment (Wang and Halpin, 2004). In this study, computer experiments are carried out through performing series of simulations such as

experimenting with different construction materials to represent hempcrete. These different construction materials are a combination of high density and low-density materials as well as high conductivity and low conductivity materials. Also, another experiment of creating a material within simulation tools to be called hempcrete will be performed. Subsequently, the heat and moisture transfer simulation will be conducted in EnergyPlus (energyplus.net) to develop the model and reveal the underlying physics of hempcrete as well as the phenomenon surrounding the performance gap. Korb and Mascaro (2010), believed that computer simulation shares epistemology with physical experiments, so they critically studied the philosophy of computer simulation for experiments. They arrived at a conclusion that experimentation with computer simulations does not just share epistemology with physical experiment, it is “full-blooded” experiment (Korb and Mascaro, 2010). Every experiment has specific problems or objectives that require the experiment to be conducted in the first place. In both physical experiments and computer experiments, there is always a relationship between what is manipulated during the investigation on the one hand, and the real-world systems that are the targets of the investigation on the other (Kalua and Jones, 2020; Winsberg, 2019).

In order to adequately conduct this research, simulation tools such as IES virtual environment (IESVE, 2018), EnergyPlus (EnergyPlus, 2016) and jEPlus+EA (jEPlus, 2018) will be used to model hempcrete buildings and carry out simulation experiments. The experimental research integrates secondary method of data collection with quantitative analysis to answer the research questions, achieve the aim as well as address the objectives of this study, respectively. The research objectives are as listed in Chapter 1, Section 1.5 and explained in Chapter 1, Section 1.6. The experiments carried out in this study, utilise some core construction techniques explored for the simulation, while investigating into the heat and moisture transfer of hempcrete as a construction material. The calibration of the experiments output is meticulously designed to effectively facilitate the reduction of simulation performance gap, by calculating root mean square error between the monitored data and simulation output. Identifying of the accurate construction component to represent hempcrete for simulation will be carried out with jEPlus+EA optimisation tool. It will further include the integration of Python 3 script and Pandas library for the multi objective optimisation. The flow chart of the experimental research methodology used in this study is shown below is Figure 6.

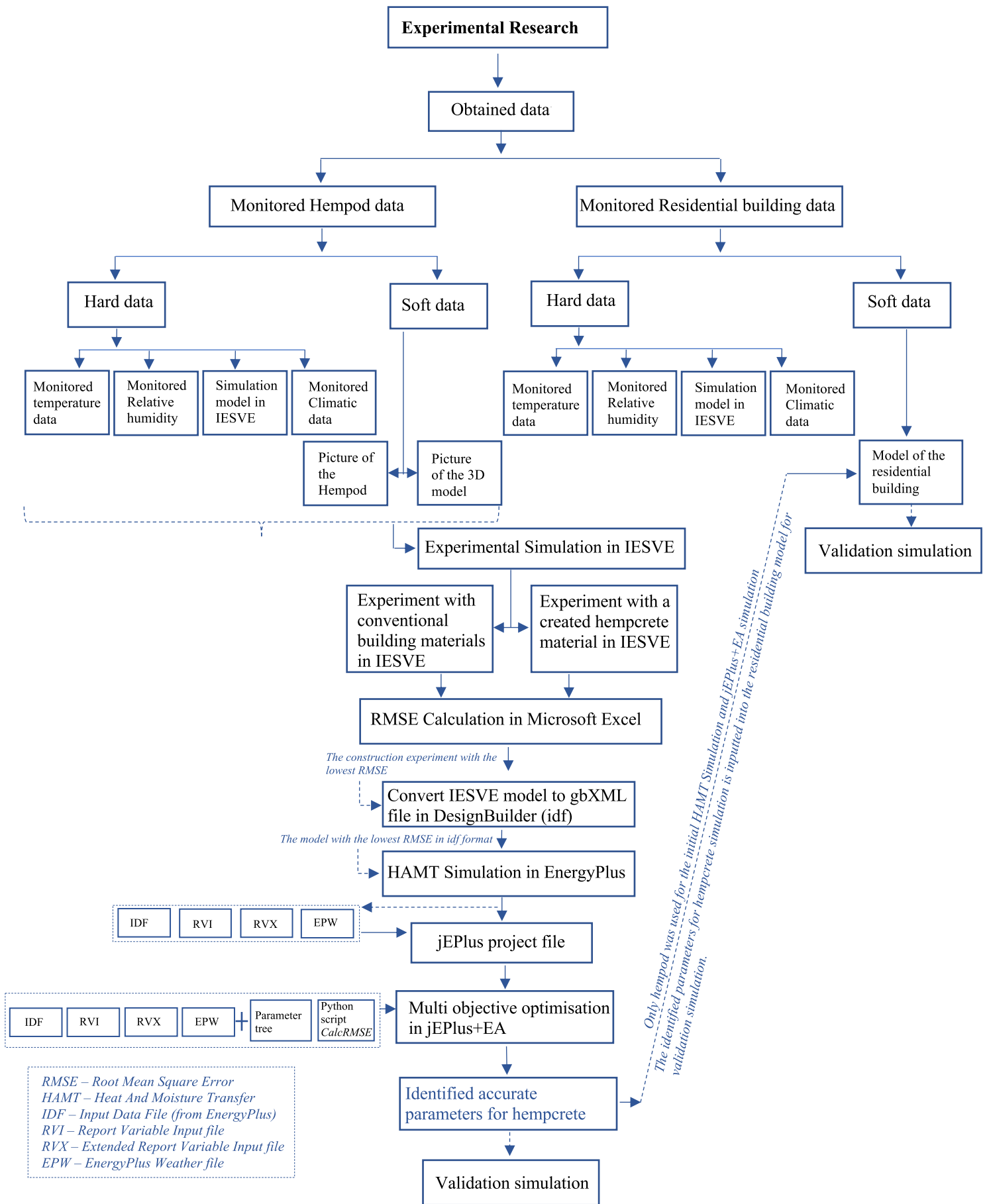


Figure 6; Flow chart of the experimental research methodology

3.2 DATA USED IN THE STUDY

This study uses secondary method of data collection, with monitored air temperature and relative humidity values of hempcrete buildings obtained from Zero Carbon Lab. The details of the obtained monitored data are as explained below:

- I. Hempod (An experimental building) - The monitored data for Hempod was obtained from Zero Carbon Lab. Hempod is a test cell/experimental building developed for experiments and research, in collaboration with University of Bath, it was constructed with hempcrete. The collected data was obtained from monitoring internal air temperature, relative humidity and other variables on hourly intervals for a period of three weeks (12th March – 05th April). The monitoring data was obtained as values in Microsoft excel (.csv) format. The dimensions of Hempod are 5.2m by 4.0m with its headroom as 2.7m high, and a mono-pitched roof. It also contains a north-facing window 1.1m wide and 1.3m high, a south facing door 0.9m wide and two south facing windows 0.6m wide and 2.25m high as seen from the image in Figure 6 below. The IES Virtual Environment model as seen from Figure 8 below, was obtained with the monitored data, including an image of the Hempod as seen in Figure 7 below.



Figure 7: Hempod.

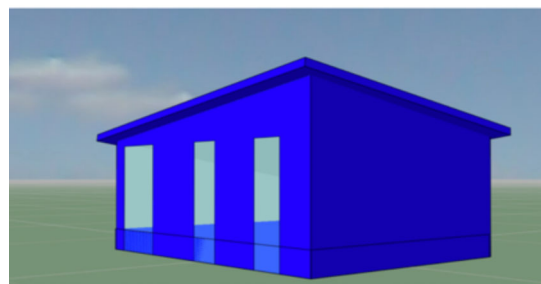


Figure 8: Hempod 3D Geometry.

The construction information for Hempod is as summarised in table 1, 2 and 3 below.

Table 1: Hempod wall construction.

Material (inner to outer layers)	Thickness (mm)	Conductivity W/(m2k)	Density (Kg/m3)	Specific heat Capacity J/(kg2k)	Resistance m2K/W
External Rendering	9.0	0.5000	1300.0	1000.0	0.0180
Hempcrete	200.0	0.0500	275.0	1750.0	4.0000
Gypsum Plastering	12.5	0.4200	1200.0	837.0	0.0214

Table 2: Hempod Floor construction.

Material (inner to outer layers)	Thickness (mm)	Conductivity W/(m2k)	Density (Kg/m3)	Specific heat Capacity J/(kg2k)	Resistance m2K/W
Chipboard floor	20.0	0.13	500.0	1600.0	0.1538
Cavity	50.0				
Insulation	150.0	0.025	700.0	1000.0	4.0000
Cast concrete	100.0	2.300	2300.0	1000.0	0.0326

Table 3: Hempod roof construction.

Material (inner to outer layers)	Thickness (mm)	Conductivity W/(m2k)	Density (Kg/m3)	Specific heat Capacity J/(kg2k)	Resistance m2K/W
Ceiling board	9.0	0.2100	700.0	1000.0	0.0595
Cavity	50.0				
Concrete deck	100.0	2.0000	2400.0	1000.0	0.0500
Felt Bitumen Layer	0.1	0.5000	1300.0	1000.0	0.0002
Roof covering	0.20	0.5000	1300.0	1000.0	0.0180
Insulation	150.0	0.0300	40.0	1450.0	5.1467

II. A Residential building – The residential terraced building, is a house constructed with hempcrete, located in Norfolk, UK. The monitored data was obtained from Zero Carbon Lab as part of the monitoring and co-heating test conducted by Jankovic (2016). The house consists of two floors (ground floor and first floor). The ground floor contains living room, kitchen, store, WC, two stores and a hallway. The first floor contains two bedrooms, store, stairs and landing. The collected data is from the monitoring of air temperature and relative humidity in the living room, bedroom and kitchen in the house, obtained in one-hour intervals, for a period of one year. The monitoring data was obtained as values in Microsoft excel (.csv) format. The IES Virtual Environment model as seen below in Figure 9, was also obtained alongside the monitored data from the same source. The Living room is 16.5m², the Kitchen is 9.45m², the ground floor WC is 3.60m², the ground floor store (1) is 1.1m², ground floor store (2) is 1.54m², first floor bedroom (1) is 16.5m², first floor bedroom (2) is 10.6m², first floor store is 1.32m², first floor bathroom is 6.2m² and the roof is 44.6m².

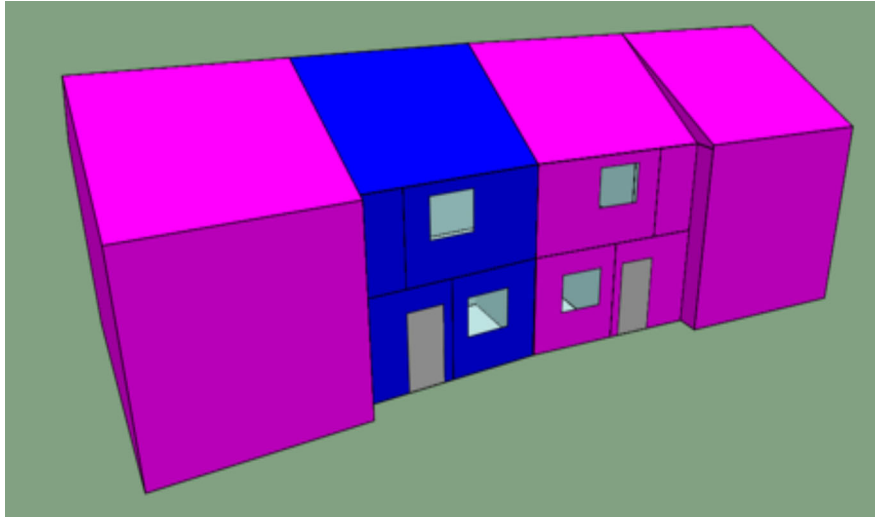


Figure 9: IES Virtual Environment, 3D Geometry of the residential building

The construction information for the residential building is as seen in table 4, 5 and 6 below.

Table 4: Wall construction of the residential building

Material (inner to outer layers)	Thickness (mm)	Conductivity W/(m2k)	Density (Kg/m3)	Specific heat Capacity J/(kg2k)	Resistance m2K/W
External Rendering	25.0	0.5000	1300.0	1000.0	0.0500
Hempcrete	250.0	0.0500	275.0	1750.0	5.0000
Gypsum Plastering	15.0	0.4200	1200.0	837.0	0.0357

Table 5: Floor construction of the residential building

Material (inner to outer layers)	Thickness (mm)	Conductivity W/(m2k)	Density (Kg/m3)	Specific heat Capacity J/(kg2k)	Resistance m2K/W
Cast concrete	100.0	1.1300	2000.0	1000.0	0.0885
Dense EPS slab insulation	200.0	0.0250	30.0	1400.0	8.0000
Timber flooring	50.0	0.1400	650.0	1200.0	0.3571

Table 6: Roof construction of the residential building

Material (inner to outer layers)	Thickness (mm)	Conductivity W/(m2k)	Density (Kg/m3)	Specific heat Capacity J/(kg2k)	Resistance m2K/W
Roofing tiles	5.0	0.8400	1900.0	800.0	0.0060
Felt/Bitumen layers	5.0	0.5000	1700.0	1000.0	0.0100
Wood blocks	150.0	0.1400	650.0	1200.0	1.0714
Glass fibre quilt	200.0	0.0400	12.0	840.0	5.0000
Cavity	50.0				
Ceiling tiles	10.0	0.0560	380.0	1000.0	0.1786

In particular case of the residential data, it was used to reduce performance gap from hemp-lime buildings outside of simulation tools (Jankovic, 2016), while this research focuses on reducing simulation performance gap from hempcrete buildings within simulation tools. The outcome from reducing the simulation performance gap from hempcrete in this study, aims to produce accurate representation of hempcrete material within simulation tools. And, facilitate a wider use of hempcrete for building design and construction through increased confidence in simulation.

3.3 EXPERIMENTAL SIMULATION

Experiments have been established as a valid approach for obtaining information about causal relationships, allowing researchers to assess the relationship between one variable and another (Robson, 1993). A principal factor of this design is that, one element is manipulated by the researcher to see whether it has any impact on the other variable (Chiang, Jhangiani and Price, 2015). Experimenters try to control all variables except the one being manipulated, which is the independent variable. And the effects of the independent variable on the dependent variable are then collected and analyzed for a subjective relationship, as applicable (Tierney, 2008). For instance, in this study, the obtained monitored air temperature and relative humidity values from the experimental hempcrete buildings are the independent variables, while the air temperature and relative humidity outputs from the simulation experiments are the dependent variables. These simulation outputs as the dependent variables will be statistically analyzed through investigating the effect of the monitored values (independent variable) on the simulated values (dependent variable), towards reducing the simulation performance gap.

In this study, computer experiments are carried out through performing series of simulations such as experimenting with different construction materials to represent hempcrete. These different construction materials are a combination of high density and low-density materials as well as high conductivity and low conductivity materials. Also, another experiment of creating a material within simulation tools to be called hempcrete will be performed. Subsequently, the heat and moisture transfer simulation will be conducted in EnergyPlus (energyplus.net) to develop the model and reveal the underlying physics of hempcrete as well as the phenomenon surrounding the performance gap.

Korb and Mascaro (2010), believed that computer simulation shares epistemology with physical experiments, so they critically studied the philosophy of computer simulation for experiments. They arrived at a conclusion that experimentation with computer simulations does not just share epistemology with physical experiment, it is full-blooded experiment. According to them, “The epistemology of computer simulation is the same as the epistemology of experimentation for the simple reason that all experiments are simulations and computer simulation experiments are just a special type” (Korb and Mascaro, 2010). For example, computer experiments carry problems, techniques and methods, such as debugging and calibration which is similar to physical experiments. Similarly, physical experiments use different types and sizes of apparatus with techniques and methods for the experiment, so also simulation experiment use different types of software (Duran, 2019; Korb and Mascaro, 2010). Every experiment has specific problems or objectives that require the experiment to be conducted in the first place. In both physical experiments and computer experiments, there is always a relationship between what is manipulated during the investigation on the one hand, and the real-world systems that are the targets of the investigation on the other (Winsberg, 2019).

The experimental simulation methodology adopted in this study, explores the use of different construction materials, to represent hempcrete within simulation tools. It also includes the simultaneous heat and moisture transfer investigation into the microstructure and macrostructure of hempcrete material, through multi objective optimisation. The reasons for performing these experiments are:

- i. A co-heating test conducted by Jankovic (2016) in a hempcrete house suggests that hempcrete as a building material may have a configuration equivalent to a series of slices of high-density material and insulation material. This is because, instead of heating on to a considerable period, it was stopped by a thermostat in half an hour and coincidentally, half an hour later, it started again (Jankovic, 2016). Hence, the investigation of heat and moisture transfer in hempcrete through simulation with slices of conventional materials and natural materials in different layers. And with different thickness to form a composite wall, which will represent hempcrete material within simulation tools in this study.
- ii. The simulation of a building requires the building material to be specified within simulation tools or require a building material to be created within simulation tools

(Garwood et al., 2018). In order to create a construction material for simulation, the material thickness, density, thermal conductivity and specific heat capacity needs to be specified by the designer. The density, thermal conductivity and specific heat enable the simulation model to calculate thermal diffusivity of the material, for dynamic simulation (Jankovic, 2017). Research on the properties of hempcrete for construction has resulted in a number of established material properties, which has been discovered through literature review, to be within a range. For instance, Amziane and Arnaud (2013), established that hempcrete is a lightweight composite material characterized with a dry density ranging from 200 kgm³ to 800 kgm³. Also, its dry thermal conductivity has been established to be between 0.04 mK and 0.2 W mK (Arnaud and Gourlay, 2012; Walker, Pavia and Mitchell, 2014; Diquelou et.al., 2015). More so, its specific heat capacity is between 1500J/kg to 1700J/kg (Abbott, 2014). It is evident that, despite hempcrete's increasing use for construction, the actual material properties have not yet been confirmed, as they are provided within a range. making it more difficult for accurate representation during design and simulation. Therefore, it is imperative to investigate the actual properties of hempcrete material to increase confidence in its simulation and facilitate design and construction with hempcrete. Hence, the idea of experimenting by investigating the microstructure and macrostructure of hempcrete within simulation tools through heat and moisture transfer simulation.

3.3.1 Reasoning

Hempcrete has carbon sequestration properties, which makes it absorb and lock in carbon from the atmosphere during the plant growth from which the material is harvested, consequently making the material carbon negative (Sutton and Black, 2011; Bevan and Woolley, 2008). As mentioned earlier in Chapter 2 Section 2.1, hempcrete is a product from plant based renewable resource, which is carbon negative, and also the hemp plants absorb CO₂ while growing. Hempcrete also known as hemp-lime is a mixture of hemp shives with lime-based binder; while hemp plants absorb CO₂ during its growth, lime on the other hand, emits CO₂ during its manufacturing process (Prabesh, 2016). It has been estimated that one cubic metre of hempcrete sequester 110kg of CO₂.

In ratio:

$6\text{CO}_2: \text{C}_6\text{H}_{10}\text{O}_5 = 1.84: 1$, which implies that 1 kg of hemp cellulose absorbs about 1.84 kg CO_2 (Prabesh, 2016). The summary of carbon sequestration or storage is summarised as presented below in Table 7.

Table 7.0: Hempcrete Carbon sequestration of 1m^3 wall (source: Bevan and Woolley, 2008)

110kg Hemp shiv	202kg CO_2 absorbed
220kg Lime	94kg CO_2 emitted
Hempcrete total carbon sequestration	108kg CO_2

Therefore, the more hempcrete is used in construction industry, the more carbon dioxide is absorbed and reduced from the built environment, making hempcrete a very powerful tool for mitigating climate change and carbon emissions. A material considered as a building/construction material, must possess the required engineering properties suitable enough for construction works. The properties of building materials are what makes it fit for construction, especially when its quality and capacity enable accurate decision to be made for the material application in buildings (Kodur and Harmathy, 2016). The general properties of building materials are:

1. Physical properties: are those properties that validate the quality and condition of the material without any external force. Such as, Porosity, Durability, Density, Fire resistance, Frost resistance, Water absorption, Water permeability and Hygroscopicity.
2. Mechanical properties: are the properties of a construction material, responsible for the behavior of the material during its operation or by applying external forces on them. These includes; Strength, Hardness, Elasticity, Plasticity, Brittleness and Abrasion resistance. For example, hempcrete's mechanical properties are
3. Thermal properties: are the properties related and/or responsible for its transfer or storage of heat, such as Thermal capacity, Thermal conductivity, Thermal resistivity, Specific heat.
4. Chemical properties: are the properties of materials responsible for its reaction to chemicals such as chemical resistance and corrosion resistance.
5. Electrical properties: are the properties of a material to conduct or to resist electricity. For example, wood have great electric resistance and stainless steel is a good conductor of electricity.

6. Magnetic properties: are properties required in the case of generators or influenced in a magnetic field. For example, iron is magnetic material (Kodur and Harmathy, 2016; theconstructor.org, 2020).

Hempcrete as a construction material, consists of different properties such as thermal, magnetic, electrical, physical, chemical and mechanical properties which all contribute in giving the material its unique properties. However, research has established the physical properties of hempcrete, its excellent thermal properties and its mechanical properties. For instance, Amziane and Arnaud (2013), established that hempcrete has dry density ranging from 200 to 800 kg m³ and the low density contributes to its high thermal properties. Also, its dry thermal conductivity has been established to be between 0.04 and 0.2 W mK (Diquelou et.al., 2015; Walker, Pavia and Mitchell, 2014; Arnaud and Gourlay, 2012). These are the properties required for simulating a material for a building design. More so, the relationship between heat and moisture within the hempcrete is responsible for its combined heat and moisture transfer property. Hempcrete's heat and moisture transfer properties are not well known, and that is why it cannot be accurately modelled in the computer. There is no sufficient understanding of the heat flux and moisture flux to be enable accurate modelling and simulation.

Given the overall objectives of this study and the methodology adopted to conduct this experimental research, the detailed investigation of a representation of a material called hempcrete will be carried out using simulation and multi objective optimization, as physical hempcrete material is very efficient in real life and exhibits a less efficient behavior when simulated. Thus, its actual material properties should be investigated within simulation tools using the material properties established from previous research and valid physical experiment of the real life hempcrete material. However, since a co-heating test conducted by Jankovic (2016) suggests, hempcrete could be represented with a combination of high- and low-density material layers. As explained in section 3.3 above, the experiments of using different conventional and natural building materials will also be explored as applicable.

Fundamentally, the experimental simulation in this study, involves three main phases (simulation, calibration and multi objective optimisation). As seen below in Figure 10.

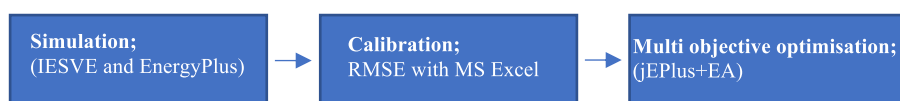


Figure 10: Phases of the simulation experiment

3.3.2 Simulation Experiment in IES Virtual Environment

The simulation experiments in IES Virtual Environment (IESVE, 2018), involves dynamic and thermal simulation. After obtaining data of the monitored hempcrete buildings, the monitored buildings were simulated to establish a base case for the subsequent simulation experiments. The IES Virtual Environment base case model simulation was set to be in free floating mode (meaning no heating or cooling was applied to the model) and this first simulation output was recorded as the base case. Subsequently, the simulation experiments involving different construction materials to represent hempcrete were conducted. The simulation experiment requires that a material is specified for the external walls and is applied to the model, followed by the simulation being conducted. In the IES Virtual Environment the experiment is prepared in the Apache construction database manager section, by editing the wall construction of the experimental building. Figure 11 below, is an example of one of the representations for Hempod, where the Hempod wall is replaced with a combination of brickwork and weather board to represent hempcrete for simulation.

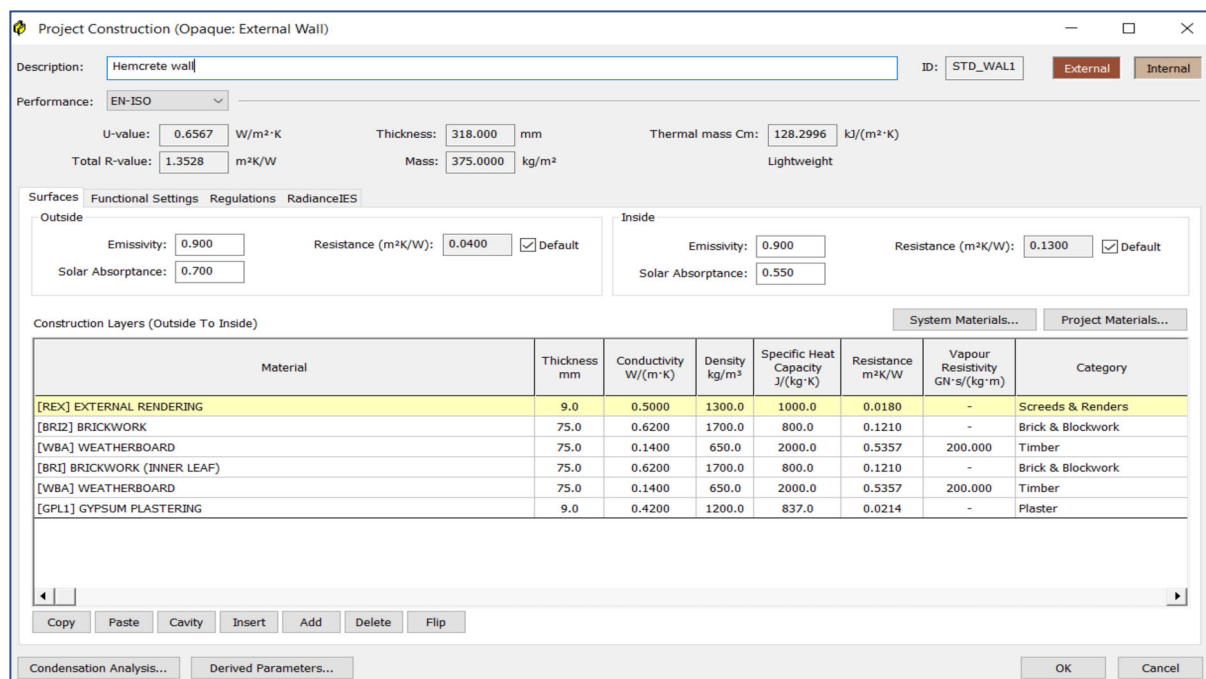


Figure 11: An example of the IES Virtual Environment simulation experiment method

All the initial simulation experiments were performed in IES Virtual Environment (IESVE, 2018), including the simulation experiment which involved creating a material called hempcrete. For creating a material called hempcrete, an insulation material from the “system materials” section was edited and its thermal conductivity, density, specific heat capacity and

vapor resistivity was replaced with that of hempcrete. It replaced the Hempod wall and represented the hempcrete wall for simulation experiment. The properties of hempcrete inputted in IES Virtual Environment (IESVE, 2018) for the simulation is from the hempcrete fact sheet – the limecrete company (Abbott, 2014). Figure 12 below, is an example from IES Virtual Environment (IESVE, 2018), of the experimental specification of hempcrete material.

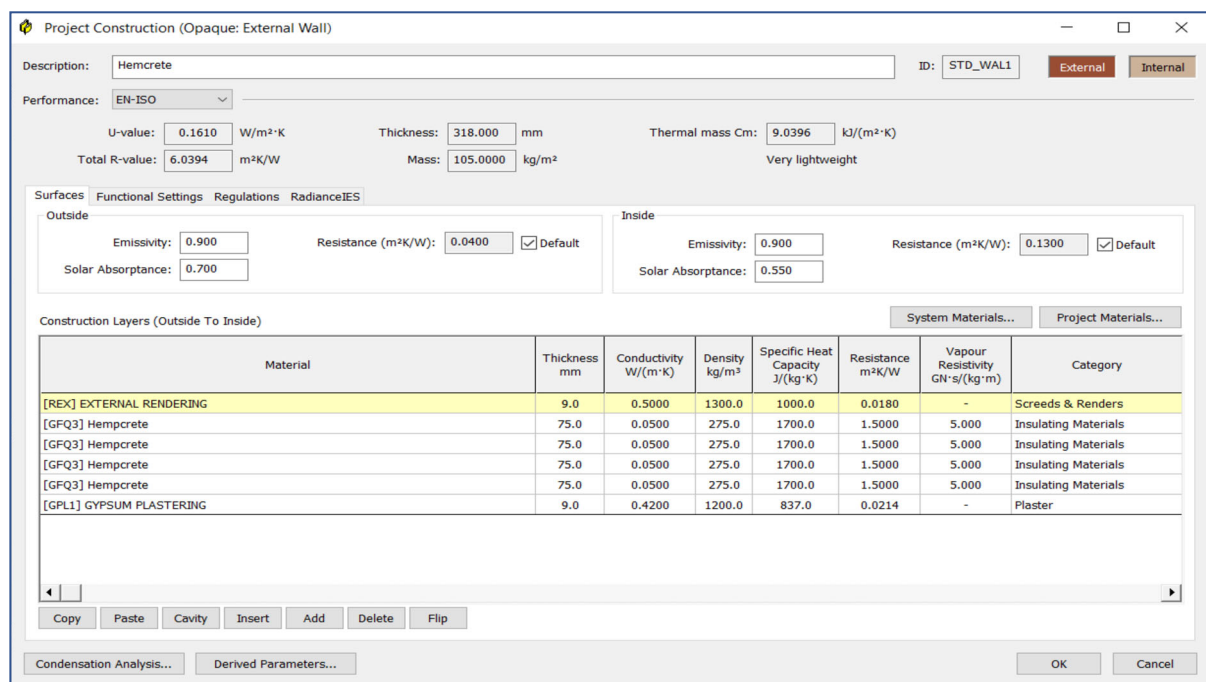


Figure 12: An example of the IES Virtual Environment simulation experiment with hempcrete material

After all of the experiments have been performed, the results of all the simulation experiment were then collated into Microsoft Excel (Microsoft office, 2018) for calibration.

3.3.3 Calibration of Experimental Simulation outputs

Simulations typically have different parameters that require calibration process, to reproduce known phenomena of the real system from the simulation output, so that good and reasonable results can be extracted through calibration (Korb and Mascaro, 2010). In this study, calibration is carried out with Microsoft Excel (Microsoft office, 2011) to calculate Root Mean Square Error with the simulation experiment output before the heat and moisture transfer simulation. The calibration in this study basically comprise of two steps as explained below:

- i Root Mean Square Error (RMSE) – the root mean square error calculation, measures how much error there is between two data sets. A lower value generally indicates a better performance of the simulation model (Cooke, 2018). The metric of root mean

square error was used to analyse the outputs from the experimental simulations. Root Mean Square Error (RMSE) is expressed as defined in Equation (1) below;

$$\Sigma = \sqrt{\frac{\sum_1^N (\text{simulated} - \text{actual})^2}{N}} \dots\dots\dots (1)$$

Where:

N – Number/size of data

Simulated – Simulation results

Actual – Monitored values

Σ – Summation

The core model of the root-mean square error calculation uses the hourly inputs of the collected monitored air temperature and relative humidity values. It is calculated as the error between the monitored (actual) values and the simulated (simulated) values for each experiment, as in Equation (3). This is to measure the discrepancy between the monitored values and the simulated values and analyse which experimental simulation output is the closest to monitored values. The experimental simulation output with the lowest root mean square error is then selected as the best model to be used for the heat and moisture transfer simulation in EnergyPlus (EnergyPlus, 2016). Calculating the error between monitoring data and simulation results is imperative, as it is the initial step towards reducing simulation performance gap. The main advantage of this model is that, the results from the root mean square error calculation is objective, because it is mathematically obtained which reduces any bias and increases reliability. Another advantage is that, it only requires a standard Microsoft excel software (Microsoft office, 2011) as the tool to calculate the root mean square error which increases the validity of the results. As mentioned earlier, the model with the lowest Root Mean Square Error is exported from IES Virtual Environment (IESVE, 2018) into EnergyPlus for conducting the heat and moisture transfer (HAMT) simulations.

- ii In order to conduct the HAMT Simulations in EnergyPlus (EnergyPlus, 2016); the simulation model has to be exported from IES Virtual Environment (iesve.com) to Design Builder (DesignBuilder, 2018), in gbXml (Green Building XML) format. The export requires the IES Virtual Environment model to be saved in gbXML format and imported into Design Builder, to be further saved into input data file (.idf) format for

EnergyPlus heat and moisture transfer (HAMT) simulations. The gbXML is a type of XML file that has over 500 types of elements and attributes that allow for the description of all aspects of a building model (gbXML, 2020). XML means eXtensible Markup Language; it is a type of text-friendly computer language that allows software programs to communicate information. XML file is versatile and can be opened using any type of text editor, information can also be easily viewed and understood in it (gbxml, 2020). "gbXML", was developed for the purpose of facilitating the safe transfer of building information, to enable the interaction as well as adequate interoperability between disparate building design and engineering analysis software tools (gbxml, 2020). IES Virtual Environment (IESVE, 2018) has an export option in the "File" menu that allows the building model to be saved and exported in "gbXML" format after the model has been created. The gbXML file includes all of the information about the building design and model. It is then imported into Design Builder as a new project, with all of the model geometry and construction properties as required to perform other simulations. The project was now saved into idf format in Design Builder (DesignBuilder, 2018), the idf format is for EnergyPlus (EnergyPlus, 2016) simulations.

In Design Builder (DesignBuilder, 2018), the general user interface contains an option at the right side of the screen "create a new file", which needs to be selected and clicked. After clicking to create a new file, the right side of the new screen has additional model options, from which there is an option "import BIM model". The import BIM model is the option for importing the gbXML model, which needs to be clicked and a dialogue box appears with further options on the file type that allows the gbXML file to be selected and opened. Once the gbXML file from IES Virtual Environment (IESVE, 2018) is opened, it shows the model as it was in IES Virtual Environment, as seen below in figure 13 and Figure 14 below.

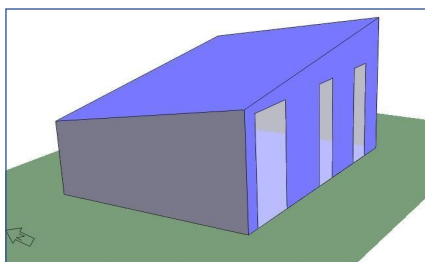


Figure 13: IES model of Hempod

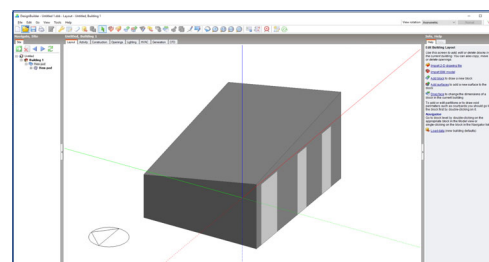


Figure 14: IES model of Hempod imported into Design Builder

Figure 15 and 16 below show the model of the residential building from IES Virtual Environment (IESVE, 2018) imported into Design Builder (DesignBuilder, 2018).

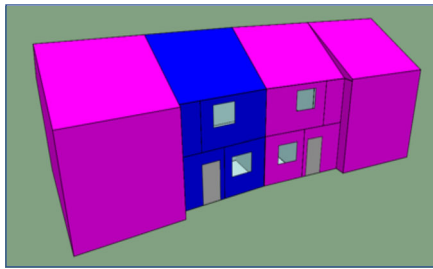


Figure 15: IES model of the residential building

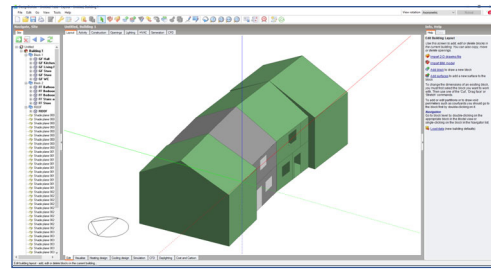


Figure 16: IES model of the residential building imported into Design Builder

From the Design Builder user interface, the “File” option at the top left of the screen, on the menu bar contains the export option. The export option is then clicked to export the model from gbXML to input data file (.idf) format for the simulation in EnergyPlus (EnergyPlus, 2016). When the export option is clicked, it opens a small dialogue tab and the first option is “Export EnergyPlus input file” which when clicked, opens a tab with options such as; Export heating design input file, Export cooling design input file and Simulation. The “simulation” option is then clicked and the input data file (.idf) is created and ready for further simulations in EnergyPlus (EnergyPlus, 2016).

It is apparent that Design Builder (DesignBuilder, 2018) was used as a plug in between IES Virtual Environment (IESVE, 2018) simulation model and EnergyPlus (EnergyPlus, 2016). The reason why the simulation and experiments were conducted in IES Virtual Environment is that, the model of the monitored buildings in IES Virtual Environment was part of the obtained data for this study. Therefore, it was considered necessary for the base case simulation and simulation experiments to be carried out in IES Virtual Environment as applicable. Especially as IES Virtual Environment is an excellent standard dynamic software that has unique capability to generate a good building geometry model and simulate the building at the same time (IESVE, 2018). This provides the user with an opportunity to perform a detailed simulation and view the building being simulated, which increases the confidence in simulation output. IES Virtual Environment (IESVE, 2018) also produce air temperature and relative humidity values, in the “vista pro” section of the software as part of the simulation output, which are particularly the outputs required from the simulation experiments. More so, IES Virtual Environment has system materials and project materials section, where

construction materials with their simulation properties are already installed. This provides the simplicity and flexibility of selecting readily available construction materials from the software and applying in to the simulation model. It also saves time and increases the opportunity of exploring and experimenting with more materials to replace hempcrete for simulation. After the simulation experiments in IES Virtual Environment is completed, the model is then transferred into EnergyPlus. After the transfer from IES Virtual Environment to idf format is completed, the idf model is then created as explained above and ready to be imported into EnergyPlus (EnergyPlus, 2016) for the HAMT simulations.

3.3.4 Heat and Moisture Transfer (HAMT) Simulation in EnergyPlus

EnergyPlus is a console-based program that reads input and writes output to text files, it enables a number of utilities including input data file (IDF) editor (EnergyPlus, 2016). An input data file (.idf) is a format for text files containing the data, describing the building and / or HVAC system to be simulated, for creating input files using a spreadsheet-like interface (EnergyPlus, 2016). EnergyPlus possess capabilities for advanced building simulations such as, combined heat and moisture transfer, conduction transfer functions, advanced fenestration models, and many other notable features (EnergyPlus, 2016). It also has the ability to investigate the heat and moisture movement within the hempcrete material as will be demonstrated in the experiments.

The reason EnergyPlus is used in this study, is for heat and moisture transfer (HAMT) model and simulation. A general link for the storage and transfer of heat, air and moisture in and between building materials, is considerably said to be missing in building design (Ming Wei et al 2019). Moisture in porous structures can significantly affect energy performance of any building. With regards to building physics, thermal transfer is entirely based on thermal performance of building components. The simultaneous heat and moisture transfer in a building envelope is very important and has an influence on the indoor environment and the overall performance of the building (Kunzel, 1995). For the experiment in this study, both heat and moisture transfer in the experimental building envelope's, alongside the corresponding indoor air, will be simultaneously considered during the heat and moisture transfer simulation. The coupled model will take into account the main hygrothermal effects in hempcrete as a construction material.

Ming Wei et al (2019) performed a Numerical Simulation of Heat and Moisture Transfer of a Wall with Insulation. The simulation was performed to improve the coupled heat and moisture transfer model with temperature and relative humidity as the driving force. Their simulation emphasizes the dependence of effective thermal conductivity and vapor permeability on temperature and relative humidity. It described the effective thermal conductivity and vapor permeability of a wall material as a function of temperature and relative humidity. They used cellulose batt as the insulation material and simulated the heat transfer and moisture transfer process of the wall. The relationship of the heat flux between the wall and the indoor air as a function of temperature, relative humidity and thickness of the insulation layer was obtained. The outputs from the performed numerical simulation of heat and moisture transfer revealed that, the heat and moisture transfer process between the wall and the air has a great influence on the comfort of the indoor air. It also has an influence on the energy consumption of the ventilation and air conditioning system in the building.

They also realised that, when there is any change in outside temperature and relative humidity, these changes the internal temperature and moisture of the wall caused by the two factors. The rate of temperature conduction in the wall is faster than the speed of water conduction, due to the fact that when the outside temperature is greater than the internal temperature. The moisture inside the wall always evaporates first, before the liquid water decreases. Also, when there is basically no change in temperature, moisture transfer causes the water vapor concentration to continuously increase, and then condensation occurs to further increase the amount of water storage. Therefore, with any increase of the thickness of insulation layer in a wall, the heat and moisture transfer intensity between a wall and its surrounding air are continuously reduced (Ming Wei et al., 2019).

As seen from the numerical simulation performed by Ming Wei et al., (2019), temperature and relative humidity are very relevant in building physics and plays an integral role in the performance of a building. As well as in conditioning the interior environment of a building, which is why heat and moisture transfer model and simulations are important to improve a building design model and building operation as applicable. The combined heat and moisture transfer (HAMT) model and simulation in EnergyPlus, are a solution algorithm which is a finite element. The model simulates the movement and storage of heat and moisture in surfaces simultaneously, from and to both the internal and external environments (EnergyPlus, 2016).

The HAMT model descriptions are dependent on some factors of the material such as the moisture content, porosity, moisture dependent thermal conductivity, moisture transfer, and convective vapour transfer (EnergyPlus, 2016). For the purpose of experimental investigation in this study, temperature and relative humidity values are the only parameters that will be considered from the simulation output of HAMT model in EnergyPlus. Frigg and Reiss (2008) defined computer simulation as the method of using a computer to solve an equation that analytically, cannot be manually solved. The heat and moisture transfer (HAMT) equations in EnergyPlus, are derived from heat and moisture balance equations from Künzle, H.M. (1995). It describes a model for the transfer of heat and moisture through a material as seen in Equation (2) and (4) below.

$$\frac{\partial H}{\partial T} \frac{\partial T}{\partial \tau} = \frac{\partial}{\partial x} \left[K_w \frac{\partial T}{\partial x} \right] + h_v \frac{\partial}{\partial x} \left[\frac{\delta \partial T}{\mu \partial x} \right] \quad (2)$$

However, Equation (3) below, describes the storage, transport and generation of heat respectively.

$$\frac{\partial H}{\partial T} \frac{\partial T}{\partial \tau} = \frac{\partial}{\partial x} \left[K_w \frac{\partial T}{\partial x} \right] + h_v \frac{\partial}{\partial x} \left[\frac{\delta \partial T}{\mu \partial x} \right] \quad (3)$$

The diagram shows Equation (3) with three terms enclosed in dashed blue boxes. Below each box is a downward-pointing arrow and a label: 'Storage' under the first term, 'Transport' under the second term, and 'Generation' under the third term.

Where:

- $\frac{\partial H}{\partial T}$ Moisture dependent heat storage capacity
- $\frac{\partial}{\partial x}$ Time step between calculations
- $\frac{\partial T}{\partial x}$ Temperature gradient heat transfer
- μ Moisture dependent vapor diffusion resistance factor
- δ Vapor diffusion coefficient in air (kg/msPa)
- K_w Moisture dependent thermal conductivity (W/mC)
- h_v Evaporation enthalpy of water (2,489, 000 J/kg)

$$\frac{\partial w \partial \phi}{\partial \phi \partial \tau} = \frac{\partial}{\partial x} \left[D_w \frac{\partial w \partial \phi}{\partial \phi \partial x} \right] + \frac{\partial}{\partial x} \left[\frac{\delta \partial T}{\mu \partial x} \right] \quad (4)$$

As seen below, Equation (5) describes the storage of moisture, the transport of liquid moisture and the transport of vapor respectively.

$$\frac{\partial w \partial \phi}{\partial \phi \partial \tau} = \frac{\partial}{\partial x} \left[D_w \frac{\partial w \partial \phi}{\partial \phi \partial x} \right] + \frac{\partial}{\partial x} \left[\frac{\delta \partial T}{\mu \partial x} \right] \quad (5)$$

Storage
Transport
Generation

Where:

- μ Moisture dependent vapor diffusion resistance factor
- δ Vapor diffusion coefficient in air
- D_w Liquid transport coefficient
- $\frac{\partial w}{\partial \phi}$ Moisture dependent moisture storage capacity (kg/m³)
- $\frac{\partial T}{\partial x}$ Temperature gradient heat transfer
- $\partial \tau$ Time step between calculations

From the Equation (5) above, only the storage and transfer of heat and moisture are used for the HAMT model simulations and analysis as described in Equation (6) and (7) below.

Basically, the HAMT simulation of storage and transfer of heat for a hempcrete wall, means that simulation is performed for all the materials that make up the wall. And simulates through layers of the wall materials, such as hempcrete, external render and internal plaster. The hempcrete material surface is further split into cells through the depth of the hempcrete material during simulation. EnergyPlus also generates no more than ten (10) cells per material, with widths thinner and near boundaries of each material demonstrating the detail transfer of heat. The HAMT simulation for hempcrete material generates 10 cells (a, b, c, d, e, f, g, h, i, j), the heat storage and transfer through the *i*th cell in the surface of hempcrete material, is described as seen in Equation (6) below. And as seen in Figure 17 below.

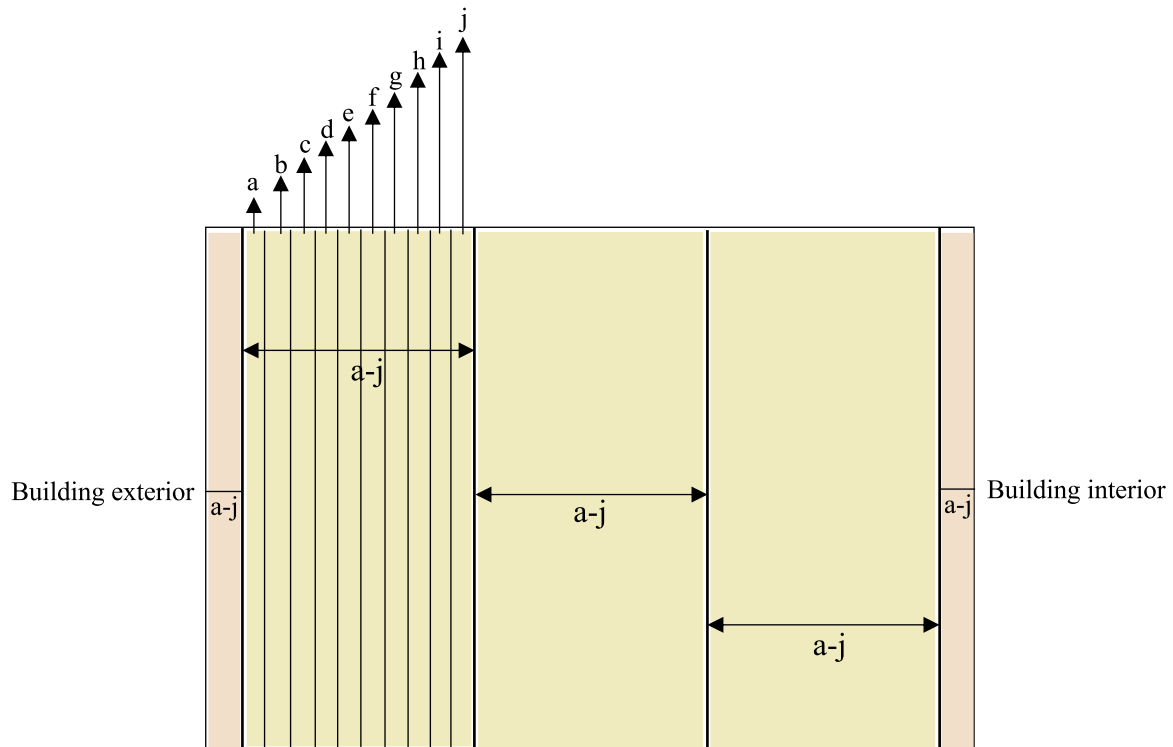


Figure 17: A cross-section of hemcrete wall surface made up of 5 material layers split into cells a-j.

Figure 17 above, represents each cell from a-j of a material in a wall surface; which means if a composite wall is made up of (8) different materials, HAMT simulations develops and runs simulations for each cell of each material, which is at least 50 cells for the composite wall. And each cell simulation can be described as seen by the Equation (6) below.

Equation (6), describes the storage and transfer of heat through the *i*th cell in a surface. As explained earlier in Section 3.3.5 of this chapter; In EnergyPlus, surfaces are made up of layers of materials and each surface is split into its constituent materials, which is further split up into cells through the depth of the material. The heat and moisture transfer model generate cells per material through the depth of the wall, which is where the material detail of a building wall model is (EnergyPlus, 2016).

$$(c_i \rho_i + c_w w_i) \Delta V_i \frac{T_i^{p+1} - T_i^p}{\Delta \tau} = \sum_j K_{wij} A_{ij} \frac{T_j^{p+L} - T_i^{p+1}}{x_{ij}} + \sum_j h_v \frac{\delta_{ij}}{\mu_{ij}} A_{ij} \frac{p_i^{p+1} - p_i^p}{x_{ij}} \dots \dots \dots (6)$$

Where:

- T Temperature (C)
- w Moisture Content (kg/m³)
- C Specific heat capacity of water (J/kgC)
- h Evaporation enthalpy of water (=2,489,000J/kg)

$\Delta\tau$	Time step between calculations (s)
ΔV_i	Cell volume (m ³)
x	Distance between cell centres (m)
P	Material porosity (m ³ / m ³)
p	Present time step (s)
i	Cell indices
j	Cell indices
V	Cell Volume (m ³)
A	Contact surface area (m ²)
K	Thermal conductivity (W/mC)
ρ	Material Density (kg/m ³)
μ	Moisture dependent vapor diffusion resistant factor
Σ	Summation
δ	Vapor diffusion coefficient in air (kg/msPa)

Equation (7) below, describes the storage and transfer of moisture through the ith cell in a surface. Moisture is transported as either liquid (w) or vapour (v) through a material. Liquid transfer is driven by difference in relative humidity while vapor transfer is driven by differences in vapor pressure.

$$\frac{dw}{d\phi_i} \Delta V_i \frac{\phi_i^{p+1} - \phi_i^p}{\Delta\tau} = \sum_j K_{ij} A_{ij} \frac{\phi_j^{p+1} - \phi_i^{p+1}}{x_{ij}} + \sum_j \frac{\delta_{ij}}{\mu_{ij}} A_{ij} \frac{p_j^{p+1} - p_i^{p+1}}{x_{ij}} \dots\dots\dots (7)$$

Where:

$\frac{\partial w}{\partial \phi}$	Moisture dependent moisture storage capacity (kg/ m ³)
Σ	Summation
j	Cell indices
ΔV_i	Cell volume (m ³)
A	Contact surface area (m ²)
K	Thermal conductivity (W/mC)
δ	Vapor diffusion coefficient in air (kg/msPa)
p	Material porosity (m ³ /m ³)
μ	Moisture dependent vapor diffusion resistant factor
x	Distance between cell centres

p	Present time step (s)
i	Cell indices
$\Delta\tau$	Time step between calculations (s)

The moisture content (w) of a cell is needed for the calculation of the heat transfer through the cell as it affects the thermal resistance and heat capacitance. The moisture content of cells in EnergyPlus, is calculated from the relative humidity (RH) of the material. The relationship between water content (w) and the relative humidity (RH) for each material is known as the sorption isotherm and measured data points are entered into EnergyPlus as a series of coordinates. HAMT interpolates between the measurements to obtain the moisture content of a material for any RH value. Equation (4) is used together with the heat Equation (3) in an alternate step by step mode to analyse and calculate the temperature and relative humidity profiles for each cell for the next time step. The eventual temperature and relative humidity profiles are the required outcome from the HAMT simulations needed for this study.

Every material in the model is represented individually, by the material property heat and moisture transfer parameters. In EnergyPlus, surfaces are made up of layers of materials and each surface is split into its constituent materials, which is further split up into cells through depth. The heat and moisture transfer model generate cells per material through the depth of the wall, which is where the material detail of a building wall model is. In order to develop the idf model to adequately investigate hempcrete's heat and moisture movement, the values of the field's in material property heat and moisture transfer parameters were replaced with search strings for the optimisation. The reason is that, the heat and moisture parameters possess the potential to reveal the underlying material physics for any material, as well as hempcrete. The model template in idf format, is then coupled into jEPlus to form the parameters for the optimization.

Additionally, EnergyPlus has the capacity to provide temperature and moisture profiles through any composite wall to demonstrate heat and moisture transfer, as well as identify surfaces with high surface humidity. Due to the specific material structure of hempcrete and its combined heat and moisture transfer, the HAMT simulation is performed to develop the model in idf, as a significant parameter for conducting the multi-objective optimisation. The EnergyPlus HAMT model contains parameters in the idf editor, which regulates the simulation outputs for the heat and moisture transfer simulation. These simulation parameters contain a class list and a tab for "explanation of objects and current field" which further defines any selected parameter

and explains the parameter's effect on the material and model. This is, including the material name, and simulation units, which are important for understanding simulation outputs. In this study, the simulation parameter for HAMT model that are integral to the investigation of hempcretes' combined heat and moisture transfer are the - Material Property Heat and Moisture Transfer: settings, sorption isotherm, suction, redistribution, diffusion and thermal conductivity, as seen below in figure 18.

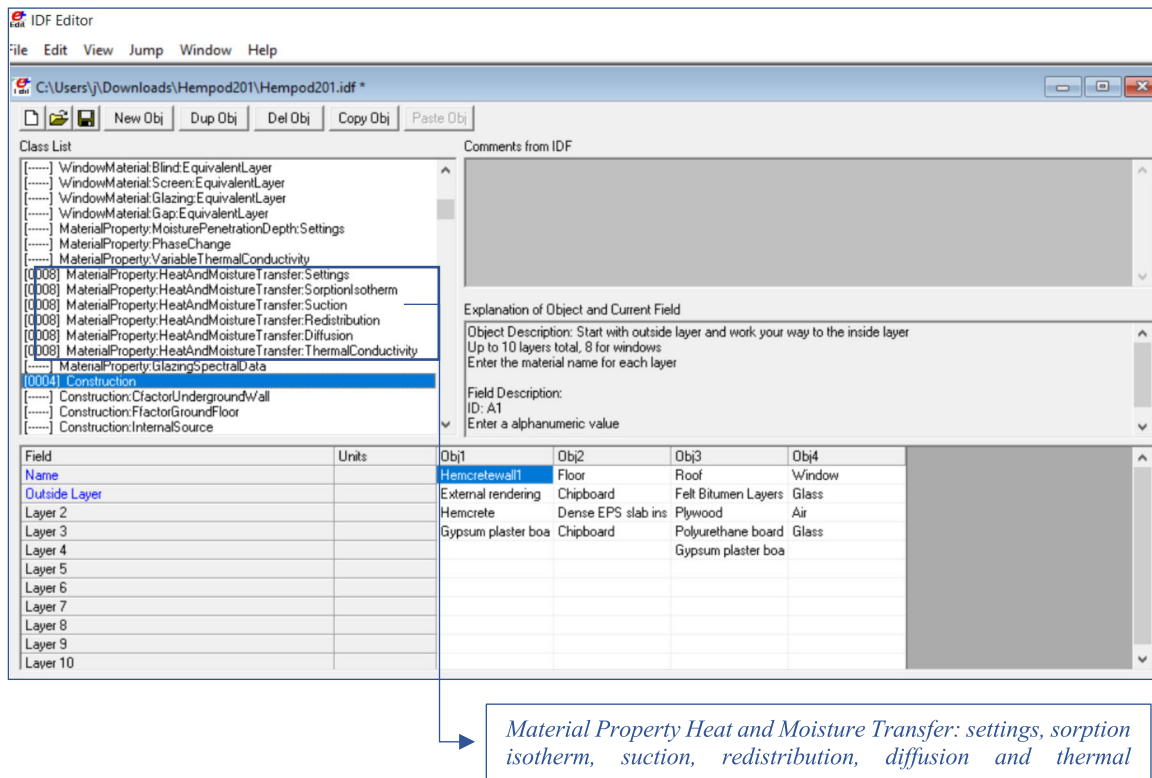


Figure 18: Showing the HAMT model parameters

The Material Property heat and moisture Transfer: Sorption Isotherm parameter includes relative humidity fraction and moisture content in its parameter field. It represents the relationship between moisture and water content (kg/m^3) of a material with its relative humidity (RH). For each humidity value, a sorption isotherm indicates the corresponding water content value at a given, constant temperature.

The Material Property heat and moisture Transfer: Suction, includes moisture content (kg/m^3) and liquid transport coefficient (m^2/s) in its parameter field. The suction parameter relates the liquid transport coefficient, under suction, to the water content of a material.

The material Property heat and moisture Transfer: Redistribution, includes moisture content (m^2/s) and liquid transport coefficient (kg/m^3) in its parameter field. The redistribution

parameter relates the liquid transport coefficient to the water content of a material under normal conditions. The liquid transport coefficient at the highest entered water content value is used for all liquid transport coefficient values above this water content.

The material Property heat and moisture Transfer: Diffusion, includes relative humidity fraction (dimensionless) and water vapour diffusion resistance factor (dimensionless) in its parameter field. The simulation parameter relates the vapor diffusion resistance factor to the relative humidity as fraction.

The material Property heat and moisture Transfer: Thermal conductivity, includes moisture content (m^2/s) and thermal conductivity ($W/m-K$) in its parameter field. The simulation parameter relates the thermal conductivity of a material to its moisture or water content.

The Material Property heat and moisture Transfer: Settings parameter includes the porosity and initial water content ratio in its parameter field. The porosity of a material in the HAMT model is the maximum fraction, of a material by volume, that can be taken up with water. In EnergyPlus HAMT the units for porosity are m^3/m^3 . The initial water content ratio (kg/kg or lb/lb) in the HAMT model is the water content assumed to be distributed evenly through the depth of the material.

Given the objectives of the study, the model with the lowest root mean square from the experiments is moved into EnergyPlus for the HAMT simulations, to investigate the movement of heat and moisture through the wall, using combined heat and moisture transfer simulations. The idf from the EnergyPlus HAMT simulations is then coupled into jEPlus to form the parameters for the analysis and optimization, used to investigate the material.

3.3.5 Multi objective optimisation

The completion of the simulation experiment in IES Virtual environment, root mean square error calculation and HAMT simulations, is followed by the multi objective optimisation stage. The model with the lowest Root Mean Square Error is developed through HAMT simulation as a model template, to be coupled into jEPlus for the simulation-based multi objective optimization in jEPlus+EA (jEPlus, 2018). An optimisation problem can be expressed as:

Minimise: $J = F(X)$

Subject to: $G(X) \leq 0$

$H(X) = 0$

Where:

$X = [X_1, X_2, \dots, X_K]$ is the vector of problem variables;

$F(X) = [F_1(X), F_2(X), \dots, F_m(X)]$ is the vector of objective functions;

$G(X) = [g_1(X), g_2(X), \dots, g_n(X)]$ is the vector of inequality constraints;

$H(X) = [h_1(X), h_2(X), \dots, h_p(X)]$ is the vector of equality constraints.

Mathematically, objectives, equality and inequality constraints are interchangeable, meaning that an equality constraint $h(X) = 0$ can also be described as an inequality constraint by introducing a small tolerance ε , i.e. $g(X) = |h(X)| - \varepsilon \leq 0$; and/or a constraint can be satiated by minimising it as an objective function. Multiple constraints can also be combined into one, for example;

$g(X) = \sum G(X) \leq 0$; are the objective functions (NEOS, 2019).

Additionally, for optimisation problems in building design and operation, objectives and constraints are often determined by the designer/user's priorities. For example, a building design can be optimised to minimize energy consumption (objective) while maintaining required comfort level (constraint). Or it can be optimised to maximize comfort level (objective) within a limited budget (constraint), or to minimise energy consumption, carbon emission, life cycle cost, discomfort, and more (objectives) all at once (Zhang, 2012). For instance, the optimisation in this study is optimised to minimise and/or maximise temperature and relative humidity simultaneously. By calculating RMSE of temperature (objective) and RMSE of relative humidity (objective) within the same time period as the monitored data. The optimisation in jEPlus+EA uses the non-dominated sorting genetic algorithm (NSGA II) in the background as an evolutionary process (Deb et al. 2002). The basic concept of jEPlus+EA is the use of Evolutionary Algorithms to search through the design space as defined by a jEPlus project (jepplus.org). Technically, jEPlus+EA is the optimisation tool that provides the interface for the integration of the Non-Sorting Genetic Algorithm (NSGA-II) to jEPlus. jEPlus is a simulation-based optimisation program, which uses EnergyPlus for managing complex parametric simulations (jEPlus, 2018). In order to conduct the optimisation in jEPlus+EA, a jEplus project (.jep) file needs to be created first.

A '.jep' project file contains all the information needed for a parametric study, as well as the simulation-based optimization variables, which includes; a weather file, idf file, and a Report

Variable Input (rvi) or extended report variable input (rvx) file. It also contains the parameter definitions, the definitions for result collection, and simulation settings such as the working directory, number of processors to deploy, and options to keep or remove temporary files and EnergyPlus outputs (jEPlus, 2018).

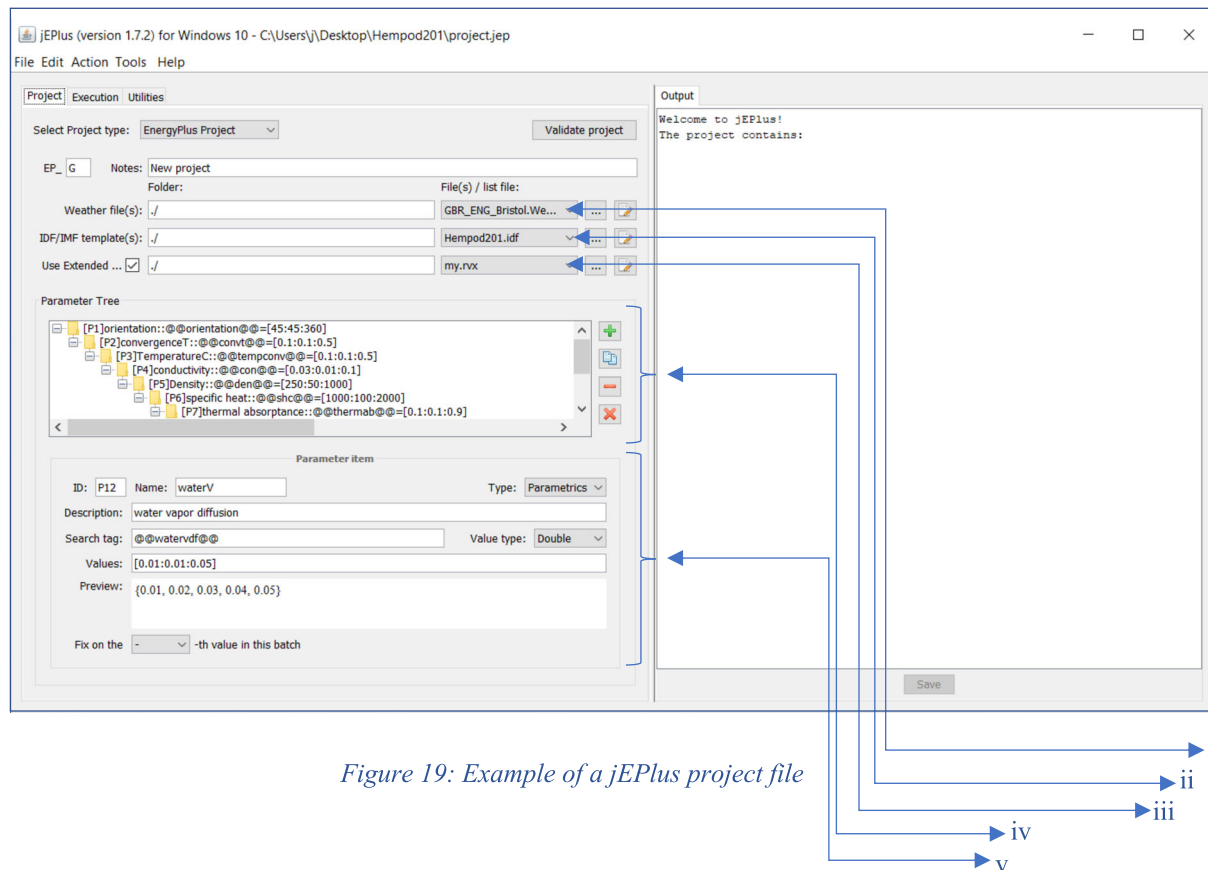


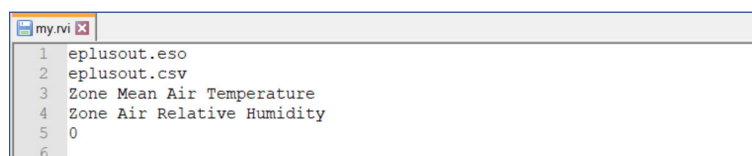
Figure 19: Example of a jEPlus project file

Figure 19 above, is an example of a jEPlus project file, showing the weather file (i), input data file (ii), rvx file (iii), parameter tree (iv) and parameter item (v). These are the main variables that make up a jEPlus file before integrating for optimization in jEPlus+EA, as will be explained below:

- i. Weather file - The weather file used, is EnergyPlus weather file (EPW) for simulation. The weather file is from energyplus.net, from the “weather data for simulation” section; the Climate.OneBuilding contains weather data files in EPW, CLM (ESP-r), and WEA (Daysim) formats from many publicly available data sets and locations from around the world. For the optimisation in this study, the EPW was requested for download by selecting and clicking on “Europe – Region 6” from the the Climate files – listed in World Metrological Organizations (WMO) Regions. After selecting Europe, United Kingdom was further selected and for the download, “GBR_ENG_Bristol.Wea.Ctr.037260_TMYx.zip” and

“GBR_ENG_Norwich.Intl.AP.034920_TMYx.zip” were downloaded. As seen from the figure above, the weather file for Bristol was downloaded instead of Bath where Hempod was originally located. The reason is, there is no available developed simulation weather file for Bath, and Bristol is the only available weather file location close to Bath. Additionally, for the residential building located in Diss – Norfolk, the simulation weather data downloaded was for Norwich.

- ii. The Input Data File (.idf) – The .idf is the EnergyPlus (EnergyPlus, 2016) building model template from which the parametric simulation and optimisation will be carried out. Specifically, it is where establishing a wide range of parameters for parametric simulation is created. For example, the material property heat and moisture transfer parameters, where search strings are inputted for performing optimisation, is set from the idf. model template, meaning that the parts of the idf model from which the heat and moisture investigation is to be carried out, are replaced numerical values where corresponding search strings are found. These search strings are created in the parameter tree as search tags for the different parameters in relation to the search string in the idf model. The parameters are further defined in the parameter item section of the parameter tree by editing the name, value type, description, search tag, and values as will be explained below.
- iii. my.rvi file - The Report Variable Input (rvi) file is a text file with a list of some selected report variables, extracted from the output variables of EnergyPlus simulation (bigladdersoftware.com). It is created from EnergyPlus output details document (eplusout.rdd) and output meter variables (eplusout.mdd) files. They are extracted based on the objectives of the optimisation, which then produce the variables inputted in the rvi file as part of the jEPlus optimization variables. For instance, the rvi file created for this study is “zone mean air temperature” and “zone air relative humidity” extracted from the EnergyPlus heat and moisture transfer (HAMT) simulation outputs. As seen below in Figure 20.



```
1 eplusout.eso
2 eplusout.csv
3 Zone Mean Air Temperature
4 Zone Air Relative Humidity
5 0
6
```

Figure 20: rvi file

my.rvx file – The rvx file, is an extended rvi text file, it contains the objectives, constraints, and rvi (bigladdersoftware.com). It is represented in JSON format (JavaScript Object Notation): a light-weight data-interchange format. It is easy to read and write, as well as easy for machines to parse and generate based on JavaScript programming language (json, 2020). It is a text format completely language independent, which uses conventions that are familiar to the C-family programmers including Python which makes JSON an ideal format of the rvx for data-interchange language (jEPlus, 2018). The rvx file is where the optimisation objectives of this study was specified. For example, the objectives for the optimisation in this study is, minimizing and/or maximizing air temperature and relative humidity through Root Mean Square Error (RMSE) calculation. It also works with the RVI file as seen below, in the Figure 21 below.

```

1  {
2
3
4
5  "notes": "Some notes about this RVX",
6
7  "rvis": [
8    {
9      "fileName": "my.rvi",
10     "tableName": "HourlyMeters",
11     "frequency": "Hourly",
12     "usedInCalc": false
13   }
14 ],
15
16 "sqls": [
17 ],
18
19 "scripts": [
20   {
21     "fileName": "CalcRMSE.py",
22     "pythonVersion": "python3",
23     "onEachJob": true,
24     "arguments": "HourlyMeters;ref.csv",
25     "tableName": "RMSE"
26   }
27 ],
28
29 "userVars": [
30   {
31     "identifier": "v0",
32     "formula": "c0",
33     "caption": "Temperature RMSE",
34     "report": false
35   },
36   {
37     "identifier": "v1",
38     "formula": "t1",
39     "caption": "Relative humidity RMSE [%]",
40     "report": false
41   }
42 ],
43
44 "constraints": [
45 ],
46
47 "objectives": [
48   {
49     "identifier": "t0",
50     "formula": "v0",
51     "caption": "Temperature RMSE [C]",
52     "scaling": false,
53     "min": "0",
54     "max": "100000",
55     "weight": "1.0"
56   },
57   {
58     "identifier": "t1",
59     "formula": "v1",
60     "caption": "Relative humidity RMSE [%]",
61     "scaling": false,
62     "min": "0",
63     "max": "1000",
64     "weight": "1.0"

```

Figure 21: rvx file

- iv. Parameter tree - A parameter tree is a structure used to identify the order of the optimisation parameters hierarchically. It is a tree structure comprising of defined parameters from the idf, replaced with search strings, it manages the definitions of

parameters as optimisation problems (jEPlus, 2018). A parameter or simulation parameter is a value, a reference or an area of the simulation model that can have more than one options. It could be a single design variable (temperature setpoint), a component (construction of a wall), a sub-system (HVAC system), and/or a complete model (model templates) (jEPlus, 2018). A parameter to be incorporated into any parametric analysis in jEPlus is ideally specified with three essential elements; a unique ID, a Search string, and a list of Alternative values (jeplus.org, 2015). As explained above in the EnergyPlus HAMT simulation section 3.3.4; the field's comprising parameters of the material property heat and moisture transfer (settings, sorption isotherm, suction, redistribution, diffusion and thermal conductivity) are replaced with search strings. Search strings are specially formulated text strings that normally do not exist in simulation model files, they are mostly created by the user for easy identification of optimisation variables (jEPlus, 2018). They are used by jEPlus to mark the locations of the parameter in the model templates, for inserting the values of the simulation parameter at the correct places. Specifically, in this study, the thermal conductivity, density and specific heat capacity of hempcrete were replaced with search strings and defined in the value type section as seen in Figure 22 below.

Additionally, the parameters of hempcrete material, from the material property heat and moisture transfer model template were also replaced with search strings, as seen in Figure 22 below. For example, the material property heat and moisture transfer diffusion parameter, of water vapour diffusion resistance factor is replaced with @@watervdf@@ as the search string, as seen in Figure 22 below. The applied search string in the parameter tree, are further defined in the parameter item section. The material property heat and moisture transfer parameters are used, to simulate and investigate the micro structure of the hempcrete material in this study. The reason is, for the including the movement of heat and moisture to identify the actual value for hempcrete water vapour resistant factor, its diffusion, etc.

Additionally, in order to investigate the actual material configuration for hempcrete wall construction components; the “construction” section in the idf model was also replaced with search strings. For instance, in the parameter tree, as seen in Figure 22 below, @@wall@@ is an example of the search string used to manually replace wall construction component in the model in the first instance. This search string is

subsequently replaced automatically with a range of numerical parameters used for parametric simulation and multi-objective optimisation, such as “Hempcretewall1” to “Hempcretewall8” as will be explained below and in the Experimentation chapter.

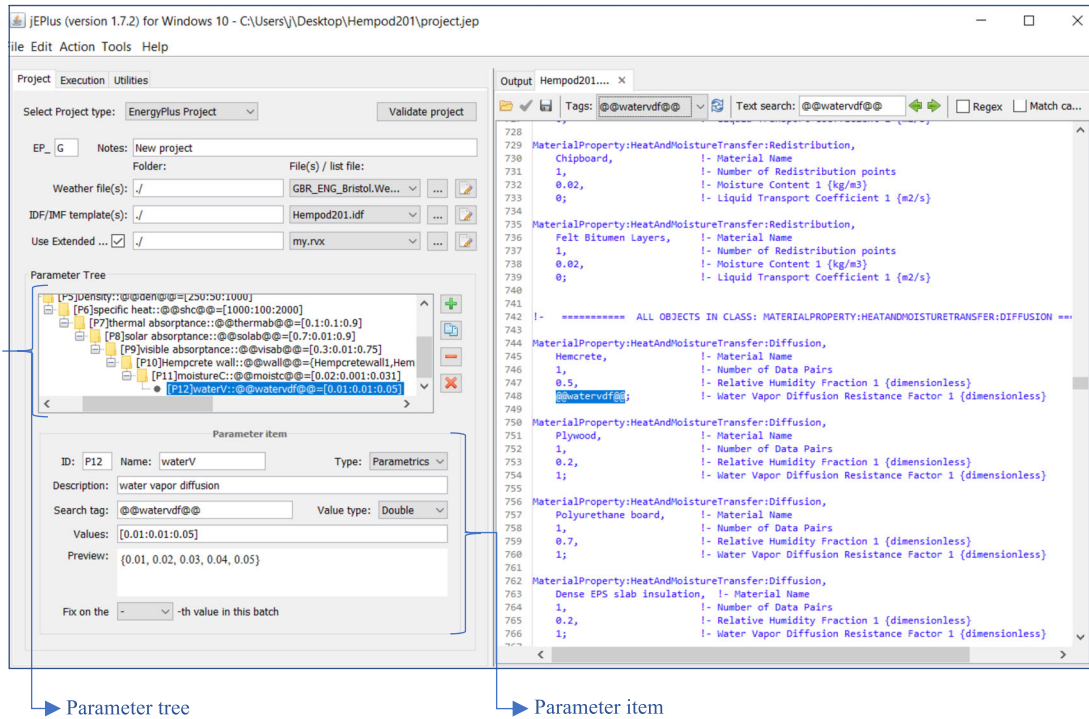


Figure 22: jEPlus interface, showing parameter tree and Parameter item

v. Parameter item – The parameter item is the section that defines each parameter on the parameter tree as seen from Figure 22 above. The parameter item section contains the parameter – ID, name, type, description, search tag, value type, value and preview. The search strings are further represented with a range of values 0.00-10.0, it relates water and moisture in the idf model template as seen in Figure 22 above.

- Parameter ID, is a short string used for identifying the optimisation parameter as applicable;
- Parameter name, is used alongside the parameter ID to form part of the optimisation job title, as well as the work directory name in which the job is to be executed;
- Parameter description, describes the optimisation parameter name in the idf model, to be replaced with the search strings as applicable;
- Search tag is where the search strings are applied, exactly as they appear in the idf model;

- Value type contains a list of strings to be used one at a time in the jEPlus parametric jobs. jEPlus supports three types of values: Discrete, Integer and Double.
- Values contain the syntax for specifying the value type of a particular parameter. Basically, there are three kinds of value type in jEPlus; double, discrete and integer. The “double” is defined with decimal numbers and double numbers. The “discrete” value type is defined with discrete numbers or with building element names such as hempcrete wall1 or window 1. The “integer” value type is defined with whole numbers as integers. More so, for the “Discrete” type of parameters, the values can be specified with a comma (,) delimited list enclosed in a pair of curly brackets ({}); for example {Hempcretewall1, Hempcretewall2, Hempcretewall3, ..}. For the “Integer” and “Double” parameters; square brackets ([]) are used to define a number series with a uniform interval. and the values within the square brackets can be specified with a colon to separate the start value, the interval value and the end value of a parameter. For example, integer values can be represented as ([1:2:9]) which means {1,3,5,7,9}. For example, double values can be represented as ([1.00:0.10:1.50]) which means {1.00,1.10,1.20,1.30,1.40,1.50}.

Essentially, conducting an optimisation in jEPlus+EA requires a folder containing a jEPlus project file (.jep), weather file, my.rvi, my.rvx file, idf, as explained above. However, in addition to the jEPlus project file (.jep), weather file, my.rvi, my.rvx and idf files, the multi objective optimisation performed in this study required the job folder to have a ref file and a CalcRMSE file as will be explained below and as seen in Figure 23 below.

Name	Date modified	Type	Size
CalcRMSE	20/11/2017 12:17	Python File	2 KB
GBR_ENG_Bristol.Wea.Ctr.037260_TMYx.e...	23/04/2019 05:32	EPW File	1,524 KB
Hempod201	22/02/2020 03:35	EnergyPlus Input D...	67 KB
my.rvi	25/01/2019 00:28	RVI File	1 KB
my.rvx	30/04/2019 16:49	RVX File	2 KB
projectjep	22/02/2020 03:23	JEP File	28 KB
ref	06/01/2020 00:50	Microsoft Excel Co...	17 KB

Figure 23: A folder ready for multi objective optimisation in jEPlus+EA

Ref file – The ref file is a Microsoft excel file, containing the obtained monitored data. It is used as the reference file from which the objective of the RMSE for temperature and relative humidity is calculated with during the optimisation process. The ref file is inputted in to the rvx file and referenced as “ref.csv” and then jEPlus integrates the ref file for the RMSE calculation during the optimisation process (jEPlus, 2018).

CalcRMSE file – The CalcRMSE file is a Python 3 script file. A script is referred to a file containing a logical sequence of orders to be executed; A text file containing Python codes that is intended to be directly executed is called script (Python.org, 2020). The Python 3 script is used for the jEPlus pre-processing to communicate with the idf model while taking account of predefined parameters in the search space of the project. jEPlus possess the facility that provides for testing Python scripts, to be used while processing data and performing optimisation (jeplus.org). The idea is that the Python 3 script can apply further operations on the idf file using arguments defined in the parameter and path names in the jEPlus. For example, the arguments for this project file was “CalcRMSE”, the Python 3 script contains information for calculating the RMSE, using the Pandas library to configure the Python 3 executable in the jEPlus project (jEPlus, 2018). Pandas is a fast and flexible data analysis and manipulation tool, built from the Python programming language. It can read any data from a .csv file using the “read_csv” function. Pandas Library provides high-performance and simple data structures for Python programming language (pandas.pydata.org). Technically, the Pandas library processes the ref file by importing it as a csv and calculating the RMSE between the ref file and the idf model template, as defined in the Python file of “CalcRMSE” as seen below in Figure 24. The CaclRMSE file explores details of the set objectives, from the extracted rvi file and the created rvx file in the idf model (jEPlus, 2018). The optimization objectives in this study, were set to minimize Root Mean Square Error (RMSE) from temperature ($t_0=v_0$) and relative humidity ($t_1=v_1$).

```

1  import pandas as pd
2  import numpy as np
3  import csv
4  import sys
5
6  # function which calculates the root mean square error
7  def rmse_function(observed, predicted, N):
8      error = observed - predicted
9      sqerror = error ** 2
10     sumsqerror = np.sum(sqerror)
11     meansqerror = sumsqerror / N
12     rmse = np.sqrt(meansqerror)
13     return rmse
14
15 # This script takes
16 args = sys.argv[4].split(';')
17
18 refdata = pd.read_csv(sys.argv[1] + args[1]) #read data from the reference file (path passed from the script)
19
20 in_file = sys.argv[2] + args[0] + ".csv"
21 indata = pd.read_csv(in_file)
22
23 rowcolno = indata.shape
24
25 heading = list(refdata.ix[:1]) #take heading row from the reference file
26
27 outname = sys.argv[3] # output file name from the parameter passed to the script
28
29 rmsedata = ["AAA"]
30
31
32 for column in range(1, rowcolno[1]):
33     observed = np.array(refdata.iloc[:, column])
34     predicted = np.array(indata.iloc[:, column])
35
36     rmse = rmse_function(observed, predicted, rowcolno[0])
37     rmsedata.append(rmse)
38 rmsedata = rmsedata
39
40 with open(outname, "w", newline='') as outfile:
41     output=csv.writer(outfile)
42     output.writerow(heading)
43     output.writerow(rmsedata)

```

Figure 24: CalcRMSE.py file

3.4 ANALYSIS

Data analysis is the process of systematically transforming data with an objective of creating useful information. Technically, quantitative analysis operates with a concept of transforming reality into numbers (Antwi and Hamza, 2015). Numbers make it easy to establish an order or sequence, as well as to measure and quantify anything; For example, equipment and objects are given serial numbers or licence numbers so that they can be quantified and/or uniquely identified. Quantitative analysis creates no room for bias, due to its numerical nature and mathematical calculations, which greatly reduces personal bias of the researcher (Imanuel, 2018). It gives structure and order to the research data while making it informative, to support or refute a decision using statistical or logical techniques to describe and evaluate data (Simpson, 2015).

The obtained data of monitored air temperature and relative humidity values in this study, are statistical information on how hempcrete buildings operates making it quantitative. Quantitative data easily provide the opportunity to conduct in depth research through detailed statistical analysis. It possesses the ease and rigoristic process adequate enough for measuring various values and numbers, into parameters in a controlled environment for mathematical derivations (Almeida, Faria and Queirós, 2017). Therefore, it comes handy as the ideal analysis

method for the experimental simulation outputs, towards addressing the objectives of this study.

After obtaining the monitored data, the analysis is carried out firstly with Microsoft excel (Microsoft office, 2011) to visually organize the data. Secondly, for calculating the Root Mean Square Error (RMSE) between the monitored and simulated data. Followed by the heat and moisture transfer simulations in EnergyPlus (EnergyPlus, 2016), from which outputs are analyzed and extracted for multi objective optimisation. The analysis of optimisation includes analyzing the solutions on the Pareto front from which the optimum solution will be identified accordingly, based on the objectives of this study. Basically, in multi objective optimisation, there's no single solution that simultaneously optimises each objective; rather, there are (possibly finite) set of solutions (Pareto optimal solutions) (NEOS, 2019). All solutions on the Pareto front are considered equally good; a solution is called Pareto optimal if no solution dominates it and none of the objective functions can be further improved in value without being detrimental to one or more of the other objective values (Mijwel, 2016). In this study, given that the articulation for multi objective optimisation solutions uses the posteriori preference method; the optimisation tool processes and generates the solution on the Pareto front, then the favourable solution from the set of solution alternatives as the optimum solution will be chosen (Augusto, Fouad and Caro, 2012).

Data visualization performed in this study is to support adequate interpretation and representation of results. As well as to understand the change in process and inform data use as applicable (MEALD Pro starter, 2019). The obtained monitored data was organised in Microsoft excel to graphically analyse performance gap by confirming the actual value of temperature and relative humidity, before any simulation experiments were performed. The graphical visualization was carried out to provide a direct comparison of the simulated and actual performance of the data. Quantitative analysis generates any frequencies and levels of difference existing in the data, requiring more visualization and interpretation. After the simulation-based optimisation case is executed, the simulation program produces a number of output files containing the useful results (jEPlus, 2018). In the multi objective optimisation, jEPlus provide various ways to extract data from the output files, including the results from the scatterplot which will be analyzed based on the Pareto optimal solutions.

3.5 VALIDATION

Validation refers to the justification of research methods and knowledge claims (Barlas and Carpenter, 1990). Validation is evidence based, as it develops a research outcome by drawing on the research process undertaken (Paré and Kitsiou, 2017). It helps to confirm the research process while emphasizing the reliability of the research results (Leung, 2015). In this study, after performing the optimisation, the identified accurate parameter for hempcrete simulation will be fed back into the simulation model and simulation will be conducted. The simulation output will then be compared with the measured data from the experimental hempcrete building for validation. It is essential that researchers ensure the quality of their work in every step of the methodology, including data collection, analysis, and interpretation of results, through appropriate validation techniques (Leung, 2015). As such, the purpose of validation in this study is to ensure that each phase of the research methodology rigorously adheres to the adequate standards of simulation quality. Sargent (1991) explicitly explained that “currently no algorithms or procedures are available to identify specific validation techniques and/or statistical tests, etc., to use in the validation process.” Therefore, validation is a challenge to all researchers, especially to those working in interdisciplinary fields such as construction, engineering and management (Lucko and Rojas, 2010). Law (2007) emphasized that validation depends on the specific purpose of the research, which is the aim and objectives of the research.

The process of validation can be broadly divided into two main areas: establishing internal and external validity. Internal validity is related to the concept of causality and is preoccupied with the derivability of relations within data. External validity is related to the concept of induction and focuses on the generalizability of results for prediction purposes (Leedy and Ormrod 2001). Internal validity is influenced by many problems, including ill-defined theoretical models that include factitious relationships or correlated explanatory variables, as well as biases in data collection that render comparisons ineffective, and failure to entertain alternative explanations during data analysis. External validity can be influenced by a variety of issues, including lack of statistical rigor in the selection of sample sizes and in collecting actual data, as well as the presence of any special circumstances during the research efforts, and oversimplification of the phenomena under study (Pannucci and Wilkins, 2010). As well as feeding the research results back into the experimental simulation model for validation, the validation of experimental and multi objective optimisation results will also be carried out with the residential building. It will be carried out by inputting the identified properties of hempcrete for simulation into the

simulation and simulating the residential building. This will demonstrate how the results from this research could be used for hempcrete simulation by any designer and also highlights the outcome of this study. The details of the experiments performed in this study, is as explained in the next chapter.

CHAPTER FOUR

EXPERIMENTATION

Chapter four is the experimentation chapter. It contains detailed explanation of the experiments performed in this study. Section 4.1 describes the simulation of the experimental buildings, which is basically the simulation of the monitored buildings for experiments. Section 4.2 explains the simulation experiments performed in IES Virtual Environment. Section 4.3 describes the calibration of simulation experiment outputs, which includes calculating of root mean square error. Section 4.4 is the Heat and Moisture Transfer Simulation in EnergyPlus, and it explains the ways in which this study investigates the heat and moisture transfer in hempcrete material while reducing the simulation performance gap. Section 4.5 is the Multi objective optimisation stage, which explains the specification of optimisation variables for identifying the accurate representation of hempcrete for simulation.

4.1 SIMULATION OF THE EXPERIMENTAL HEMPCRETE BUILDING

The simulation of the monitored hempcrete buildings was carried out in IES Virtual Environment (IESVE, 2018). The monitored data used for this study was obtained alongside the IES Virtual Environment model of the monitored hempcrete buildings, from Zero Carbon Lab. The monitored hempcrete buildings were first simulated, before performing simulation experiments and the simulation of the hempcrete building model was carried out in IES Virtual Environment (IESVE, 2018). However, the model had to be edited in accordance with the objective of this study. For instance, the original construction materials used for the real-life Hempod building in the walls, roofs and floors had to be re-assigned in the model after it had been obtained. The simulation was then conducted while the model was in passive unregulated free-floating mode, so that no heating or cooling was assigned to the model during the simulations. The simulation output was then collected as the base case model and the root mean square error was calculated between the base case model and the monitored data.

4.2 SIMULATION EXPERIMENTS IN IES VIRTUAL ENVIRONMENT

The experiment ideas explained in chapter 3, section 3.2.1 were used to conduct the experiments for Hempod and for the residential building. The simulation experiments in IES Virtual Environment (IESVE, 2018) includes simulation experiments with conventional and natural materials, as will be explained below in section 4.2.1. Section 4.2.2 contains the simulation experiment in IES Virtual Environment (IESVE, 2018), to investigate properties of

a created material called hempcrete. Section 4.2.1 and 4.2.2 contains details of the experimental simulation for Hempod only. The reason is, Hempod will be used for the IES Virtual Environment (IESVE, 2018) experiments, EnergyPlus simulations and calibration, as well as multi objective optimisation to identify the parameters for hempcrete simulation. The results obtained from the optimisation as the identified parameters for hempcrete simulation, will then be used to simulate the residential building in EnergyPlus (EnergyPlus, 2016) for validation.

4.2.1 Simulation with conventional and natural materials:

In IES virtual Environment (IESVE, 2018) the walls of Hempod was replaced with a combination of different conventional and natural materials, applied to the external walls of Hempod model to replace hempcrete for experimentation. The construction component of Hempod walls was adjusted severally and simulation was performed consecutively, to observe the variations in simulation outputs, including how the construction changes in the walls could affect the performance gap positively by reducing it. A complete detail of all the Hempod simulation experiments conducted with conventional and natural materials using IES Virtual Environment, is shown in Table 8 in Chapter 5, section 5.2. Figure 25 below shows the experiment conducted by using layers of brickwork and weatherboard to represent hempcrete in IES Virtual Environment (IESVE, 2018). It is a detailed example of how all the other experiments with conventional and natural materials were carried out for Hempod, using IES Virtual Environment (IESVE, 2018).

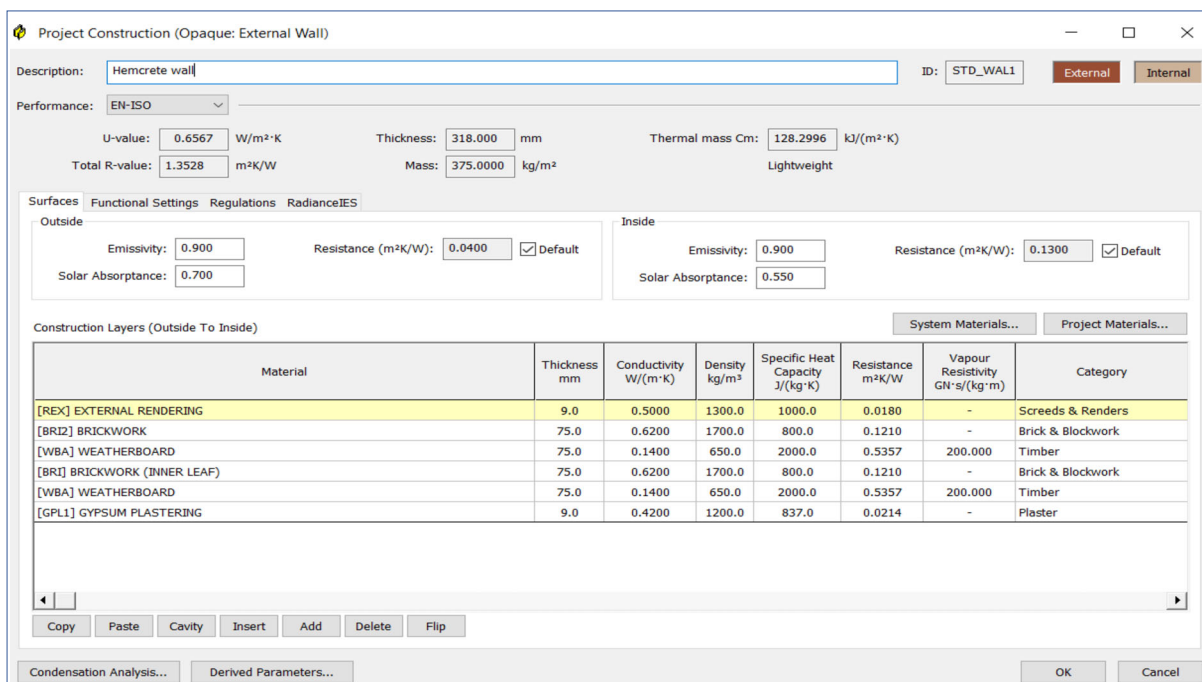


Figure 25: An example of the IES Virtual Environment simulation experiment method

4.2.2 Simulation to investigate properties of a created material named hempcrete:

The simulation of a created material named hempcrete was carried out by using an insulation material from the “system materials” section in IES Virtual Environment (IESVE, 2018). The material was edited and its thermal conductivity, density, specific heat capacity and vapor resistivity was replaced with that of hempcrete as specified by Hempcrete Fact Sheet (Abbott, 2014). The created hempcrete material replaced the Hempod external wall as the hempcrete wall for the simulation experiment. A complete detail of all the Hempod simulation experiments conducted with hempcrete material in IES Virtual Environment, is shown in Table 9 in Chapter 5, section 5.2. However, Figure 26 below is an example from IES of the experiments conducted by creating hempcrete material with layers of 75mm thickness.

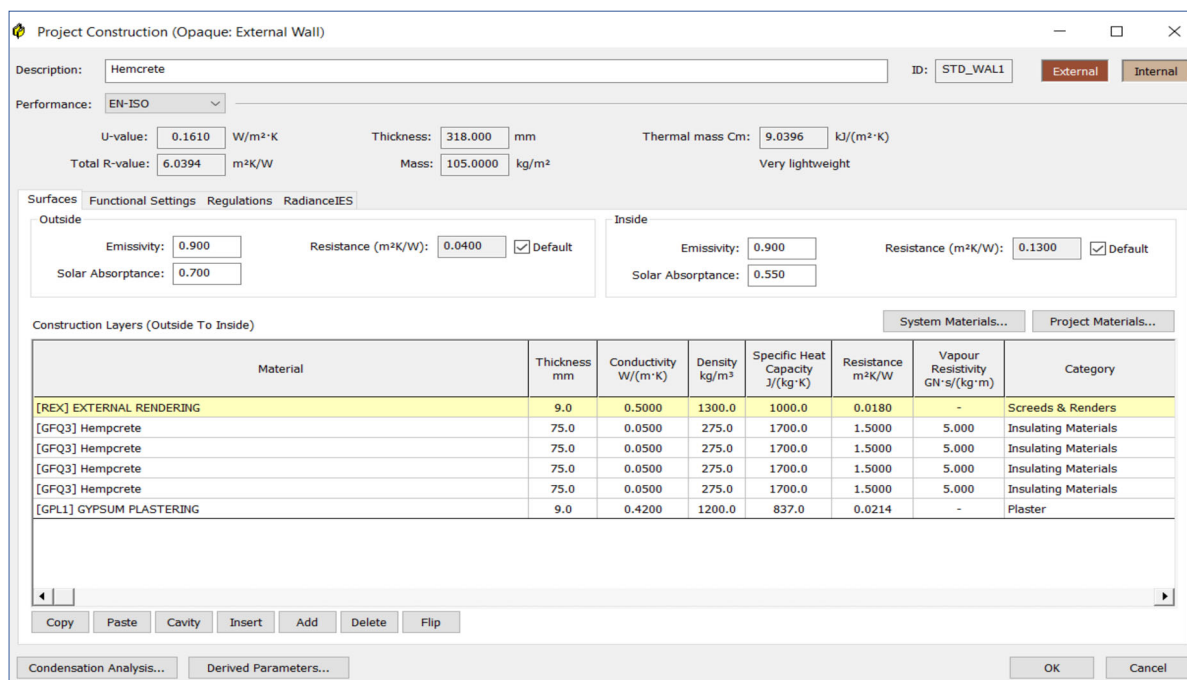


Figure 26: An example of the IES simulation experiment with hempcrete material of 75mm layers thickness

In total, 201 simulation experiments were conducted for Hempod, including experiments with different construction material layers and with the created hempcrete material of different thickness. After the experiments were conducted, the simulation outputs were collected for calibration and for calculating of the root mean square error with the monitored Hempod values, as applicable.

4.3 RMSE CALCULATION WITH SIMULATION EXPERIMENT OUTPUT

The experimental simulation outputs were all collected and collated for calculating root mean square error. Overall, the results from the calibration and root mean square error calculation for Hempod experiments, is compiled, analysed and shown in Table 8 in section 5.2. It shows the simulation experiment done with conventional and natural materials with its corresponding root mean square error results for temperature and relative humidity.

After conducting and calculating the RMSE for the 201 Hempod experiments, the simulation model with the lowest RMSE, is the model to be transported in gbXML format from IES Virtual Environment into Design Builder as explained previously in Chapter 3, Section 3.3.3. The model will then be converted from gbXML into idf format in Design Builder (DesignBuilder, 2018) for EnergyPlus simulations and calibration, towards coupling as an optimisation parameter in jEPlus+EA (jEPlus, 2018).

4.4 ENERGYPLUS HEAT AND MOISTURE TRANSFER SIMULATION

The reason for using heat and moisture transfer (HAMT) simulations is as explained in Chapter 1 Section 1.6 and Chapter 3 in section 3.3.4.

In EnergyPlus (EnergyPlus, 2016), the idf model was imported and opened using the idf editor, below are the details of the HAMT simulations conducted in EnergyPlus;

- i. The Combined Heat and Moisture Finite Element module was selected as the simulation algorithm. EnergyPlus has five heat balance simulation algorithms; the combined heat and moisture finite element was selected as the algorithm for heat and moisture transfer simulation (HAMT) as seen in the Figure 27 below.

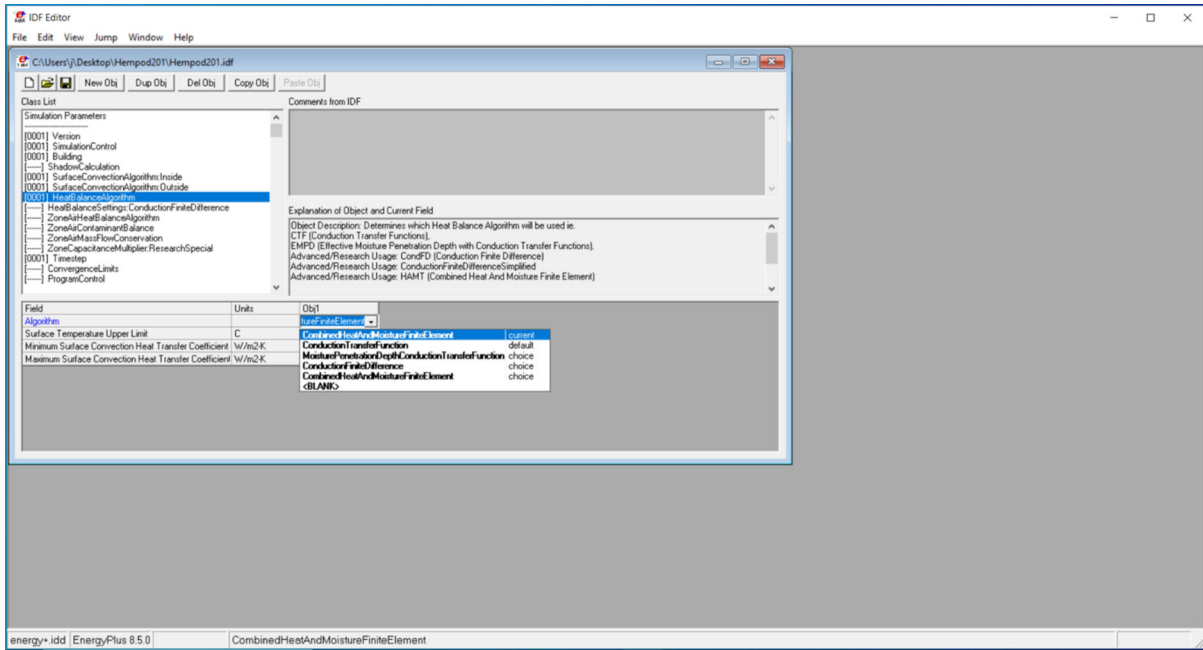


Figure 27: Combined Heat and Moisture Finite Element

- ii. The site location of the Hempod was specified as GBR_ENG_Bristol.Wea.Ctr, which is the EnergyPlus weather file extracted from the downloaded weather zip folder (GBR_ENG_Bristol.Wea.Ctr.037260_TMYx.zip) from EnergyPlus.net. As explained in the “weather file” section of Chapter three section 3.3.5. “Europe – Region 6” from the Climate files – listed in World Metrological Organizations (WMO) Regions. For the heat and moisture transfer simulation, the weather file is as seen below, in Figure 28.

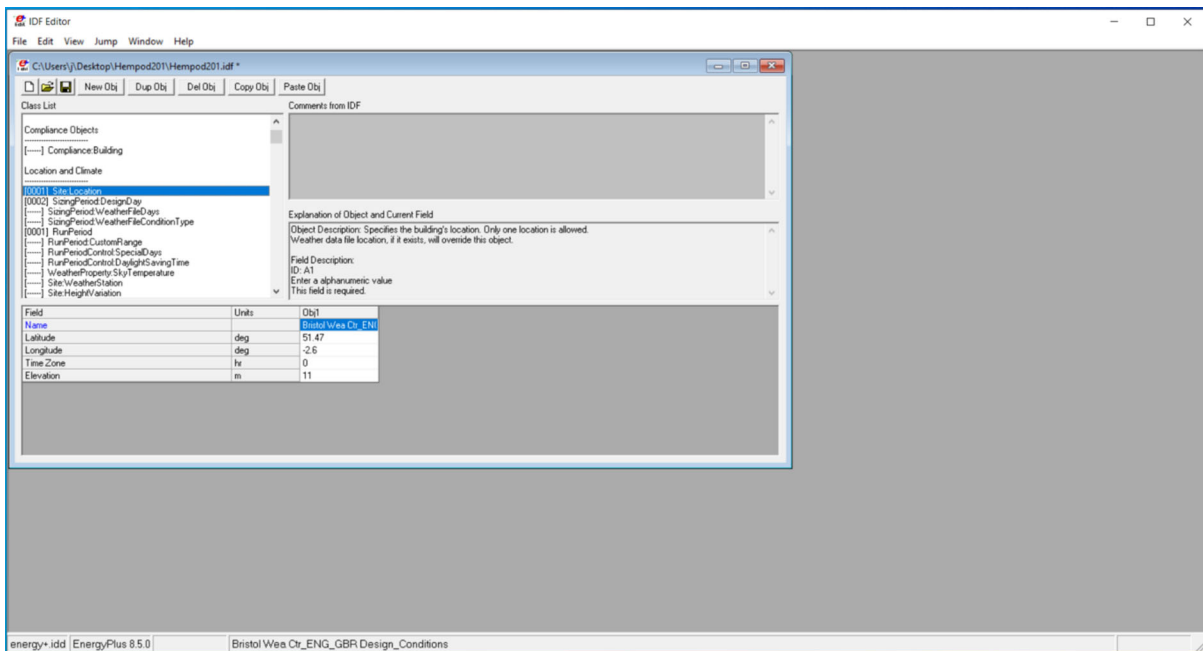


Figure 28: Site location setting for HAMT simulations

- iii. Setting up a model for conducting heat and moisture transfer simulation involves specifying a run period for the simulations. The run period for the heat and moisture simulation was specified for the same period as the monitored Hempod data, which is from 12th March to 4th April (12/3 – 4/4). The begin month and begin day of month as well as end month and end day of month for the simulation was specified in EnergyPlus (EnergyPlus, 2016), as indicated in the Figure 29 below.

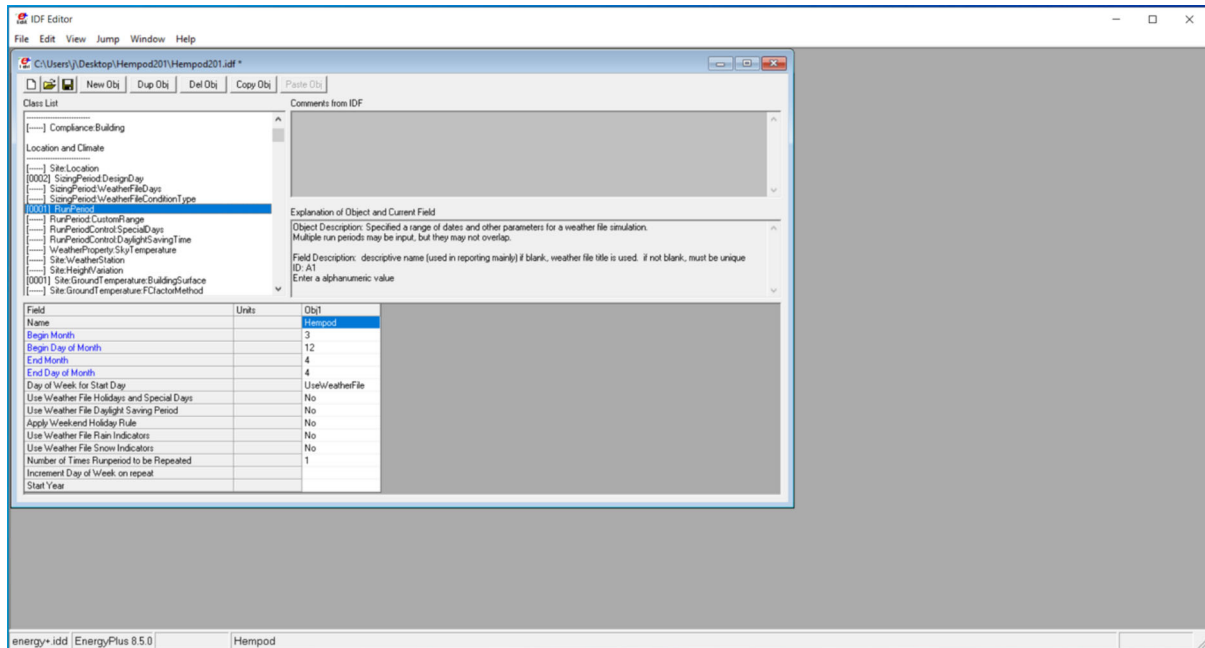


Figure 29: Run Period of HAMT Simulation

- iv. For heat and moisture transfer simulations, there is a material class section in the idf editor that provides for inputting details on material properties required for the simulation of the model. The materials for Hempod was specified in the material section of the idf editor. And the hempcrete material properties (conductivity, density and specific heat) used for the simulation experiments in IES Virtual Environment (IESVE, 2018), were also specified as the hempcrete material properties in EnergyPlus (EnergyPlus, 2016). The material thickness, conductivity, density and specific heat will later be replaced with search strings to investigate for accurate representation of hempcrete material property for simulation. As seen from Figure A1 in Appendix A, the column named “Obj1” for the “material name” was named hempcrete.

- v. In order to carry out detailed investigation of hempcrete material for heat and moisture transfer, the field for material property heat and moisture transfer containing the porosity and initial water content ratio for the material was set to zero. The relationship of porosity and initial water content ratio for hempcrete is unknown. For this reason, the zero value will be replaced with search strings as part of investigating the heat and moisture transfer in the hempcrete material through optimisation. Figure A2 in Appendix A shows the porosity as zero and the initial water content ratio as zero in the column “Obj1”, with material name hempcrete.

- vi. The heat and moisture transfer simulation (HAMT) require that the material property for hempcrete sorption isotherm to be specified. It is represented through the relationship between moisture content and relative humidity fraction in the heat and moisture transfer: sorption isotherm class. However, the moisture content and relative humidity fraction for hempcrete is unknown. Therefore, in order to investigate it, Figure A3 in Appendix A shows the field of moisture content and relative humidity fraction for hempcrete material in the column “Obj3” has zero. The zero will be replaced with search strings later for the optimisation.

- vii. The heat and moisture transfer simulation algorithm also contain the class for heat and moisture transfer called suction, which is the relationship between liquid transport coefficient and moisture content in a material. However, the liquid transport coefficient and moisture content for hempcrete is unknown, therefore the column “Obj1” for hempcrete material is set to zero as seen in Figure A4 in Appendix A.

- viii. The heat and moisture finite element solution algorithm for the heat and moisture transfer simulations (HAMT), contains the Redistribution class. The redistribution represents the relationship between liquid transport coefficient and moisture content of a material for simulation. However, the liquid transport coefficient and moisture content in hempcrete material is unknown. Therefore, the column named “Obj1” with material name hempcrete, has its moisture content and liquid transport coefficient field set as zero as indicated in Figure A5 Appendix A, which will later be replaced with search strings for optimisation.

- ix. The heat and moisture finite element solution algorithm for the heat and moisture transfer simulations contains the Diffusion class. The material property heat and moisture transfer: Diffusion, represents the relationship between water vapor diffusion and relative humidity fraction of a material for simulation. However, the relative humidity fraction and water vapor diffusion resistance factor of hempcrete is unknown. Figure A6 in Appendix A, shows the column “Obj1” with material name hempcrete, has its relative humidity fraction and water vapor diffusion resistance factor as zero. These zeros will be replaced with search string for optimisation.
- x. The heat and moisture finite element solution algorithm for the heat and moisture transfer simulations, contains the moisture dependent thermal conductivity class. The material property heat and moisture transfer: thermal conductivity represents the relationship between thermal conductivity and moisture content for simulation. However, the moisture content and relative humidity value of hempcrete for simulation is unknown. Figure A7 in Appendix A, shows the column named “Obj1” with material name hempcrete, has the moisture content field as zero. And thermal conductivity field was set to 0.05, which is same as the conductivity value used for the simulation experiments of creating the hempcrete material in IES Virtual Environment (IESVE, 2018). However, the moisture content and thermal conductivity value will be replaced with search strings for the optimisation of investigating the appropriate specification for hempcrete simulation.
- xi. The construction class in EnergyPlus, provides for inputting the construction component of the building in layers. It is designed to be specified from the outside layers to the inside layers, for the walls, roofs, floors and windows. It also allows for up to 10 layers of building construction component to be specified. As shown in Figure A8 Appendix A, the construction component for the walls is specified in layers from external rendering through to the internal layer of gypsum plaster board as highlighted in the column “Obj1”.

- xii. Building surface detailed allows for the detailed entry of the building heat transfer surfaces such as walls, floors and roofs for simulations. In the field for construction name, “Walls” was specified from construction class as explained from Figure A8. In the “name” field for building surface detailed class, the four walls in Hempod was specified as south wall, east wall, north wall and west wall as shown in “Obj1 to Obj4” from Figure A9 in Appendix A. This means that the construction component for the south, east, north and west walls has the same hempcrete wall layers as explained in the construction class section.

- xiii. Output variables class settings; command picks variables to be put onto the standard output file after simulations have been conducted in EnergyPlus, as some variables may not be reported for every simulation. However, a list of variables that can be reported are on the report dictionary file (.rdd) with the simulation outputs. Heat and moisture transfer simulation automatically has some default variables in the simulation outputs, such as the zone mean air temperature and zone air relative humidity. As explained in chapter three section 3.3.5 using Figure 20, the list of output variables from EnergyPlus is where optimisation objectives specified in the rvi are extract from. However, if a simulation setting is not correct or not in accordance with the selected heat balance algorithm, there will be no output variables report, only an error report. As seen in Figure A10 Appendix A, “Obj 1” contains Zone mean air temperature and “Obj2” is Zone air relative humidity in the output variables class settings.

After all of the heat and moisture transfer simulation settings in EnergyPlus idf editor for Hempod was concluded, the model was saved, and simulation was performed. Simulation was performed in EnergyPlus because EnergyPlus provides error report with simulation outputs. It is necessary to make sure there are no errors from the EnergyPlus heat and moisture transfer simulations, before saving the idf to be used for optimisation. The reason is, during the course of the experiments and calibration in this study, an idf model with errors was coupled into jeplus for optimisation and there were no results from the optimisation. Instead, there was an error report from jEPlus+EA referring to an error in the EnergyPlus idf model. Therefore, after the heat and moisture transfer simulations was conducted, the idf was saved to be coupled into jEPlus as will be explained in the section 4.5 below.

4.5 MULTI OBJECTIVE OPTIMISATION IN jEPlus+EA

Performing the multi objective optimisation follows on from the EnergyPlus heat and moisture transfer simulations. In order to perform the optimisation in jEPlus+EA (jEPlus, 2018), the “Hempod 201” model is transported from EnergyPlus in idf format into a job folder, to create the jEPlus project. As explained using Figure 19 in section 3.3.5 of chapter three, a jEPlus project file contains a weather file, a rvi or rvx file, EnergyPlus input data file (.idf), parameter tree and parameter item section. Figure 30 below, shows the jEPlus project used in this study, the list of parameter trees and parameter item.

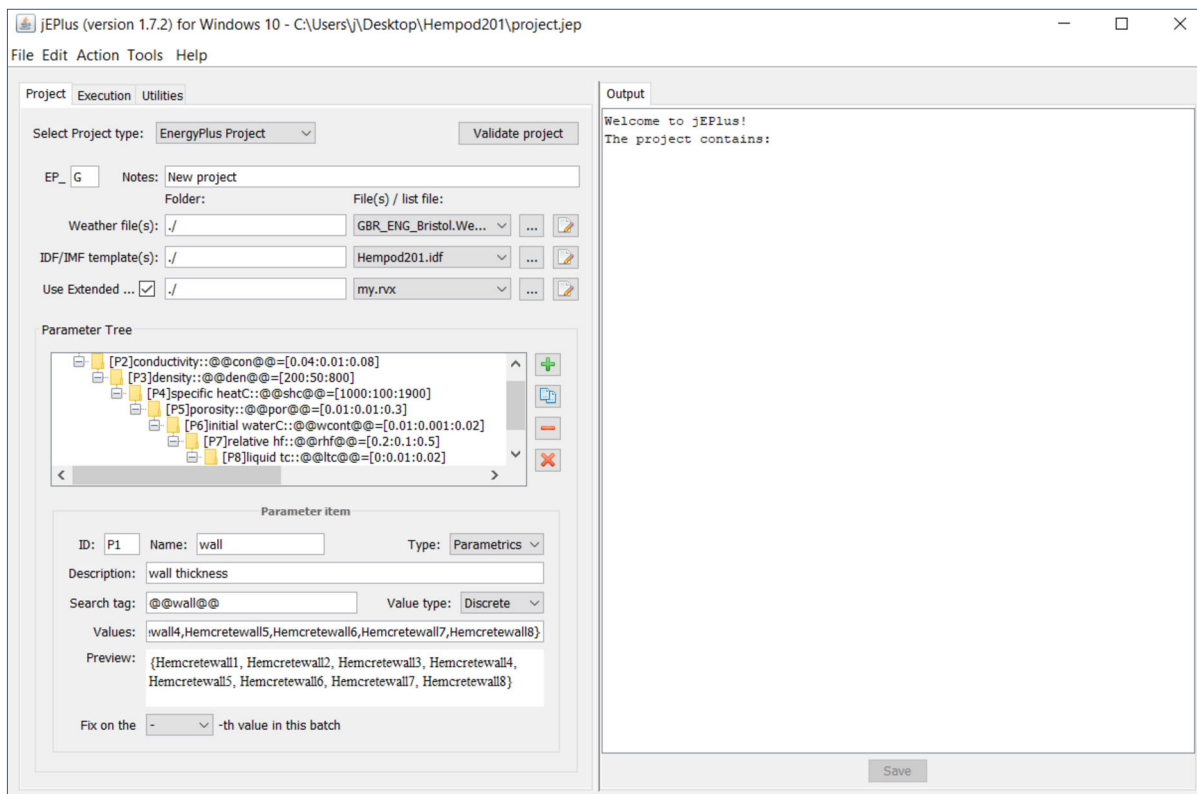


Figure 30: A jEPlus project

The list of parameter tree and their corresponding parameter item is as explained below:

- i. Wall is Parameter P1; The wall thickness is important in order to identify the accurate parameters for hempcrete simulation. As seen above from the experiments conducted in IES Virtual Environment (IESVE, 2018), specifying the thickness of a material or construction component during simulation is important. In order to investigate the wall thickness for hempcrete simulation, the wall construction component from the “construction class” above in Section 4.4 explained using Figure A8, was renamed from “Walls” to “Hemcretewall”. Seven more wall construction components were

added in the construction class section of the idf. by creating a wall thickness of 0.05m to 0.4m through representing it as Hemcretewall1 (0.05m), Hemcretewall2 (0.1m), Hemcretewall3 (0.15m), Hemcretewall4 (0.2m), Hemcretewall5 (0.25m), Hemcretewall6 (0.3m), Hemcretewall7 (0.35m) and Hemcretewall8 (0.4m) as seen from Figure 31 and 32 below.

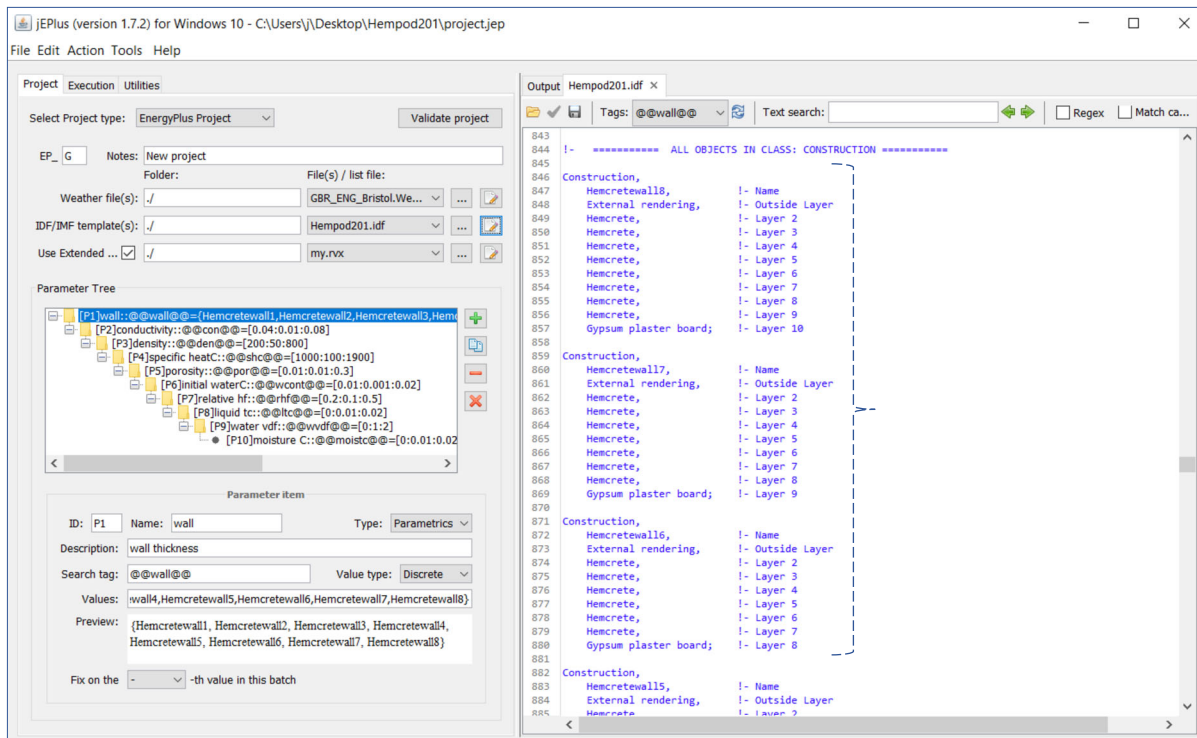


Figure 31: Showing Hemcretewall8, Hemcretewall7 and Hemcretewall6

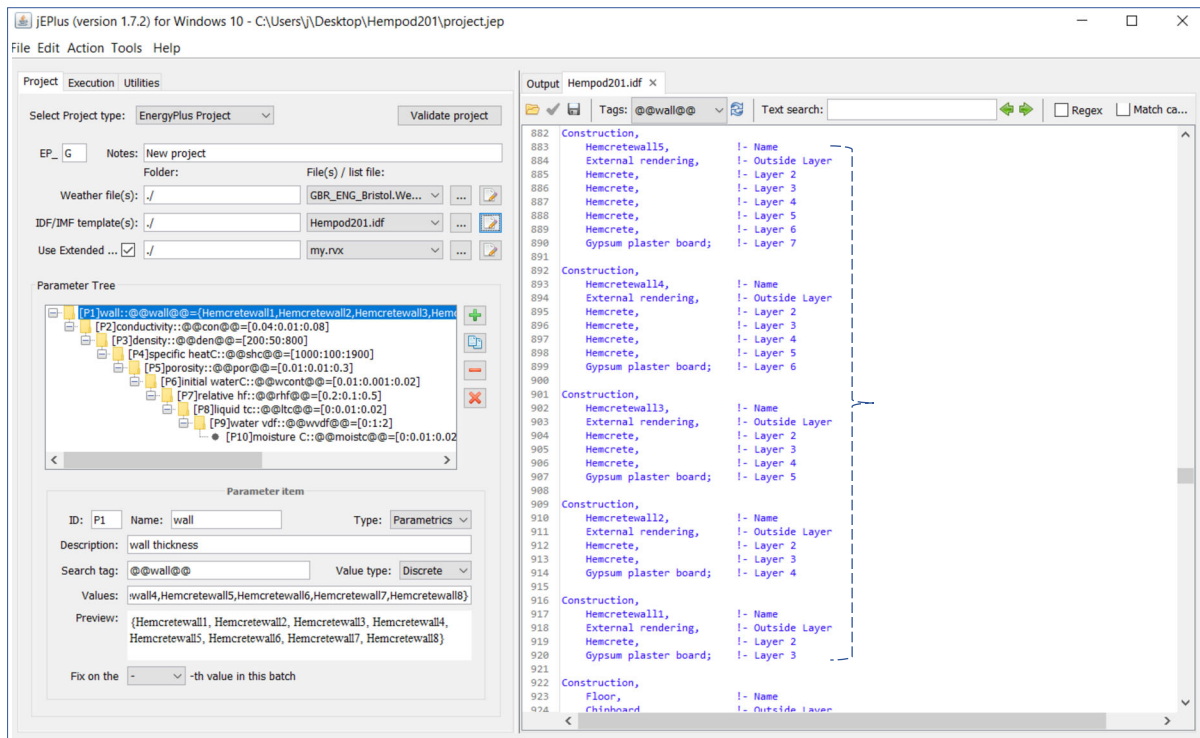


Figure 32: Showing Hemcretewall5, Hemcretewall4, Hemcretewall3, Hemcretewall2 and Hemcretewall1

After the material layer from the construction class section in the idf was replaced with different composition of Hemcretewall1 to Hemcretewall8. A parameter was created, named walls and described as “wall thickness” in the parameter description section as seen in the Figure 33 below. The search tag for the “Walls” parameter is @@wall@@, the parameter value type is discrete, and the values were represented as {Hemcretewall1,Hemcretewall2,Hemcretewall3,Hemcretewall4,Hemcretewall5,Hemcretewall6,Hemcretewall7,Hemcretewall8} as seen in the Figure 33 below.

In the building surface: detailed class of the idf, the field of construction name which was previously named “Walls” for the south, east, north and west wall from Figure A9 is now replaced with the search string @@wall@@. This means that the optimisation will investigate the appropriate wall thickness to reduce the simulation performance gap for the south, east, north and west wall from the wall options of: Hemcretewall1 (0.05m), Hemcretewall2 (0.1m), Hemcretewall3 (0.15m), Hemcretewall4 (0.2m), Hemcretewall5 (0.25m), Hemcretewall6 (0.3m), Hemcretewall7 (0.35m) and Hemcretewall8 (0.4m) as seen from Figure 33 below. The search string @@wall@@ will be replaced by the above values when conducting parametric simulations and multi-objective optimisation.

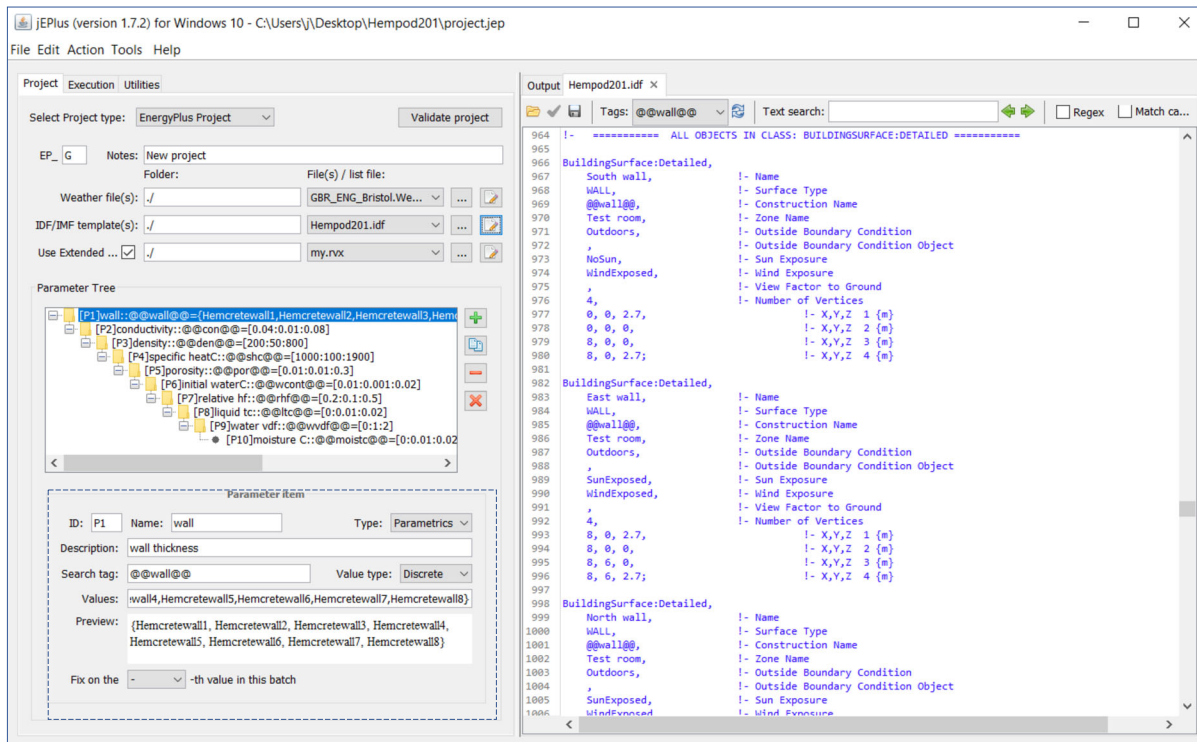


Figure 33: Showing the wall optimisation parameter specification

- ii. Thermal Conductivity: in order to investigate the thermal conductivity for the hempcrete material simulation, the material property section in the .idf for Hempod 201 model was edited. It was edited by representing thermal conductivity with the search string @@con@@ as seen in the search tag section of Figure B1 in Appendix B. The value type for the conductivity parameter was selected as double, with the values ranging from 0.04 to 0.2 at 0.01 interval. Therefore, optimisation for thermal conductivity with this specified parameter, means that the wall conductivity will be explored at 0.04, 0.05, 0.06, 0.07, 0.08, 0.09, 0.1, 0.11, 0.12, 0.13, 0.14, 0.15, 0.16, 0.17, 0.18, 0.19 and 0.2 as seen in the “preview” section from Figure B1 in Appendix B.
- iii. Density: the density of the hempcrete material for simulation, was investigated by representing the material class section with search string @@den@@ as the search tag. The value type for the density parameter was selected as integer, with the values ranging from 200 to 800 as seen from Figure B2 in Appendix B.
- iv. Specific Heat Capacity: The specific heat capacity for the hempcrete material was replaced with a search string @@shc@@ in the material class section of the idf

model. And the range for the optimisation parameter of specific heat capacity was 1000 to 2500 as seen in Figure B3 in Appendix B.

- v. The material property: Heat and moisture transfer: settings, contains the porosity field. To investigate the porosity from the material property heat and moisture transfer simulation, the porosity field, which was set to zero as explained using Figure A2, is replaced with the search string @@por@@. And the parameter value type was double, with the values ranging from 0.01 to 0.5 as seen in Figure B4 in Appendix B.
- vi. The material property; Heat and moisture transfer: settings class, also contains the initial water content ratio field. The initial water ratio field for hempcrete is 0 as explained in section 4.4 using Figure A2. Therefore, in order to investigate for simulation, the initial water content ratio field which was set to zero is replaced with the search string @@wcont@@ as the search tag. The value type was selected as double, with the values ranging from 0.01 to 0.05 as seen in Figure B5 in Appendix B.
- vii. The Material Property heat and moisture Transfer; Sorption Isotherm - represents the relationship between moisture content and its corresponding relative humidity fraction in the material. For each humidity value, a sorption isotherm indicates the corresponding water content value at a given, constant temperature. It includes relative humidity fraction and moisture content in the parameter field. The moisture content field for hempcrete is zero as explained in Section 4.4, using Figure A3. Therefore, in order to investigate for simulation, the moisture content field which was set to zero is replaced with the search string @@moistc@@ as the search tag. And the value type was selected as double with the values in range of 0.0 to 0.02 as seen in Figure B6 in Appendix B.
- viii. The Material Property heat and moisture Transfer; Sorption Isotherm contains the relative humidity fraction field. The relative humidity fraction field for hempcrete is zero as explained in Section 4.4 using Figure A3. Therefore, in order to investigate for simulation, the relative humidity fraction field which was set to zero is replaced with the search string @@rhf@@ as the search tag. The value type for the parameter

was selected as double, with the values ranging from 0.1 to 1.0 as seen in Figure B7 in Appendix B.

- ix. The Material Property heat and moisture Transfer; Suction - relates the liquid transport coefficient in suction, to the water content of a material. It includes moisture content and liquid transport coefficient in its parameter field. The moisture content field for hempcrete is zero as explained in Section 4.4 using Figure A4. Therefore, in order to investigate for simulation, the moisture content field which was set to zero is replaced with the search string @@moistc@@ as the search tag. The value type was selected as double and the values was in range of 0.0 to 0.02 as seen in Figure B8 in Appendix B.
- x. The Material Property heat and moisture Transfer; Suction contains the liquid transport coefficient. The liquid transport coefficient field, for hempcrete is zero as explained in Section 4.4 using Figure A4. Therefore, in order to investigate for simulation, the liquid transport coefficient which was set to zero is replaced with the search string @@lrc@@ as the search tag. The value type was selected as double and the values was in range of 0.0 to 0.02 as seen in Figure B9 in Appendix B.
- xi. The material Property heat and moisture Transfer; Redistribution - relates the liquid transport coefficient to the water content of a material under normal conditions (energyplus.net). It includes moisture content and liquid transport coefficient in its parameter field, the liquid transport coefficient at the highest entered water content value is used for all liquid transport coefficient values above this water content. The liquid transport coefficient field, for hempcrete is zero as explained in Section 4.4 using Figure A5. Therefore, in order to investigate for simulation, the liquid transport coefficient which was set to zero is replaced with the search string @@lrc@@ as the search tag. The value type was selected as double and the values was in range of 0.0 to 0.02 as seen in Figure B10 in Appendix B.
- xii. The material Property heat and moisture Transfer; Redistribution also contains the moisture content field. The moisture content field for hempcrete is zero as explained in Section 4.4 using Figure A5. Therefore, in order to investigate for simulation, the moisture content field which was set to zero is replaced with the search string

@@moistc@@ as the search tag. The value type was selected as double and the values was in range of 0.0 to 0.02 as seen in Figure B11 in Appendix B.

- xiii. The material Property heat and moisture Transfer; Diffusion - relates the vapor diffusion resistance factor to its relative humidity fraction in the material. It includes relative humidity fraction and water vapour diffusion resistance factor in the parameter field. The relative humidity fraction field for hempcrete is zero as explained in Section 4.4 using Figure A6. Therefore, in order to investigate for simulation, the relative humidity fraction field which was set to zero is replaced with the search string @@rhf@@ as the search tag. The value type for the parameter was selected as double, with the values ranging from 0.1 to 1.0 as seen in Figure B12 in Appendix B.
- xiv. The material Property heat and moisture Transfer; Diffusion also contains the water vapour diffusion resistance factor field. The water vapour diffusion resistance factor field for hempcrete is zero as explained in Section 4.4 using Figure A6 and the zero was replaced with the search string @@wvdf@@ as the search tag. The value type was selected as integer and the values was in range of zero to 10 as seen in Figure B13 in Appendix B.

After all the optimisation parameters have been specified and the search strings applied to the idf, the jEPlus project is then saved in the optimisation folder. As earlier explained in Chapter three, Section 3.3.5 using Figure 23; a jEPlus+EA optimisation contains a ref file, CalcRMSE, jEPlus project file (.jep), weather file, my.rvi, my.rvx file and idf.

The ref file is the monitored Hempod values in Microsoft excel. The CalcRMSE file is the Python 3 script file, which uses the details of the set objectives, from the extracted rvi file and the created rvx file in the idf model (jeplus.org). The optimization objectives in this study, were set to minimize Root Mean Square Error (RMSE) from temperature ($t_0=v_0$) and relative humidity ($t_1=v_1$). The jEPlus+EA optimisation folder was created as seen below in Figure 34 and optimisation.

Name	Date modified	Type	Size
CalcRMSE	20/11/2017 12:17	Python File	2 KB
GBR_ENG_Bristol.Wea.Ctr.037260_TMYx.e...	23/04/2019 05:32	EPW File	1,524 KB
Hempod201	22/02/2020 03:35	EnergyPlus Input D...	67 KB
my.rvi	25/01/2019 00:28	RVI File	1 KB
my.rvx	30/04/2019 16:49	RVX File	2 KB
projectjep	22/02/2020 03:23	JEP File	28 KB
ref	06/01/2020 00:50	Microsoft Excel Co...	17 KB

Figure 34: jEPlus+EA Optimisation folder

The optimisation parameters was saved and the jEPlus project was then launched for optimization in jEPlus+EA. The jEPlus project file was opened in jEPlus+EA (jEPlus, 2018), the optimisation parameters specified in jEPlus project was then validated and passed in jEPlus+EA. The optimisation is ready to be performed by clicking the “start” tab indicated in the user interface for jEPlus+EA as seen in Figure 35 below.

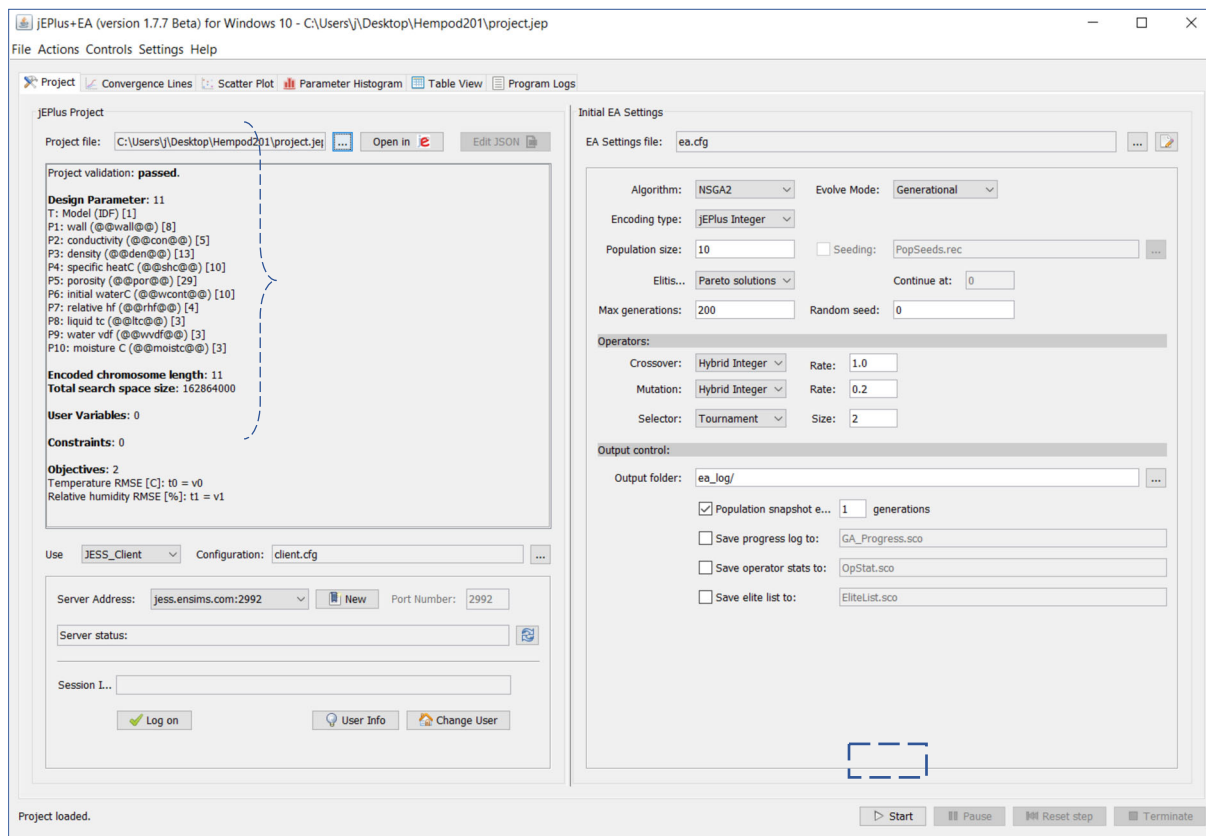


Figure 35: jEPlus+EA interface showing loaded jEPlus project with parameters ready for optimisation

Multi objective Optimization was carried out as explained in Chapter 3 Section 3.3.5 and in Section 4.5 to identify the optimum solution from the *Hempod 201* simulations. After the jEPlus project was launched for optimization in jEPlus+EA (jEPlus, 2018), the optimization generated a scatterplot from the post processing showing the optimum solutions from the Pareto solutions as optimisation outputs. Figure 36 below, is a scatterplot from the post processing showing the optimum solution chosen from the generated Pareto solutions as optimisation outputs. The properties of hemcrete simulation was identified for: Conductivity, Density, Specific Heat Capacity, Porosity, Initial water content, Relative humidity fraction, Liquid transport co-efficient, Water vapor diffusion resistance factor and Moisture content, as seen from the Figure 36 below.

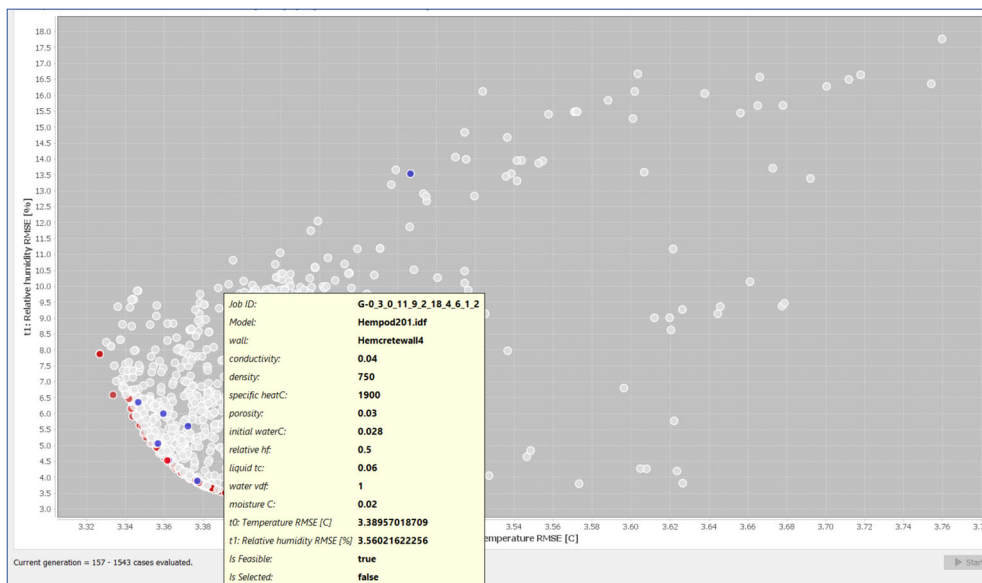


Figure 36: Scatterplot from the multi objective optimisation

The optimisation solution detail from Figure 36 above, was inputted back into EnergyPlus for analysis and validation. The EnergyPlus simulation reported a severe error as seen in Figure 37 below.

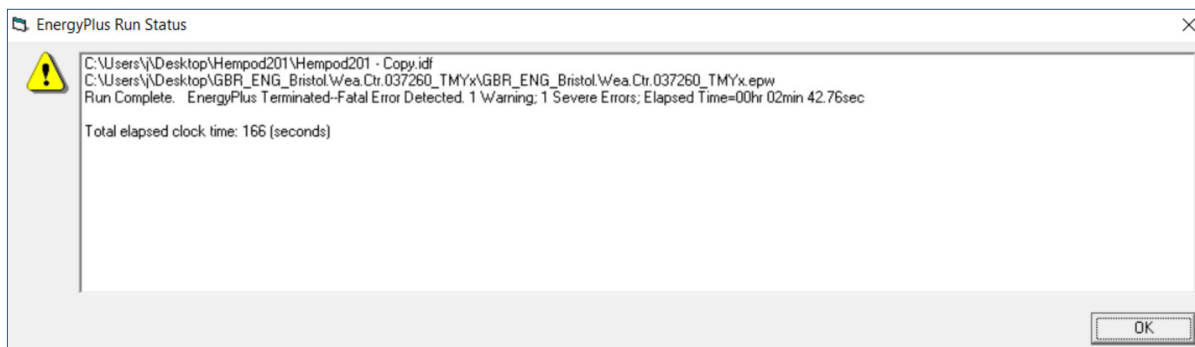


Figure 37: EnergyPlus simulation output for the optimisation results from Figure 36

The severe error reported “*temperature high out of bounds for the Hempod surface – south wall*”. Over the course of the simulations in this study, it has been observed that whenever an EnergyPlus simulation comes back with “severe error”, it also means that there is no available output for that simulation. Specifically, the excel file simulation outputs needed for calculating root mean square error as applicable. After the error in Figure 37 was reported, the optimisation process was reiterated.

The reiteration of multi objective optimisation was carried out by editing the EnergyPlus .idf. The class list “Building” parameter for EnergyPlus heat and moisture transfer simulation is used to describe parameters that are used during the simulation of the building. The reason is, there are necessary correlations between the entries for this object and some entries in the site weather station and site height variation, specifically the terrain field (EnergyPlus, 2016). In the “Building” simulation parameter, the field for orientation and the field for temperature convergence tolerance value which is 0.4 by default will be replaced with search strings. Figure 38 below shows the “Building” class list parameter in EnergyPlus for heat and moisture transfer simulation.

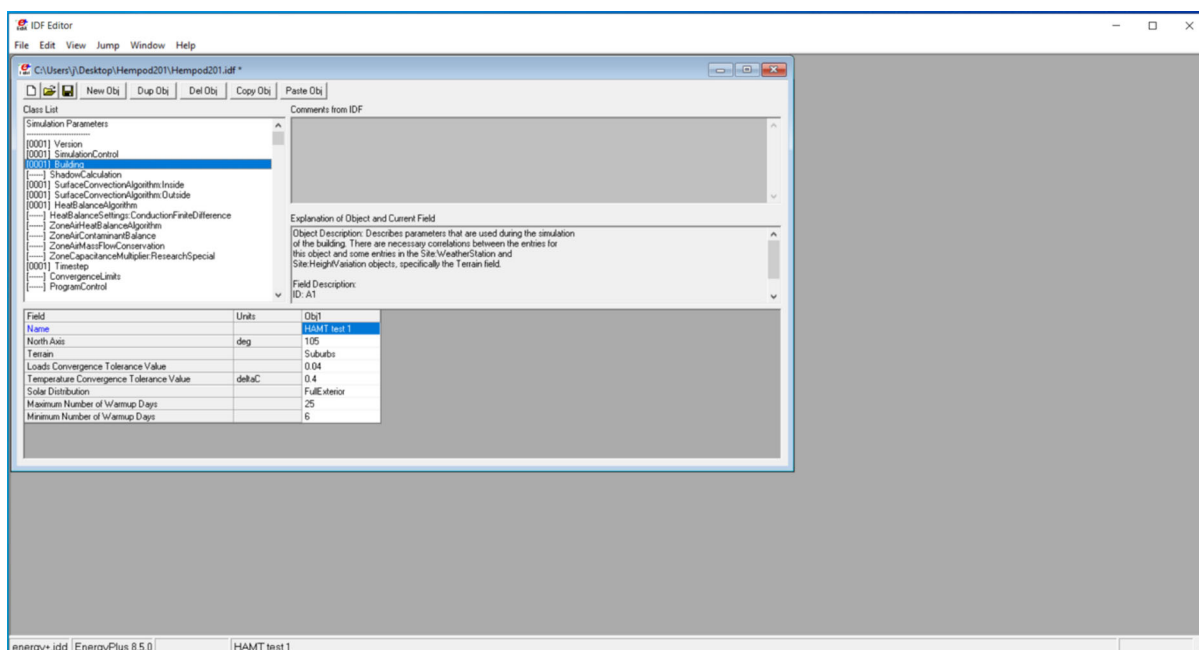


Figure 38: Building parameter for HAMT Simulations

The orientation field was replaced with a search string @@orientation@@ as the search tag. The value type for the orientation parameter was selected as integer, with the values ranging from 0° to 360°, with 15° interval as seen in Figure B14 in Appendix B.

The field name for temperature convergence tolerance value, was replaced with search string @@tempconv@@ as the search tag. The value type was selected as double, ranging from 0.001 to 0.4 with an interval of 0.001 as seen in Figure B15 in Appendix B.

The material property; heat and moisture transfer settings field for porosity and initial water content ratio was also replaced with search strings. Porosity was replaced with the search string @@por@@, the parameter value type was selected as double, with the values ranging from 0.01 to 0.5 as seen in Figure B16 in Appendix B.

The initial water content ratio field was replaced with the search string @@moistr@@ as the search tag and the values type was double, ranging from 0.001 to 0.1 as seen in Figure B17 in Appendix B.

All the field's for "Material" class was investigated to identify the parameter for hempcrete simulation. The material thickness, conductivity, density, specific heat, thermal, solar and visible absorptance as shown in Figure B18 in Appendix B, will be replaced with search strings for optimisation.

For material thickness, the search tag for the "Walls" parameter was still @@wall@@, the parameter value type was selected as discrete, and the values were represented as {Hempcretewall1,Hempcretewall2,Hempcretewall3,Hempcretewall4,Hempcretewall5,Hempcretewall6,Hempcretewall7,Hempcretewall8} same as the earlier optimisation.

In the building surface: detailed class of the idf, the field of construction name which was previously named "Walls" for the south, east, north and west wall is replaced with the search string @@wall@@ as seen in Figure 39 below. This means that the optimisation will investigate the appropriate wall thickness to reduce the simulation performance gap for the south, east, north and west wall from the wall options of: Hempcretewall1 (0.05m), Hempcretewall2 (0.1m), Hempcretewall3 (0.15m), Hempcretewall4 (0.2m), Hempcretewall5 (0.25m), Hempcretewall6 (0.3m), Hempcretewall7 (0.35m) and Hempcretewall8 (0.4m) as seen from Figure 39 below.

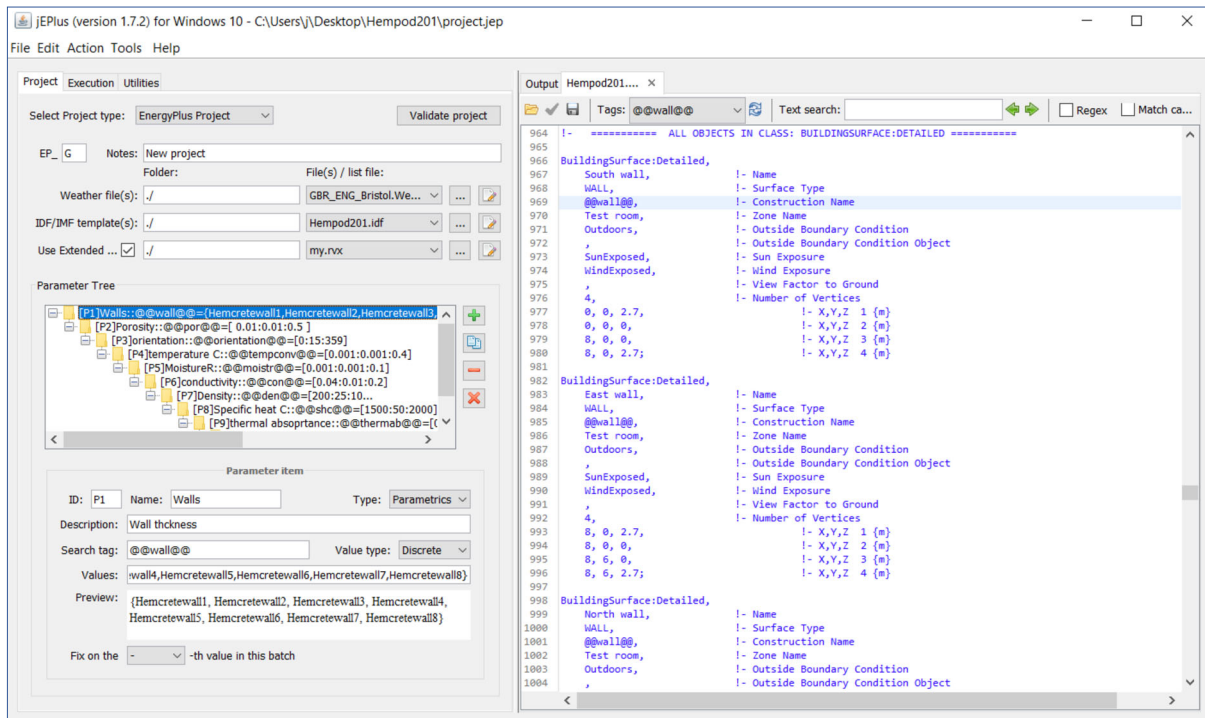


Figure 39: showing the wall optimisation parameter specification

The investigation of thermal conductivity for the hempcrete material simulation, was performed by representing thermal conductivity with the search string @@con@@ as the search tag. The value type for the conductivity parameter was selected as double, with the values ranging from 0.04 to 0.2 at 0.01 interval as seen in Figure B19 in Appendix B.

In order to investigate density of the hempcrete material for simulation, the material class section for density was replaced with search string @@den@@ as the search tag. The value type for the density parameter was selected as integer, with the values ranging from 200 to 1000 at an interval of 25 as seen in Figure B20 in Appendix B.

The investigation of specific heat capacity for the hempcrete material simulation was performed by replacing specific heat capacity with the search string @@shc@@ as the search tag. The value type was selected as integer and the value range from 1500 to 2000 at interval of 50 as seen in Figure B21 in Appendix B.

As mentioned earlier, the fields for solar absorptance, thermal absorptance and visible absorptance was replaced with search strings. They are fields in the “Material” class list in

EnergyPlus HAMT simulation settings, responsible for simulating the solar, thermal and visible absorptance of a material.

The thermal absorptance field was replaced with the search string `@@thermab@@` as the search tag. The thermal absorptance value of hempcrete for simulation is unknown. However, EnergyPlus has defined that the thermal absorptance, solar absorptance and visible absorptance of any material is between 0.0 to 0.9. Therefore, it cannot be lower than 0.0 or higher than 0.9. Hence, the value type for thermal absorptance was selected as double, ranging from 0.1 to 0.9 with interval of 0.05 as seen in Figure B22 in Appendix B.

The visible absorptance was replaced with search string `@@visab@@` as the search tag and the value type was selected as double, ranging from 0.1 to 0.9 with interval of 0.05 as seen in Figure B23 in appendix B.

The solar absorptance for hempcrete simulation was investigated using search string `@@solab@@` as the search tag. The value type was selected as double, ranging from 0.1 to 0.9 with interval of 0.05 as seen in Figure B24 in appendix B.

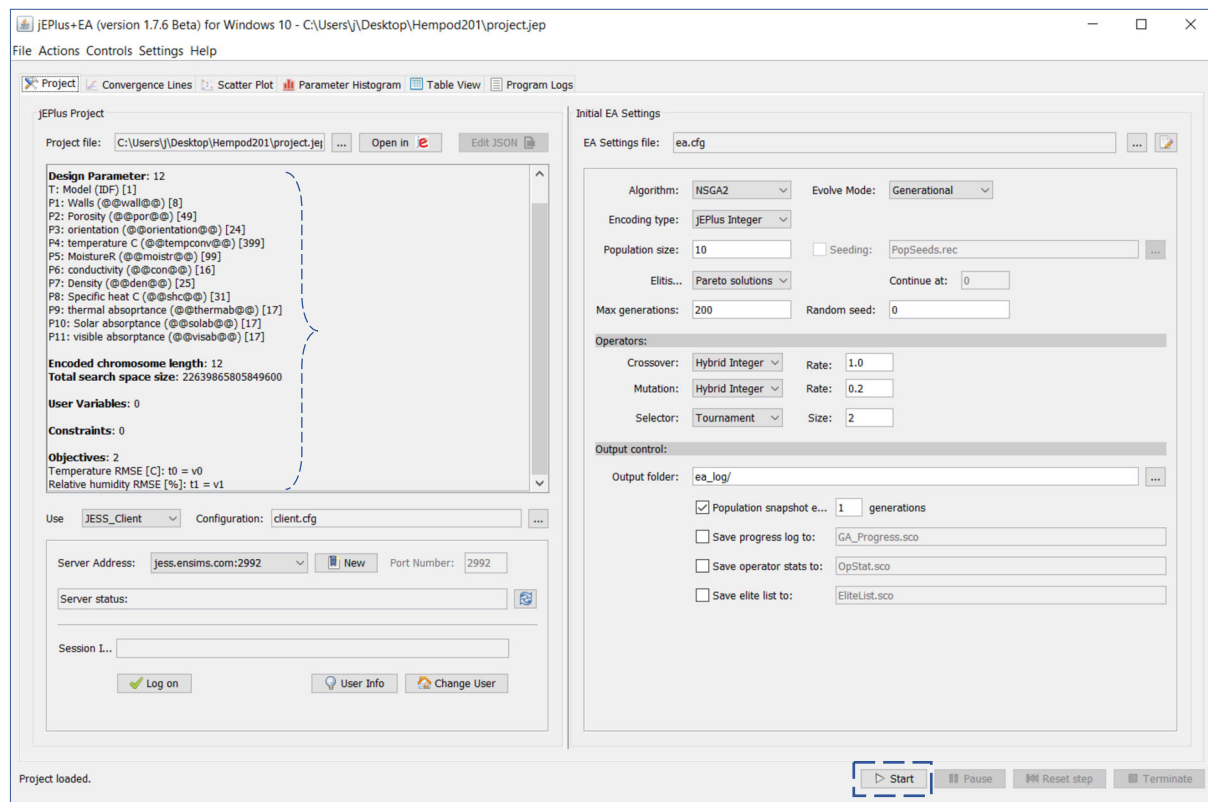


Figure 40: jEPlus+EA interface showing loaded jEPlus project with parameters ready for optimisation

Figure 40 above shows the optimisation interface of a loaded project. After setting up the parameters in the EnergyPlus (idf) for multi objective optimisation, the jEPlus project was saved again into a new folder for jEPlus+EA optimisation and the optimisation was launched. The jEPlus project file was opened in jEPlus+EA, the optimisation parameters specified in jEPlus project was then validated and passed in jEPlus+EA. The optimisation job variables, had a total of 12 design parameters and total search space of over one billion to be explored, during the optimisation process as seen in the Figure 40 above. The optimisation process was then performed by clicking the “start” tab indicated in the user interface for jEPlus+EA as seen in Figure 40 above. The details of the optimisation will be analyzed in the next chapter.

CHAPTER FIVE

ANALYSIS

Chapter five is the analysis chapter, where the data analysis, simulation output analysis and optimisation solution analysis will be carried out. Section 5.1 is the monitored and simulated analysis section. Section 5.2 is the root mean square error analysis for the simulation experiments carried out in this study. Section 5.3 contains the analysis of the multi objective optimisation results from the Pareto front and identifies the parameters for hempcrete simulation. Section 5.4 contains the reference list for this chapter.

5.1 MONITORED AND SIMULATED DATA ANALYSIS

The obtained monitored data was organised in Microsoft excel to analyse performance gap by confirming the actual value of temperature, relative humidity and the weather/climatic data before simulation experiments were performed.

Figure 41 below show the monitored weather values for temperature of Hempod and Figure 42 show the monitored weather values for relative humidity of Hempod.

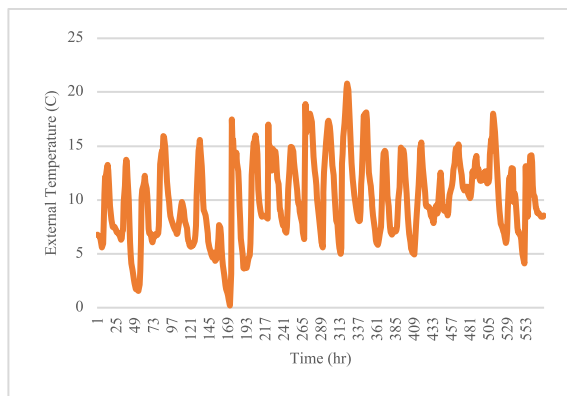


Figure 41: Monitored external Temperature Values

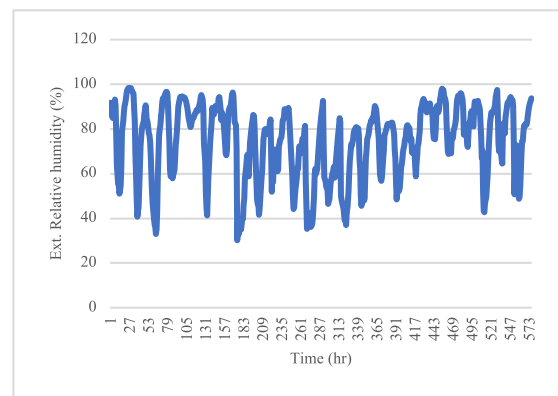


Figure 42: Monitored external Rel. humidity values

Figure 43 below show the IESVE simulated weather values for temperature of Hempod and Figure 44 show the IESVE simulated weather values for relative humidity of Hempod respectively.

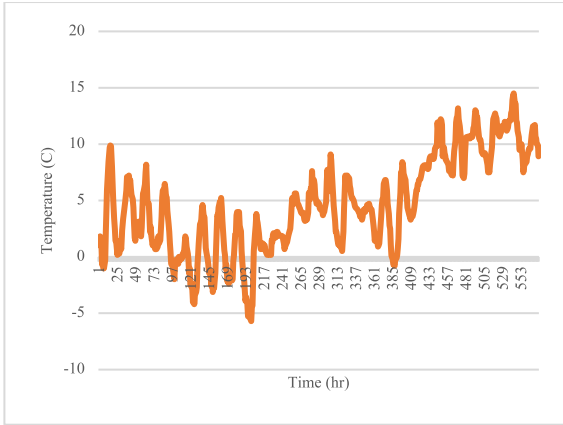


Figure 43: Hempod simulated temperature

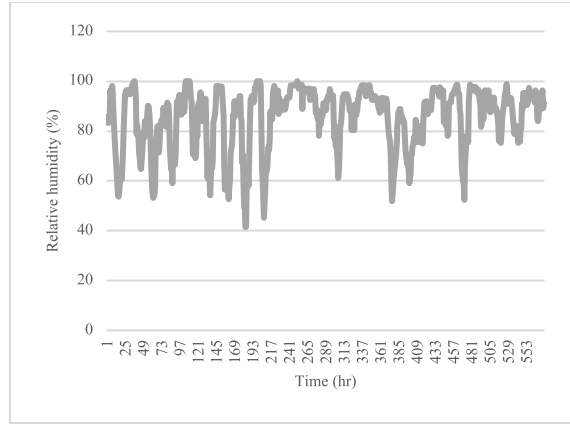


Figure 44: Hempod simulated rel. humidity

Figure 45 below show the monitored weather values for temperature of the residential building and Figure 46 below, show the monitored weather values for relative humidity of the residential building respectively.

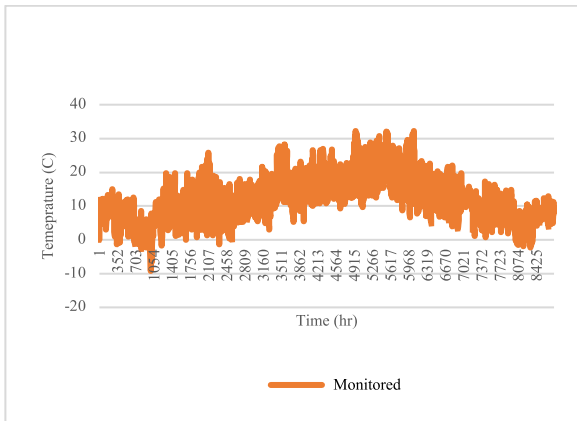


Figure 45: Monitored external Temperature Values

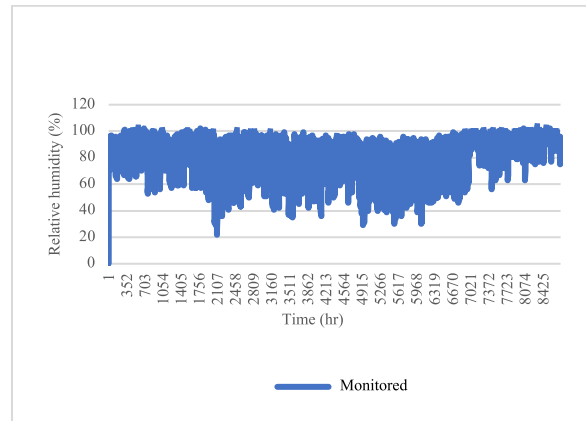


Figure 46: Monitored external Rel. humidity values

Figure 47 below show the IESVE simulated weather values for temperature of the residential building and Figure 48 show the IESVE simulated weather values for relative humidity of the residential building respectively.

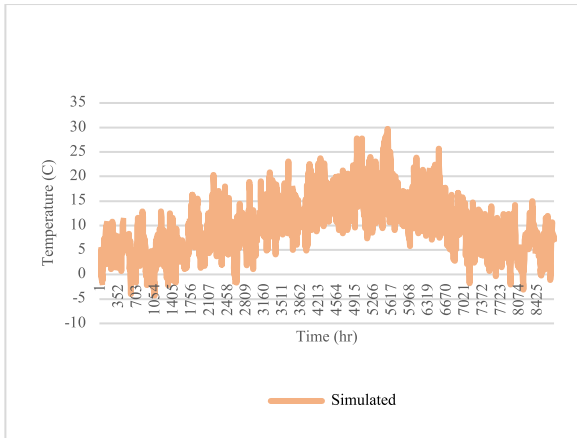


Figure 47: Simulated weather for temperature

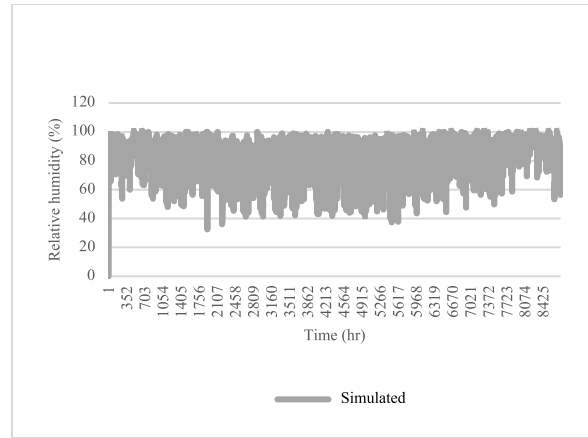


Figure 48: Simulated weather for rel. humidity

5.1.1 Base case simulation analysis for Hempod

Before any experimental modelling and simulations were performed, the obtained Hempod model was simulated in passive unregulated free-floating mode to create the base case scenario. Figure 49 below show the monitored internal temperature values for hempod and Figure 50 below, show the monitored internal relative humidity values of Hempod respectively.

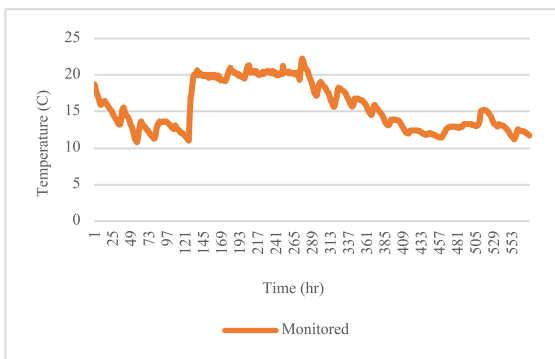


Figure 49: Monitored Temperature Values

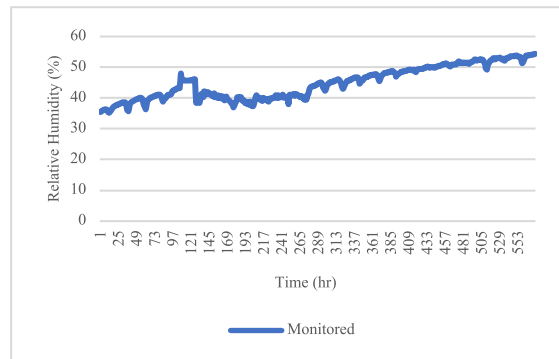


Figure 50: Monitored Rel. humidity values

Figure 51 below show the simulated internal temperature values for hempod and Figure 52 below, show the simulated internal relative humidity values of Hempod respectively.

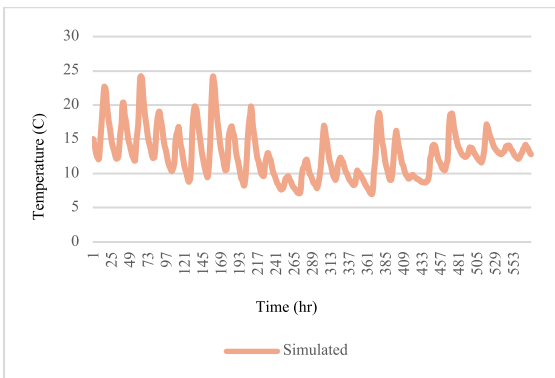


Figure 51: Hempod simulated temperature

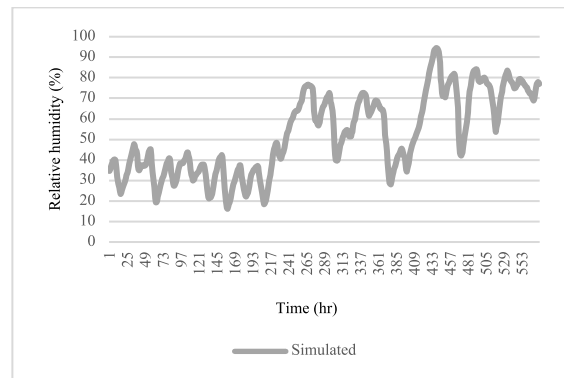


Figure 52: Hempod simulated rel. humidity

In order to analyse and obtain the base case for Hempod, the difference between the monitored and simulated values were graphically visualised and root mean square error calculated. Figure 53 below show the base case for the internal temperature of hempod, which is the output of RMSE as 5.5°C and Figure 54 below show the base case for relative humidity as 18.0%.

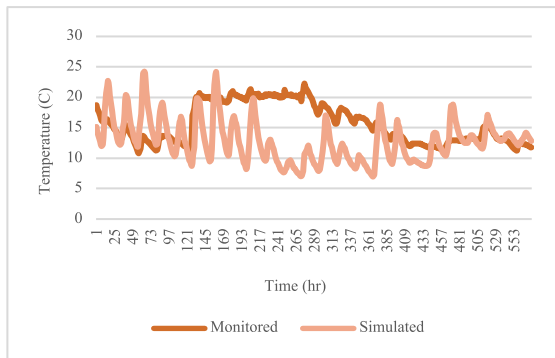


Figure 53: Hempod monitored and simulated temperature values

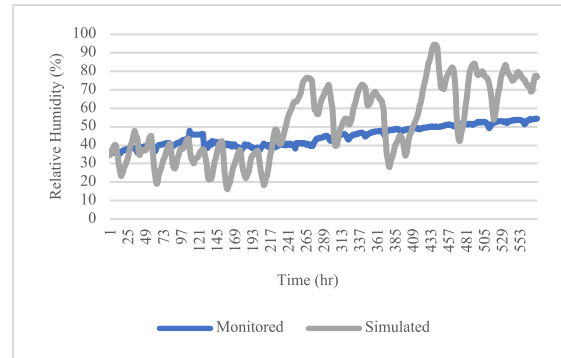


Figure 54: Hempod monitored and simulated relative humidity values

The base case simulation for the monitored climatic data and the IESVE climatic data was calculated as the RMSE between the monitored (actual) weather data and the IESVE weather data. The root mean square error for temperature was 7.21°C and the root mean square error for relative humidity was 21.71%. Figure 55 below shows the discrepancy between the monitored and IESVE simulated weather values for temperature and Figure 56 shows that of Relative humidity respectively.

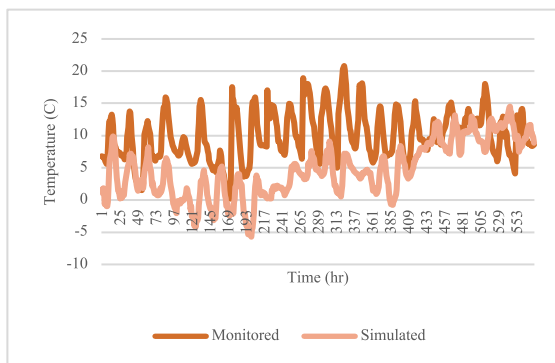


Figure 55: Hempod monitored and simulated weather values for temperature

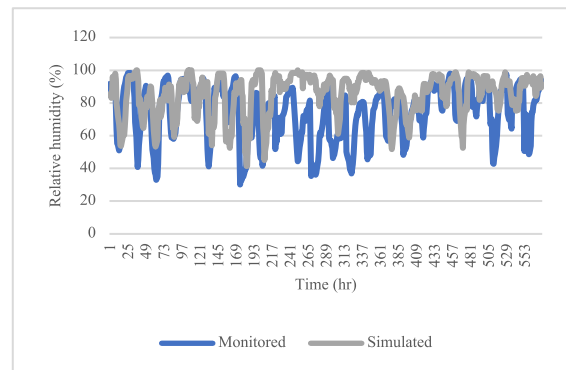


Figure 56: Hempod monitored and simulated weather values for rel. humidity

5.1.2 Base case simulation analysis for the residential building

The obtained model of the residential building was simulated in passive unregulated free-floating mode to establish the base case scenario. The base case for the residential building was also obtained through calculating the root mean square error as applicable. The Living room

had a temperature base case of 4.1°C and that of relative humidity was 4.9%. The base case for the kitchen was 5.1°C for temperature and relative humidity was 10.7%. And the base case of the bedroom for temperature was 4.2°C and relative humidity was 4.7% accordingly.

The base case simulation for the monitored climatic data and the IESVE climatic data of the residential building was calculated. The root mean square error for temperature was 1.04°C and the root mean square error for relative humidity was 3.09%. Figure 57 below shows the discrepancy between the monitored and IESVE simulated weather values for temperature and Figure 58 shows that of Relative humidity respectively.

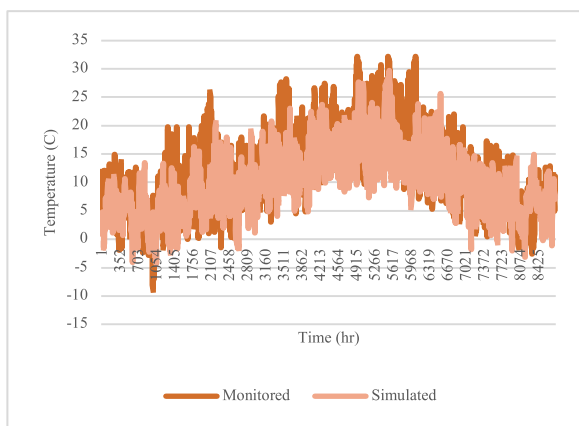


Figure 57: Monitored and simulated weather values for temperature.

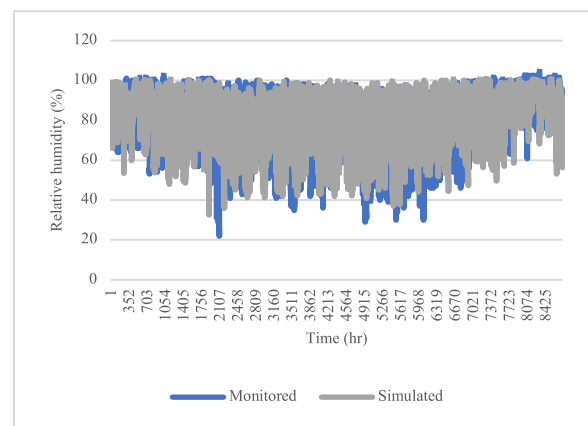


Figure 58: Monitored and simulated weather values for relative humidity.

5.2 ROOT MEAN SQUARE ERROR (RMSE) CALCULATION

The outputs of experimental simulation for Hempod and the measured monitored values were transferred into Microsoft excel spreadsheet to calculate the root mean square error.

As explained in Chapter 3 section 3.3.1, the experiments were carried out using a combination of natural and conventional construction materials to represent hempcrete in simulation tools. Some of the materials used for the experiments are concrete, rammed earth, timber, corkboard, chipboard, aerated concrete, london clay, stone chippings, weather board, e.t.c. The choice of experiments was guided by decisions and reasoning explained in Chapter 3 Section 3.3. The rationale for exchanging the material placement in the experiment is to investigate the movement of heat and moisture and understand the physics of hempcrete wall. Building walls are thermal elements, separating inside the building from outer space while allowing the transfer of heat inside or outside (Paraschiv et.al., 2020; The Building Regulations, 2010). The details of the experiments done by combining rammed earth and timber in different wall layers

to represent hempcrete, for simulation are seen below in Figure 59, Figure 60, Figure 61, Figure 62, Figure 63 and Figure 64. It is also an example of how the experiments with the other construction materials were conducted.

Figure 59 show a wall of 218mm thickness which comprises of two layers of 50mm rammed earth and two layers of 50mm chipboard, including 9mm external rendering and gypsum plastering placed in a sandwich form, to represent hempcrete. Figure 60 show a wall of 243mm thickness which comprises of two layers of 75mm rammed earth and one layer of 75mm chipboard, including 9mm external rendering and gypsum plastering placed in a sandwich form, to represent hempcrete.

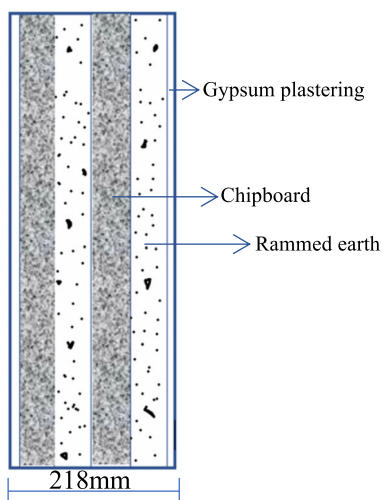


Figure 59: 218mm wall experiment with rammed earth and chipboard

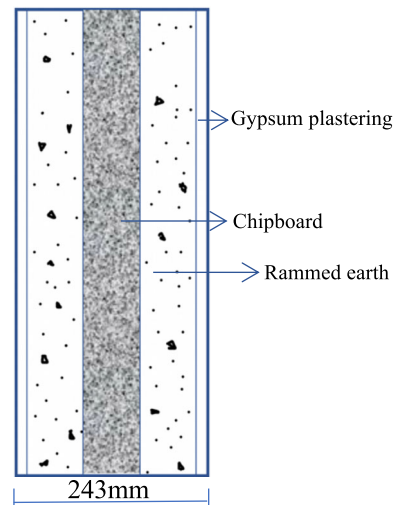


Figure 60: 243mm wall experiment with rammed earth and chipboard

Figure 61 below, show a wall of 268mm thickness which comprises of two layers of 50mm rammed earth and three layers of 50mm chipboard, placed in a sandwich form to represent hempcrete. Figure 62 below, show a wall of 318mm thickness which comprises of two layers of 75mm rammed earth and two layers of 75mm chipboard including 9mm external rendering and gypsum plastering placed in a sandwich form, to represent hempcrete.

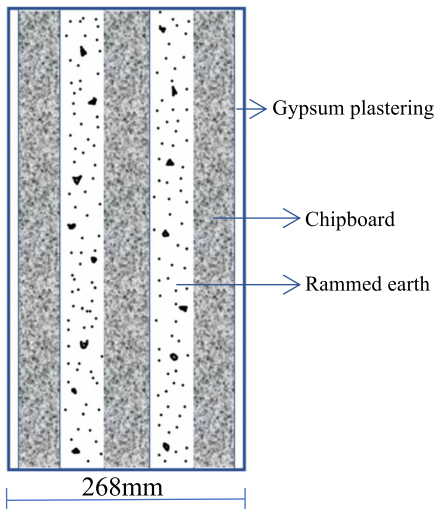


Figure 61: 268mm wall experiment with rammed earth and chipboard

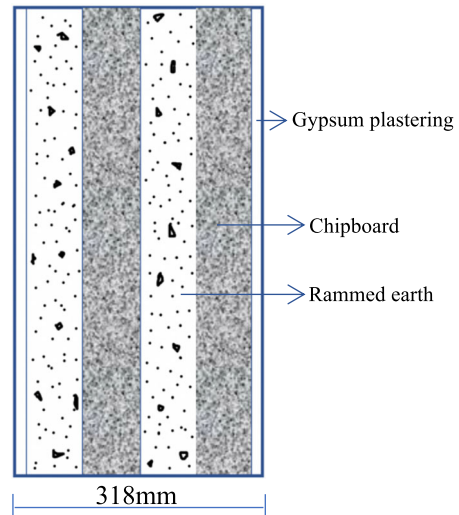


Figure 62: 318mm wall experiment with rammed earth and chipboard

Figure 63 below, show a wall of 318mm thickness which comprises of two layers of 100mm rammed earth and one layer of 100mm chipboard, including 9mm external rendering and gypsum plastering placed in a sandwich form, to represent hempcrete. Figure 64 below, show a wall of 418mm thickness which comprises of two layers of 100mm rammed earth and two layers of 100mm chipboard, including 9mm external rendering and gypsum plastering placed in a sandwich form, to represent hempcrete.

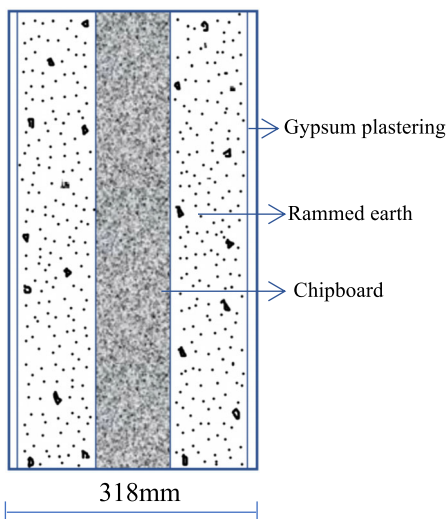


Figure 63: 318mm wall experiment with rammed earth and chipboard

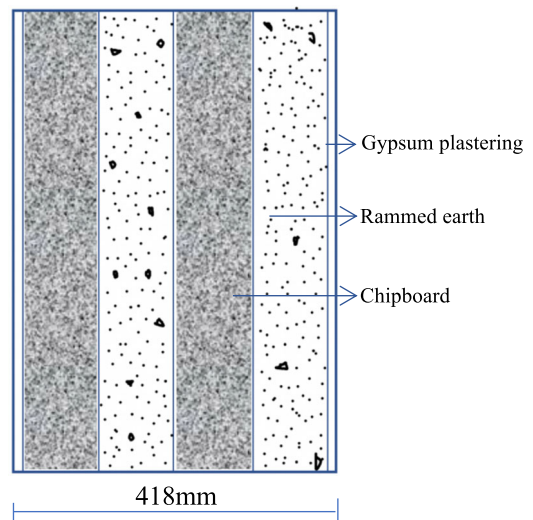


Figure 64: 418mm wall experiment with rammed earth and chipboard

Separating the walls into layers of different thickness for the simulation experiments is a process of detailed investigation into the hempcrete wall, following a co-heating test conducted

by Jankovic (2016) suggesting that hempcrete could be represented with a combination of high- and low-density material layers. Additionally, the heat conduction through a single layer of wall is proportional to its temperature difference across the wall layer, the thermal conductivity of the material and the heat transfer of the wall area but inversely proportional to the layer thickness of the wall. Also, the heat transfer through a multilayer plane wall is proportional to the temperature difference across the wall layers, to the heat transfer area and with the overall heat transfer coefficient of the wall thickness (Paraschiv et.al., 2020). The thickness of materials used in a wall construction play an important role in thermal performance and regulating any heat loss or gain of the building. The Physical as well as structural specifications of any building wall have some significant impact on energy consumption, heat and moisture transfer (Jannat et.al., 2020).

The experiments by combining natural and conventional building materials to represent hempcrete for simulation were carried out as seen from experiment 1-150. The corresponding result of the RMSE for air temperature ranges from 9.9°C to 5.0°C and RMSE of relative humidity ranges from 29.4% to 16.5% for experiments 1-150 as seen below in Table 8. Also, the experiments of combining natural construction materials of high density and low density to represent hempcrete is as seen in Table 8 from experiment 151-196. Where the corresponding RMSE results for air temperature ranges from 8.0°C to 5.0°C while RMSE of relative humidity ranges between 24.8% to 16.2%.

Table 8 below shows the details and output of root mean square error from the experiments conducted. In table 8 below, column one is the serial number of the conducted experiments and as seen, there were 201 experiments carried out. Column two contains details of the construction composition done with different thickness of materials for wall layers to represent hempcrete wall. Column three shows the overall wall thickness of the experiments done to represent hempcrete wall as explained using Figure 59, Figure 60, Figure 61, Figure 62, Figure 63 and Figure 64 above. Column four shows the output of RMSE for air temperature calculated from the output of the conducted experiment and the monitored values. Column five is the output of RMSE for relative humidity, calculated from the output of conducted experiment and the monitored relative humidity values.

Table 8: Hempod simulation experiment with conventional and natural materials

S/No	Construction Composition (outside to inside)	Wall Thickness	RMSE air temperature (C)	RMSE relative humidity (%)
1	External rendering (9mm), Chipboard (50mm), Rammed earth (50mm), Chipboard (50mm), Rammed earth (50mm), Gypsum plastering (9mm)	218mm	8.0°C	24.5%
2	External rendering (9mm), Rammed earth (75mm), Chipboard (75mm), Rammed earth (75mm), Gypsum plastering (9mm)	243mm	8.2°C	25.2%
3	External rendering (9mm), Chipboard (75mm), Rammed earth (75mm), Chipboard (75mm), Gypsum plastering (9mm)	243mm	7.3°C	23.1%
4	External rendering (9mm), Chipboard (50mm), Rammed earth (50mm), Chipboard (50mm), Rammed earth (50mm), Chipboard (50mm), Gypsum plastering (9mm)	268mm	7.2°C	23.2%
5	External rendering (9mm), Rammed earth (50mm), Chipboard (50mm), Rammed earth (50mm), Chipboard (50mm), Rammed earth (50mm), Gypsum plastering (9mm)	268mm	7.8°C	24.4%
6	External rendering (9mm), Rammed earth (75mm), Chipboard (75mm), Rammed earth (75mm), Chipboard (75mm), Gypsum plastering (9mm)	318mm	7.2°C	23.2%
7	External rendering (9mm), Rammed earth (100mm), Chipboard (100mm), Rammed earth (100mm), Gypsum plastering (9mm)	318mm	7.6°C	24.3%
8	External rendering (9mm), Chipboard (100mm), Rammed earth (100mm), Chipboard (100mm), Gypsum plastering (9mm)	318mm	6.5°C	21.9%
9	External rendering (9mm), Rammed earth (100mm), Chipboard (100mm), Rammed earth (100mm), Chipboard (100mm), Gypsum plastering (9mm)	418mm	6.3°C	21.9%
10	External rendering (9mm), Chipboard (50mm), Cast concrete (50mm), Chipboard (50mm), Cast concrete (50mm), Gypsum plastering (9mm)	218mm	7.9°C	24.3%
11	External rendering (9mm), Cast concrete (75mm), Chipboard (75mm), Cast concrete (75mm), Gypsum plastering (9mm)	243mm	8.2°C	25.1%
12	External rendering (9mm), Chipboard (75mm), Cast concrete (75mm), Chipboard (75mm), Gypsum plastering (9mm)	243mm	7.3°C	23.1%
13	External rendering (9mm), Chipboard (50mm), Cast concrete (50mm), Chipboard (50mm), Cast concrete (50mm), Chipboard (50mm), Gypsum plastering (9mm)	268mm	7.3°C	23.1%
14	External rendering (9mm), Cast concrete (50mm), Chipboard (50mm), Cast concrete (50mm), Chipboard (50mm), Cast concrete (50mm), Gypsum plastering (9mm)	268mm	7.8°C	24.3%
15	External rendering (9mm), Cast concrete (75mm), Chipboard (75mm), Cast concrete (75mm), Chipboard (75mm), Gypsum plastering (9mm)	318mm	7.2°C	23.2%
16	External rendering (9mm), Cast concrete (100mm), Chipboard (100mm), Cast concrete (100mm), Gypsum plastering (9mm)	318mm	7.7°C	24.3%

17	External rendering (9mm), Chipboard (100mm), Cast concrete (100mm), Chipboard (100mm), Gypsum plastering (9mm)	318mm	6.6°C	21.9%
18	External rendering (9mm), Cast concrete (100mm), Chipboard (100mm), Cast concrete (100mm), Chipboard (100mm), Gypsum plastering (9mm)	418mm	6.4°C	21.9%
19	External rendering (9mm), Cork board (50mm), Concrete block (50mm), Cork board (50mm), Concrete block (50mm), Gypsum plastering (9mm)	218mm	5.4°C	16.5%
20	External rendering (9mm), Concrete block (75mm), Cork board (75mm), Concrete block (75mm), Gypsum plastering (9mm)	243mm	5.8°C	17.3%
21	External rendering (9mm), Cork board (75mm), Concrete block (75mm), Cork board (75mm), Gypsum plastering (9mm)	243mm	5.5°C	17.0%
22	External rendering (9mm), Cork board (50mm), Concrete block (50mm), Cork board (50mm), Concrete block (50mm), Cork board (50mm), Gypsum plastering (9mm)	268mm	5.4°C	16.8%
23	External rendering (9mm), Concrete block (50mm), Cork board (50mm), Concrete block (50mm), Cork board (50mm), Concrete block (50mm), Gypsum plastering (9mm)	268mm	5.3°C	16.5%
24	External rendering (9mm), Concrete block (75mm), Cork board (75mm), Concrete block (75mm), Cork board (75mm), Gypsum plastering (9mm)	318mm	5.5°C	17.0%
25	External rendering (9mm), Concrete block (100mm), Cork board (100mm), Concrete block (100mm), Gypsum plastering (9mm)	318mm	5.0°C	15.9%
26	External rendering (9mm), Cork board (100mm), Concrete block (100mm), Cork board (100mm), Gypsum plastering (9mm)	318mm	5.2°C	16.3%
27	External rendering (9mm), Concrete block (100mm), Cork board (100mm), Concrete block (100mm), Cork board (100mm), Gypsum plastering (9mm)	418mm	5.2°C	16.4%
28	External rendering (9mm), Straw bale (50mm), Brickwork (50mm), Straw bale (50mm), Brickwork (50mm), Gypsum plastering (9mm)	218mm	6.6°C	19.5%
29	External rendering (9mm), Straw bale (50mm), Brickwork (50mm), Straw bale (50mm), Brickwork (50mm), Straw bale (50mm), Gypsum plastering (9mm)	268mm	6.3°C	18.9%
30	External rendering (9mm), Brickwork (50mm), Straw bale (50mm), Brickwork (50mm), Straw bale (50mm), Brickwork (50mm), Gypsum plastering (9mm)	268mm	6.5°C	19.3%
31	External rendering (9mm), Brickwork (75mm), Straw bale (75mm), Brickwork (75mm), Straw bale (75mm), Gypsum plastering (9mm)	318mm	6.4°C	19.1%
32	External rendering (9mm), Brickwork (100mm), Straw bale (100mm), Brickwork (100mm), Gypsum plastering (9mm)	318mm	6.2°C	18.6%
33	External rendering (9mm), Straw bale (100mm), Brickwork (100mm), Straw bale (100mm), Gypsum plastering (9mm)	318mm	6.0°C	18.2%
34	External rendering (9mm), Brickwork (100mm), Straw bale (100mm), Brickwork (100mm), Straw bale (100mm), Gypsum plastering (9mm)	418mm	5.9°C	18.1%

35	External rendering (9mm), Straw bale (50mm), Cast concrete (50mm), Straw bale (50mm), Cast concrete (50mm), Gypsum plastering (9mm)	218mm	6.6°C	19.9%
36	External rendering (9mm), Straw bale (50mm), Cast concrete (50mm), Straw bale (50mm), Cast concrete (50mm), Straw bale (50mm), Gypsum plastering (9mm)	268mm	6.3°C	19.3%
37	External rendering (9mm), Cast concrete (50mm), Straw bale (50mm), Cast concrete (50mm), Straw bale (50mm), Cast concrete (50mm), Gypsum plastering (9mm)	268mm	6.6°C	19.8%
38	External rendering (9mm), Cast concrete (75mm), Straw bale (75mm), Cast concrete (75mm), Straw bale (75mm), Gypsum plastering (9mm)	318mm	6.4°C	19.6%
39	External rendering (9mm), Cast concrete (100mm), Straw bale (100mm), Cast concrete (100mm), Gypsum plastering (9mm)	318mm	6.3°C	19.2%
40	External rendering (9mm), Straw bale (100mm), Cast concrete (100mm), Straw bale (100mm), Gypsum plastering (9mm)	318mm	5.9°C	18.6%
41	External rendering (9mm), Cast concrete (100mm), Straw bale (100mm), Cast concrete (100mm), Straw bale (100mm), Gypsum plastering (9mm)	418mm	5.4°C	15.9%
42	External rendering (9mm), Adobe (50mm), Cast concrete (50mm), Adobe (50mm), Cast concrete (50mm), Gypsum plastering (9mm)	218mm	9.8°C	29.4%
43	External rendering (9mm), Adobe (50mm), Cast concrete (50mm), Adobe (50mm), Cast concrete (50mm), Adobe (50mm), Gypsum plastering (9mm)	268mm	9.5°C	28.5%
44	External rendering (9mm), Cast concrete (50mm), Adobe (50mm), Cast concrete (50mm), Adobe (50mm), Cast concrete (50mm), Gypsum plastering (9mm)	268mm	9.6°C	28.9%
45	External rendering (9mm), Cast concrete (75mm), Adobe (75mm), Cast concrete (75mm), Adobe (75mm), Gypsum plastering (9mm)	318mm	9.3°C	28.2%
46	External rendering (9mm), Cast concrete (100mm), Adobe (100mm), Cast concrete (100mm), Gypsum plastering (9mm)	318mm	9.4°C	28.7%
47	External rendering (9mm), Adobe (100mm), Cast concrete (100mm), Adobe (100mm), Gypsum plastering (9mm)	318mm	9.2°C	27.9%
48	External rendering (9mm), Cast concrete (100mm), Adobe (100mm), Cast concrete (100mm), Adobe (100mm), Gypsum plastering (9mm)	418mm	8.8°C	27.9%
49	External rendering (9mm), Bamboo (50mm), Cast concrete (50mm), Bamboo (50mm), Cast concrete (50mm), Gypsum plastering (9mm)	218mm	9.7°C	29.0%
50	External rendering (9mm), Cast concrete (75mm), Bamboo (75mm), Cast concrete (75mm), Gypsum plastering (9mm)	243mm	9.1°C	27.4%
51	External rendering (9mm), Bamboo (75mm), Cast concrete (75mm), Bamboo (75mm), Gypsum plastering (9mm)	243mm	8.9°C	26.5%
52	External rendering (9mm), Bamboo (50mm), Cast concrete (50mm), Bamboo (50mm), Cast concrete (50mm), Bamboo (50mm), Gypsum plastering (9mm)	268mm	9.3°C	27.8%

53	External rendering (9mm), Cast concrete (50mm), Bamboo (50mm), Cast concrete (50mm), Bamboo (50mm), Cast concrete (50mm), Gypsum plastering (9mm)	268mm	9.5°C	28.4%
54	External rendering (9mm), Cast concrete (75mm), Bamboo (75mm), Cast concrete (75mm), Bamboo (75mm), Gypsum plastering (9mm)	318mm	9.2°C	27.4%
55	External rendering (9mm), Cast concrete (100mm), Bamboo (100mm), Cast concrete (100mm), Gypsum plastering (9mm)	318mm	9.3°C	28.0%
56	External rendering (9mm), Bamboo (100mm), Cast concrete (100mm), Bamboo (100mm), Gypsum plastering (9mm)	318mm	9.0°C	26.9%
57	External rendering (9mm), Cast concrete (100mm), Bamboo (100mm), Cast concrete (100mm), Bamboo (100mm), Gypsum plastering (9mm)	418mm	8.6°C	26.5%
58	External rendering (9mm), Bamboo (50mm), Rammed earth (50mm), Bamboo (50mm), Rammed earth (50mm), Gypsum plastering (9mm)	218mm	9.1°C	27.2%
59	External rendering (9mm), Rammed earth (75mm), Bamboo (75mm), Rammed earth (75mm), Gypsum plastering (9mm)	243mm	9.2°C	27.5%
60	External rendering (9mm), Bamboo (75mm), Rammed earth (75mm), Bamboo (75mm), Gypsum plastering (9mm)	243mm	8.9°C	26.6%
61	External rendering (9mm), Bamboo (50mm), Rammed earth (50mm), Bamboo (50mm), Rammed earth (50mm), Bamboo (50mm), Gypsum plastering (9mm)	268mm	8.8°C	26.4%
62	External rendering (9mm), Rammed earth (50mm), Bamboo (50mm), Rammed earth (50mm), Bamboo (50mm), Rammed earth (50mm), Gypsum plastering (9mm)	268mm	9.0°C	27.0%
63	External rendering (9mm), Rammed earth (75mm), Bamboo (75mm), Rammed earth (75mm), Bamboo (75mm), Gypsum plastering (9mm)	318mm	8.7°C	26.4%
64	External rendering (9mm), Rammed earth (100mm), Bamboo (100mm), Rammed earth (100mm), Gypsum plastering (9mm)	318mm	8.8°C	27.0%
65	External rendering (9mm), Bamboo (100mm), Rammed earth (100mm), Bamboo (100mm), Gypsum plastering (9mm)	318mm	8.6°C	25.7%
66	External rendering (9mm), Rammed earth (100mm), Bamboo (100mm), Rammed earth (100mm), Bamboo (100mm), Gypsum plastering (9mm)	418mm	8.3°C	25.7%
67	External rendering (9mm), Chipboard (50mm), Aerated concrete (50mm), Chipboard (50mm), Aerated concrete (50mm), Gypsum plastering (9mm)	218mm	7.7°C	23.0%
68	External rendering (9mm), Chipboard (50mm), Aerated concrete (50mm), Chipboard (50mm), Aerated concrete (50mm), Chipboard (50mm), Gypsum plastering (9mm)	268mm	7.0°C	21.6%
69	External rendering (9mm), Aerated concrete (50mm), Chipboard (50mm), Aerated concrete (50mm), Chipboard (50mm), Aerated concrete (50mm), Gypsum plastering (9mm)	268mm	7.3°C	22.1%

70	External rendering (9mm), Aerated concrete (75mm), Chipboard (75mm), Aerated concrete (75mm), Chipboard (75mm), Gypsum plastering (9mm)	318mm	6.7°C	21.0%
71	External rendering (9mm), Aerated concrete (100mm), Chipboard (100mm), Aerated concrete (100mm), Gypsum plastering (9mm)	318mm	6.9°C	21.4%
72	External rendering (9mm), Chipboard (100mm), Aerated concrete (100mm), Chipboard (100mm), Gypsum plastering (9mm)	318mm	6.4°C	20.6%
73	External rendering (9mm), Aerated concrete (100mm), Chipboard (100mm), Aerated concrete (100mm), Chipboard (100mm), Gypsum plastering (9mm)	418mm	5.8°C	19.6%
74	External rendering (9mm), Bamboo (50mm), Aerated concrete (50mm), Bamboo (50mm), Aerated concrete (50mm), Gypsum plastering (9mm)	218mm	8.8°C	26.2%
75	External rendering (9mm), Aerated concrete (75mm), Bamboo (75mm), Aerated concrete (75mm), Gypsum plastering (9mm)	243mm	7.6°C	22.1%
76	External rendering (9mm), Bamboo (75mm), Aerated concrete (75mm), Bamboo (75mm), Gypsum plastering (9mm)	243mm	8.1°C	23.6%
77	External rendering (9mm), Bamboo (50mm), Aerated concrete (50mm), Bamboo (50mm), Aerated concrete (50mm), Bamboo (50mm), Gypsum plastering (9mm)	268mm	8.5°C	25.0%
78	External rendering (9mm), Aerated concrete (50mm), Bamboo (50mm), Aerated concrete (50mm), Bamboo (50mm), Aerated concrete (50mm), Gypsum plastering (9mm)	268mm	8.3°C	24.2%
79	External rendering (9mm), Aerated concrete (75mm), Bamboo (75mm), Aerated concrete (75mm), Bamboo (75mm), Gypsum plastering (9mm)	318mm	8.0°C	23.5%
80	External rendering (9mm), Aerated concrete (100mm), Bamboo (100mm), Aerated concrete (100mm), Gypsum plastering (9mm)	318mm	7.8°C	22.9%
81	External rendering (9mm), Bamboo (100mm), Aerated concrete (100mm), Bamboo (100mm), Gypsum plastering (9mm)	318mm	8.2°C	24.1%
82	External rendering (9mm), Aerated concrete (100mm), Bamboo (100mm), Aerated concrete (100mm), Bamboo (100mm), Gypsum plastering (9mm)	418mm	7.3°C	21.8%
83	External rendering (9mm), Cob wall (50mm), Cast concrete (50mm), Cob wall (50mm), Cast concrete (50mm), Gypsum plastering (9mm)	218mm	9.9°C	29.7%
84	External rendering (9mm), Cob wall (50mm), Cast concrete (50mm), Cob wall (50mm), Cast concrete (50mm), Cob wall (50mm), Gypsum plastering (9mm)	268mm	9.6°C	28.8%
85	External rendering (9mm), Cast concrete (50mm), Cob wall (50mm), Cast concrete (50mm), Cob wall (50mm), Cast concrete (50mm), Gypsum plastering (9mm)	268mm	9.7°C	29.1%

86	External rendering (9mm), Cast concrete (75mm), Cob wall (75mm), Cast concrete (75mm), Cob wall (75mm), Gypsum plastering (9mm)	318mm	9.4°C	28.4%
87	External rendering (9mm), Cast concrete (100mm), Cob wall (100mm), Cast concrete (100mm), Gypsum plastering (9mm)	318mm	9.5°C	28.8%
88	External rendering (9mm), Cob wall (100mm), Cast concrete (100mm), Cob wall (100mm), Gypsum plastering (9mm)	318mm	9.3°C	28.2%
89	External rendering (9mm), Cast concrete (100mm), Cob wall (100mm), Cast concrete (100mm), Cob wall (100mm), Gypsum plastering (9mm)	418mm	8.9°C	28.1%
90	External rendering (9mm), Cob wall (50mm), Concrete block (50mm), Cob wall (50mm), Concrete block (50mm), Gypsum plastering (9mm)	218mm	9.5°C	28.5%
91	External rendering (9mm), Cob wall (50mm), Concrete block (50mm), Cob wall (50mm), Concrete block (50mm), Cob wall (50mm), Gypsum plastering (9mm)	268mm	9.2°C	27.6%
92	External rendering (9mm), Concrete block (50mm), Cob wall (50mm), Concrete block (50mm), Cob wall (50mm), Concrete block (50mm), Gypsum plastering (9mm)	268mm	9.2°C	27.5%
93	External rendering (9mm), Concrete block (75mm), Cob wall (75mm), Concrete block (75mm), Cob wall (75mm), Gypsum plastering (9mm)	318mm	8.9°C	27.0%
94	External rendering (9mm), Concrete block (100mm), Cob wall (100mm), Concrete block (100mm), Gypsum plastering (9mm)	318mm	8.9°C	26.9%
95	External rendering (9mm), Cob wall (100mm), Concrete block (100mm), Cob wall (100mm), Gypsum plastering (9mm)	318mm	9.0°C	27.1%
96	External rendering (9mm), Concrete block (100mm), Cob wall (100mm), Concrete block (100mm), Cob wall (100mm), Gypsum plastering (9mm)	418mm	8.4°C	26.1%
97	External rendering (9mm), Brickwork (50mm), Rammed earth (50mm), Brickwork (50mm), Rammed earth (50mm), Gypsum plastering (9mm)	218mm	9.3°C	28.1%
98	External rendering (9mm), Brickwork (50mm), Rammed earth (50mm), Brickwork (50mm), Rammed earth (50mm), Brickwork (50mm), Gypsum plastering (9mm)	268mm	9.1°C	27.7%
99	External rendering (9mm), Rammed earth (50mm), Brickwork (50mm), Rammed earth (50mm), Brickwork (50mm), Rammed earth (50mm), Gypsum plastering (9mm)	268mm	9.2°C	28.1%
100	External rendering (9mm), Rammed earth (75mm), Brickwork (75mm), Rammed earth (75mm), Brickwork (75mm), Gypsum plastering (9mm)	318mm	8.9°C	27.7%
101	External rendering (9mm), Rammed earth (100mm), Brickwork (100mm), Rammed earth (100mm), Gypsum plastering (9mm)	318mm	9.0°C	28.1%
102	External rendering (9mm), Brickwork (100mm), Rammed earth (100mm), Brickwork (100mm), Gypsum plastering (9mm)	318mm	8.8°C	27.3%
103	External rendering (9mm), Rammed earth (100mm), Brickwork (100mm), Rammed earth	418mm	8.5°C	27.4%

	(100mm), Brickwork (100mm), Gypsum plastering (9mm)			
104	External rendering (9mm), Chipboard (50mm), Brickwork (50mm), Chipboard (50mm), Brickwork (50mm), Gypsum plastering (9mm)	218mm	8.2°C	24.5%
105	External rendering (9mm), Chipboard (50mm), Brickwork (50mm), Chipboard (50mm), Brickwork (50mm), Chipboard (50mm), Gypsum plastering (9mm)	268mm	7.5°C	23.2%
106	External rendering (9mm), Brickwork (50mm), Chipboard (50mm), Brickwork (50mm), Chipboard (50mm), Brickwork (50mm), Gypsum plastering (9mm)	268mm	8.0°C	24.2%
107	External rendering (9mm), Brickwork (75mm), Chipboard (75mm), Brickwork (75mm), Chipboard (75mm), Gypsum plastering (9mm)	318mm	7.3°C	22.9%
108	External rendering (9mm), Brickwork (100mm), Chipboard (100mm), Brickwork (100mm), Gypsum plastering (9mm)	318mm	7.7°C	23.8%
109	External rendering (9mm), Chipboard (100mm), Brickwork (100mm), Chipboard (100mm), Gypsum plastering (9mm)	318mm	6.8°C	22.0%
110	External rendering (9mm), Brickwork (100mm), Chipboard (100mm), Brickwork (100mm), Chipboard (100mm), Gypsum plastering (9mm)	418mm	6.5°C	21.6%
111	External rendering (9mm), glass-fibre quilt (50mm), Cast concrete (50mm), glass-fibre quilt (50mm), Cast concrete (50mm), Gypsum plastering (9mm)	218mm	5.5°C	17.0%
112	External rendering (9mm), glass-fibre quilt (50mm), Cast concrete (50mm), glass-fibre quilt (50mm), Cast concrete (50mm), glass-fibre quilt (50mm), Gypsum plastering (9mm)	268mm	5.7°C	17.5%
113	External rendering (9mm), Cast concrete (50mm), glass-fibre quilt (50mm), Cast concrete (50mm), glass-fibre quilt (50mm), Cast concrete (50mm), Gypsum plastering (9mm)	268mm	5.4°C	17.0%
114	External rendering (9mm), Cast concrete (75mm), glass-fibre quilt (75mm), Cast concrete (75mm), glass-fibre quilt (75mm), Gypsum plastering (9mm)	318mm	5.9°C	17.9%
115	External rendering (9mm), Cast concrete (100mm), glass-fibre quilt (100mm), Cast concrete (100mm), Gypsum plastering (9mm)	318mm	5.1°C	16.1%
116	External rendering (9mm), glass-fibre quilt (100mm), Cast concrete (100mm), glass-fibre quilt (100mm), Gypsum plastering (9mm)	318mm	5.6°C	17.3%
117	External rendering (9mm), Weather board (50mm), Brickwork (50mm), Weather board (50mm), Brickwork (50mm), Gypsum plastering (9mm)	218mm	8.1°C	24.1%
118	External rendering (9mm), Weather board (50mm), Brickwork (50mm), Weather board (50mm), Brickwork (50mm), Weather board (50mm), Gypsum plastering (9mm)	268mm	7.4°C	22.7%
119	External rendering (9mm), Brickwork (50mm), Weather board (50mm), Brickwork (50mm), Weather board (50mm), Brickwork (50mm), Gypsum plastering (9mm)	268mm	7.9°C	23.7%

120	External rendering (9mm), Brickwork (75mm), Weather board (75mm), Brickwork (75mm), Weather board (75mm), Gypsum plastering (9mm)	318mm	7.3°C	22.4%
121	External rendering (9mm), Weather board (100mm), Brickwork (100mm), Weather board (100mm), Gypsum plastering (9mm)	318mm	6.7°C	21.5%
122	External rendering (9mm), Brickwork (100mm), Weather board (100mm), Brickwork (100mm), Weather board (100mm), Gypsum plastering (9mm)	418mm	7.6°C	23.3%
123	External rendering (9mm), Silicon (50mm), Concrete block (50mm), Silicon (50mm), Concrete block (50mm), Gypsum plastering (9mm)	218mm	8.4°C	24.8%
124	External rendering (9mm), Silicon (50mm), Concrete block (50mm), Silicon (50mm), Concrete block (50mm), Silicon (50mm), Gypsum plastering (9mm)	268mm	7.9°C	23.4%
125	External rendering (9mm), Concrete block (50mm), Silicon (50mm), Concrete block (50mm), Silicon (50mm), Concrete block (50mm), Gypsum plastering (9mm)	268mm	8.2°C	24.2%
126	External rendering (9mm), Concrete block (75mm), Silicon (75mm), Concrete block (75mm), Silicon (75mm), Gypsum plastering (9mm)	318mm	7.5°C	22.8%
127	External rendering (9mm), Concrete block (100mm), Silicon (100mm), Concrete block (100mm), Gypsum plastering (9mm)	318mm	8.5°C	25.1%
128	External rendering (9mm), Silicon (100mm), Concrete block (100mm), Silicon (100mm), Gypsum plastering (9mm)	318mm	8.0°C	23.7%
129	External rendering (9mm), Concrete block (100mm), Silicon (100mm), Concrete block (100mm), Silicon (100mm), Gypsum plastering (9mm)	418mm	6.6°C	21.4%
130	External rendering (9mm), Cratherm board (50mm), Concrete block (50mm), Cratherm board (50mm), Concrete block (50mm), Gypsum plastering (9mm)	218mm	6.6°C	19.6%
131	External rendering (9mm), Cratherm board (50mm), Concrete block (50mm), Cratherm board (50mm), Concrete block (50mm), Cratherm board (50mm), Gypsum plastering (9mm)	268mm	5.9°C	17.8%
132	External rendering (9mm), Concrete block (50mm), Cratherm board (50mm), Concrete block (50mm), Cratherm board (50mm), Concrete block (50mm), Gypsum plastering (9mm)	268mm	5.9°C	17.8%
133	External rendering (9mm), Concrete block (75mm), Cratherm board (75mm), Concrete block (75mm), Cratherm board (75mm), Gypsum plastering (9mm)	318mm	5.9°C	18.0%
134	External rendering (9mm), Concrete block (100mm), Cratherm board (100mm), Concrete block (100mm), Gypsum plastering (9mm)	318mm	5.6°C	17.1%
135	External rendering (9mm), Cratherm board (100mm), Concrete block (100mm), Cratherm board (100mm), Gypsum plastering (9mm)	318mm	5.6°C	17.3%
136	External rendering (9mm), Timber board (50mm), Reinforced concrete (50mm), Timber board (50mm), Reinforced concrete (50mm), Gypsum plastering (9mm)	218mm	8.7°C	26.0%

137	External rendering (9mm), Timber board (50mm), Reinforced concrete (50mm), Timber board (50mm), Reinforced concrete (50mm), Timber board (50mm), Gypsum plastering (9mm)	268mm	7.9°C	24.5%
138	External rendering (9mm), Reinforced concrete (50mm), Timber board (50mm), Reinforced concrete (50mm), Timber board (50mm), Reinforced concrete (50mm), Gypsum plastering (9mm)	268mm	8.5°C	25.9%
139	External rendering (9mm), Reinforced concrete (75mm), Timber board (75mm), Reinforced concrete (75mm), Timber board (75mm), Gypsum plastering (9mm)	318mm	7.6°C	24.3%
140	External rendering (9mm), Reinforced concrete (100mm), Timber board (100mm), Reinforced concrete (100mm), Gypsum plastering (9mm)	318mm	8.4°C	25.8%
141	External rendering (9mm), Timber board (100mm), Reinforced concrete (100mm), Timber board (100mm), Gypsum plastering (9mm)	318mm	7.3°C	23.2%
142	External rendering (9mm), Reinforced concrete (100mm), Timber board (100mm), Reinforced concrete (100mm), Timber board (100mm), Gypsum plastering (9mm)	418mm	6.6°C	22.8%
143	External rendering (9mm), Plywood (50mm), Aerated- concrete (50mm), Plywood (50mm), Aerated- concrete (50mm), Gypsum plastering (9mm)	218mm	7.5°C	21.9%
144	External rendering (9mm), Plywood (75mm), Aerated- concrete (75mm), Plywood (75mm), Gypsum plastering (9mm)	243mm	7.1°C	20.9%
145	External rendering (9mm), Plywood (50mm), Aerated- concrete (50mm), Plywood (50mm), Aerated- concrete (50mm), Plywood (50mm), Gypsum plastering (9mm)	268mm	6.9°C	20.3%
146	External rendering (9mm), Aerated- concrete (50mm), Plywood (50mm), Aerated- concrete (50mm), Plywood (50mm), Aerated- concrete (50mm), Gypsum plastering (9mm)	268mm	7.0°C	20.6%
147	External rendering (9mm), Aerated- concrete (75mm), Plywood (75mm), Aerated- concrete (75mm), Plywood (75mm), Gypsum plastering (9mm)	318mm	6.4°C	19.4%
148	External rendering (9mm), Aerated- concrete (100mm), Plywood (100mm), Aerated- concrete (100mm), Gypsum plastering (9mm)	318mm	6.6°C	19.8%
149	External rendering (9mm), Plywood (100mm), Aerated- concrete (100mm), Plywood (100mm), Gypsum plastering (9mm)	318mm	6.4°C	19.3%
150	External rendering (9mm), Aerated- concrete (100mm), Plywood (100mm), Aerated- concrete (100mm), Plywood (100mm), Gypsum plastering (9mm)	418mm	5.8°C	18.3%
151	External rendering (9mm), Timber (50mm), Straw bale (50mm), Timber (50mm), Straw bale (50mm), Gypsum plastering (9mm)	218mm	6.7°C	19.6%
152	External rendering (9mm), Straw bale (75mm), Timber (75mm), Straw bale (75mm), Gypsum plastering (9mm)	243mm	6.3°C	18.3%

153	External rendering (9mm), Timber (75mm), Straw bale (75mm), Timber (75mm), Gypsum plastering (9mm)	243mm	6.2°C	18.1%
154	External rendering (9mm), Timber (50mm), Straw bale (50mm), Timber (50mm), Straw bale (50mm), Timber (50mm), Gypsum plastering (9mm)	268mm	5.9°C	17.6%
155	External rendering (9mm), Straw bale (50mm), Timber (50mm), Straw bale (50mm), Timber (50mm), Straw bale (50mm), Gypsum plastering (9mm)	268mm	6.1°C	18.0%
156	External rendering (9mm), Straw bale (75mm), Timber (75mm), Straw bale (75mm), Timber (75mm), Gypsum plastering (9mm)	318mm	5.2°C	16.2%
157	External rendering (9mm), Straw bale (100mm), Timber (100mm), Straw bale (100mm), Gypsum plastering (9mm)	318mm	5.8°C	17.6%
158	External rendering (9mm), Timber (100mm), Straw bale (100mm), Timber (100mm), Gypsum plastering (9mm)	318mm	5.6°C	16.8%
159	External rendering (9mm), Straw bale (100mm), Timber (100mm), Straw bale (100mm), Timber (100mm), Gypsum plastering (9mm)	418mm	5.6°C	17.1%
160	External rendering (9mm), Adobe (50mm), Timber (50mm), Adobe (50mm), Timber (50mm), Gypsum plastering (9mm)	218mm	8.4°C	24.8%
161	External rendering (9mm), Adobe (50mm), Timber (50mm), Adobe (50mm), Timber (50mm), Adobe (50mm), Gypsum plastering (9mm)	268mm	8.1°C	24.1%
162	External rendering (9mm), Timber (50mm), Adobe (50mm), Timber (50mm), Adobe (50mm), Timber (50mm), Gypsum plastering (9mm)	268mm	7.7°C	23.2%
163	External rendering (9mm), Timber (75mm), Adobe (75mm), Timber (75mm), Adobe (75mm), Gypsum plastering (9mm)	318mm	7.3°C	22.7%
164	External rendering (9mm), Timber (100mm), Adobe (100mm), Timber (100mm), Gypsum plastering (9mm)	318mm	7.1°C	22.1%
165	External rendering (9mm), Adobe (100mm), Timber (100mm), Adobe (100mm), Gypsum plastering (9mm)	318mm	7.8°C	23.7%
166	External rendering (9mm), Timber (100mm), Adobe (100mm), Timber (100mm), Adobe (100mm), Gypsum plastering (9mm)	418mm	6.4°C	21.3%
167	External rendering (9mm), Chipboard (50mm), Adobe (50mm), Chipboard (50mm), Adobe (50mm), Gypsum plastering (9mm)	218mm	8.1°C	24.4%
168	External rendering (9mm), Chipboard (50mm), Adobe (50mm), Chipboard (50mm), Adobe (50mm), Chipboard (50mm), Gypsum plastering (9mm)	268mm	7.4°C	23.1%
169	External rendering (9mm), Adobe (50mm), Chipboard (50mm), Adobe (50mm), Chipboard (50mm), Adobe (50mm), Gypsum plastering (9mm)	268mm	7.9°C	24.0%
170	External rendering (9mm), Adobe (75mm), Chipboard (75mm), Adobe (75mm), Chipboard (75mm), Gypsum plastering (9mm)	318mm	7.2°C	22.8%

171	External rendering (9mm), Adobe (100mm), Chipboard (100mm), Adobe (100mm), Gypsum plastering (9mm)	318mm	7.6°C	23.6%
172	External rendering (9mm), Chipboard (100mm), Adobe (100mm), Chipboard (100mm), Gypsum plastering (9mm)	318mm	6.8°C	21.9%
173	External rendering (9mm), Adobe (100mm), Chipboard (100mm), Brick (100mm), Chipboard (100mm), Gypsum plastering (9mm)	418mm	6.4°C	21.4%
174	External rendering (9mm), Chipboard (50mm), Cob wall (50mm), Chipboard (50mm), Cob wall (50mm), Gypsum plastering (9mm)	218mm	8.2°C	24.5%
175	External rendering (9mm), Chipboard (50mm), Cob wall (50mm), Chipboard (50mm), Cob wall (50mm), Chipboard (50mm), Gypsum plastering (9mm)	268mm	7.5°C	23.1%
176	External rendering (9mm), Cob wall (50mm), Chipboard (50mm), Cob wall (50mm), Chipboard (50mm), Cob wall (50mm), Gypsum plastering (9mm)	268mm	8.0°C	24.1%
177	External rendering (9mm), Cob wall (75mm), Chipboard (75mm), Cob wall (75mm), Chipboard (75mm), Gypsum plastering (9mm)	318mm	7.3°C	22.9%
178	External rendering (9mm), Cob wall (100mm), Chipboard (100mm), Cob wall (100mm), Gypsum plastering (9mm)	318mm	7.7°C	23.8%
179	External rendering (9mm), Chipboard (100mm), Cob wall (100mm), Chipboard (100mm), Gypsum plastering (9mm)	318mm	6.8°C	22.0%
180	External rendering (9mm), Cob wall (100mm), Chipboard (100mm), Cob wall (100mm), Chipboard (100mm), Gypsum plastering (9mm)	418mm	6.4°C	21.5%
181	External rendering (9mm), glass-fibre quilt (50mm), Rammed earth (50mm), glass-fibre quilt (50mm), Rammed earth (50mm), Gypsum plastering (9mm)	218mm	5.4°C	16.7%
182	External rendering (9mm), Rammed earth (75mm), glass-fibre quilt (75mm), Rammed earth (75mm), Gypsum plastering (9mm)	243mm	5.8°C	17.6%
183	External rendering (9mm), glass-fibre quilt (75mm), Rammed earth (75mm), glass-fibre quilt (75mm), Gypsum plastering (9mm)	243mm	5.8°C	17.7%
184	External rendering (9mm), glass-fibre quilt (50mm), Rammed earth (50mm), glass-fibre quilt (50mm), Rammed earth (50mm), glass-fibre quilt (50mm), Gypsum plastering (9mm)	268mm	5.6°C	17.3%
185	External rendering (9mm), Rammed earth (50mm), glass-fibre quilt (50mm), Rammed earth (50mm), glass-fibre quilt (50mm), Rammed earth (50mm), Gypsum plastering (9mm)	268mm	5.3°C	16.8%
186	External rendering (9mm), Rammed earth (75mm), glass-fibre quilt (75mm), Rammed earth (75mm), glass-fibre quilt (75mm), Gypsum plastering (9mm)	318mm	5.8°C	17.8%
187	External rendering (9mm), Rammed earth (100mm), glass-fibre quilt (100mm), Rammed earth (100mm), Gypsum plastering (9mm)	318mm	5.0°C	16.1%
188	External rendering (9mm), glass-fibre quilt (100mm), Rammed earth (100mm), glass-fibre quilt (100mm), Gypsum plastering (9mm)	318mm	5.6°C	17.1%

189	External rendering (9mm), Phenolic foam (50mm), Rammed earth (50mm), Phenolic foam (50mm), Rammed earth (50mm), Gypsum plastering (9mm)	218mm	5.4°C	16.7%
190	External rendering (9mm), Rammed earth (100mm), Phenolic foam (100mm), Rammed earth (100mm), Gypsum plastering (9mm)	243mm	5.8°C	17.7%
191	External rendering (9mm), Phenolic foam (100mm), Rammed earth (100mm), Phenolic foam (100mm), Gypsum plastering (9mm)	243mm	5.8°C	17.7%
192	External rendering (9mm), Phenolic foam (50mm), Rammed earth (50mm), Phenolic foam (50mm), Rammed earth (50mm), Phenolic foam (50mm), Gypsum plastering (9mm)	268mm	5.6°C	17.3%
193	External rendering (9mm), Rammed earth (50mm), Phenolic foam (50mm), Rammed earth (50mm), Phenolic foam (50mm), Rammed earth (50mm), Gypsum plastering (9mm)	268mm	5.3°C	16.8%
194	External rendering (9mm), Rammed earth (75mm), Phenolic foam (75mm), Rammed earth (75mm), Phenolic foam (75mm), Gypsum plastering (9mm)	318mm	5.8°C	17.8%
195	External rendering (9mm), Rammed earth (100mm), Phenolic foam (100mm), Rammed earth (100mm), Gypsum plastering (9mm)	318mm	5.0°C	16.1%
196	External rendering (9mm), Phenolic foam (100mm), Rammed earth (100mm), Phenolic foam (100mm), Gypsum plastering (9mm)	318mm	5.5°C	17.1%

Table 9 below show the simulation experiments 197-201 and it is the experiments done with the created hempcrete wall of different thickness. The corresponding root mean square error for temperature ranges between 5.5°C to 5.0°C and relative humidity between 18.0% to 15.4%.

Table 9: Hempod simulation with hempcrete material

S/No	Construction Composition (outside to inside)	Wall Thickness	RMSE air temperature (C)	RMSE relative humidity (%)
197	External rendering (9mm), Hempcrete (50mm), Hempcrete (50mm), Hempcrete (50mm), Gypsum plastering (9mm)	218mm	5.5	18.0
198	External rendering (9mm), Hempcrete (75mm), Hempcrete (75mm), Hempcrete (75mm), Gypsum plastering (9mm)	243mm	5.3	15.9
199	External rendering (9mm), Hempcrete (50mm), Hempcrete (50mm), Hempcrete (50mm), Hempcrete (50mm), Gypsum plastering (9mm)	268mm	5.2	15.6
200	External Rendering (9mm), Hempcrete (75mm), Hempcrete (75mm), Hempcrete (75mm), Gypsum plastering (9mm)	318mm	5.2	15.4
201	External rendering (9mm), Hempcrete (100mm), Hempcrete (100mm), Hempcrete (100mm), Hempcrete (100mm), Gypsum plastering (9mm)	418mm	5.0	15.4

After conducting all the experiments and analysing the results by calculating the RMSE. The Figure 65 below, show the *Experiment 1 and Experiment 2* simulation outputs and RMSE values for Hempod temperature.

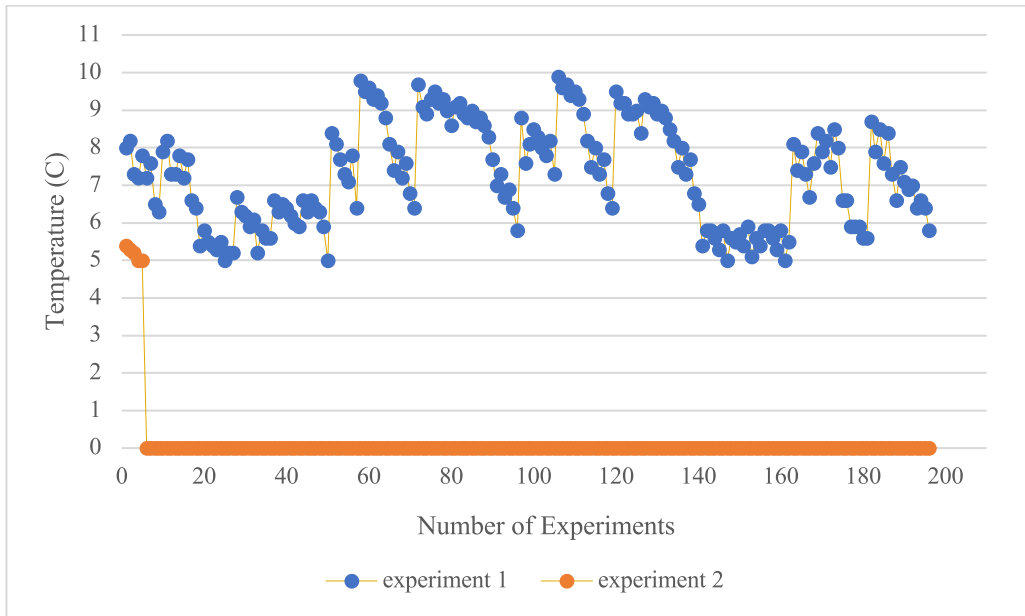


Figure 65: Hempod Experiment1 and Experiment2 showing the temperature values

The Figure 66 below, show the *Experiment 1 and Experiment 2* simulation outputs and RMSE values for Hempod relative humidity.

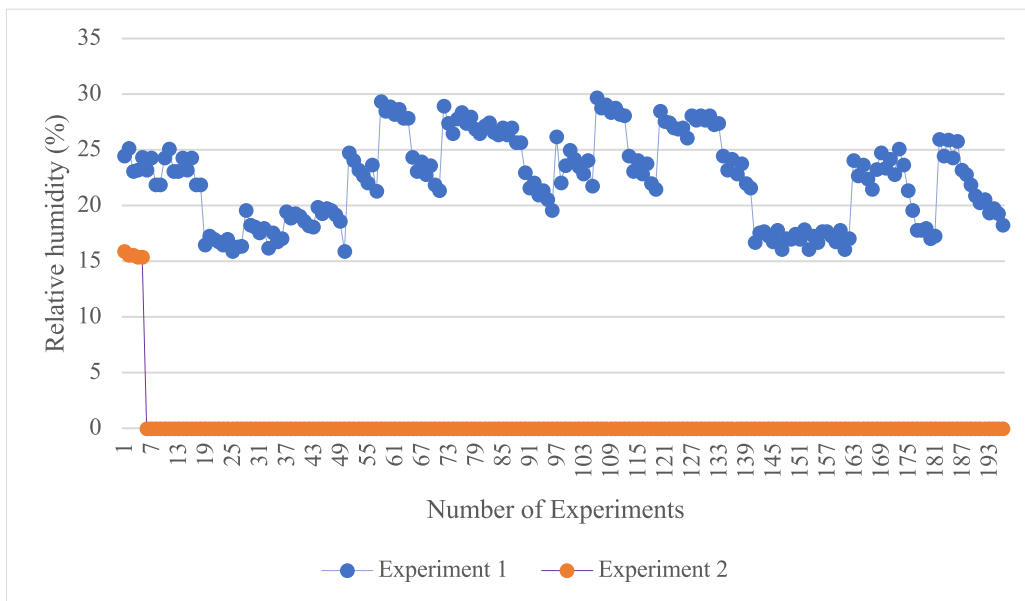


Figure 66: Hempod Experiment1 and Experiment2 showing the relative humidity values

The Hempod 201 IES Virtual Environment simulation output with root mean square error (RMSE) of 5.0°C for temperature and Relative humidity 15.4% was visually organised alongside the monitored values as seen in Figure 67 and Figure 68 below. This was done to analyse the difference between the simulation values and the monitored values before performing optimisation.

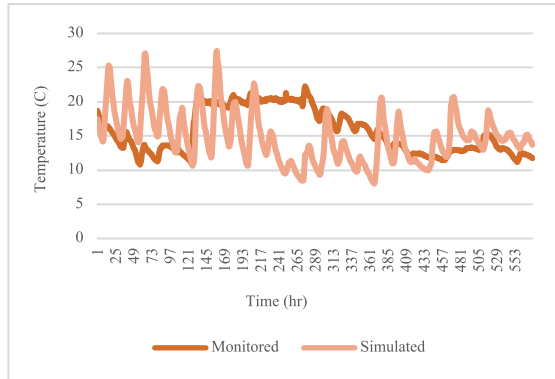


Figure 67: Hempod 201 and Hempod monitored temperature values

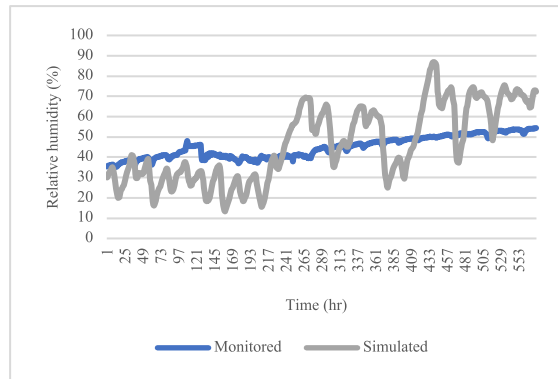


Figure 68: Hempod 201 and Hempod monitored Rel. humidity

5.3 Multi Objective Optimisation using jEPlus+EA

As indicated in the previous chapters, the optimization performed in this study was carried out using the Non-dominated Sorting Genetic Algorithm II (NSGA-II) (Deb et al., 2002). The set of output for the non-dominated solutions, was derived from the set of all solutions generated over the run. A nondominated solution is the one that provides a suitable compromise between all objectives without degrading any of them (Mkaouer and Kessentini, 2014). The basic technique of NSGA-II (Deb et al. 2002) is driven by an algorithm where firstly a population of solutions represented as points is initialized. Then the process is repeated similar to a generational loop and it comprises two parts; in the first part, the population goes through variations and the second part results in new generation-population, which is where selection takes place. The optimization in this study was performed for 200 generations and the resulting nondominated solutions were obtained as Pareto solutions. All the other solutions that are not on the Pareto front are considered as suboptimal solutions. The solutions are considered nondominated when improvement in any of the objective will be at the expense of at least one or the other objective. (Rondeau and Bostian, 2009; Flemming, 1999).

The optimisation in this study uses the posteriori preference method (Hwang and Masud, 1979), where no preference of the user is considered, because the outputs are generated through

the process of the optimisation. After the Pareto set has been generated, the favourable solution from the set of solution alternatives is chosen, as the optimum solution (Augusto, Fouad and Caro, 2012). From the optimisation settings performed in Chapter 4, Section 4.5, Figure 40 shows the total search space size, with parameters and variables to be considered, for the optimisation. The optimisation was performed, and the solutions were generated. In jEPlus+EA (jEPlus, 2018), the scatter plot shows all of the explored solutions including those in the current population (blue) and on the current Pareto Front (red), where the solutions shown in white are from the previous generations, as seen below in Figure 69 from the scatter plot.

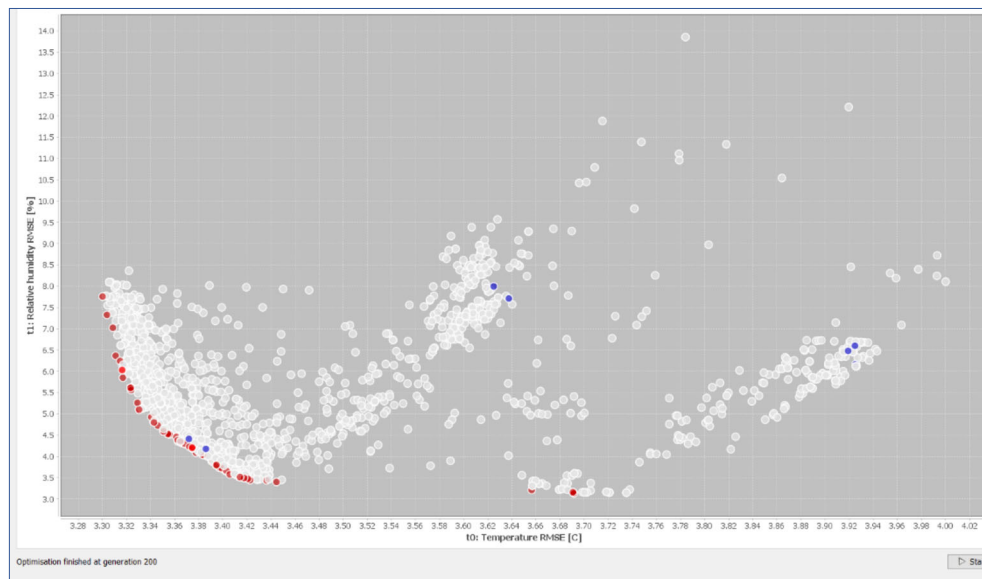


Figure 69: Scatter plot showing all the optimization outputs and the Pareto

The convergence line charts show the convergence of each objective alongside the progression of iterations. As seen below in Figure 70, the optimization finished at 200th generation; the upper part of the chart shows the solution count, where t0 represents the objective of “temperature RMSE” and t1 represents the objective of “relative humidity RMSE”. The red on the chart represents the number of new solutions on the Pareto front as also seen from the scatter plot. The blue represents numbers of Pareto solutions generated; the green represents the population size.

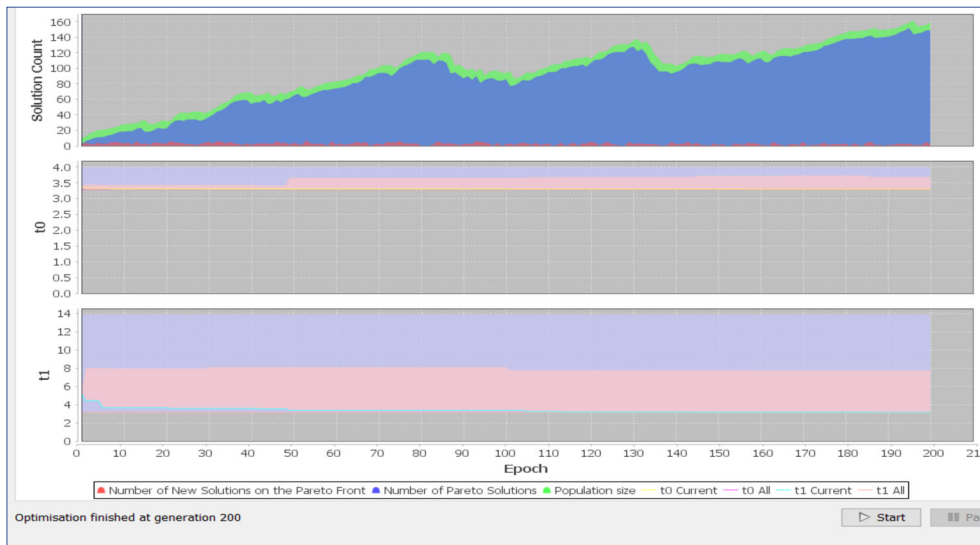


Figure 70: Scatter plot showing all the optimisation outputs and the Pareto

The optimisation produced the outputs of Pareto front, which represents the optimal parameter configurations for the optimisation. The points of the solutions on the Pareto front are considered mathematically indifferent with respect to each other. Given that the optimisation uses posteriori preference method, the selection stage is based on Multiple Criteria Decision Making (MCDM), which basically means making choices in the presence of multiple conflicting criteria (Köksalan, Wallenius, and Zionts 2011). This will involve exploration of the Pareto front and eventually selecting a solution from the available set of solutions. In multi objective optimisation, the Pareto front is regarded as the main index for evaluation of the results (Emmerich and Deutz, 2018; Chiandussi, Codegone, Ferrero and Varesio, 2012). A basic approach could be to use a quantitative metric such as the correlation coefficient or other metrics to filter out the solutions that show a lower correlation with the objectives for more detailed analysis (Brownlee and Wright, 2012). However, in this study, manual exploration and selection of solution from the attained Pareto frontier will be performed. The reason is the objective of the optimisation is calculating root mean square error for temperature and relative humidity which is already a metric.

The scatter plot view produced from the optimisation, is where all the explored solutions can be visually browsed to view the details of each solution. Figure 71, Figure 72, Figure 73 and Figure 74 shows the best solutions on the Pareto front with the reasonable lowest root mean square errors from the optimisation. As seen in the Figure 71 below, the root mean square error for temperature is 3.39°C and the root mean square error for relative humidity is 3.72% respectively.

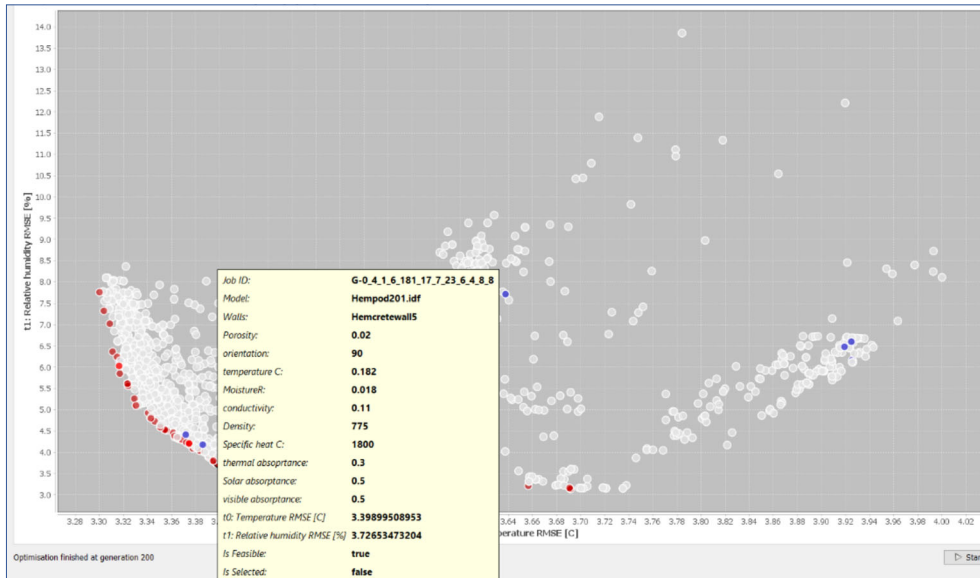


Figure 71: showing a solution chosen from the Pareto front

As seen from the Figure 72 below, the root mean square error for temperature is 3.37°C and the root mean square error for relative humidity is 4.08% respectively.

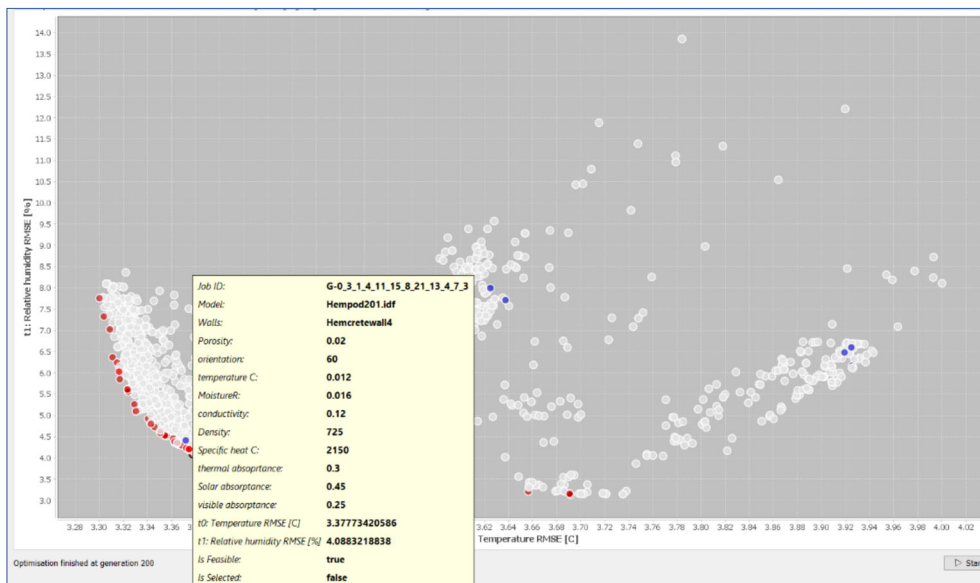


Figure 72: showing a solution chosen from the Pareto front

In the Figure 73 below, the root mean square error for temperature is 3.38°C and the root mean square error for relative humidity is 4.03% respectively.

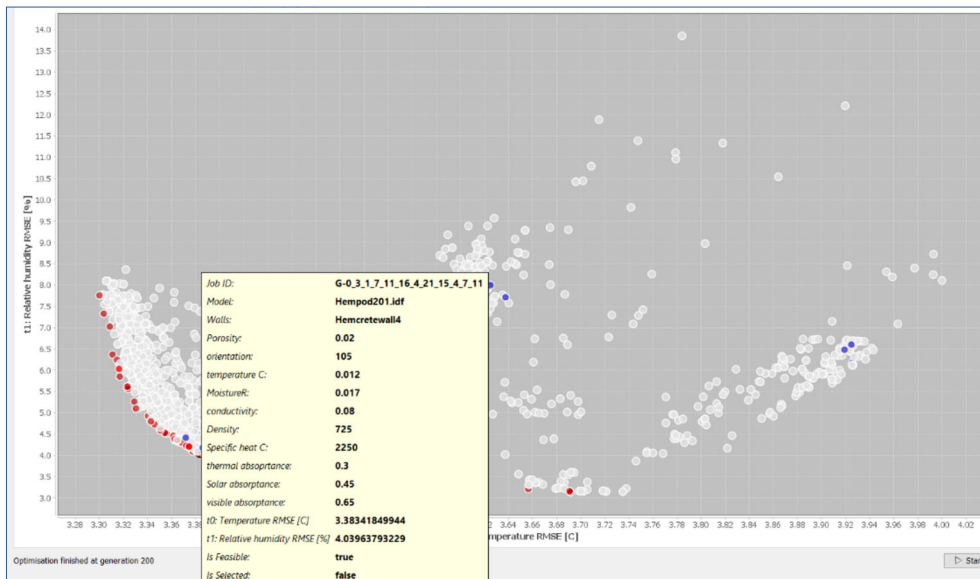


Figure 73: showing a solution chosen from the Pareto front

In the Figure 74 below, the root mean square error for temperature is 3.45°C and the root mean square error for relative humidity is 3.56% respectively.

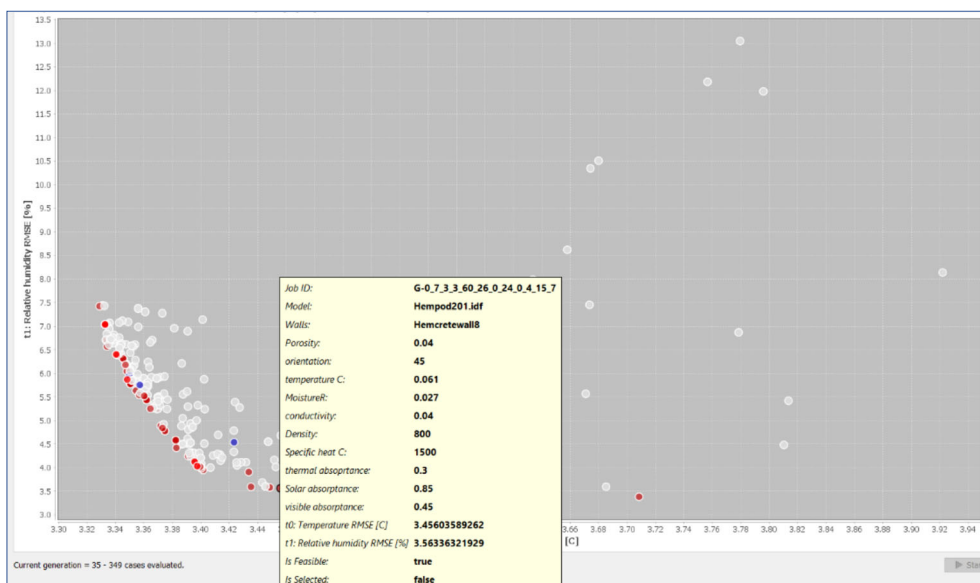


Figure 74: showing the optimum solution chosen from the Pareto front

The solution from Figure 74 was selected as the identified optimum solution from the multi objective optimisation. The reasoning is that, compared to the other solutions, this particular solution simultaneously reduces the root mean square error for both objectives (temperature and relative humidity) accordingly. Even though the RMSE for temperature in the solution represented with Figure 71 is 3.39°C, the corresponding RMSE for relative humidity was 3.72%. While in Figure 72, the RMSE for temperature was 3.37°C which is lower than the

RMSE for temperature in Figure 73 as 3.45°C, however, its corresponding relative humidity RMSE was 4.08% which is higher than 3.56% in Figure 74. Additionally, the details realized from the solution in Figure 74 was inputted back into EnergyPlus to verify and validate the experimental simulation and multi objective optimisation results. From the validation simulation, the root mean square error was calculated with the monitored data in excel format. The root mean square error for temperature was 3.45°C and the root mean square error for relative humidity was 3.56%, which is the same as the RMSE from the multi objective optimisation.

The construction wall identified as the accurate parameter for hempcrete simulation, contains the @@wall@@ with eight layers of 0.05mm of hempcrete. As explained in section 5.2 above, separating the wall layers was done to observe the detail movement of heat and moisture in and through the hempcrete wall. However, eight layers of 0.05m of hempcrete is 0.4m of hempcrete wall. Meaning that, 400mm (0.4m) of hempcrete wall using the identified hygrothermal properties for hempcrete from this study, are the accurate parameters for hempcrete simulation. It is also not different from the “hempcrete wall8” comprising of eight layers of 0.05mm of hempcrete. Figure 75 below, show the simulation conducted in EnergyPlus to confirm that eight layers of 0.05m of hempcrete is the same as 0.4m of hempcrete. After this simulation was conducted, the simulation outputs for eight layers of 0.05m of hempcrete, was the same as 0.4m (400mm) of hempcrete.

The screenshot shows the EnergyPlus IDF Editor interface. On the left, a 'Class List' shows various material and window-related classes. The main area displays a table comparing properties for Obj1 (Hempcrete) and other materials. The table includes columns for Field, Units, Obj1, Obj2, Obj3, Obj4, Obj5, and Obj6. The 'Name' row is highlighted for Obj1 as 'Hempcrete'.

Field	Units	Obj1	Obj2	Obj3	Obj4	Obj5	Obj6
Name		Hempcrete	Plywood	Polyurethane board	Dense EPS slab ins	External rendering	Gypsum plaster boa
Roughness		MediumRough	MediumSmooth	MediumRough	MediumRough	MediumSmooth	MediumSmooth
Thickness	m	0.4	0.01	0.2	0.2	0.009	0.009
Conductivity	W/m-K	0.04	0.15	0.04	0.04	0.5	0.16
Density	kg/m3	800	700	30	30	1300	801
Specific Heat	J/kg-K	1500	1420	1400	1400	1000	837
Thermal Absorptance		0.3	0.9	0.9	0.9	0.9	0.9
Solar Absorptance		0.85	0.1	0.1	0.1	0.1	0.1
Visible Absorptance		0.45	0.3	0.3	0.3	0.3	0.3

Figure 75: Simulation to confirm eight layers of hempcrete is the same as 400mm of hempcrete

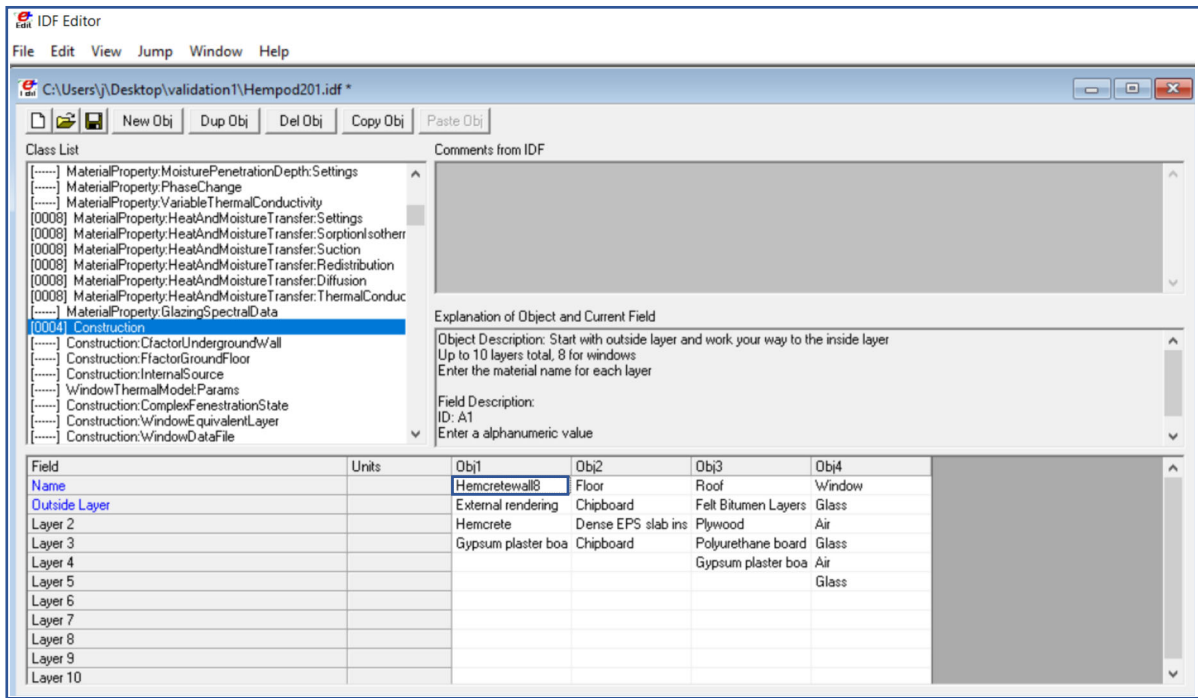


Figure 76: EnergyPlus simulation interface to confirm “hemcretewall8” is the same 400mm of hemcrete

CHAPTER SIX

RESULTS AND DISCUSSION

Chapter six is the results and discussion chapter. It explains, validates and discusses the results from this research study. Section 6.1 explains the results obtained from the conducted experimental simulations and optimisation. Section 6.1.1 contains the validation of the optimisation outputs, which includes feeding back the optimisation results into a simulation model to validate the research method and results. Section 6.1.2 contains the validation of experimental results using the residential building model. Section 6.2 is the discussion section where the viability of research outputs, simulation variables and optimisation parameters are discussed, including importance of the research results. Section 6.3 contains the reference list for this chapter.

6.1 RESULTS

This study extensively investigated hempcrete simulation to reduce performance gap, the results show that simulation performance gap was indeed reduced. As seen from the experimental simulations performed, the metric of root mean square error was used to calculate the difference between measured and simulated values of Hempod. The results from the root mean square error calculation represents the performance gap and it is evident that root mean square error was reduced after multi objective optimization was performed.

The root mean square error of the base case for Hempod temperature before experimentation was 5.5°C and it was reduced to 5°C in *Hempod201* from the simulation experiments in IES Virtual Environment. From the multi objective optimisation performed, the root mean square error for temperature was further reduced to 3.45°C. Similarly, the root mean square error of the base case for Hempod relative humidity was 18.0% before any experiments were performed. It was reduced to 15.4% in *Hempod 201* from the experiments in IES Virtual Environment and from the optimisation outputs, it was further reduced to 3.56%. The results of the optimisation chosen as the optimum solution from the performed optimisation in this study, are as seen in the jEPlus+EA (jEPlus, 2018) scatter plot in Figure 90 below.

Research question 1, seeks to find out to what extent can multi-objective optimisation reduce the simulation performance gap from hempcrete? As explained above and seen from the multi-objective optimisation outputs in Figure 77 below, the performance gap has been reduced from hempcrete as applicable.

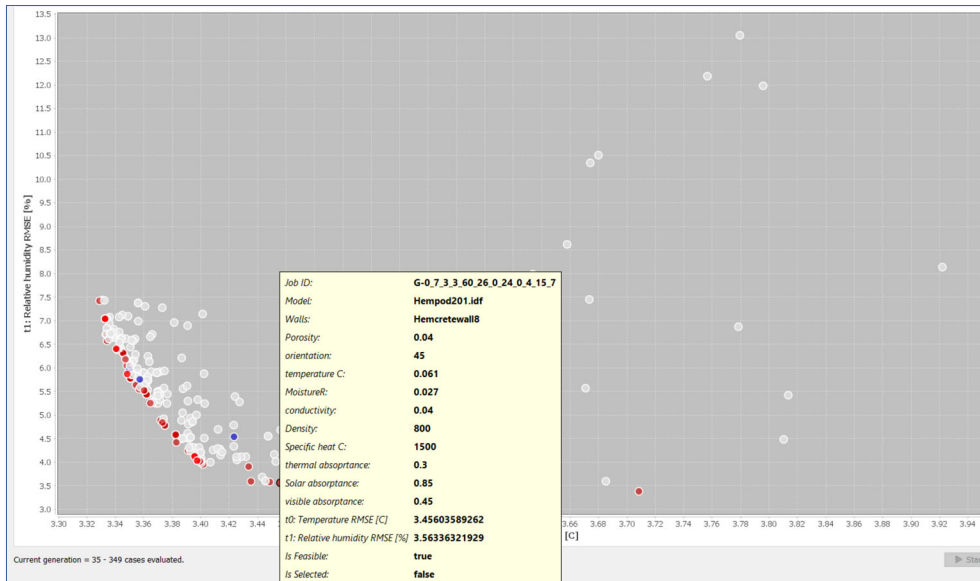


Figure 77: showing the optimum solution chosen from the Pareto front

From the optimum solution as seen in Figure 77, the “Hemcretewall8” is the wall construction identified, with porosity (0.04), initial water content ratio as “moistureR” (0.027), conductivity (0.04), Density (800), specific heat capacity (1500), thermal absorptance (0.3), solar absorptance (0.85) and visible absorptance (0.45). These results together with the inputted value for moisture content (0.02), relative humidity fraction (0.5), liquid transport coefficient (0.06) and water vapor diffusion resistance factor (1) from the optimisation results in Figure 36, have been identified as the parameters for hempcrete simulation, as seen in Table 10 below.

Table 10: Representation of hempcrete for reduced simulation performance gap

Material (outside to inside)	Thickness (m)	Conductivity (W/m ² K)	Density (Kg/m ³)	Specific Heat Capacity (J//kg ² k)	Thermal Absorptance	Solar Absorptance	Visible Absorptance	Porosity (m ³ /m ³)	Initial Water Content Ratio (kg/kg)	Moisture Content (kg/m ³)	Liquid Transport Coefficient (m2/s)	Relative Humidity Fraction	Water Vapor Diffusion Resistance Factor
External Rendering	0.009	0.5000	1300.0	1000.0	0.1	0.02	0.9	0.1	0.021	0	0	0.25	7
Hempcrete	0.05	0.04	800	1500	0.3	0.85	0.45	0.04	0.027	0.02	0.06	0.5	1
Hempcrete	0.05	0.04	800	1500	0.3	0.85	0.45	0.04	0.027	0.02	0.06	0.5	1
Hempcrete	0.05	0.04	800	1500	0.3	0.85	0.45	0.04	0.027	0.02	0.06	0.5	1
Hempcrete	0.05	0.04	800	1500	0.3	0.85	0.45	0.04	0.027	0.02	0.06	0.5	1
Hempcrete	0.05	0.04	800	1500	0.3	0.85	0.45	0.04	0.027	0.02	0.06	0.5	1
Hempcrete	0.05	0.04	800	1500	0.3	0.85	0.45	0.04	0.027	0.02	0.06	0.5	1
Hempcrete	0.05	0.04	800	1500	0.3	0.85	0.45	0.04	0.027	0.02	0.06	0.5	1
Hempcrete	0.05	0.04	800	1500	0.3	0.85	0.45	0.04	0.027	0.02	0.06	0.5	1
Gypsum Plastering	0.009	0.420	1200	837	0.3	0.02	0.9	0.3	0.027	0	0	0.2	5

6.1.1 Validation of results with Hempod

The identified hempcrete simulation properties as detailed from Table 10 above, was fed back into Hempod EnergyPlus model, for parametric simulation to validate the optimisation results.

The validation of experimental results for Hempod is as explained below:

- I. The material field for hempcrete was inputted and the properties of hempcrete for simulation, identified from the multi objective optimisation results were entered. As seen in the column named “Obj1”, Thermal conductivity ($0.04\text{W/m}^2\text{K}$), Density (800kgm^3), specific heat capacity ($\text{J/kg}\cdot\text{K}$), thermal absorptance (0.3), solar absorptance (0.85) and visible absorptance (0.45) accordingly, as shown in Figure C1 in appendix C.
- II. The material property:Heat and Moisture Transfer; Settings section, where hempcrete field property for porosity and initial water content ratio was set to zero in Figure A2 are now specified accordingly, after replacing the zero with search strings as explained with Figure B4 and B5 for optimisation. The values of porosity and initial water content ratio identified from the multi objective optimisation results, are 0.04 for porosity and 0.027 for initial water content ratio. They were specified as the value of porosity and initial water content ratio accordingly, for Hempod simulation as seen in the column “Obj1” in Figure C2 in appendix C.
- III. The material property:Heat and Moisture Transfer; Sorption isotherm section, where hempcrete field property for relative humidity fraction and moisture content was inputted as zero in Figure A3 are now set accordingly. After replacing the zero with search strings as explained with Figure B6 and Figure B7 for optimisation. The values of relative humidity fraction and moisture content identified from the multi objective optimisation results, are 0.5 for relative humidity fraction and 0.02 for moisture content. They were specified as the value of relative humidity fraction and moisture content accordingly, for Hempod simulation as seen in the column “Obj3” from Figure C3 in appendix C.
- IV. The material property:Heat and Moisture Transfer; Suction section, where hempcrete field property for moisture content and liquid transport coefficient was set to zero in Figure A4 are now specified accordingly, after replacing the zero with search strings as explained with Figure B8 and Figure B9 for optimisation. The values of moisture content and liquid transport coefficient identified from the multi objective optimisation results, are 0.02 for moisture content and 0.06 for liquid transport coefficient. They

were specified as the value of moisture content and liquid transport coefficient accordingly, for Hempod simulation as seen in the column “Obj1” in the Figure C4 in appendix C.

- V. The material property:Heat and Moisture Transfer; Redistribution section, where hempcrete field property for moisture content and liquid transport coefficient was set to zero in Figure A5 are now set accordingly, after replacing the zero with search strings as explained with Figure B10 and Figure B11 for optimisation. The values of moisture content and liquid transport coefficient identified from the multi objective optimisation results, are 0.02 for moisture content and 0.06 for liquid transport coefficient. They were specified as the value of moisture content and liquid transport coefficient accordingly, for Hempod simulation as seen in the column “Obj1” in the Figure C5 in appendix C.
- VI. The material property:Heat and Moisture Transfer; Diffusion section, where hempcrete field property for relative humidity fraction and water vapor diffusion resistance factor was set to zero in Figure A6 are now set accordingly, after replacing the zero with search strings as explained with Figure B12 and Figure B13 for optimisation. The values of relative humidity fraction and water vapor diffusion resistance factor identified from the multi objective optimisation results, are 0.5 for relative humidity fraction and 1 for water vapor diffusion resistance factor. They were specified as the value of relative humidity fraction and water vapor diffusion resistance factor accordingly, for Hempod simulation as seen in the column “Obj1” in the Figure C6 in appendix C.
- VII. The material property:Heat and Moisture Transfer; Thermal conductivity section, where hempcrete field property for moisture content and thermal conductivity were replaced with search strings are now set accordingly. The values of moisture content and thermal conductivity identified from the multi objective optimisation results, are 0.02 for moisture content and 0.04 for conductivity. They were specified as the value of moisture content and thermal conductivity accordingly, for Hempod simulation as seen in the column “Obj1” in the Figure C7 in appendix C.
- VIII. In the construction class field for walls, “Hemcretewall8” was set as the wall construction as seen in the column “Obj1” in the Figure C8 in appendix C.

In the building surface detailed class list of simulation parameters, the wall construction name was selected as Hempcretewall8 from the construction class list as explained with Figure C8 in appendix C. After the South wall, East wall, North wall and West wall of Hempod were replaced with the search string @@wall@@ as explained with Figure 39 for optimisation, these are now set to Hempcretewall8 as identified from the multi objective optimisation results. This was entered for Hempod validation simulation as seen in Figure C9 in appendix C.

After inputting all the hempcrete simulation parameters identified from the optimisation results into the EnergyPlus model for simulation, the model was saved and simulation was launched. The results from the validation simulation was obtained and used for calculating root mean square error with the monitored values of Hempod. The root mean square error for temperature was 3.45°C and the root mean square error for relative humidity was 3.56% respectively. Figure 78 below shows the validation simulation values for Hempod temperature, with the monitored temperature value of Hempod. And Figure 79 below, shows the validation simulation values for Hempod relative humidity with the monitored relative humidity value for Hempod.

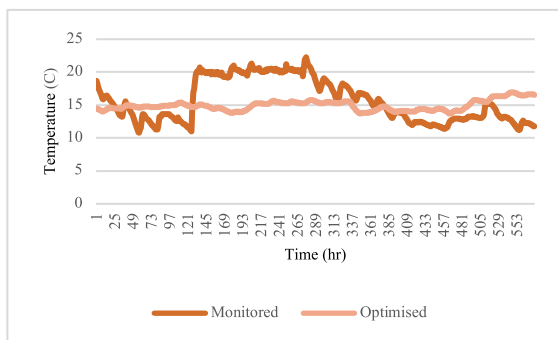


Figure 78: Optimised and monitored temperature

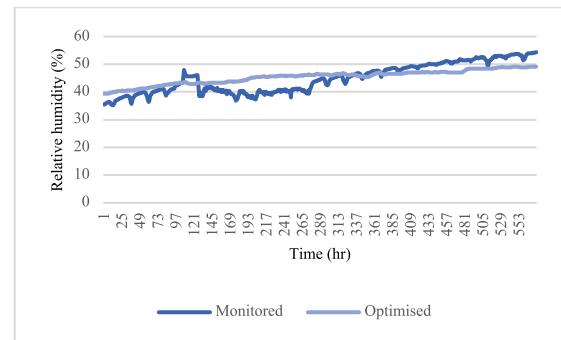


Figure 79: Optimised and monitored Relative humidity

6.1.2 Validation of results with residential building

The validation of results with the residential building was conducted by performing a simulation of the residential building in EnergyPlus, using the identified simulation properties of hempcrete from the multi objective optimisation. The IES Virtual Environment model of the residential building was transferred into idf format via DesignBuilder (DesignBuilder, 2018) and opened in EnergyPlus for heat and moisture transfer simulation. The validation of experimental results using the residential building is as explained below:

I. In EnergyPlus, the combined heat and moisture finite algorithm was selected as the heat balance algorithm for the simulation as seen in the Figure 80 below.

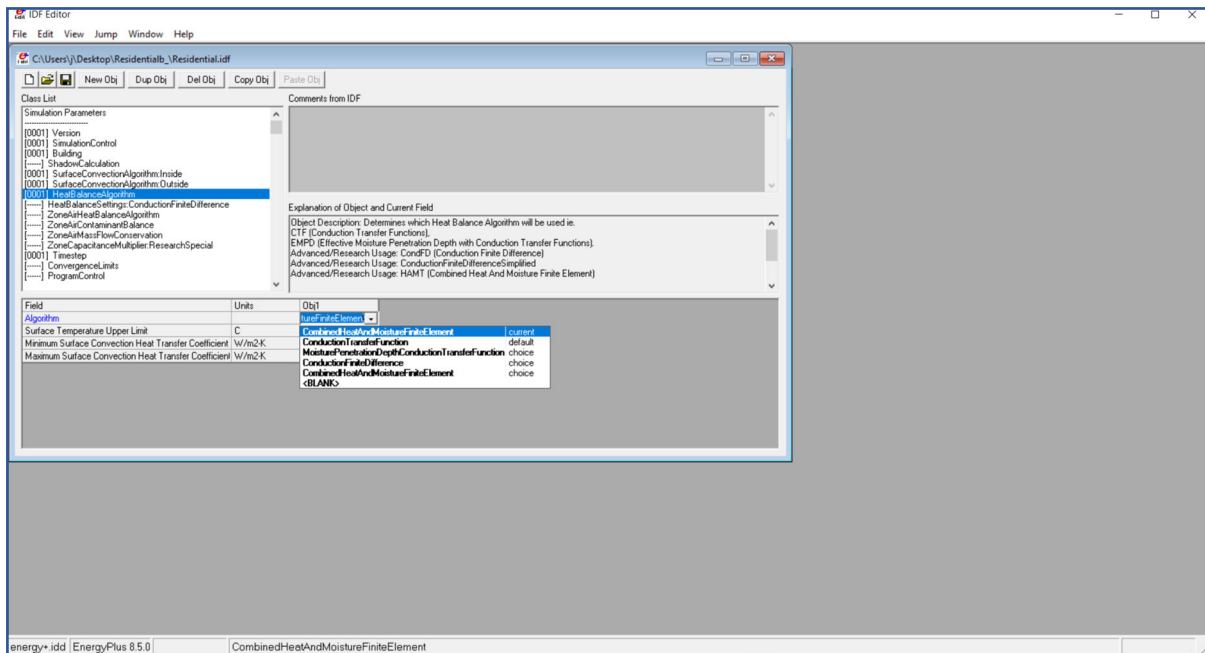


Figure 80: heat balance algorithm for HAMT Simulation

II. The site location for the simulation was inputted as GBR_ENG_Norwich which is the location of the monitored residential building. The weather file used, is the EnergyPlus weather file (GBR_ENG_Norwich.Intl.AP.034920_TMYx.zip) downloaded from EnergyPlus.net as explained in the “weather file” section of Chapter three section 3.3.5. “Europe – Region 6” from the the Climate files – listed in World Metrological Organizations (WMO) Regions; GBR_ENG_Norwich.Intl.A.P was used as seen in the Figure 81 below.

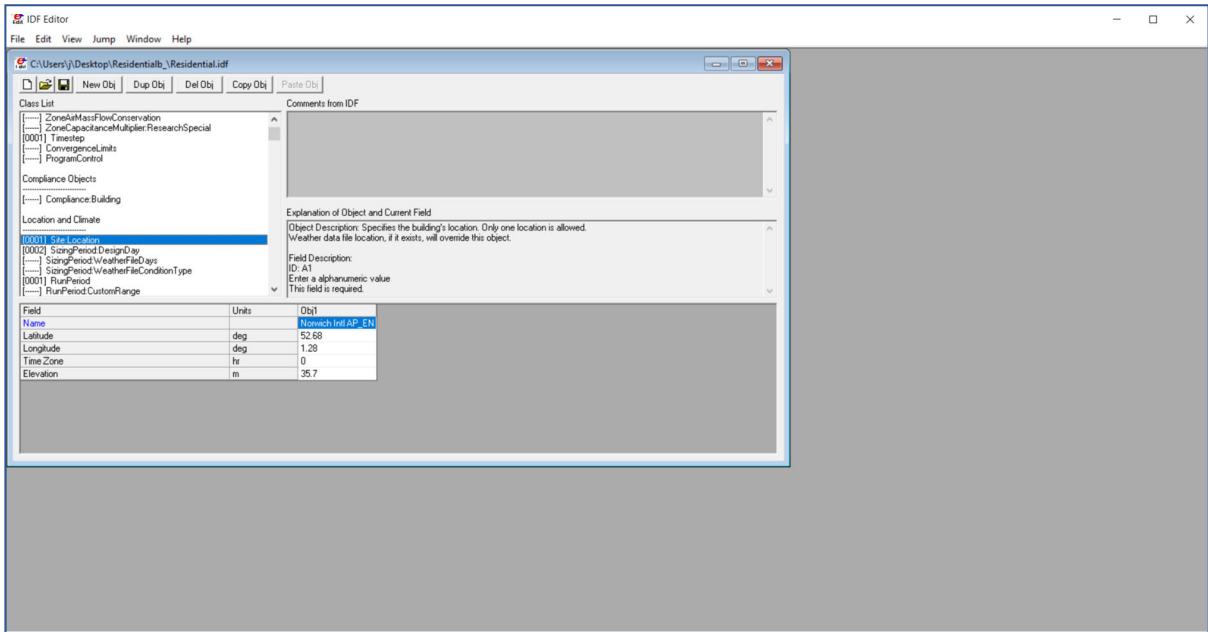


Figure 81: Showing the selected site location for the residential building HAMT simulation

III. The Run period of the simulation was specified for the same period as the monitored residential data, which is from 1st January to 31st December (1/1 – 31/12). The begin month and begin day of month, as well as end month and end day of month for the simulation was specified in EnergyPlus, as indicated in the Figure 82 below.

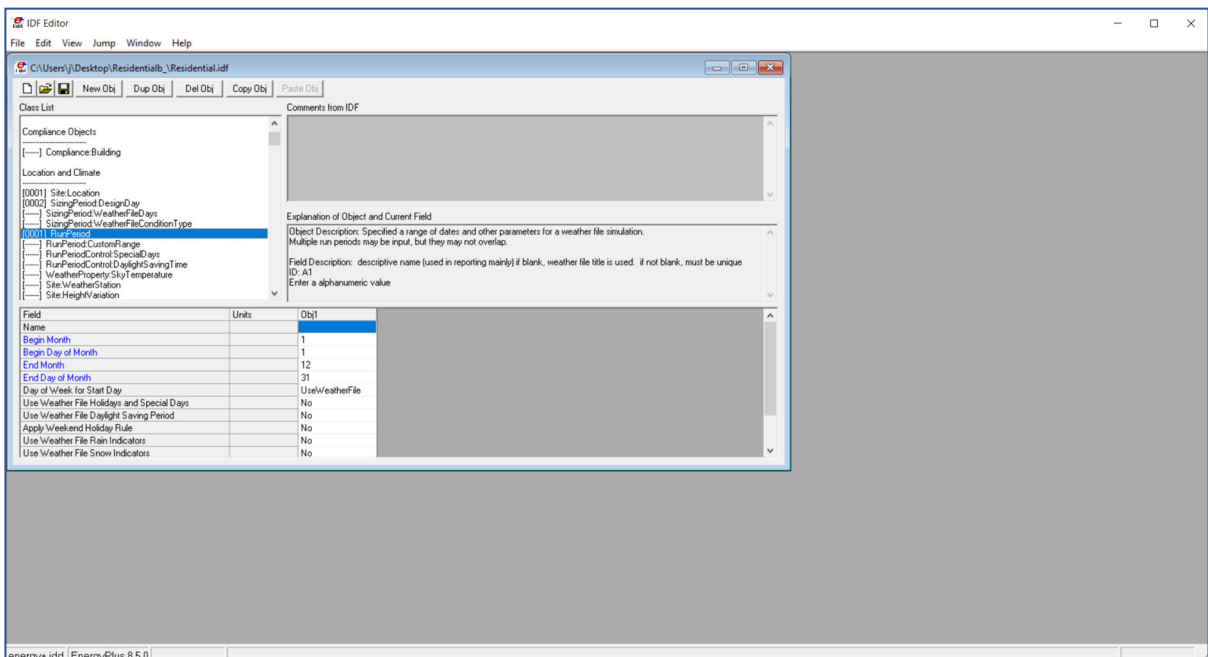


Figure 82: Showing the specified run period for the residential building HAMT Simulation

- IV. In the “Material” class list for the heat and moisture transfer simulation parameter, a material field was inputted and named hempcrete. Due to the console based layout of EnergyPlus, material and material property have to be entered for any simulations. The material field for hempcrete was entered as identified from the multi objective optimisation. As seen in the column named “Obj1”, these were set to the wall thickness (0.4m), thermal conductivity (0.04W/m²K), Density (800kgm³), specific heat capacity (J/kg·K), thermal absorptance (0.3), solar absorptance (0.85) and visible absorptance (0.45). As seen in Figure D1 in appendix D.
- V. In the material property:Heat and Moisture Transfer; settings section, the hempcrete material field property for porosity and initial water content ratio were entered. The values of porosity and initial water content ratio identified from the multi objective optimisation results, were 0.04 for porosity and 0.027 for initial water content ratio. They were specified as the value of porosity and initial water content ratio accordingly, as seen in the column “Obj1” in Figure D2 in appendix D.
- VI. In the material property:Heat and Moisture Transfer; sorption isotherm section, the hempcrete material property field for relative humidity fraction and moisture content were entered. The values of relative humidity fraction and moisture content identified from the multi objective optimisation results, are 0.5 for relative humidity fraction and 0.02 for moisture content. They were specified as the value of relative humidity fraction and moisture content accordingly, as seen in the column “Obj1” in Figure D3 in appendix D.
- VII. In the material property:Heat and Moisture Transfer; suction section, the hempcrete material property field for moisture content and liquid transport coefficient were identified from the optimisation. The value for moisture content is 0.02 and the value for liquid transport coefficient is 0.06. The values were specified as the values of moisture content and liquid transport coefficient accordingly, as seen in the column “Obj1” in Figure D4 in appendix D.
- VIII. In the material property:Heat and Moisture Transfer; redistribution section, the hempcrete material property field for moisture content and liquid transport coefficient were identified from the optimisation. The value for moisture content is 0.02 and the value for liquid transport coefficient is 0.06. The values were specified as the values of

moisture content and liquid transport coefficient accordingly, as seen in the column “Obj1” in Figure D5 in appendix D.

- IX. In the material property:Heat and Moisture Transfer; Diffusion section, the hempcrete material property field for relative humidity fraction and water vapor diffusion resistance factor were identified from the optimisation. The value for relative humidity fraction is 0.5 and the value for water vapor diffusion resistance factor is 1. The values were inputted and specified as the values of relative humidity fraction and water vapor diffusion resistance factor accordingly, as seen in the column “Obj1” in Figure D6 in appendix D.
- X. In the material property:Heat and Moisture Transfer; thermal conductivity section, the hempcrete material property field for moisture content and thermal conductivity were identified from the optimisation. The value for moisture content is 0.02 and the value for thermal conductivity is 0.04. The values were specified as the values of moisture content and thermal conductivity accordingly, as seen in the column “Obj1” in Figure D7 in appendix D.
- XI. The construction class provides for inputting the construction component of the building in layers. It is designed to be entered from the outside layers to the inside layers, for the walls, roofs, floors and windows. The hempcrete material specified above and explained in Figure 40 was selected and used as the wall construction component as seen below in column “Obj14” and the wall construction was named “Hemcretewall”. As seen from the Figure D8 in appendix D, the construction component for the Hemcretewall is specified in layers from external rendering through to the internal layer of gypsum plaster board.

In EnergyPlus heat and moisture transfer simulation, a zone defines the thermal area of the building to be simulated. For instance, the simulation of the residential building required that every room in the building should be defined as a zone, to increase the detail in the simulation output. The reason is that, the temperature and relative humidity outputs for the living room, kitchen and bedroom will be obtained from the simulation and used to calculate root mean square error with the monitored values. The ceiling height, volume and floor area of each room is specified to define it as a zone for the simulation. This information was collected from the IES Virtual Environment model of the residential building. In the “zone” class all the areas in the building were defined as seen in the Figure D9 in appendix D, where the column “Obj1”

defines the living room as a zone, as well as column “Obj5” defines the kitchen and column “Obj 7 and Obj10 define the bedrooms as zones.

Building surface detailed allows for the detailed entry of the building heat transfer surfaces such as walls, floors and roofs for simulations. In the field for zone name, every zone in the building was selected as defined in the “zone” class and explained above using Figure 13, the surface type for each zone was also selected accordingly. In the field for construction name, the walls of the Living room, kitchen and bedroom were assigned hempcretewall as specified and explained above using Figure 40. This means that the hempcrete wall contains properties identified from the multi objective optimisation results as the properties of hempcrete for simulation. For example, in Columns “Obj5, Obj 6 and Obj7” of Figure D10 in appendix D, hempcrete wall is applied to the wall of the Living room. And in the same way, it was applied to the kitchen and bedroom.

After entering all the hempcrete simulation parameters identified from the optimisation results into the EnergyPlus residential building model for simulation, the model was saved and simulation was launched. The results from the validation simulation was obtained and used for calculating root mean square error with the monitored values of the living room, kitchen and bedroom. The root mean square error for temperature of the living room was 2.27°C and the root mean square error for relative humidity of the living room was 2.06% respectively. Figure 83 below shows the simulation values for living room temperature, with the monitored temperature value of the living room. Figure 84 below, shows the simulation values for the living room relative humidity with the monitored relative humidity value for the living room.



Figure 83: Simulated and monitored living room temperature

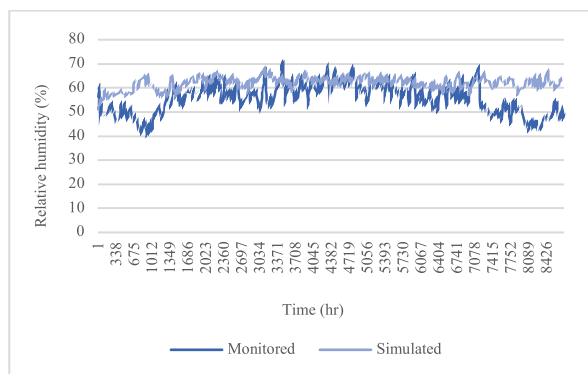


Figure 84: Simulated and monitored living room relative humidity

The root mean square error for temperature of the kitchen was 1.94°C and the root mean square error for relative humidity of the kitchen was 1.21% respectively. Figure 85 below show the simulation values for kitchen temperature, with the monitored temperature value of the kitchen. Figure 86 below, show the simulation values for the kitchen relative humidity with the monitored relative humidity values of the kitchen.



Figure 85: Simulated and monitored kitchen temperature

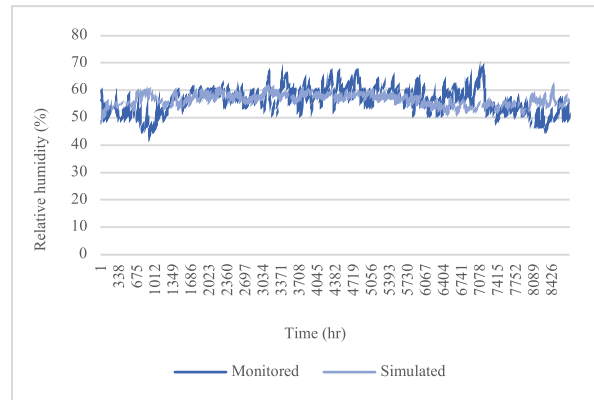


Figure 86: Simulated and monitored kitchen relative humidity

The root mean square error for temperature of the bedroom was 1.55°C and the root mean square error for relative humidity of the kitchen was 2.51% respectively. Figure 87 below shows the validation simulation values for the bedroom temperature, with the monitored temperature values of the bedroom. Figure 88 below, show the simulation values for the bedroom relative humidity with the monitored relative humidity values of the bedroom.

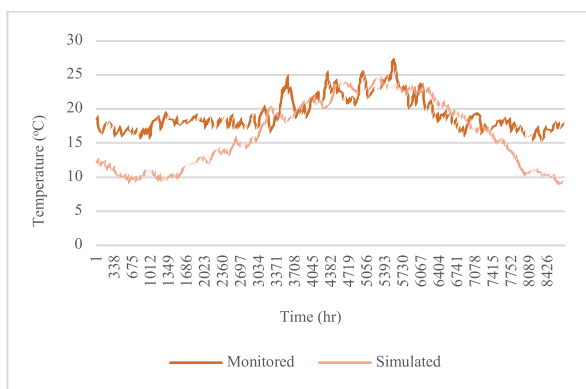


Figure 87: Simulated and monitored bedroom temperature

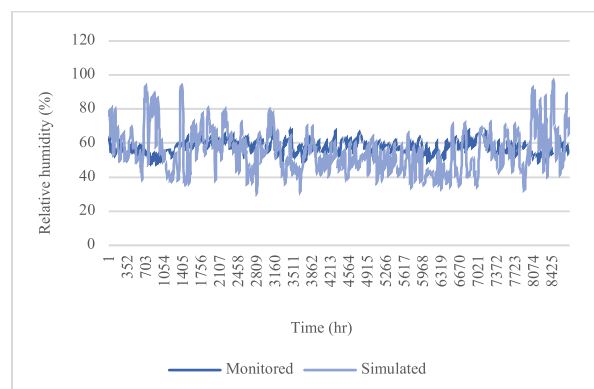


Figure 88: Simulated and monitored bedroom relative humidity

Research question 1a seeks to find out to what extent can identifying the appropriate parameters for hempcrete simulation reduce the simulation performance gap? As seen from the validation

simulation, where the identified appropriate parameters for hempcrete simulation was entered for simulating the residential building. From the validation of the experimental results using the residential building, it is evident that root mean square error has been reduced from the residential building. The root mean square error of the Living room base case for temperature was 4.1°C and it has been reduced to 2.27°C, the base case relative humidity was 4.9% and has been reduced to 2.06%. Similarly, the root mean square error of the kitchen base case for temperature was 5.1°C and it has been reduced to 1.94°C, the relative humidity base case was 10.7% and has been reduced to 1.21%. Also, the root mean square error of the bedroom base case for temperature was 4.2°C and has been reduced to 1.55°C while the base case relative humidity was 4.7% and reduced to 2.51%.

6.2 DISCUSSION

The results from this experimental study show that simulation performance gap was significantly reduced. However, the simulation experiments and validation were only performed in the walls, where hempcrete was used for the actual building construction of the monitored buildings. This suggests that, if hempcrete was used for the floor and roof construction, there is a good potential to eliminate the simulation performance gap from the whole building. This also highlights the efficiency of the research method adopted to conduct this study.

Humphreys (2009) philosophically addressed computer simulations as an ‘amplification instrument’ that speeds up what the unaided human could not easily do within reasonable time (Humphreys, 2009; Humphreys, 2002). As seen from the multi objective optimisation conducted in this study, there was over several millions of optimisation variables in the total search space as seen from Figure 40, which ordinarily would have taken few weeks, months or years to run as individual simulations. However, the optimisation simultaneously executed the simulations and explored all the parameters and variables within hours. Similarly, the heat and moisture transfer simulation are a computational representation of the heat and moisture generation, heat and moisture storage as well as heat and moisture transfer equations (EnergyPlus, 2016). Ordinarily, solving these equations manually or analytically will take years. More so, computer simulation has become a reliable and efficient contributor towards adequate investigation in the fields of science such as biology, physics, chemistry and building

science (Winsberg, 2019). According to Tedre and Moisseinen (2014); the context in which computer experiments are approached in computing, ‘experimentation’ as a terminology is used the same in other fields such as, physics (Franklin, 2012) and biology (Weber, 2012) for physical experiments. For instance, experimental checks and calibration, using apparatus to investigate a phenomenon is similar to both physical and simulation experiments (Tedre and Moisseinen 2014). The introduction or production of intervention, in which the experimenter manipulates the object under observation is same as in physical experiment and simulation experiments (Korb and Mascaro, 2010). Simulation is informative of real-world phenomena, as seen in this study, real life hempcrete buildings were monitored and then simulated to address the problem of hempcrete simulation and performance gap using simulation tools. This study extensively investigated how to reduce simulation performance gap from hempcrete within simulation tools, by identifying the parameters for hempcrete simulation.

Experiments are carried out for various reasons, but, with a sole aim of finding out something of interest or creating something from a natural phenomenon. While there are many possible complications and nuances in the real world, experiments have a main concept of using one physical process, or type of process, to simulate another (Korb and Mascaro, 2010). The parameters used in the simulation experiments are a mixture of experimental and estimated values. In order to make prior estimates, the results from previous hempcrete studies was used to extrapolate some key values in the experiment such as conductivity, density and specific heat capacity. As indicated in Chapter 3 and Chapter 4, these values were used because, in order to conduct a simulation, the conductivity, density and specific heat of a material need to be assigned. These values were used for the experiments before being replaced with search strings for the multi objective optimisation to identify the accurate parameter of hempcrete for simulation. There is the potential for things to go wrong in experiments such as the experimental outcome not being as expected. And/or, for the experiment to be uninformative as a result of the experimental subject failing to simulate the target subject, due to the homomorphism between reality and the experimental process failing (Mascaro et al., 2015). Barclay, Holcroft and Shea (2014), experimentally researched methods to determine the whole building hygrothermal performance of hempcrete buildings for moisture buffer. A set of hygrothermal material properties for hempcrete was presented from laboratory, which was then inputted and used for simulation in Wufi and EnergyPlus. The results from the study highly recommended that, increasing resolution of EnergyPlus using HAMT model should be part of

efficient attempts to improve simulation accuracy for hempcrete (Barclay, Holcroft and Shea, 2014). The hygrothermal property for hempcrete simulation is still unknown which also contributes to the existing performance gap. As seen in this study, coupling EnergyPlus heat and moisture transfer model with multi objective optimisation has identified the thermal and hygric parameter for hempcrete simulation as applicable.

Additionally, photosynthetic and natural fiber construction materials such as hempcrete, tend to have higher vapor permeability than conventional building materials such as concrete. However, a significant barrier to the wider use and simulation of hempcrete is the shortage of a complete sets of hygroscopic material property (Colinart et al., 2013). The high vapor permeability of hempcrete is really important, as it plays a vital role in the thermal performance of the material. While the vapor permeability property of hempcrete can be useful, the hygroscopic complex behavior presents challenges in describing the thermal performance, and subsequently affects the whole building performance analysis as well as its simulation (Mazhoud, Collet, Pretot and Chamoin, 2016; Walker and Pavia, 2014). Even though a number of tools such as Wufi, EnergyPlus and ESP-r have successfully integrated heat and moisture transport algorithm for models, there are still some barriers to its widespread use for hempcrete simulation, such as the material property data for hempcrete simulation being unavailable (Barclay, Holcroft and Shea, 2014). This study investigated in detail how to reduce simulation performance gap from hempcrete within simulation tools, by identifying the parameters required for hempcrete simulation. As well as having good thermal and insulative properties, hempcrete also possess a moderate thermal inertia, meaning it provides efficient heat store that improves the overall thermal efficiency of any building built with hempcrete (Everard 2008).

The combined heat and moisture simulation are a type of simulation algorithm, used to simulate buildings for research or construction purpose. Research question 1b seeks to find out how the heat and moisture transfer in hempcrete can be modelled for simulation? As seen from the multi objective optimisation results, the heat and moisture transfer in hempcrete can be modelled and simulated by using the identified properties of hempcrete from the multi-objective optimisation.

The parameters required for combined heat and moisture simulation are: Density, Porosity, specific heat capacity, moisture dependent thermal conductivity, liquid transport coefficient

for suction (energyplus.net; Künzel, 1995). These are the parameters whose values were identified from this study for hempcrete simulation.

Thermal conductivity is the correlation between heat flux per unit area and temperature gradient (Mulopo and Abdulsalam, 2019). It represents the quantity of thermal energy that flows per unit time through a unit area with a temperature gradient of 1°C per unit distance. It is the ability of a material to conduct heat and it is a necessary feature that helps dissipate thermal energy in a material or system (Vengatesan, Varghese and Mittal, 2018). The results from this research, established a thermal conductivity for hempcrete simulation as 0.04W/m²K from the results of the multi objective optimisation.

Specific heat capacity is the amount of heat supplied to or taken out of the unit mass of a material or system in order to increase or decrease its temperature by one degree (Feidt, 2017). It is essential for the heat balances of a material or any system under investigation (Janotte et al., 2017). The value of specific heat capacity for hempcrete simulation was identified as 1500J/kg-K from the results of the multi objective optimisation.

Porosity can be defined as any space between micro-units that is greater than normal atomic dimensions so that foreign molecules such as water can penetrate it (Sereda, 2020). The porosity of a material is an input variable which is the maximum fraction by volume of a material that can be taken up with moisture (EnergyPlus, 2016). The value of porosity for hempcrete simulation was identified as 0.04m³/m³ from the multi objective optimisation in this study.

Density has a significant effect on the hygrothermal properties of hempcrete (Barclay, Holcroft and Shea, 2014). The value of Density for hempcrete simulation was identified as 800kg/m³ from the multi objective optimisation performed in this study.

Thermal absorptance for hempcrete simulation was identified as 0.3, solar absorptance value of hempcrete for simulation was identified as 0.85 and the visible absorptance for hempcrete simulation was identified as 0.45 from the multi objective optimisation.

The water vapour diffusion resistance factor is an actual reciprocal of the water vapour permeance (ISO 12572:2016).The water vapor diffusion resistant factor for hempcrete have been established from laboratory and previous research as 4 to 10 (Abbott, 2014) and 5 to 12, which is very low compared to other materials (Collet and Pretot, 2014). The value of water vapor diffusion resistance factor for hempcrete simulation was identified as 1 from the optimisation performed in this study.

Moisture content is needed for calculating the heat transfer through the cells of a material in the walls, floor or roof, it also affects thermal resistance and heat capacitance of any material. The value of moisture content for hempcrete simulation was identified as $0.02\text{kg}/\text{m}^3$ from the performed multi objective optimisation.

Initial water content ratio describes the water/material density ratio of the material, the value obtained for hempcrete simulation from the multi objective optimisation is $0.027\text{kg}/\text{kg}$.

Liquid transport coefficient is moisture dependent and affects two different coefficients within the material, for suction with wet surface and for redistribution where the surface of the material is no longer wet but has been absorbed into the material. The value of liquid transport coefficient for hempcrete simulation was obtained as $0.06\text{m}^2/\text{s}$ from the multi objective optimisation results.

Also, the value of relative humidity fraction for hempcrete simulation was identified as 0.5 from the multi objective optimisation results.

This suggests that an efficient way to model and simulate hempcrete for design and construction is to use the heat and moisture transfer simulation technique. More so, in a hygroscopic field, the water content of a building material is influenced and described by sorption isotherm. At a relative humidity below 50%, the water molecules are closely bound to the pores, such that liquid transport coefficient can be excluded. However, at relative humidity above 50%, capillary condensation occurs within the micropores of the material. Also, in building materials, the vapor diffusion resistance is attributable to liquid transport, which is superimposed and driven by diffusion (Krus and Holm, 1999). If the sorption isotherm for a material is known, the capillary transport coefficient can be calculated from the difference between mass flows or transfer in the higher humidity area and those measured in dry state (Krus, 1996). Since this study researched into reducing simulation performance gap from hempcrete to increase confidence in hempcrete simulation, the detailed description and explanation of hempcrete hygrothermal properties is outside the focus of this work.

However, since the liquid transport coefficient for hempcrete simulation has been identified in this study, this means that the capillary action within hempcrete can be researched and can be modelled and simulated for advancing its effect on the built environment. Similarly, the results from the multi objective optimisation have revealed the hygroscopic properties of hempcrete for simulation, which can potentially inspire ideas and develop research using hempcrete for climate change mitigation.

CHAPTER SEVEN

CONCLUSION

Chapter seven is the conclusion chapter. It highlights the conclusion of the research study and explains the benefits of the research results. Section 7.1 is the research conclusion, which draws the conclusion from this research study. Section 7.1.1 is the research outcome section and it discusses the outcome of this study accordingly. Section 7.1.2 contains the contribution to knowledge from this research. Section 7.1.3 explains future work.

7.1 RESEARCH CONCLUSION

Currently, the technological advancement and increased development of computer virtual technology has amplified the use of simulation tools for building design and simulations especially as it saves time and energy. For instance, it is used by architects, designers and other built environment professionals for increased detail and faster designs. The current issues of climate change in the built environment has made it imperative to design and construct buildings that actually perform in reality, rather than buildings that only theoretically perform on paper. More so, a growing number of design and analytical approaches based on simulations have gradually paved the way for new ways of designing in the AEC industry (an extensive account of such approaches is presented in Lam 2020). Computer aided designs and simulation tools demonstrates the flexibility and reinforces the feasibility of integrating space, time and function virtually, into a comprehensive system such as buildings. In this study, simulation based multi-objective optimisation was employed as a computational framework to investigate and address the problem of performance gap in hempcrete simulation, which is, to reduce simulation performance gap. As illustrated, the experiment focused more on investigating the material properties of hempcrete for reducing the simulation performance gap and improving hempcrete simulation. This was carried out as a means to increase the confidence in hempcrete simulation and facilitate a wider use of hempcrete by professionals and students in the built environment as applicable.

As explored in the literature review, there are many benefits of using hempcrete as a construction material such as it's good thermal and hygric properties with high vapor permeability. To a great extent, hempcrete provides sustainable solution to the increasing

demand for energy efficient construction strategies that are also low carbon, healthy, and breathable. The good thermal properties of hempcrete mean that, it has the potential to mitigate climate change related issues from the built environment such as overheating, increased precipitation, and energy consumption. Therefore, understanding the behaviour and physics of hempcrete material is key to defining the material properties needed for its accurate simulation. From the experiments conducted in this study, as seen in experiment 1, it is evident that hempcrete cannot be easily substituted with other conventional materials and natural construction materials. Experiment 2 revealed the importance of investigating the physics properties, hygrothermal behavior and properties of hempcrete for simulation, as a construction material. EnergyPlus heat and moisture transfer simulation requires thermal and hygroscopic properties of materials to be inputted in order to conduct the simulation. Since the appropriate properties and parameters for hempcrete simulation is not known, it instigated the investigation with calibration into the EnergyPlus heat and moisture transfer simulation parameters for optimisation in this study. More so, the method of coupling parametric simulation with multi objective optimisation used in this study, has demonstrated to be efficient for investigating material properties within simulation tools. The study has also illustrated how simulation models can potentially be integrated with parametric analysis for genetic algorithm optimisation. And it presented a number of Pareto-optimal models for hempcrete simulation with reduced performance gap. However, in comparing the root mean square error of the best performing models, the model which reasonably and simultaneously reduced the performance gap for both objectives was selected as the optimum solution. Evidently, this approach also allowed for locating the desirable solutions within the Pareto Frontier that are more likely to meet expectations of reducing performance gap and identifying hempcrete simulation parameters. Altogether, the mechanism for analysing the multi objective optimization results led to a better understanding of the objectives of this study while identifying hempcrete simulation parameters as required. The results from the multi objective optimisation also shows a significant reduction of the simulation performance gap as applicable, which explains the answer to research question 1.

The validation of experimental and optimisation results conducted with Hempod demonstrated the viability of the research method and results in this study. Similarly, as demonstrated in the previous chapter, the optimisation results were also used to simulate the residential building using the identified hempcrete simulation parameter from the optimisation. Evidently, the root

mean square error for the residential building was reduced, which confirms the research results and reinforces the viability of the research method. Additionally, the residential building and Hempod are buildings from different location, as seen from the validation, different weather files was used for the simulation. This suggests that the results from this study is weather and climate independent, meaning the identified parameters for hempcrete simulation can be used for hempcrete simulation no matter the weather.

The representation of hempcrete consisting of the following material properties; Conductivity ($0.04\text{W}/(\text{m}^2\text{K})$), Density ($800\text{Kg}/\text{m}^3$), Specific Heat Capacity ($1500\text{ J}/(\text{Kg}^2\text{K})$), Thermal absorptance (0.3), Solar absorptance (0.85), Visible absorptance (0.45), Porosity ($0.04\text{ m}^3/\text{m}^3$), Initial water content ratio ($0.027\text{ Kg}/\text{Kg}$), Moisture content ($0.02\text{Kg}/\text{m}^3$), Liquid Transport coefficient ($0.06\text{ m}^2/\text{s}$), Relative humidity fraction (0.5) and Water Vapor Diffusion Resistance Factor (1) leads to a reduction of performance gap when used for simulation, as evidenced from the validation simulation carried out in Chapter 6 Section 6.1.1 and 6.1.2. This representation enables architects and designers using conventional simulation tools to simulate hempcrete accurately with reduced performance gap. More so, research has established and corroborated the good thermal and hygroscopic properties of hempcrete as a construction material. Therefore, reducing the performance gap and identifying the parameters for appropriate hempcrete simulation is a sustainable way to increase the built environment's resilience to climate change.

7.1.1 RESEARCH OUTCOME

The outcome of this study addresses the early-stage of design and construction for sustainable building projects. The reasoning is, before a building construction is carried out, the design has to be created and the simulation conducted. Therefore, before hempcrete buildings can be constructed and built, they need to be designed and simulated as well, the results from this research will come in handy for design and simulation of hempcrete buildings. The identified parameters for hempcrete simulation and construction obtained in this study from the multi objective optimisation, will be helpful to design and construction professionals. Specifically, it will increase confidence for architects and building engineers when designing and simulating hempcrete buildings with the readily available representation of hempcrete. Additionally, the outcome from this research will facilitate a wider use of hempcrete. This is because, hempcrete is a construction material and has the potential to be used for construction of houses, offices,

warehouses, schools. It can also be used to construct other outdoor and landscape structures such as pergola's, gazebos and pavements as applicable.

7.1.2 CONTRIBUTION TO KNOWLEDGE

Prior to this research, the simulation of hempcrete was difficult using conventional simulation tools, which had led to a significant performance gap. As seen from the results of this research, hempcrete can now be simulated with conventional simulation tools using the hempcrete material representation discovered in this research with substantially reduced performance gap. This opens up new opportunities in terms of:

- I. The results from the experiments demystifies hempcrete simulation as it demonstrates how hempcrete can be represented in conventional simulation tools, using the identified material properties. The established hempcrete properties for simulation can be directly applied into a simulation project for design and construction of sustainable buildings. An example is seen from the validation performed with the residential building.
- II. Software engineers can also use the readily available hempcrete properties and input hempcrete into the simulation tools, for example there are readily available materials with their simulation properties in IES Virtual Environment, which gives ease and simplicity of selecting concrete as a construction material and applying it to the building model for simulation. These identified material properties for hempcrete simulation can be installed into simulation software's such as IES Virtual Environment as a system material for model and simulation.
- III. The results will transform hempcrete simulation for research and diversely increase the use of hempcrete with improved confidence for further research for the benefit of the built environment's resilience to climate change. Specifically, the heat and moisture transfer simulation method identified as the simulation algorithm for hempcrete simulation will also be advantageous to researchers.

7.1.3 FUTURE WORK

As seen from the simulation outputs, the RMSE and simulation performance gap have been significantly reduced. However, the results could be considered to not follow the dynamics of the corresponding monitored values. While this is a potential limitation of this study in addition to the data used and simulation run period as explained in Chapter 1, Section 1.7. The results from this study have identified the accurate parameters to be used for hempcrete simulation

with a reduced performance gap. Additionally, the validation simulation carried out by using the identified parameters for hempcrete simulation to simulate the residential building, demonstrates the extent to which identifying the appropriate parameters for hempcrete simulation can increase confidence in hempcrete simulation. Especially as the root mean square error was significantly reduced during the validation simulation which answers research question 1a as applicable. These parameters can be used by researchers to further look into investigating the performance gap of hempcrete within simulation tools to achieve a more dynamic correspondence between the monitored values and the simulation results.

As explained in Chapter 6 Section 6.2, the results from the multi objective optimisation revealed the hygroscopic properties of hempcrete for simulation which can potentially inspire ideas and develop research using hempcrete. The heat and moisture transfer in hempcrete can be modelled and simulated to facilitate hempcrete simulation using the identified properties of hempcrete for simulation as seen from the multi objective optimisation results which answers research question 1b. For instance, the liquid transport coefficient for hempcrete simulation has been identified in this study alongside the parameters shown in Table 10. This means that the natural capillary action occurring within hempcrete can be investigated for advancing design and simulation of buildings towards climate change mitigation, which is currently an impending need in the built environment.

7.2 RECOMMENDATION

This research and experiment was conducted with data from a monitored test cell called Hempod and the results were validated using Hempod and the residential building with their corresponding weather data. Therefore, this study should be replicated using other climatic/weather areas, to examine and confirm the validity of the results since the study produced climate independent results from the experimental simulations. This research could potentially be the catalyst for creating more strategic action plans for reducing simulation performance gap from hempcrete for more accurate hempcrete simulation focused on transforming the built environment's resilience to climate change. Additionally, it is good for more studies to be done with data from a different type of hempcrete building using the identified parameter for hempcrete simulation from this study, to increase confidence in hempcrete simulation.

LIST OF REFERENCES

- Abbott, T., (2014). *Hempcrete Factsheet - Essential Hempcrete Info - The Limecrete Company*. [online] Limecrete.co.uk. Available at: <<http://limecrete.co.uk/hempcrete-factsheet/>> [Accessed 11 June. 2019].
- Afonja, B. (2001). *Introduction statistics*. Evans Brothers (Nig) publishers Ltd Ibadan-Nigeria.
- Ahmad, M., and Culp, H. C. (2006). Uncalibrated Building Energy Simulation Modeling Results. *Hvac Research*, 12. 1141-1155. 10.1080/10789669.2006.10391455.
- Allard, I., Olofsson, T. and Nair, G. (2018). Energy evaluation of residential buildings: Performance gap analysis incorporating uncertainties in the evaluation methods. *Building Simulation*, 11(4), pp.725-737.
- Almalki, S., (2016). Integrating Quantitative and Qualitative Data in Mixed Methods Research—Challenges and Benefits. *Journal of Education and Learning*, [online] 5(3), p.288. Available at: <<http://dx.doi.org/10.5539/jel.v5n3p288>> [Accessed 21 April 2021].
- Almeida, F., Faria, D. and Queirós, A., (2017). Strengths and Limitations of Qualitative and Quantitative Research Methods. *European Journal of Education Studies*, 3(9), pp.369-379.
- Altomonte, S., (2009). Climate Change and Architecture: Mitigation and Adaptation Strategies for a Sustainable Development. *Journal of Sustainable Development*, 1(1).
- Ammeri, A., Hachicha, W., Masmoudi, F., and Chabchoub, H. (2014). Iterative simulation optimisation approach-based genetic algorithm for lot-sizing problem in make-to-order sector. *International Journal of Business Performance and Supply Chain Modelling*. Vol. 6. PP. 376-394.
- Amziane, S., and Arnaud, L. (2014). Bio-aggregate-based building materials - *Applications to hemp concretes*, 508 Wiley-ISTE, London, 2013.
http://onlinelibrary.wiley.com/book/10.1002/9781118576809_509 [accessed 20 August. 2019].
- Amziane, S. and Sonebi, M. (2016). Overview on bio-based building material made with plant aggregate. [online] Pureadmin.qub.ac.uk. Available at: https://pureadmin.qub.ac.uk/ws/portalfiles/portal/47919763/Overview_on_bio_based_building.pdf [Accessed 19 Oct. 2019].
- Antwi, S.K., and Hamza, K. (2015). Qualitative and Quantitative Research Paradigms in Business Research: A Philosophical Reflection. *European Journal of Business and Management*, 7, 217-225.
- Anyanwu, S. A. C. (2002). *Descriptive statistics for Business science and Engineering students* spring field publishers Owerri-Nigeria.

Apuke, O., (2017). Quantitative Research Methods : A Synopsis Approach. *Kuwait Chapter of Arabian Journal of Business and Management Review*, 6(11), pp.40-47.

Arnaud, L. (2009). Comparative study of hygrothermal performances of building materials In: *Proceedings of 11th International Conference on Nonconventional Materials and Technologies (NOCMAT 2009)*, Bath, United Kingdom, 6-9 September 2009.

Arnaud, L., and Gourlay, E. (2011). Experimental study of parameters influencing mechanical properties of 511 hemp concretes, *Construction and Building Materials*. 50–56.

Architecture.com. (2020). *Royal Institute Of British Architects*. [online] Available at: <<https://www.architecture.com>> [Accessed 11 July 2019].

Architizer Editors. Journal. (2020). *Architecture 101: What Is A Section Drawing? - Architizer Journal*. [online] Available at: <<https://architizer.com/blog/practice/details/architecture-101-what-is-a-section/>> [Accessed 11 May 2019].

Architecture, V., (2020). *Importance Of Architectural Detailing - Vita Architecture*. [online] Vita Architecture. Available at: <<https://www.vitaarchitecture.com/architectural-detailing/>> [Accessed 11 March 2020].

Arizzi, A., Brummer, M., Martin-Sanchez, I., Cultrone, G., and Viles, H. (2015). “The Influence of the Type of Lime on the Hygric Behaviour and Bio-Receptivity of Hemp Lime Composites Used for Rendering Applications in Sustainable New Construction and Repair Works.” *PLoS One*, 10(5), 1-19

Attia, S., Hensen, J., Beltrán, L. and De Herde, A., (2012). Selection criteria for building performance simulation tools: contrasting architects' and engineers' needs. *Journal of Building Performance Simulation*, 5(3), pp.155-169.

Augenbroe, G. (2011). The Role of Simulation in Performance Based Building. In “*Building Performance Simulation for Design and Operation*” Edited by Jan L.M. Hensen and Roberto Lamberts. Spon Press.

Augusto, O., Bennis, F. and Caro, S. (2012). A new method for decision making in multi-objective optimization problems. *Research gate*, 32(2), pp.331-369.

Austin, Z. and Sutton, J., (2014). Qualitative Research: Getting Started. *The Canadian Journal of Hospital Pharmacy*, 67(6).

Baglivo, C., Congedo, P. and D’Agostino, D. (2018). Multi-Objective Analysis for the Optimization of a High-Performance Slab-on- Ground Floor in a Warm Climate. *Energies*, 11(11), p.2988.

Bana, A. and Jankovic, L., (2019). Reducing Simulation Performance Gap from Hempcrete Buildings Using Multi Objective Optimization. In: *16th International Building Performance*

Simulation Association Conference. [online] Rome, Italy: IBPSA, pp.425-432. Available at: <<https://doi.org/10.26868/25222708.2019.210914>> [Accessed 1 May 2020].

Banks, J., Carson, J. S., Nelson, B. L., Nicol, D. M. (2009). Discrete-Event Simulation System. 5. *Prentice-Hall International Series in Industrial and Systems Engineering*; 2009.

Barclay, M., Holcroft, N. and Shea, A., (2014). Methods to determine whole building hygrothermal performance of hemp–lime buildings. *Building and Environment*, 80, pp.204-212.

Bejat, T., Piot, A., Jay, A. and Bessette, L. (2015). Study of two hemp concrete walls in real weather conditions. *International Building Physics Conference, IBPC*, 6(78), pp.1605-1610.

Benfratello, S., Capitano, C., Peri, G., Rizzo, G., Scaccianoce, G., and Sorrentino, G. (2013). Thermal and structural properties of a hemp–lime biocomposite. *Construction and Building Materials*. 48. 745-754.

Bevan, R., and Woolley, T. (2008). *Hemp Lime Construction - A guide to building with hemp lime composites*. Bracknell, UK: IHS BRE Press. ISBN 978-1-84806- 033-3

Boutin, M.P., Flamin, C., Quinton, S., Gosse, G. (2006). Study on the Environmental Characteristics of Hemp through the Analysis of its Life Cycle. *Ministry of Agriculture, Agrifood and Forestry*. Paris, France.

Brady, T., and Yellig, E. (2005). Simulation data mining: A New Form of Computer Simulation Output. In: *Kuhl ME, Steiger NM, Armstrong FB, Joines JA, editors. Proceedings of the 2005 Winter Simulation Conference*. New Jersey: Institute of Electrical and Electronics Engineers, Inc; 2005. pp. 285–289.

BRE (2002). Final report on the Construction of the Hemp Houses at Haverhill, Suffolk.

Bre, F., Silva, Arthur., Ghisi, E., and Fachinotti, V. (2016). Residential building design optimisation using sensitivity analysis and genetic algorithm. *Energy and Buildings*. 133. 10.1016/j.enbuild.2016.10.025.

Bruijn, P. (2012). Material properties and full-scale rain exposure of lime-hemp concrete walls - Epsilon Open Archive. [online] Pub.epsilon.slu.se. Available at: <https://pub.epsilon.slu.se/9007/> [Accessed 19 Nov. 2019].

Burman, E., Rigamonti, D., Kimpain, J. and Mumovic, D. (2012). Performance gap and thermal modelling: a comparison of simulation results and actual energy performance for an academy in North West England. In: *Building Simulation and Optimization Conference*. Loughborough, UK.

Carlucci, S., Cattarn, G., Causone, F., and Pagliano, L. (2015). Multi-objective optimization of a nearly zero-energy building based on thermal and visual discomfort minimization using a non-dominated sorting genetic algorithm. *Energy and Buildings*. 104, 378–3940.

- Carter, J., Cavan, G., Connelly, A., Guy, S., Handley, J. and Kazmierczak, A., (2015). Climate change and the city: Building capacity for urban adaptation. *Progress in Planning*, 95, pp.1-66.
- Cecs.wright.edu. (2021). [online] Available at: <<http://cecs.wright.edu/~stthomas/htchapter03.pdf>> [Accessed 14 April 2021].
- Chalmers, P., (2014). *Climate Change: Implications For Buildings*. [online] Cisl.cam.ac.uk. Available at: <https://www.cisl.cam.ac.uk/business-action/low-carbon-transformation/ipcc-climate-science-business-briefings/pdfs/briefings/IPCC_AR5__Implications_for_Buildings__Briefing__WEB_EN.pdf> [Accessed 1 March 2020].
- Chang, K. (2015). Design Theory and Methods Using CAD/CAE, [online] pp.325-406. Available at: <https://www.sciencedirect.com/science/article/pii/B9780123985125000050> [Accessed 29 May 2019].
- Chastas, P., Theodosiou, T. and Bikas, D., (2016). Embodied energy in residential buildings-towards the nearly zero energy building: A literature review. *Building and Environment*, 105, pp.267-282.
- Chen, S., Jiang, Z., Yang, S., Apley, D. W., and Chen, W. (2016) Non-hierarchical multi-model fusion using spatial random processes. *International Journal, Numerical Mathematical and Engineering* 106:503-526
- Chel, A. and Kaushik, G., (2018). Renewable energy technologies for sustainable development of energy efficient building. *Alexandria Engineering Journal*, 57(2), pp.655-669.
- Cheng, H. and Phillips, M., (2014). Secondary analysis of existing data: opportunities and implementation. *Shanghai Archive of Psychiatry*, 26(4), pp.371–375.
- Chiandussi, G., Codegone, M., Ferrero, S. and Varesio, F. (2012). Comparison of multiobjective optimization methodologies for engineering applications. *Computers and Mathematics with Applications*, 63, pp.912–942.
- Cho, R. (2017). *How We Know Today's Climate Change Is Not Natural*. [online] State of the Planet. Available at: <https://blogs.ei.columbia.edu/2017/04/04/how-we-know-climate-change-is-not-natural/> [Accessed 18 Oct. 2019].
- Cibse.org. (2013). *CIBSE - TM54: Evaluating Operational Energy Performance of Buildings at the Design Stage*. [online] Available at: <https://www.cibse.org/Knowledge/knowledgeitems/detail?id=a0q20000008I7f7AAC> [Accessed 25 May 2019].
- Cimato, F. and Mullan, M., (2010). *Adapting To Climate Change: Analysing The Role Of Government*. [online] Assets.publishing.service.gov.uk. Available at: <https://assets.publishing.service.gov.uk/government/uploads/system/uploads/attachment_data/file/69194/pb13341-analysing-role-government-100122.pdf> [Accessed 1 March 2020].

- Clarke, J. and Hensen, J., (2015). Integrated building performance simulation: Progress, prospects and requirements. *Building and Environment*, 91, pp.294-306.
- Coakley, D., Raftery, P. and Keane, M., (2014). A review of methods to match building energy simulation models to measured data. *Renewable and Sustainable Energy Reviews*, 37, pp.123-141.
- Coello, C., Veldhuizen, D. and Lamont, G., (2013). *Evolutionary Algorithms for Solving Multi-Objective Problems*. [online] Google Books. [Accessed 17 March 2020].
- Colinart, T., Glouannec, P., Pierre, T., Chauvelon, P. and Magueresse, A., (2013). Experimental Study on the Hygrothermal Behavior of a Coated Sprayed Hemp Concrete Wall. *Buildings*, 3(1), pp.79-99.
- Collet, F., and Pretot S. (2014). Experimental highlight of hygrothermal phenomena in hemp concrete wall. *Building and Environment*, Elsevier, 2014, 82, pp.459-466.
- Cooke, M. (2018). Analysis of implication and value of the process of calibration of Building Energy Models (BEMs). *Energy Technology Partnership*.
- Daniel, E., (2016). The Usefulness of Qualitative and Quantitative Approaches and Methods in Researching Problem-Solving Ability in Science Education Curriculum. *Journal of Education and Practice*, 7(15), pp.91-98.
- Deb, K., Pratap, A., Agarwal, S. and Meyarivan, T. (2002). A fast and elitist multiobjective genetic algorithm: *NSGA-II*. *IEEE Transactions on Evolutionary Computation*, 6(2), pp.182-197
- Delgarm, N., Sajadi, B., and Delgarm, S. (2016). Multi-Objective Optimization of Building Energy Performance and Indoor Thermal Comfort: A New Method using Artificial Bee Colony (ABC). *Energy and Buildings*. 131. 10.1016/j.enbuild.2016.09.003.
- Designbuilder.co.uk. (2020). *Simulation Made Easy*. [online] Available at: <<https://designbuilder.co.uk/>> [Accessed 11 March 2020].
- De Wilde, P., (2018). *Building Performance Analysis*. 1st ed. John Wiley & Sons Ltd.
- De Wilde, P. (2017). [online] Available at: <https://journals.sagepub.com/doi/full/10.1177/0143624417728431> [Accessed 30 Mar. 2019].
- De Wilde, P. (2014). The gap between predicted and measured energy performance of buildings: *a framework for investigation*. *Automated. Construction*. 41, 40–49.
- Dhakal, U., Berardi, U., Gorgolewski, M. and Richman, R. (2017). Hygrothermal performance of hempcrete for Ontario (Canada) buildings. *Journal of Cleaner Production*, 142, pp.3656-3665.
- Diquélou, Y., Gourlay, E., Arnaud, L., and Kurek, B. (2015). Impact of hemp shiv on cement setting and 513 hardening: *Influence of the extracted components from the aggregates and*

study of the interfaces 514 with the inorganic matrix, Cement Concrete Compositions. 55; 112–121.

Docs.Python.org. (2020). 6. Modules — Python 3.3.7 Documentation. [online] Available at: <<https://docs.Python.org/3.3/tutorial/modules.html>> [Accessed 6 March 2020].

Dowling, D. (1999). Experimenting on theories. *Sci. Context* 12, 261–273.

Dubrow, D. T., and Krarti, M. (2010). Genetic-algorithm based approach to optimize building envelope design for residential buildings. *Buildings and Environment.* 45, 1574–1581.

Ducoulombier, L. and Lafhaj, Z., (2017). Comparative study of hygrothermal properties of five thermal insulation materials. *Case Studies in Thermal Engineering*, 10, pp.628-640.

Dudovskiy, J., (2019). *Data Collection Methods - Research-Methodology.* [online] ResearchMethodology. Available at: <<https://research-methodology.net/research-methods/datacollection/>> [Accessed 6 June 2020].

Dudas, C., Ng, A., Boström, H. (2009). Information extraction from solution set of simulation-based multi-objective optimization using data mining.

Dumas II, J., (2016). *Computer Architecture: Fundamentals And Principles Of Computer Design.*, 2nd ed. Boca Raton: Chapman and Hall/CRC.

Durán, J., (2019). *Computer Simulations In Science And Engineering - Concepts - Practices - Perspectives.* [online] arXiv.org. Available at: <<https://arxiv.org/abs/1904.01053>> [Accessed 17 March 2020].

Durán, J., (2020). What is a Simulation Model?. *Minds and Machines.*,

Durán, J., (2019). A Formal Framework for Computer Simulations: Surveying the Historical Record and Finding Their Philosophical Roots. *Philosophy & Technology.*,

Elfordy, S., Lucas, F., Tancret, F., Scudeller, Y., and Goudet, L. (2008). Mechanical and thermal properties of lime 517 and hemp concrete (“hemcrete”) manufactured by a projection process, *Construction and Building Materials.* 518 22; 2116–2123.

Energy.gov. (2015). *An Assessment of Energy Technologies and Research Opportunities.* [online] Available at: <<https://www.energy.gov/sites/prod/files/2017/03/f34/qtr-2015-chapter5.pdf>> [Accessed 14 April 2021].

Energyplus.net. (2016). *Engineering Reference.* [online] Available at: <https://energyplus.net/sites/all/modules/custom/nrel_custom/pdfs/pdfs_v8.5.0/EngineeringReference.pdf> [Accessed 11 March 2020].

English, C. and Validation, R., (2020). *Research And Validation | Validity And Validation | Cambridge English.* [online] Cambridgeenglish.org. Available at:

<<https://www.cambridgeenglish.org/research-and-validation/validity-and-validation/>>
[Accessed 5 March 2020].

Epa.gov. (2013). *Our Built And Natural Environment*. [online] Available at:
<<https://www.epa.gov/sites/production/files/2014-03/documents/our-built-and-natural-environments.pdf>> [Accessed 1 March 2020].

Evrard, A. (2008). Transient Hygrothermal Behaviour of Lime-Hemp Materials. *PhD Thesis. Leuven, Belgium:Université Catholique de Louvain*.

Evrard, A. (2008). Transient Hygrothermal Behaviour of Lime-Hemp Materials. *PhD Thesis. Leuven, Belgium:Université Catholique de Louvain*.

Evrard, A., De Herde, A. and Minet, J. (2006). Dynamical interactions between heat and mass flows in Lime-Hemp Concrete. *Research in Building Physics and Building Engineering* ISBN 0-415-41675-2.

Evrard, A. (2003). Bétons de Chanvre - Synthèse des Propriétés Physiques Saint Valérien: *Construire en Chanvre*. In French.

Fàbregues, Sergi (@sfabreguesf). “@socioloxia Perform an alternative analysis with the aim of generating new insights from previous analyses” 10th of December 2013, 11:33 AM.

Fabrizio, E. and Monetti, V., (2015). Methodologies and Advancements in the Calibration of Building Energy Models. *Energies*, 8(4), pp.2548-2574.

Favoino, F., Loonen, R., Doya, M., Goia, F., Bedon, C. and Babich, F., (2018). *Building Performance Simulation And Characterisation Of Adaptive Facades – Adaptive Facade Network*. [online] Tu1403.eu. Available at: <<http://tu1403.eu/wp-content/uploads/Vol%203-2%20linked%20for%20web%201123.pdf>> [Accessed 17 March 2020].

Feidt, M., (2017). From Thermostatics to Non-equilibrium Thermodynamics. *Finite Physical Dimensions Optimal Thermodynamics 1*, pp.1-41.

Freitas, A., (2004). A critical review of multi-objective optimization in data mining. *ACM SIGKDD Explorations Newsletter*, 6(2), pp.77-86.

Frigg, R. and J. Reiss (2008). A critical look at the philosophy of simulation. Synthese. forthcoming.

Garwood, T., Hughes, B., Oates, M., O’Connor, D. and Hughes, R., (2018). A review of energy simulation tools for the manufacturing sector. *Renewable and Sustainable Energy Reviews*, 81, pp.895-911.

Gbxml.org. (2020). *Gbxml - An Industry Supported Standard For Storing And Sharing Building Properties Between 3D Architectural And Engineering Analysis Software*. [online] Available at: <<https://www.gbxml.org>> [Accessed 6 March 2020].

Geiger, O., (2011) “Hempcrete Blocks.” *Geopolymer House Blog*,
<<https://geopolymerhouses.wordpress.com/2011/08/17/hempcrete-blocks/>>

Glé, P., Gourdon, E. and Arnaud, L., (2011). Characterization and modelling of the acoustical properties of hemp shiv and hemp concrete. In: *Symposium on the Acoustics of Poro-Elastic Materials*. Ferrara (Italy), pp.1-2.

Goldberg, D. E (1993): *Genetic Algorithms in Search, Optimization, and Machine Learning*. Reading, Mass. Addison-Wesley, 1989

Gossard, D., Lartigue, B., and Thellier, F. (2013). Multi-objective optimization of a building envelope for thermal performance using Genetic Algorithms and Artificial Neural Network. *Energy and Buildings*. 67. 253-260.

Goundar, S., (2012). (PDF) *Chapter 3 - Research Methodology and Research Method*. [online] ResearchGate. Available at:
<https://www.researchgate.net/publication/333015026_Chapter_3_-_Research_Methodology_and_Research_Method> [Accessed 23 March 2021].

Gourdon, E., and Arnaud, L. (2011). Acoustical properties of materials made of vegetable particles with 503 several scales of porosity, *Appl. Acoust.* 72; 249–259. 504.

Gourlay, E., Glé, P., Marceau, S., Foy, C. and Moscardelli, S. (2017). Effect of water content on the acoustical and thermal properties of hemp concretes. *Construction and Building Materials*, 139, pp.513-523.

GOV.UK. (2019). *Climate change explained*. [online] Available at:
<https://www.gov.uk/guidance/climate-change-explained> [Accessed 18 Oct. 2019].

Gunantara, N. (2018). A review of multi-objective optimization: Methods and its applications. *Cogent Engineering*, 5(1502242), pp.1-16.

Gray, J. and Cutter, A., (2014). Mainstreaming *Caenorhabditis elegans* in experimental evolution. *Proceedings of the Royal Society B: Biological Sciences*, 281(1778), p.20133055.

Hamdy, M. and Mauro, G. (2017). Multi-Objective Optimization of Building Energy Design to Reconcile Collective and Private Perspectives: CO₂-eq vs. *Discounted Payback Time*. energies.

Hamdy, M., Palonen, M., and Hasan, A. (2012). Implementation of Pareto-Archive NSGA-II Algorithms to a Nearly-Zero-Energy Building Optimisation problem.

Hammond, G. and Jones, C., (2008). Embodied energy and carbon in construction materials. *Proceedings of the Institution of Civil Engineers - Energy*, 161(2), pp.87-98.

Han, Y., Yu, H. and Sun, C., (2017). Simulation-Based Multiobjective Optimization of Timber-Glass Residential Buildings in Severe Cold Regions. *Sustainability*, 9(12), p.2353.

Hartmann, S., (1994). *Models As A Tool For Theory Construction: Some Strategies Of Preliminary Physics*. [online] Philsci-archive.pitt.edu. Available at: <<http://philsciarchive.pitt.edu/2410/1/Models.pdf>> [Accessed 18 May 2020].

Hartmann, S. (1996). The world as a process: Simulation in the natural and social sciences. In R. Hegselmann, U. Müller, and K. Troitzsch (Eds.), *Modelling and Simulation in the Social Sciences from the Philosophy of Science Point of View*, pp. 77–100. Kluwer.

Heckbert, P., (1995). *Fourier Transforms And The Fast Fourier Transform (FFT) Algorithm*. [online] Cs.cmu.edu. Available at: <<http://www.cs.cmu.edu/afs/andrew/scs/cs/15-463/2001/pub/www/notes/fourier/fourier.pdf>> [Accessed 11 March 2020].

Hemp Basics | Natural Hemp Products. (2020). *Hemp Uses, Information Facts - Hemp Basics*. [online] Available at: <<https://www.hempbasics.com/shop/general-hemp-information>> [Accessed 17 March 2020].

Hensen, J. and Lamberts, R. (2011). Building Performance Simulation for Design and Operation. *1st ed. London: Routledge*, pp.1-536.

Hirst, E., Walker, P., Paine, K. and Yates, T., (2010). Characterisation of Low-Density Hemp-Lime Composite Building Materials under Compression Loading. In: *Second International Conference on Sustainable Construction Materials and Technologies*. [online] Ancona, Italy, pp.1-11. Available at: <<http://www.claisse.info/proceedings.htm>> [Accessed 17 March 2020].

Hong, T., Langevin, J. and Sun, K., (2018). Building simulation: Ten challenges. *Building Simulation*, 11(5), pp.871-898.

Humphreys, P. (2009) The philosophical novelty of computer simulation methods. *Synthese*. 169, 615–626.

Humphreys, P. (2002). Computational models. *Philosophy of Science*, 69(3), S1–S11.

Humphreys, P. W. (1990). Computer simulations. *Philosophy of Science Association*, 2, 497–506.

Hussain, A., Calabria-Holley, J., Lawrence, M., and Jiang, Y. (2019). Hygrothermal and mechanical characterisation of novel hemp shiv based thermal insulation composites. *Construction and Building Materials*. 212. 561-568. 10.1016/j.conbuildmat.2019.04.029.

IEA Annex 21, (2016). Annex 21 Environmental Performance webpage [online]. Available from <http://www.ecbcs.org/annexes/annex21.htm> [Accessed 07 Oct. 2019]

Iesve.com. (2020). *IES Virtual Environment | The Leading Integrated Suite For Accurate Whole Building Performance Simulation*. [online] Available at: <<https://www.iesve.com/software/virtual-environment>> [Accessed 11 March 2020].

Industrialstrategy.dialogue-app.com. (2018). Model beyond compliance to address the ‘performance gap’ and reduce building energy use — *Department for Business, Energy and Industrial Strategy Dialogue*. [online] Available at:

<https://industrialstrategy.dialogueapp.com/clean-growth/model-beyond-compliance-to-address-the-2018performance-gap2019and-reduce-building-energy-use> [Accessed 19 Oct. 2019].

Ingrao, C., Lo Giudice, A., Bacenetti, J., Tricase, C., Dotelli, G., Fiala, M., Siracusa, V. and Mbohwa, C., (2015). Energy and environmental assessment of industrial hemp for building applications: A review. *Renewable and Sustainable Energy Reviews*, 51, pp.29-42.

Ipscc.ch. (2018). *IPCC — Intergovernmental Panel On Climate Change*. [online] Available at: <<https://www.ipcc.ch>> [Accessed 1 May 2019].

Iso.org. (2020). [online] Available at: <<https://www.iso.org/obp/ui/#iso:std:iso:12572:ed-1:v1:en>> [Accessed 23 May 2020].

Jankovic, L., (2016). Reducing Simulation Performance Gap in Hemp-Lime Buildings Using Fourier Filtering †. *Sustainability*, 8(9), p.864.

Jannat, N., Hussien, A., Abdullah, B. and Cotgrave, A., (2020). A Comparative Simulation Study of the Thermal Performances of the Building Envelope Wall Materials in the Tropics. *Sustainability*, 12(12), p.4892.

Jami, T. and Kumar, S., (2017). Assessment of Carbon Sequestration of Hemp Concrete. In: *International Conference on Advances in Construction Materials and Systems*. [online] Chennai, India, pp.1-7. Available at: <<http://DOI: 10.13140/RG.2.2.29338.95683>> [Accessed 11 March 2020].

Janotte, N., Wilbert, S., Sallaberry, F., Schroedter-Homscheidt, M. and Ramirez, L., (2017). Principles of CSP performance assessment. *The Performance of Concentrated Solar Power (CSP) Systems*, pp.31-64.

Jeplus.org. (2020). *Jeplus – An Energyplus Simulation Manager For Parametrics*. [online] Available at: <<http://www.jeplus.org/wiki/doku.php>> [Accessed 11 March 2020].

Jianling, C. (2009). Multi-Objective Optimization of Cutting Parameters with Improved NSGA-II. 10.1109/ICMSS.2009.5302835.

Jones RV, Fuertes A, Wilde P de. (2015). The Gap Between Simulated and Measured Energy Performance: A Case Study Across Six Identical New-Build Flats in The UK Rory V. Jones, Alba Fuertes, Pieter De Wilde Building Performance Analysis Group, School of Architecture, Design and Environment. *International Conference of the International Building Performance Simulation Association*.

Json.org. (2020). *JSON*. [online] Available at: <<https://www.json.org/json-en.html>> [Accessed 6 March 2020].

Kabir, S., (2016). *Basic Guidelines For Research: An Introductory Approach For All Disciplines*. 1st ed. Chittagong: Book Zone Publication, Chittagong-4203, Bangladesh, p.Chapter 9.

- Kalua, A. and Jones, J., (2020). Epistemological Framework for Computer Simulations in Building Science Research: Insights from Theory and Practice. *Philosophies*, 5(4), p.30.
- Karaguzel, O., Zhang, R. and Lam, K. (2013). Coupling of whole-building energy simulation and multi-dimensional numerical optimization for minimizing the life cycle costs of office buildings. *Building Simulation*, 7(2), pp.111-121.
- Kibira, D., Hatim, Q., Kumara, S., and Shao, G. (2015). Integrating data analytics and simulation methods to support manufacturing decision making. 2100-2111.
- Kinnane, O., McGranaghan, G., Walker, R., Pavia, S., Byrne, G., and Robinson, A. (2015). Experimental investigation of thermal inertia properties in hemp-lime concrete walls. In *Proceedings of the 10th Conference on Advanced Building Skins*. Economic Forum, pp. 942-949, 10th Conference on Advanced Building Skins, Bern, Switzerland, 03 November 2015.
- Kodali, S. P., Kudikala, R. and Deb, K. (2008). Multi-objective optimization of surface grinding process using NSGA II. City, 2008.
- Kodur, V., (2014). Properties of Concrete at Elevated Temperatures. *ISRN Civil Engineering*, 2014, pp.1-15.
- Korb, K. and Mascaro, S., (2010). *The Philosophy Of Computer Simulation*. [online] Pdfs.semanticscholar.org. Available at: <<https://pdfs.semanticscholar.org/cca0/b36d8511c30e1a7410bb8948d25bc584df16.pdf>> [Accessed 18 March 2020].
- Krus, M., (1996). *Moisture Transport And Storage Coefficient Of Porous Mineral Building Materials*. [online] Wufi.de. Available at: <<https://wufi.de/literatur/Krus%201996%20-%20Moisture%20Transport%20and%20Storage%20Coefficients.pdf>> [Accessed 23 May 2020].
- Krus, M. and Holm, A., (1999). Simple methods to approximate the liquid transport coefficients describing the absorption and drying process. In: *Proceedings of the 5th Symposium 'Building Physics in the Nordic Countries*. Göteborg: Fraunhofer Institute for Building Physics.
- Künzel, H.M. (1995) *Simultaneous Heat and Moisture Transport in Building Components. One- and two-dimensional calculation using simple parameters*. IRB Verlag 1995
- Lam, Khee Poh. "Sustainability Performance Simulation Tools for Building Design." *Sustainable Built Environments* (2020): 589-655).
- Lane, T. (2006). Beer, Cannabis, Glue and a Generous Helping of Lime. *Building Magazine* (45), 46-50.
- Langelier, G., Sahraoui, H. and Poulin, P., (2005). Visualization-based analysis of quality for large-scale software systems. *Proceedings of the 20th IEEE/ACM international Conference on Automated software engineering - ASE '05*,.

- Latif, E., Lawrence, M., Shea, A. and Walker, P. (2015). Moisture buffer potential of experimental wall assemblies incorporating formulated hemp-lime. *Building and Environment*, 93, pp.200-210.
- Lazar, J., Feng, J. and Hochheiser, H., (2017). *Research Methods in Human Computer Interaction*. 2nd ed. Morgan Kaufmann Publishers., pp.25-44.
- Leal, S., Zucker, G., Hauer, S. and Judex, F., (2014). A Software Architecture for Simulation Support in Building Automation. *Buildings*, 4(3), pp.320-335.
- Leedy, P. and Ormrod, J., (2015). *Practical Research Planning And Design*. 1st ed. Harlow: Pearson Education Limited, pp.229-260.
- Legislation.gov.uk. (2021). *The Building Regulations 2010*. [online] Available at: <<https://www.legislation.gov.uk/ukxi/2010/2214/regulation/2/made#regulation-2-3>> [Accessed 14 April 2021].
- Law, A. M. and Kelton, W. D. (2000). *Simulation Modeling and Analysis*, 3rd ed. McGrawHill, New York.
- Leung, C. and Lau, H., (2018). Multiobjective Simulation-Based Optimization Based on Artificial Immune Systems for a Distribution Center. *Journal of Optimization*, 2018, pp.1-15.
- Leung, L., (2015). Validity, reliability, and generalizability in qualitative research. *Journal of Family Medicine and Primary Care*, 4(3), p.324.
- Liang, L. and Jakubiec, J. (2018). A Three-Part Visualisation Framework to Navigate Complex Multi-Objective (>3) Building Performance Optimisation Design Space. In: *4th Building Simulation and Optimization Conference*. Cambridge, UK, p.192.
- Li, S., Liu, L. and Peng, C., (2020). A Review of Performance-Oriented Architectural Design and Optimization in the Context of Sustainability: Dividends and Challenges. *Sustainability*, 12(4), p.1427.
- Liu, S., Sun, J., Wei, F. and Lu, M., (2018). Numerical simulation and experimental research on temperature and stress fields in TIG welding for plate of RAFM steel. *Fusion Engineering and Design*, 136, pp.690-693.
- LLC, B., (2020). *Combined Heat And Moisture Transfer (HAMT) Model: Engineering Reference — Energyplus 8.0*. [online] Bigladdersoftware.com. Available at: <<https://bigladdersoftware.com/epx/docs/8-0/engineering-reference/page-018.html>> [Accessed 6 March 2020].
- Lucko, G. and Rojas, E., (2010). Research Validation: Challenges and Opportunities in the Construction Domain. *Journal of Construction Engineering and Management*, 136(1).
- Mack, N., Woodsong, C., Macqueen, K., Guest, G. and Namey, E., (2005). *Qualitative Research Methods*. [online] Fhi360.org. Available at: <<https://www.fhi360.org/sites/default/files/media/documents/Qualitative%20Research%20M>

ethods%20-%20A%20Data%20Collector%27s%20Field%20Guide.pdf> [Accessed 23 April 2021].

Marler, R. and Arora, J., (2004). Survey of multi-objective optimization methods for engineering. *Structural and Multidisciplinary Optimization*, 26(6), pp.369-395.

Mazhoud, B., Collet, F., Pretot, S. and Chamoin, J., (2016). Hygric and thermal properties of hemp-lime plasters. *Building and Environment*, 96, pp.206-216.

Mealdprostarter.org. (2019). *Data Analysis, Visualization And Interpretation | MEALD Pro Starter*. [online] Available at: <<https://mealdprostarter.org/n-data-analysis-visualization-andinterpretation/>> [Accessed 5 February 2020].

McMillan, C., & González, R. F. (1968). *Systems Analysis: A Computer Approach to Decision Models*. Homewood/Ill: Irwin.

Mitra, K., and Gopinath, R. (2004). Multiobjective Optimization of an Industrial Grinding Operation Using Elitist Nondominated Sorting Genetic Algorithm. *Chemical Engineering Science*. 59. 385-396.

Mijwel, M., (2016). Genetic Algorithm Optimization by Natural Selection. *Computer Science*, 1, pp.1-7.

Mitchell, M., (2020). *An Introduction To Genetic Algorithms*. 1st ed. Michigan: MIT Press, 1998, pp.20-133.

Mitchell, O. (2015). *Experimental Research Design*. [online] Available at: <https://doi.org/10.1002/9781118519639.wbecpx113> [Accessed 27 Dec. 2019].

Moffatt, S. and Kohler, N., (2008). Conceptualizing the built environment as a social-ecological system. *Building Research & Information*, 36(3), pp.248-268.

Monfet, D., Charneux, R., Zmeureanu, R. and Lemire, N. (2009). *Calibration of a Building Energy Model Using Measured Data*. ASHRAE Transactions 115(1), pp. 348–359.

Mulopo, J. and Abdulsalam, J., (2019). Energy storage properties of graphene nanofillers. *Graphene-Based Nanotechnologies for Energy and Environment*, pp.155-179.

Naylor, R. (2003). Galileo, Copernicanism and the Origins of the New Science of Motion. *The British Journal for the History of Science*, 36(2), 151-181. Retrieved June 6, 2020, from www.jstor.org/stable/4028231

Negendahl, K., and Nielsen, T.R. (2015). Building energy optimization in the early design stages: A simplified method. *Energy Build; 105*, 88–99.

Neos-guide.org. (2019). *Multiobjective Optimization | NEOS*. [online] Available at: <<https://neos-guide.org/content/multiobjective-optimization>> [Accessed 6 March 2020].

- Nikjoofar, A., and Zarghami, M. (2013). Water Distribution Networks Designing by the Multiobjective Genetic Algorithm and Game Theory. *Metaheuristics in Water Resources, Geotechnical and Transportation Engineering*. 43-77.
- Niyigena, C., Amziane, S., Chateauneuf, A., Arnaud, L., Bessette, L., Collet, F., Escadeillas, G., Lanos, Lawrence M., Magniont C., Marceau S., Pavia S., Peter U., Picandet V., Sonebi M., Walker R. (2015) RRT3: 527 statistical analysis of hemp concrete mechanical properties variability, in: Proc. *1st Int. Conf. Bio528 Based Build. Mater., RILEM*, Clermont-Ferrand, France, 2015: pp. 334–340.
- Nozahic, V., Amziane, S., Torrent, G., Saïdi, K., and De Baynast, H. (2012). Design of green concrete made of plant-derived aggregates and a pumice-lime binder. *Cement and Concrete Composites*. 34. 10.1016/j.cemconcomp.2011.09.002.
- Nguyen, A. T., & Reiter, S. (2015). A performance comparison of sensitivity analysis methods for building energy models. *Building Simulation*, Vol. 8, No. 6, pp. 651-664
- Nguyen, A., Reiter, S. and Rigo, P., (2014). A review on simulation-based optimization methods applied to building performance analysis. *Applied Energy*, 113, pp.1043-1058.
- Nguyen, T.-T., Picandet, V., Amziane, S., and Baley, C. (2010). Effect of compaction on 536 mechanical and thermal properties of hemp concrete, *Eur. J. Environment and Civil Engineering*. 14. 545– 537 560.
- Nguyen, T.-T., Picandet, V., Amziane, S., and Baley, C. (2009). Influence of compactness and hemp hurd 533 characteristics on the mechanical properties of lime and hemp concrete, *Eur. J. Environment and Civil Engineering*. 534 13. 1039–1050.
- Office.com. (2020). *Office 365 Login | Microsoft Office*. [online] Available at: <<https://www.office.com>> [Accessed 6 March 2020].
- Openstudio.net. (2020). *Openstudio | Openstudio*. [online] Available at: <<https://www.openstudio.net>> [Accessed 11 March 2020].
- Osanyintola, O. and Simonson, C. (2006). Moisture buffering capacity of hygroscopic building materials: Experimental facilities and energy impact. *Energy and Buildings*, 38, pp.1270–1282.
- Panagiotidou, M. and Aye, L. (2018). Comparison of Multi-objective Optimisation Tools for Building Performance Simulation with TRNSYS 18. In: *4th Building Simulation and Optimization Conference*. Cambridge, UK, pp.215-216.
- Pandas.pydata.org. (2020). *Pandas Documentation — Pandas 1.0.4 Documentation*. [online] Available at: <<https://pandas.pydata.org/docs/>> [Accessed 6 March 2020].
- Pannucci, C. and Wilkins, E., (2010). Identifying and Avoiding Bias in Research. *Plastic and Reconstructive Surgery*, 126(2), pp.619-625.
- Paré G, Kitsiou S. Chapter 9 Methods for Literature Reviews. In: Lau F, Kuziemsy C, editors. Handbook of eHealth Evaluation: An Evidence-based Approach [Internet]. Victoria

(BC): University of Victoria; 2017 Feb 27. Available from: <https://www.ncbi.nlm.nih.gov/books/NBK481583/>

Paraschiv, L., Acomi, N., Serban, A. and Paraschiv, S., (2020). A web application for analysis of heat transfer through building walls and calculation of optimal insulation thickness. *Energy Reports*, 6, pp.343-353.

Peev, P. (2012). *Is industrial hemp a sustainable construction material?*. via university college, horsens denmark, 7, pp.12-14.

Pervaiz, M. and Sain, M., (2003). Carbon storage potential in natural fiber composites. *Resources, Conservation and Recycling*, 39(4), pp.325-340.

Piot, A., Bejat, T., Jay, A., Bessette, L., Wurtz, E. and Davin, L. (2017). Study of a hempcrete wall exposed to outdoor climate: *Effects of the coating*. *Construction and Building materials*, 139, pp.540-550.

Pochwała, S., Makiola, D., Anweiler, S. and Böhm, M., (2020). The Heat Conductivity Properties of Hemp–Lime Composite Material Used in Single-Family Buildings. *Materials*, 13(4), p.1011.

Polson, D., Zacharis, E., Lawrie, O. and Vagiou, D., (2017). Multi-Objective Optimisation In Early Stage Design. Case Study: Northampton University Creative Hub Building. In: *15th IBPSA Conference*. [online] San Francisco, CA, USA, : IBPSA, pp.1637-1645. Available at: <<https://doi.org/10.26868/25222708.2017.435>> [Accessed 17 March 2020].

Prabesh, K., (2016). *HEMPCRETE NOISE BARRIER WALL FOR HIGHWAY NOISE INSULATION*. [online] Theseus.fi. Available at: <https://www.theseus.fi/bitstream/handle/10024/121363/Hempcrete_Noise_Barrier_Walls_K_C.pdf?sequence=1&isAllowed=y> [Accessed 4 March 2020].

Preiser, W. and J. Vischer, eds. (2005). *Assessing building performance*. Oxford: Butterworth-Heinemann.

Prétot, S., Collet, F. and Garnier, C., (2013). *Life Cycle Assessment of a Hemp Concrete Wall: Impact of Thickness and Coating*. [online] Hal.archives-ouvertes.fr. Available at: <<https://hal.archives-ouvertes.fr/hal-00916557/document>> [Accessed 17 March 2020].

Pretot, S., Collet, F. and Garnier, C., (2014). Life Cycle Assessment of a hemp concrete wall : impact of thickness and coating. *Building and Environment*, 72, pp.223-231.

Przyborski, P. and Levy, R., (2010). *Global Warming*. [online] Earthobservatory.nasa.gov. Available at: <<https://earthobservatory.nasa.gov/features/GlobalWarming/page4.php>> [Accessed 1 May 2019].

Queirós, A., Faria, D. and Almeida, F., (2017). STRENGTHS AND LIMITATIONS OF QUALITATIVE AND QUANTITATIVE RESEARCH METHODS. *European Journal of Education Studies*, 3(9), pp.369 - 383.

Raslan, R., and Davies, M. (2010). Results variability in accredited building energy performance compliance demonstration software in the UK: An inter-model comparative study. *Journal of Building Performance Simulation*. 3. 63-85.

Riffat, S., Powell, R. and Aydin, D., (2016). *Future Cities And Environmental Sustainability*.

Rotimi, A., Bahadori-Jahromi, A., Mylona, A., Godfrey, P. and Cook, D., (2017). Estimation and Validation of Energy Consumption in UK Existing Hotel Building Using Dynamic Simulation Software. *Sustainability*, 9(8), p.1391.

Sargent, R.G. (1991). Simulation Model Verification and Validation, *Proceedings of 1991 Winter Simulation Conference*, edited by Nelson, Kelton, and Clark, Phoenix, AZ, pp. 37-47.

Sariyildiz, S., Bittermann, S., and Ciftcioglu, Ö. (2015). multi-objective optimization in the construction industry. *Research Gate*.

Schwartz, Y., Raslan, R., Korolija, I. and Mumovic, D., (2017). Integrated Building Performance Optimisation: Coupling Parametric Thermal Simulation Optimisation and Generative Spatial Design Programming. In: *Proceedings of the 15th IBPSA Conference*. [online] San Francisco, CA, USA: IBPSA, pp.1222-1229. Available at: <<http://DOI:10.26868/25222708.2017.316>> [Accessed 17 March 2020].

Seltman, H., (2018). *Experimental Design And Analysis*. [online] Stat.cmu.edu. Available at: <<http://www.stat.cmu.edu/~hseltman/309/Book/Book.pdf>> [Accessed 17 March 2020].

Sereda, P., (2020). *CBD-127. The Structure Of Porous Building Materials - NRC-IRC*. [online] Web.mit.edu. Available at: <http://web.mit.edu/parmstr/Public/NRCan/CanBldgDigests/cbd127_e.html> [Accessed 17 July 2020].

Shea, A., Lawrence, M. and Walker, P. (2012). Hygrothermal performance of an experimental hemp–lime building. *Construction and Building Materials*, 36, pp.270-275.

Shi, Q., Yan, Y., Zuo, J. and Yu, T. (2016). Objective conflicts in green buildings projects: A critical analysis. *Building and Environment*, 96, pp.107-117.

Shi, X., Si, B., Zhao, J., Tian, Z., Wang, C., Jin, X. and Zhou, X. (2019). Magnitude, Causes, and Solutions of the Performance Gap of Buildings: A Review. *Sustainability*, 11(937), pp.120.

Shihyi Wang and D. W. Halpin (2004). "Simulation experiment for improving construction processes," *Proceedings of the 2004 Winter Simulation Conference, 2004.*, Washington, DC, USA, 2004, pp. 1252-1259 vol.2, doi: 10.1109/WSC.2004.1371457.

Simpson, S., (2015). Creating a Data Analysis Plan: What to Consider When Choosing Statistics for a Study. *The Canadian Journal of Hospital Pharmacy*, 68(4).

Snow, M. and Prasad, D. (2011). *Climate Change Adaptation for Building Designers: An Introduction*. Environment Design Guide, 66, pp.2-10.

Sousa, J. (2012). *Energy Simulation Software for Buildings: Review and Comparison*. [online] Ceur-ws.org. Available at: <http://ceur-ws.org/Vol-923/paper08.pdf> [Accessed 13 Mar. 2019]. <http://ceur-ws.org/Vol-923/paper08.pdf>

Spitler, J.D. (2006) Building Performance Simulation: *The Now and the Not Yet*’, HVAC&R Research 12(3a): 549-551.

Sustainabledevelopment.un.org. (2019). *Global Sustainable Development Report*. [online] Available at: https://sustainabledevelopment.un.org/content/documents/24797GSDR_report_2019.pdf [Accessed 1 March 2020].

Sutton, A. and Black, D. (2011). *An introduction to low-impact building materials*. [online] Available at: http://www.bre.co.uk/filelibrary/pdf/projects/low_impact_materials/ip14_11.pdf

Sutton, J. and Austin, Z., (2015). Qualitative Research: Data Collection, Analysis, and Management. *The Canadian Journal of Hospital Pharmacy*, 68(3).

Tedre, M. and Moisseinen, N., (2014). Experiments in Computing: A Survey. *The Scientific World Journal*, 2014, pp.1-11.

Teichroew, D., & Lubin, J. F. (1966). Computer simulation - discussion of the technique and comparison of languages. *Communications of the ACM*, 9(10), 723–741.

The Constructor. (2020). *The Constructor - Civil Engineering Home For Civil Engineers*. [online] Available at: <https://theconstructor.org> [Accessed 6 March 2020].

Tian, Z., Zhang, X., Jin, X., Zhou, X., Si, B., and Shi, X. (2017). Towards adoption of building energy simulation and optimization for passive building design: A survey and a review. *Energy and Buildings*. 158.

Tierney, S. (2008). *Experimental (quantitative) studies: An overview and general issues*. [online] Pdfs.semanticscholar.org. Available at: <https://pdfs.semanticscholar.org/4da8/5b8cc2af1a47b65c5e0127df4fba99df59a8.pdf> [Accessed 27 Dec. 2019].

Tofield B (2012). Delivering a low-energy low energy building: Making quality commonplace. *Build with CaRe report*, University of East Anglia, Norwich.

Tolwinski, N., (2017). Introduction: Drosophila—A Model System for Developmental Biology. *Journal of Developmental Biology*, 5(3), p.9.

Tomandl, M., Mieling, T., Losert-Valiente Kroon, C., Hopf, M. and Arndt, M., (2015). Simulated Interactive Research Experiments as Educational Tools for Advanced Science. *Scientific Reports*, 5(1).

Torres-Rivas, A., Palumbo, M., Haddad, A., Cabeza, L., Jiménez, L. and Boer, D. (2018). Multi-objective optimisation of bio-based thermal insulation materials in building envelopes considering condensation risk. [online] Ideas.repec.org. Available at: <https://ideas.repec.org/a/eee/appene/v224y2018icp602-614.html> [Accessed 19 Oct. 2019].

Tran A.D., Maalouf, C., Mai, T.H., Wurtz, E., and Collet, F. (2010). Transient hygrothermal behaviour of a hemp 498 concrete building envelope, *Energy Build.* 42: 1797–1806. 499

Tran Le, A., Maalouf, C., Mai, T., Wurtz, E. and Collet, F., (2010). Transient hygrothermal behaviour of a hemp concrete building envelope. *Energy and Buildings*, 42(10), pp.1797-1806.

Theclimategroup.org. (2020). *SMART 2020: Enabling The Low Carbon Economy In The Information Age*. [online] Available at: <https://www.theclimategroup.org/sites/default/files/archive/files/Smart2020Report.pdf> [Accessed 11 March 2020].

UK Hempcrete. (2020). *Building With Hempcrete - UK Hempcrete*. [online] Available at: <https://www.ukhempcrete.com/building-with-hempcrete/> [Accessed 1 March 2020].

Uusitalo, L., Lehikoinen, A., Helle, I. and Myrberg, K. (2015). An overview of methods to evaluate uncertainty of deterministic models in decision support. *Environmental Modelling & Software*, 63, pp.24-31.

van Dronkelaar, C., Dowson, M., Spataru, C. and Mumovic, D., (2016). A Review of the Regulatory Energy Performance Gap and Its Underlying Causes in Non-domestic Buildings. *Frontiers in Mechanical Engineering*, 1.

Vardoulakis, S., Dimitroulopoulou, C., Thornes, J., Lai, K., Taylor, J., Myers, I., Heaviside, C., Mavrogianni, A., Shrubsole, C., Chalabi, Z., Davies, M. and Wilkinson, P., (2015). Impact of climate change on the domestic indoor environment and associated health risks in the UK. *Environment International*, 85, pp.299-313.

Vengatesan, M., Varghese, A. and Mittal, V., (2018). Thermal properties of thermoset polymers. *Thermosets*, pp.69-114.

Walker, R. and Pavia, S. (2014). Moisture transfer and thermal properties of hemp–lime concretes. *Construction and Building Materials*, 64, pp.270-276.

Walker, R., Pavia, S., and Mitchell, R. (2014). Mechanical properties and durability of hemplime concretes, 520 *Construction and. Building Materials*. 61; 340–348.

Wallner, J., Hochegger, K., Chen, X., Mischak, I., Reinbacher, K., Pau, M., Zrnc, T., Schwenzer-Zimmerer, K., Zemann, W., Schmalstieg, D. and Egger, J., (2018). Clinical evaluation of semi-automatic open-source algorithmic software segmentation of the mandibular bone: Practical feasibility and assessment of a new course of action. *PLOS ONE*, 13(5), p.e0196378.

Wang, S. and Halpin, D., (2004). Simulation Experiment for Improving Construction Processes. West Lafayette- U.S.A: *R. G. Ingalls, M. D. Rossetti, J. S. Smith, and B. A. Peters, eds.*, pp.1252-1259.

Wang, W., Zmeureanu, R. and Rivard, H. (2005). Applying multi-objective genetic algorithms in green building design optimization. [online] Isiarticles.com. Available at: <http://isiarticles.com/bundles/Article/pre/pdf/61625.pdf> [Accessed 19 Oct. 2019].

Wei, M., Wang, B. and Liu, S., (2019). Numerical Simulation of Heat and Moisture Transfer of Wall with Insulation. In: *3rd International Conference on Fluid Mechanics and Industrial Applications*. Xian, China: IOP Publishing, pp.1-6.

Woolley, T. (2006) Natural Building Materials: a Guide to Materials and Techniques. *The Crowood Press*, Wiltshire, UK.

Worldgbc.org. (2017). *GLOBAL STATUS REPORT 2017*. [online] Available at: https://www.worldgbc.org/sites/default/files/UNEP%20188_GABC_en%20%28web%29.pdf [Accessed 11 May 2019].

Winsberg, E., (2003). Simulated Experiments: Methodology for a Virtual World. *Philosophy of Science*, 70(1), pp.105-125.

Winsberg, E. (2008). A tale of two methods. *Synthese*, 169(3), pp.575-592.

Winsberg, E., (2019). *Computer Simulations In Science (Stanford Encyclopedia Of Philosophy)*. [online] Plato.stanford.edu. Available at: <https://plato.stanford.edu/entries/simulationsscience/> [Accessed 23 March 2020].

Wisdom, J. and Creswell, J., (2013). *Mixed Methods: Integrating Quantitative and Qualitative Data Collection and Analysis While Studying Patient-Centered Medical Home Models | PCMH Resource Center*. [online] Pcmh.ahrq.gov. Available at: <https://pcmh.ahrq.gov/page/mixed-methods-integrating-quantitative-and-qualitative-data-collection-and-analysis-while> [Accessed 23 March 2021].

Wright, S., (2016). *6 Ways Construction Technology Has Transformed The Industry*. [online] Blog.capterra.com. Available at: <https://blog.capterra.com/6-ways-construction-technology-has-transformed-the-industry/> [Accessed 4 May 2019].

Xu, X., Feng, G., Chi, D., Liu, M. and Dou, B. (2018). Optimization of Performance. Parameter Design and Energy Use Prediction for Nearly Zero Energy Buildings. [online] Energies. Available at: <https://www.mdpi.com/1996-1073/11/12/3252>.

Yassin, A.A., Sheta, S.A., Elwazeer, M.A. (2017). Parametric Study on Window-Wall Ratio (WWR) for Day lighting Optimization in Multi-Story Residential Buildings: Case Study of an Apartment Complex in Mansoura City, Egypt. *Int. Advanced Research Journal. Science and Engineering Technology*. 4, 21–32.

Yates, T. (2003). [online] Projects.bre.co.uk. Available at: <http://projects.bre.co.uk/hemp/hemp/HempThermographicReport.pdf> [Accessed 19 Sept. 2019]

Yu, W., Li, B., Jia, H., Zhang, M. and Wang, D., (2015). Application of multi-objective genetic algorithm to optimize energy efficiency and thermal comfort in building design. *Energy and Buildings*, 88, pp.135-143.

Yusoff, Y., Ngadiman, M. and Zain, A. (2011). Overview of NSGA-II for Optimizing Machining Process Parameters. *Procedia Engineering*, 15, pp.3978-3983.

Zhang, A., Bokel, R., Dobbelsteen, A., Sun, Y., Huang, Q., and Zhang, Q. (2017). Optimization of thermal and daylight performance of school buildings based on a multiobjective genetic algorithm in the cold climate of China. *Energy and Buildings*. 139. 371– 384.

Zhang, Y., (2012). Use jEPlus as an efficient building design optimisation tool. In: *CIBSE ASHRAE Technical Symposium, Imperial College, London UK*. London, UK: Imperial College, London, pp.1-12.

APPENDICES

APPENDIX A: ENERGYPLUS HEAT AND MOISTURE TRANSFER SIMULATION

This section contains all the diagrams referenced from section 4.4 as applicable.

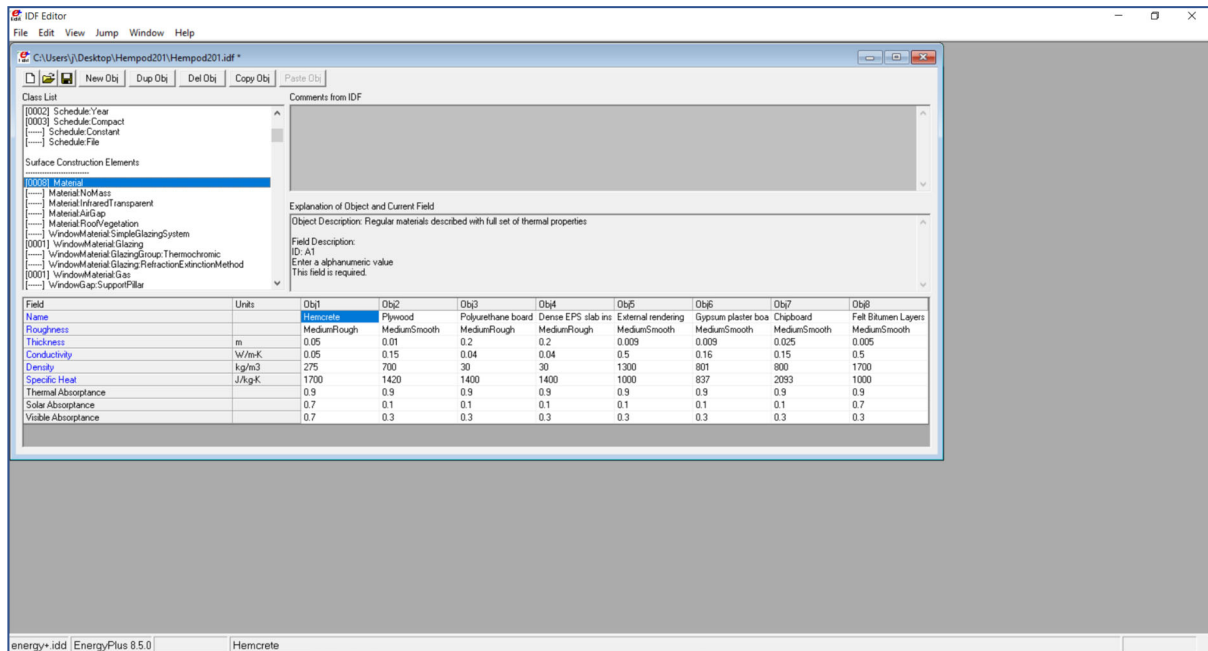


Figure A1: The created Hemcrete material property for simulation

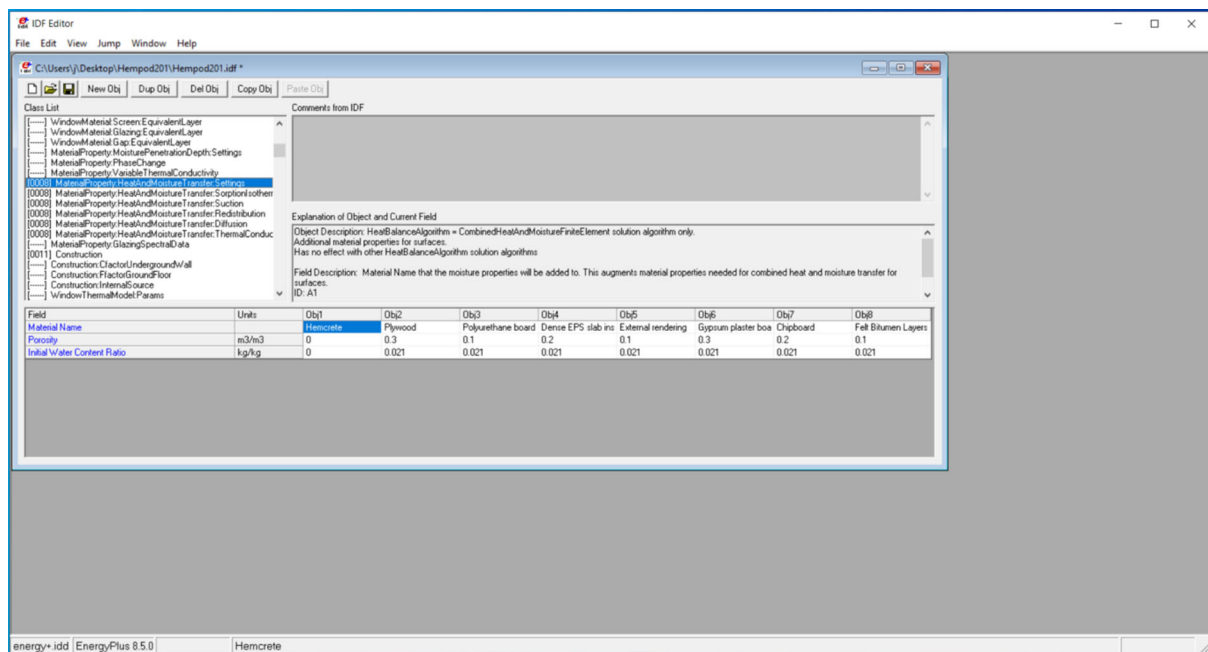


Figure A2: Material property heat and moisture transfer: settings

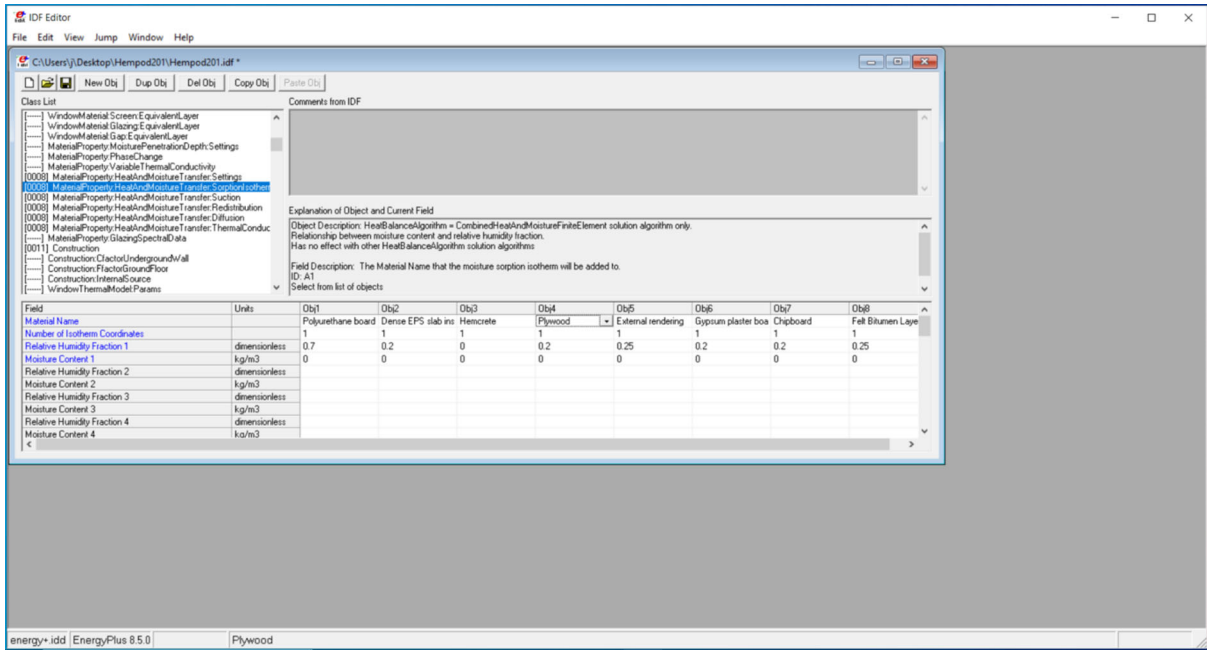


Figure A3: Material property heat and moisture transfer: sorption isotherm

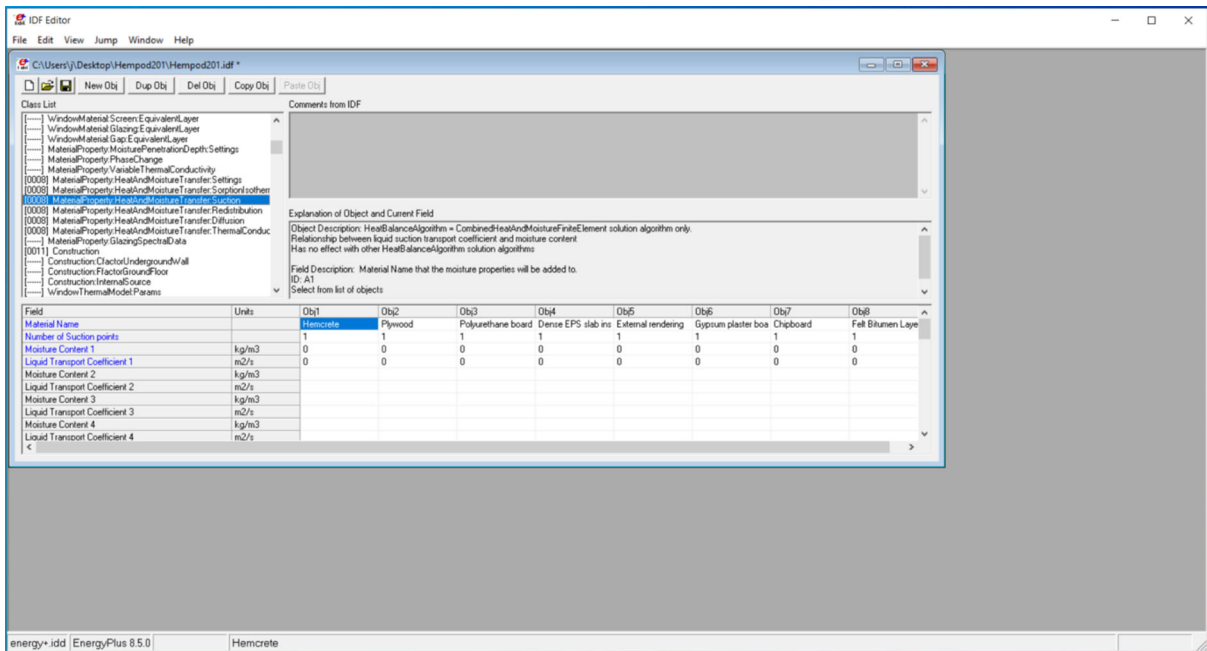


Figure A4: Material property heat and moisture transfer: suction

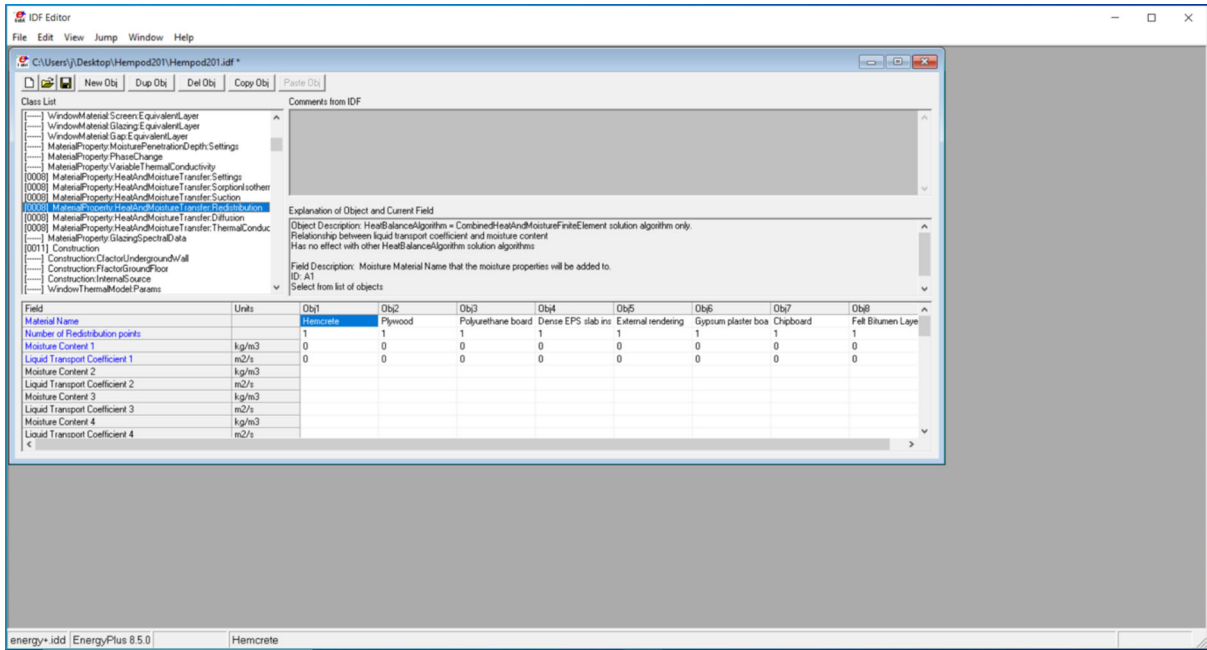


Figure A5: Material property heat and moisture transfer: Redistribution

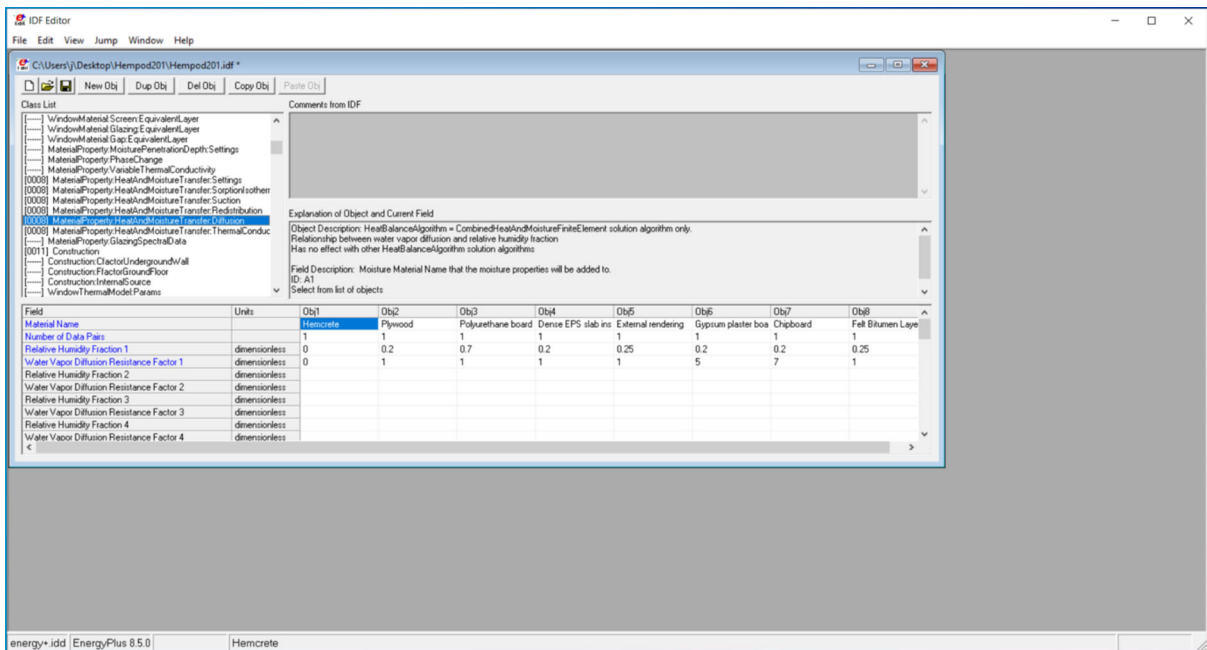


Figure A6: Material property heat and moisture transfer: Diffusion

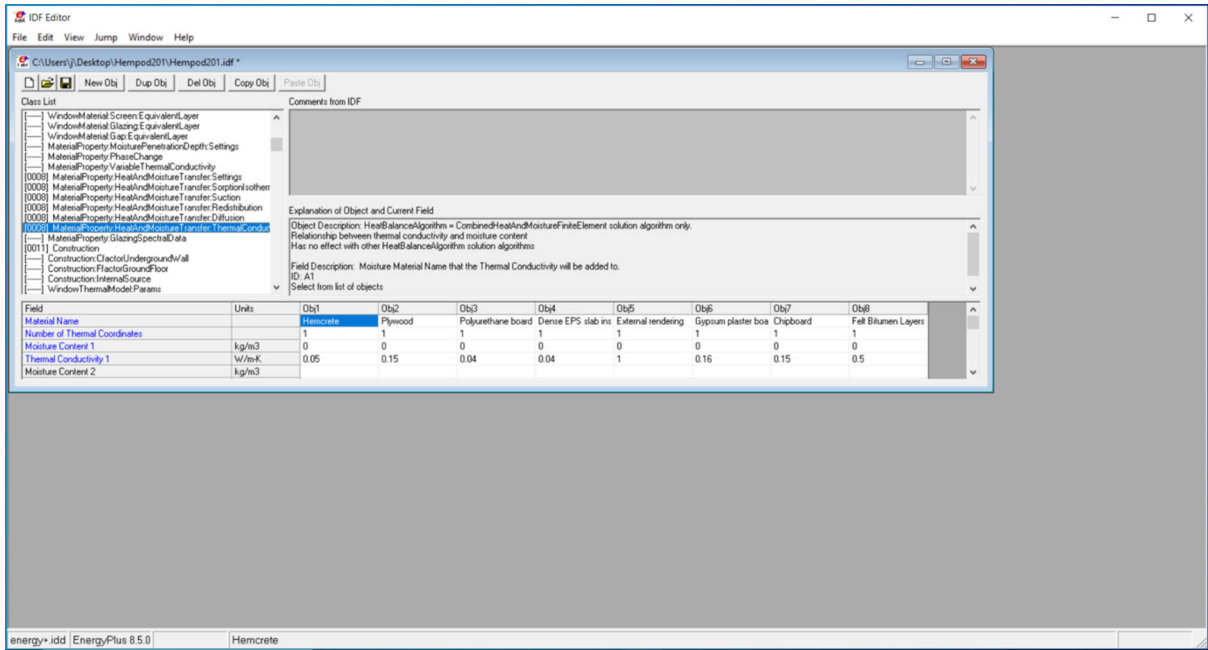


Figure A7: Material property heat and moisture transfer: thermal conductivity

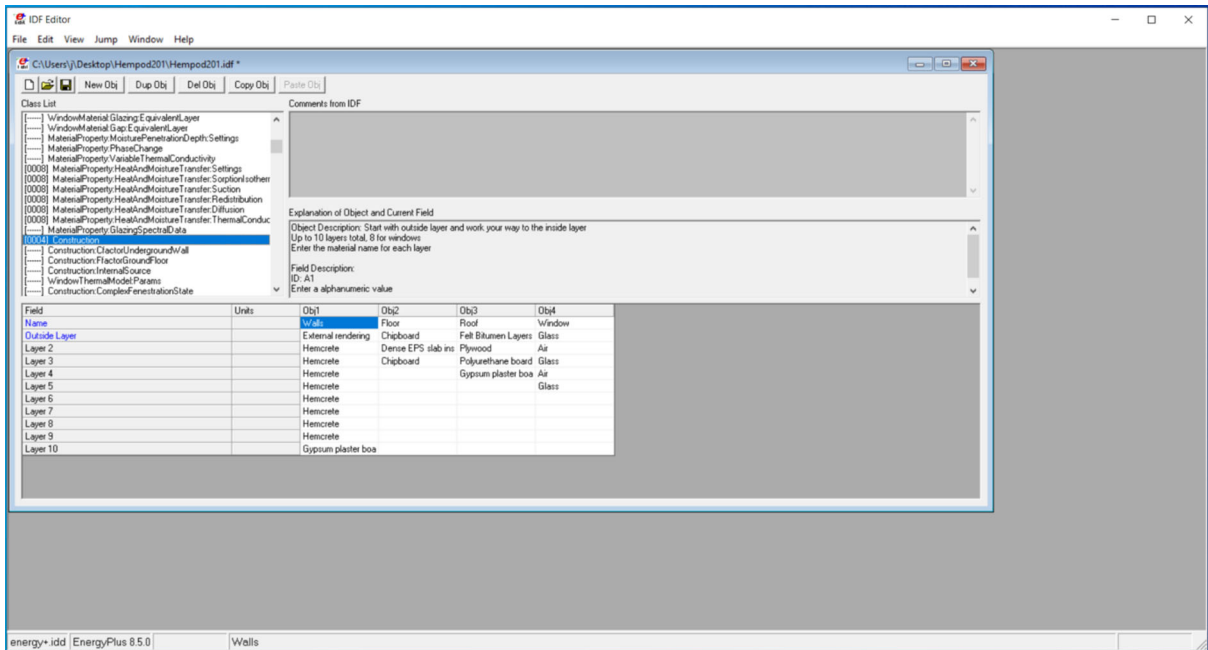


Figure A8: Construction component of hempod showing the wall layers

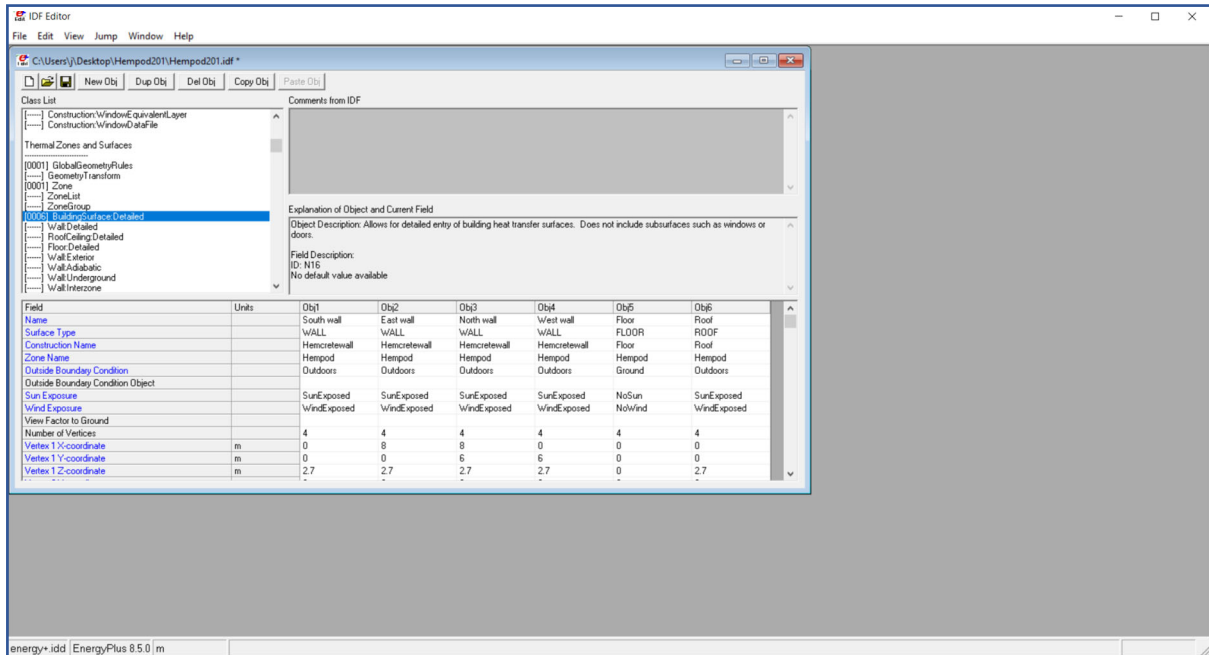


Figure A9: Building surface detailed for Heat and Moisture transfer simulation

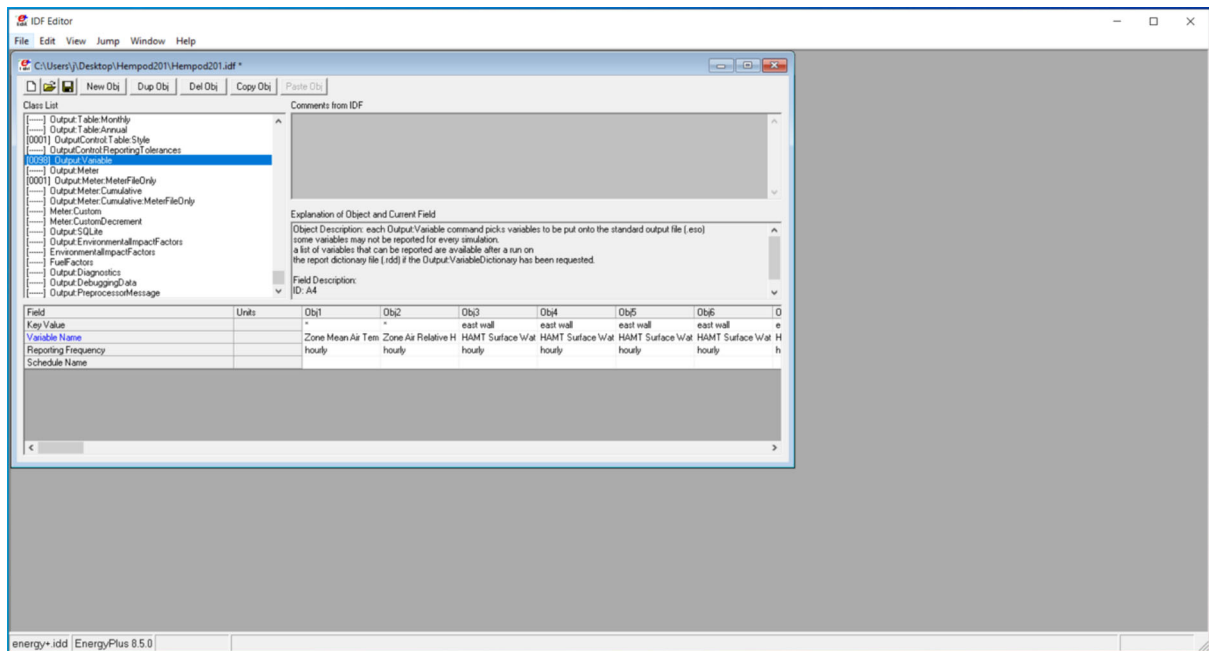


Figure A10: Output variables for Heat and Moisture transfer simulation

APPENDIX B: MULTI OBJECTIVE OPTIMISATION IN jEPlus+EA

This section contains all the diagrams referenced in section 4.5 as applicable.

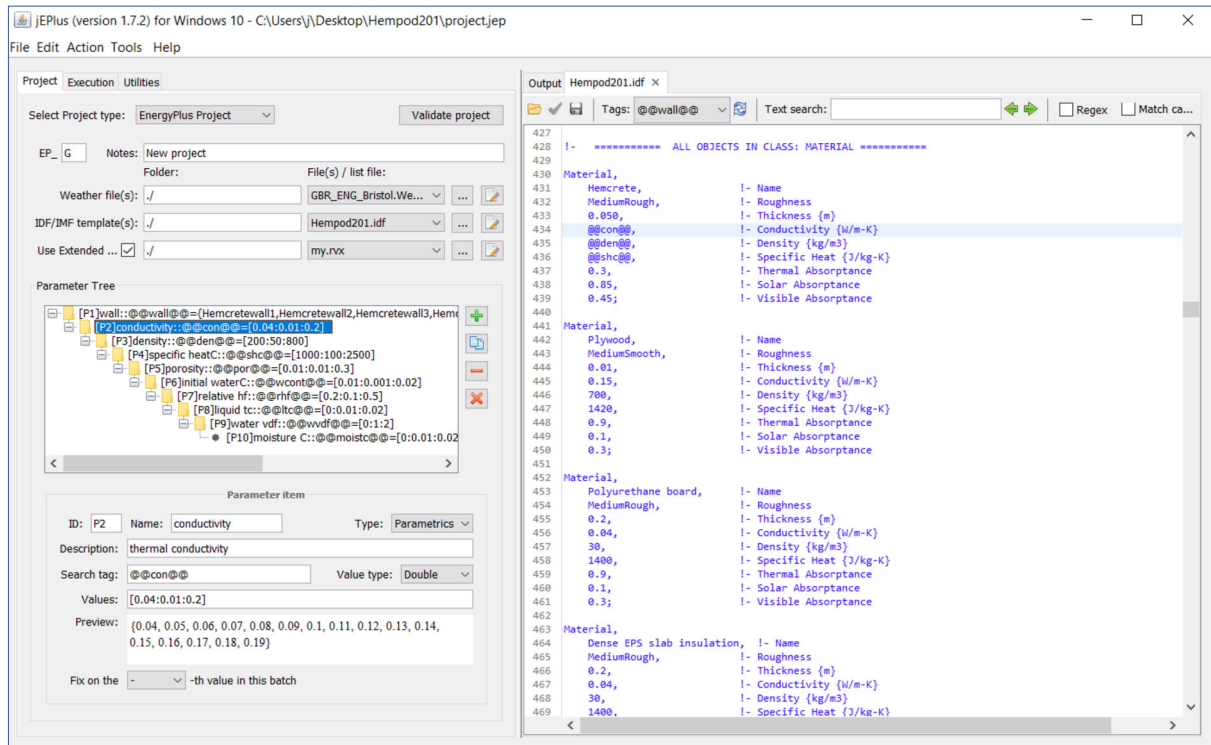


Figure B1: Showing the thermal conductivity optimisation parameter specification

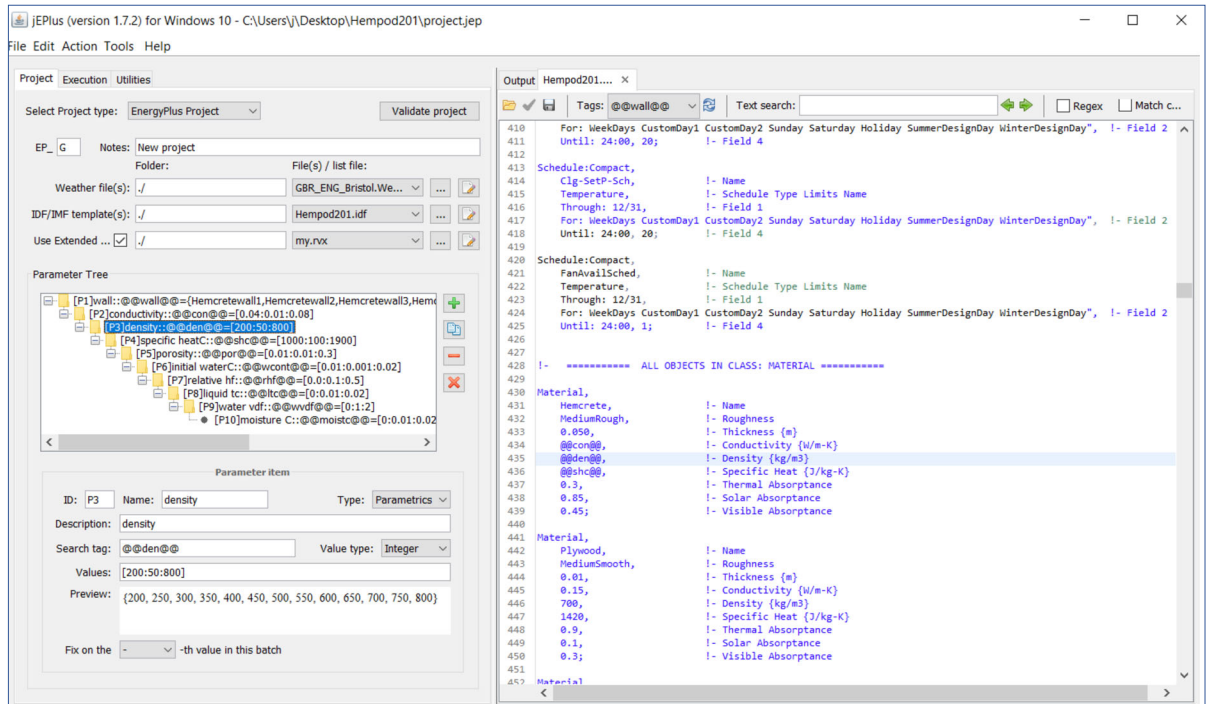


Figure B2: Showing the Density optimisation parameter specification

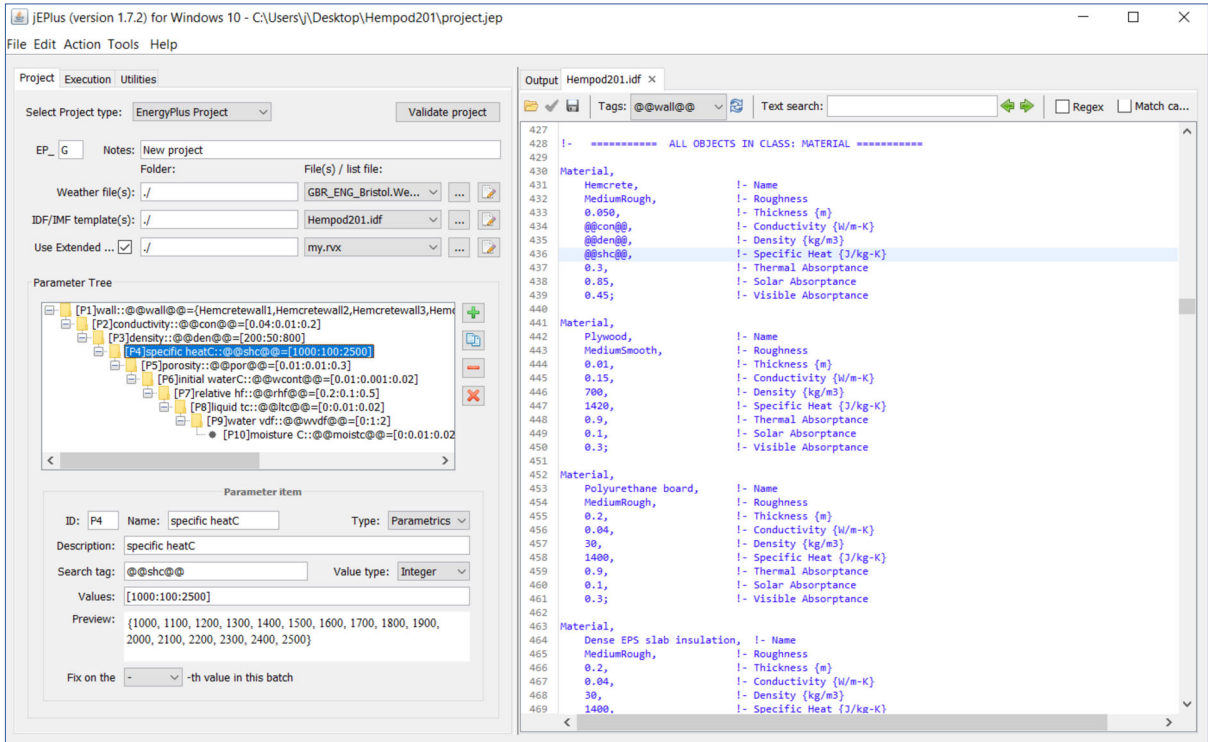


Figure B3: Showing specific heat capacity optimisation parameter specification

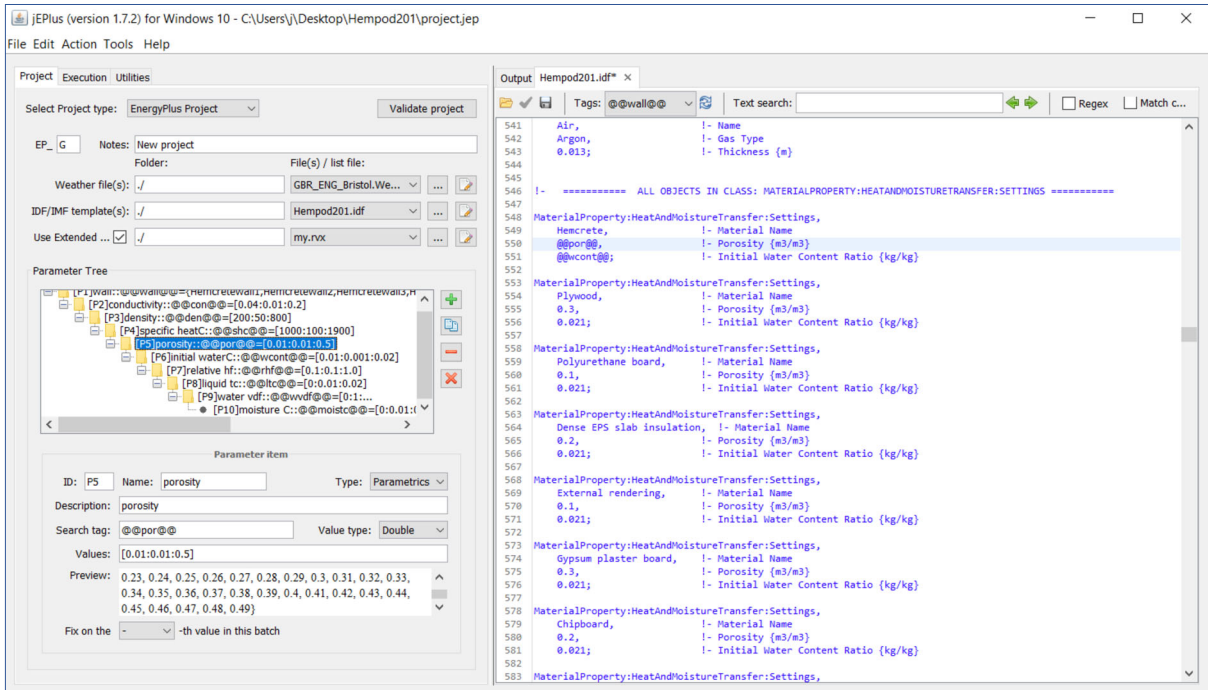


Figure B4: Showing the porosity optimisation parameter specification

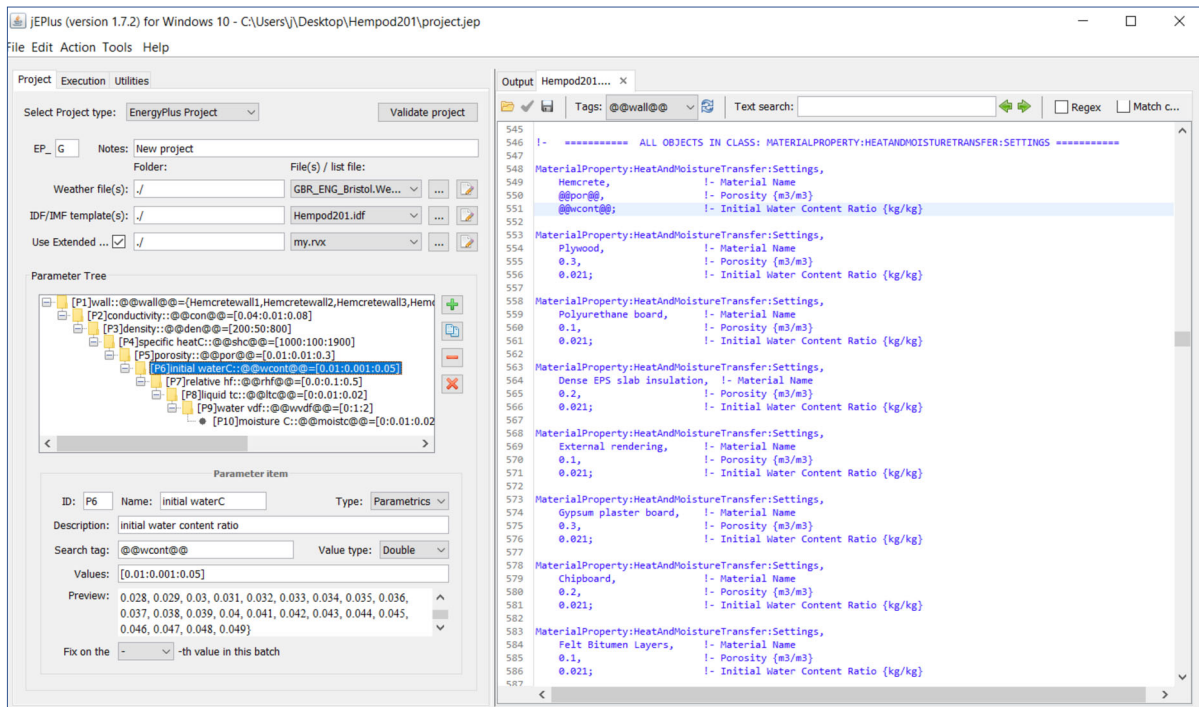


Figure B5: Showing initial water content ratio optimisation parameter

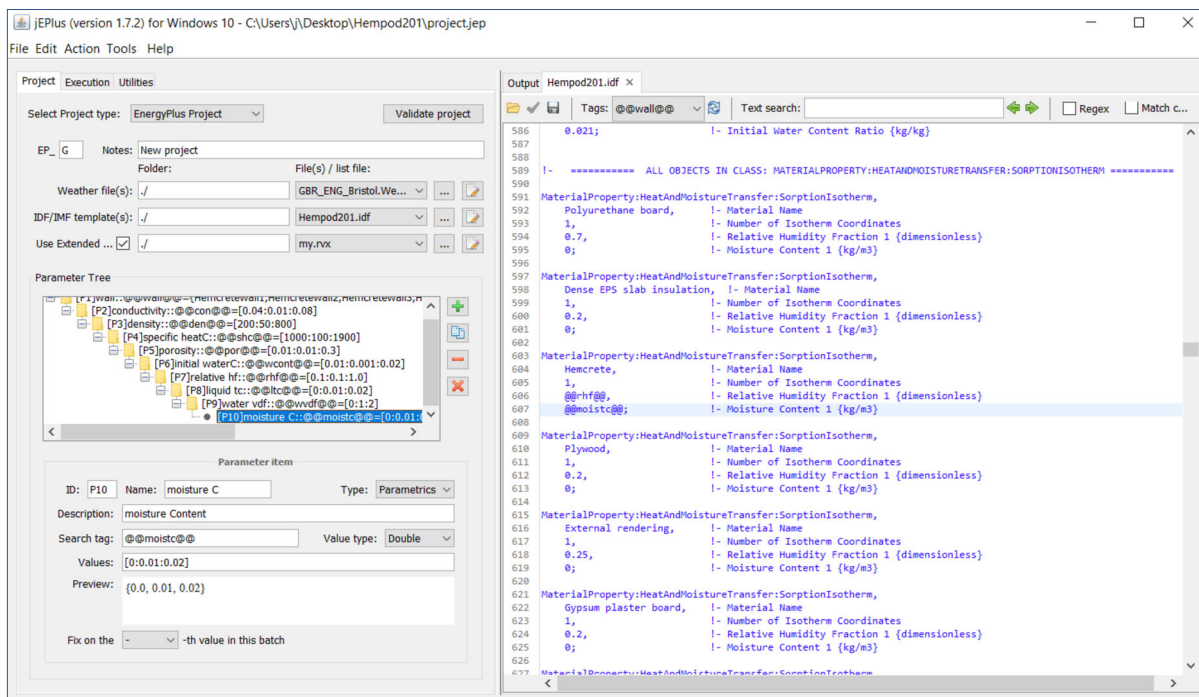


Figure B6: Showing moisture content optimisation parameter - sorption isotherm

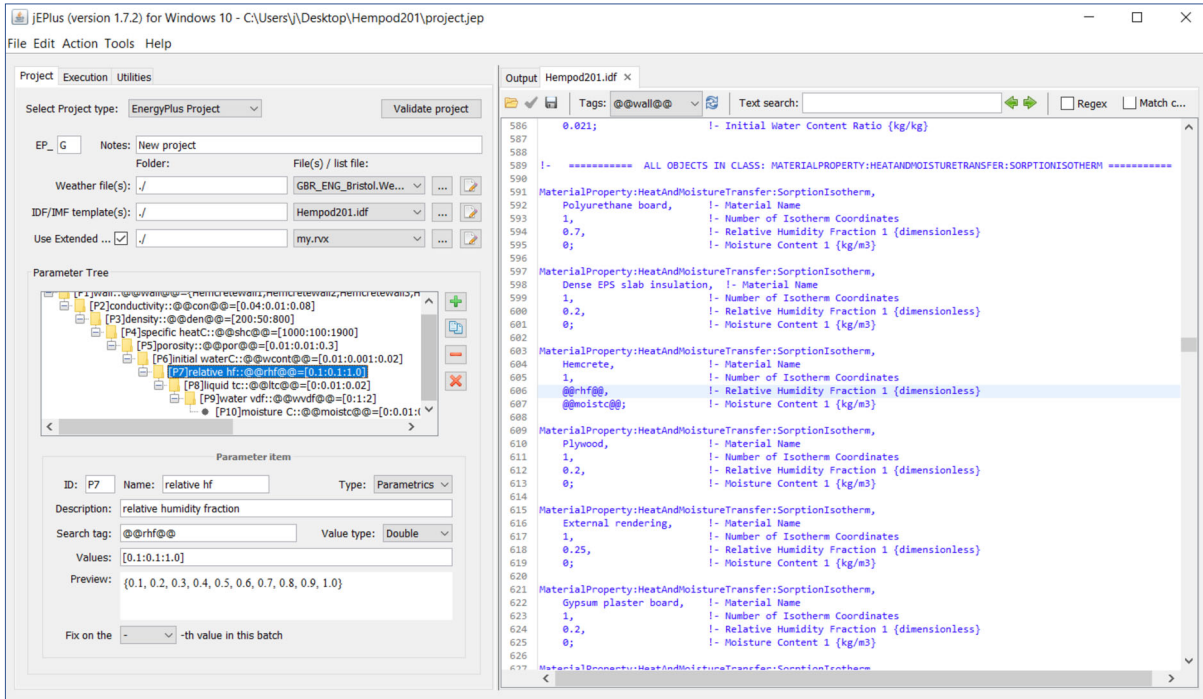


Figure B7: Showing relative humidity fraction optimisation parameter - sorption isotherm

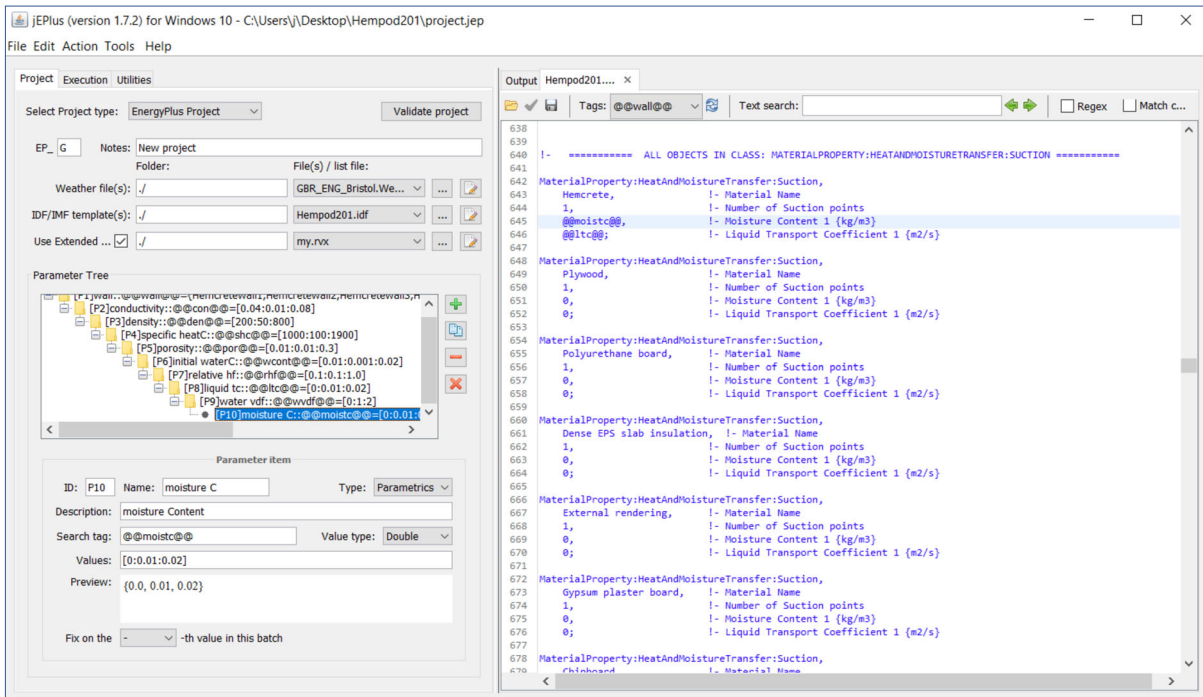


Figure B8: Showing moisture content optimisation parameter – suction

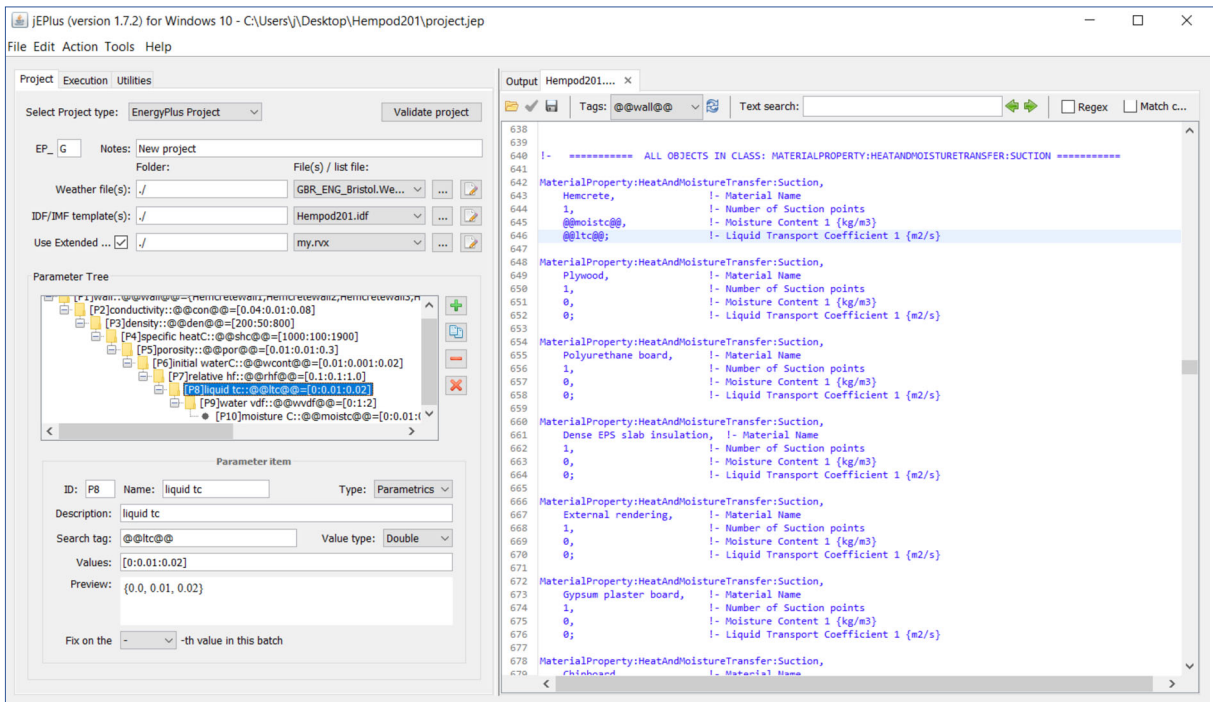


Figure B9: Showing the liquid transport coefficient optimisation parameter – suction

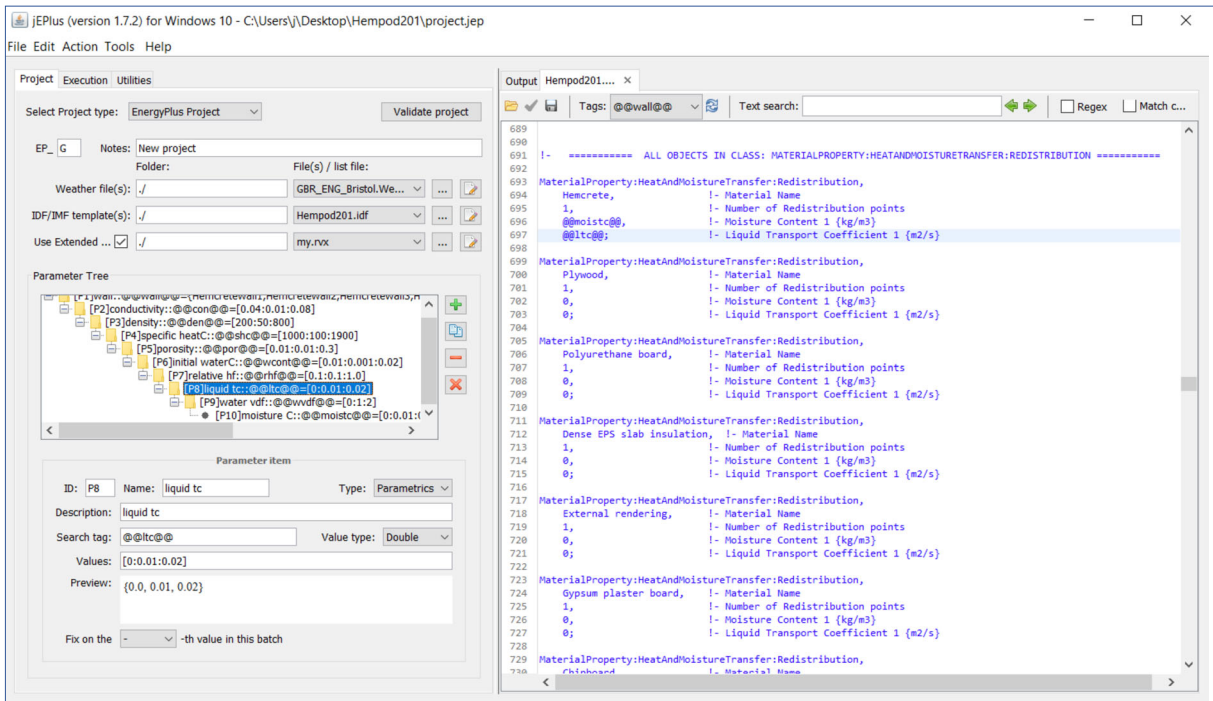


Figure B10: Showing the liquid transport coefficient optimisation parameter – redistribution

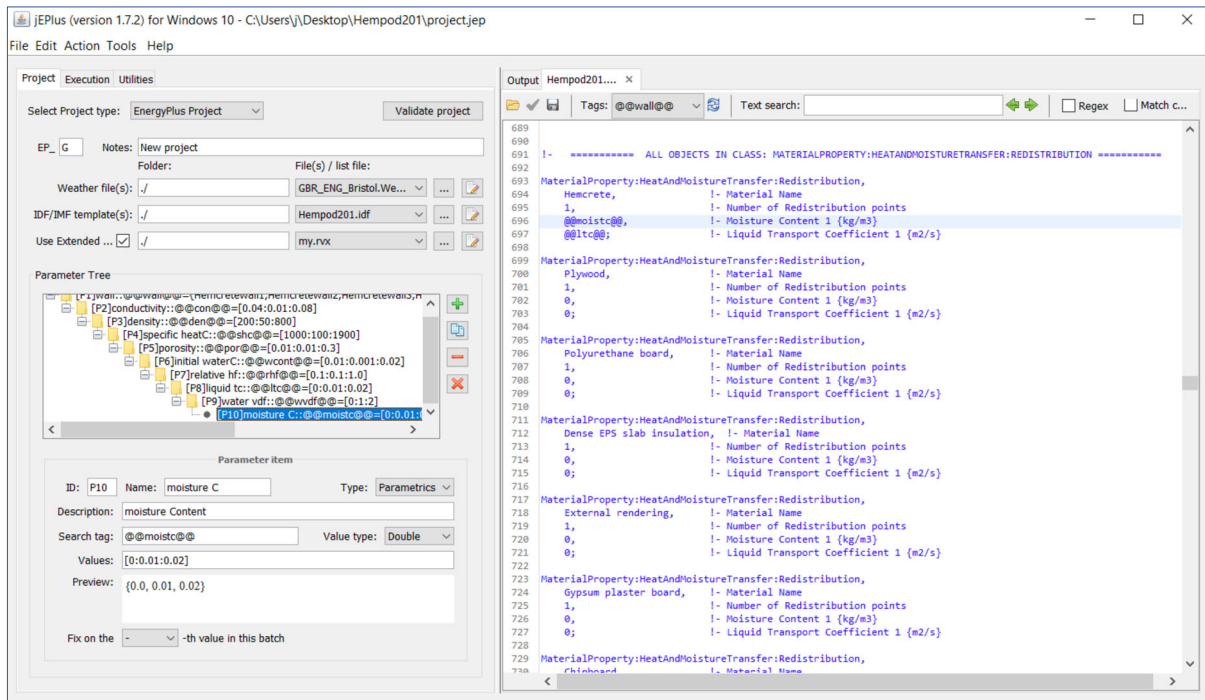


Figure B11: Showing moisture content optimisation parameter – redistribution

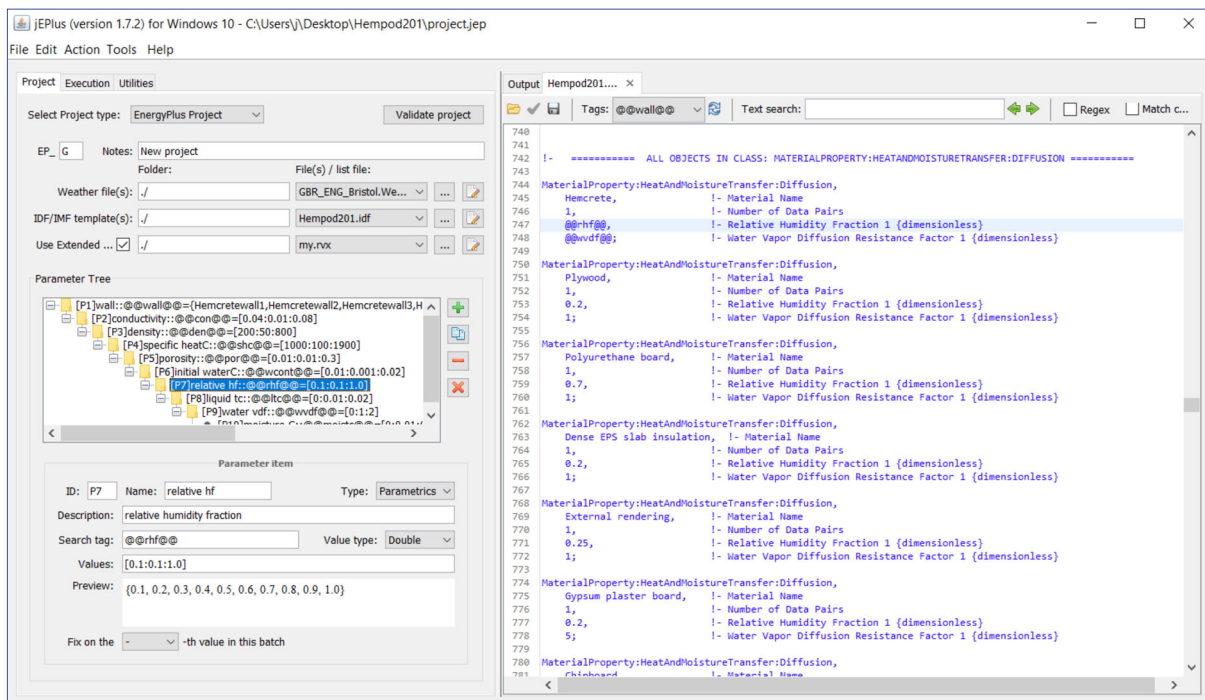


Figure B12: Showing relative humidity fraction optimisation parameter – diffusion

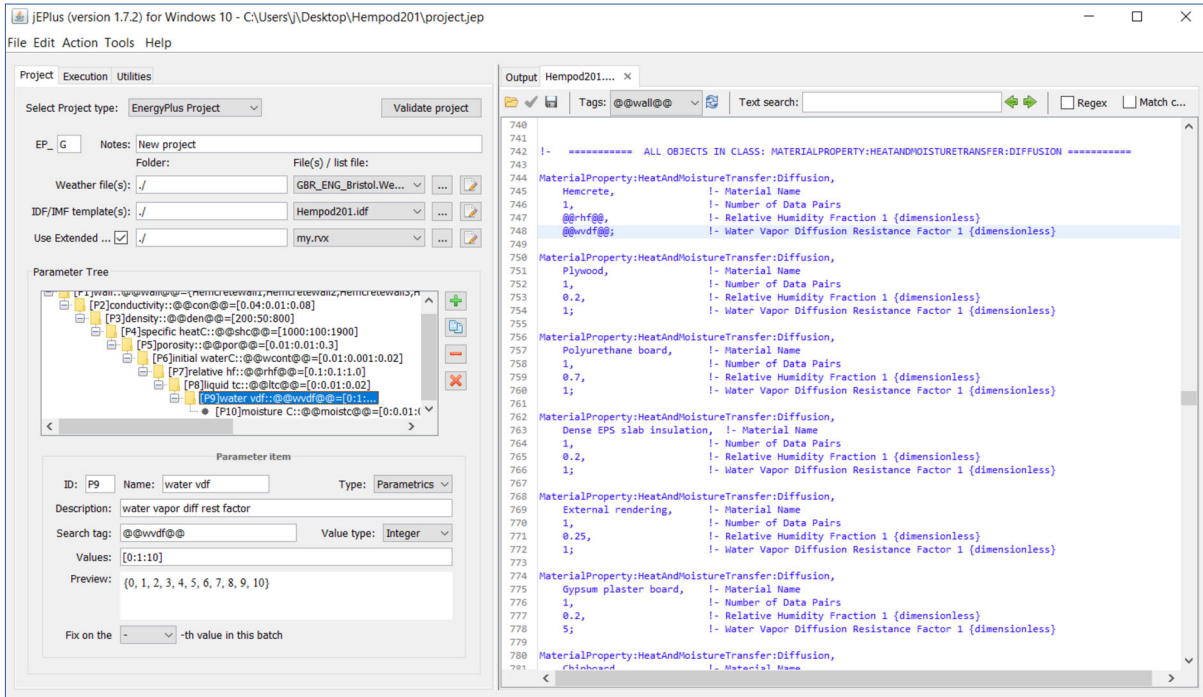


Figure B13: Showing water vapour diffusion resistance factor optimisation parameter – diffusion

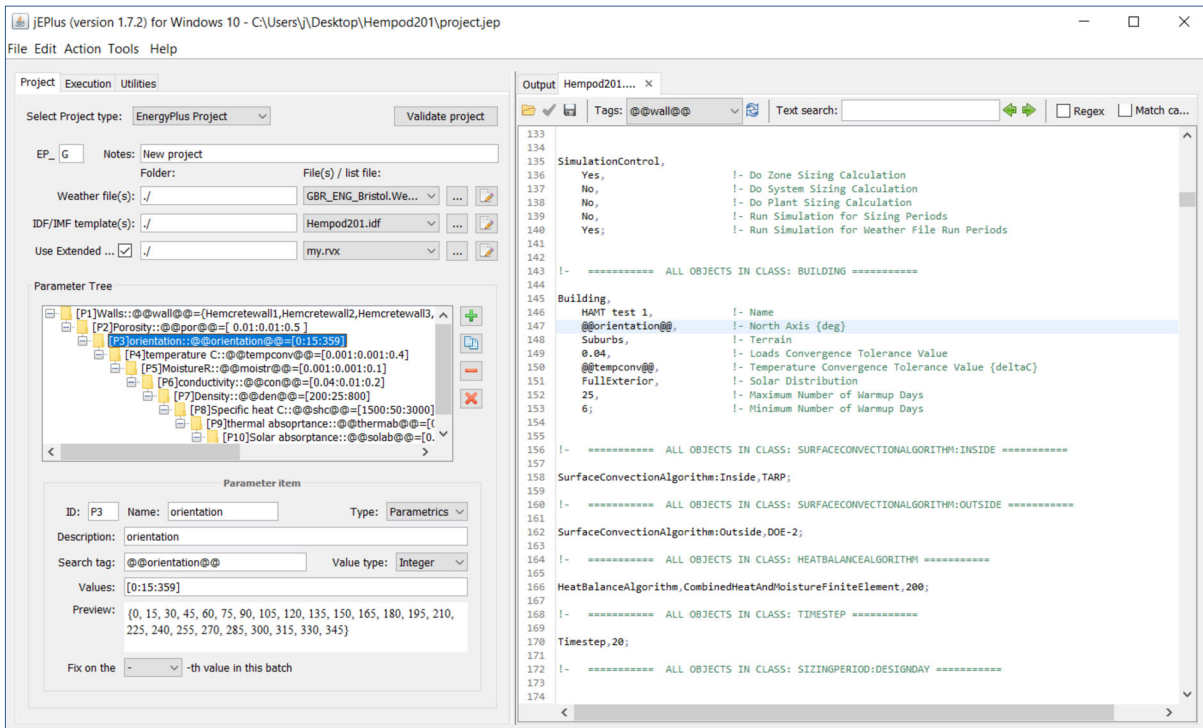


Figure B14: Showing the orientation optimisation parameter

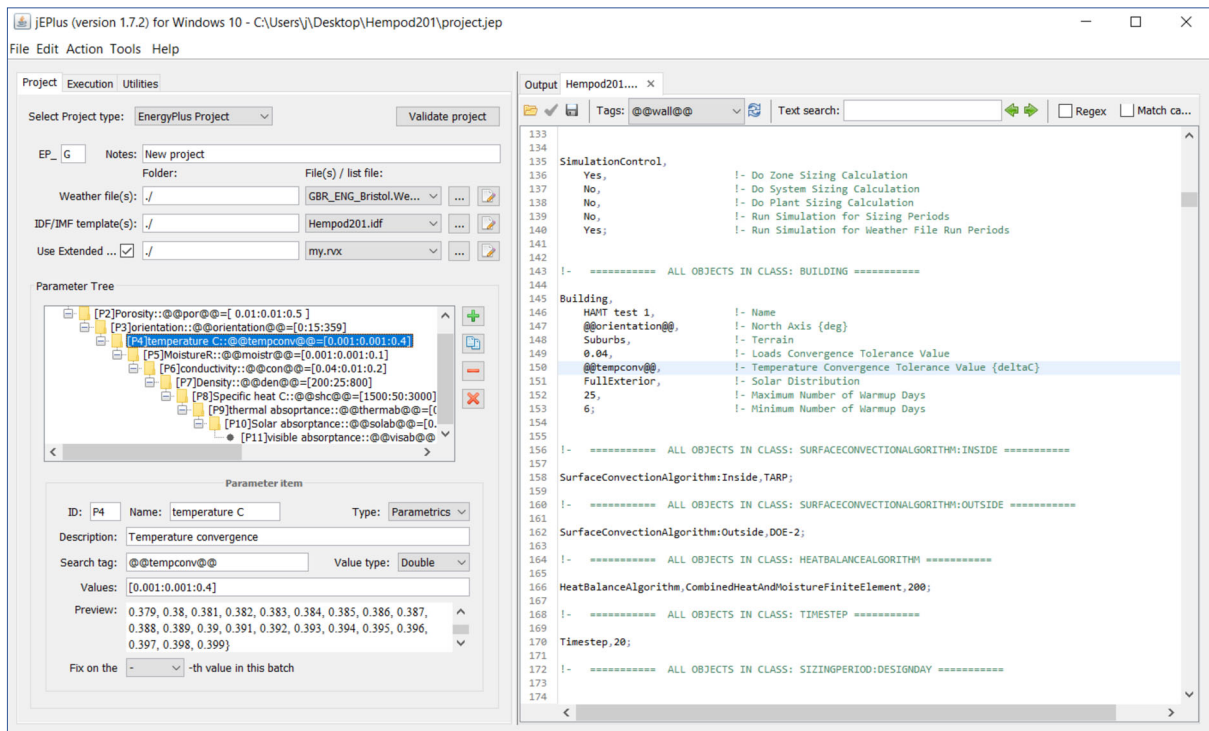


Figure B15: Showing the temperature convergence tolerance value optimisation parameter

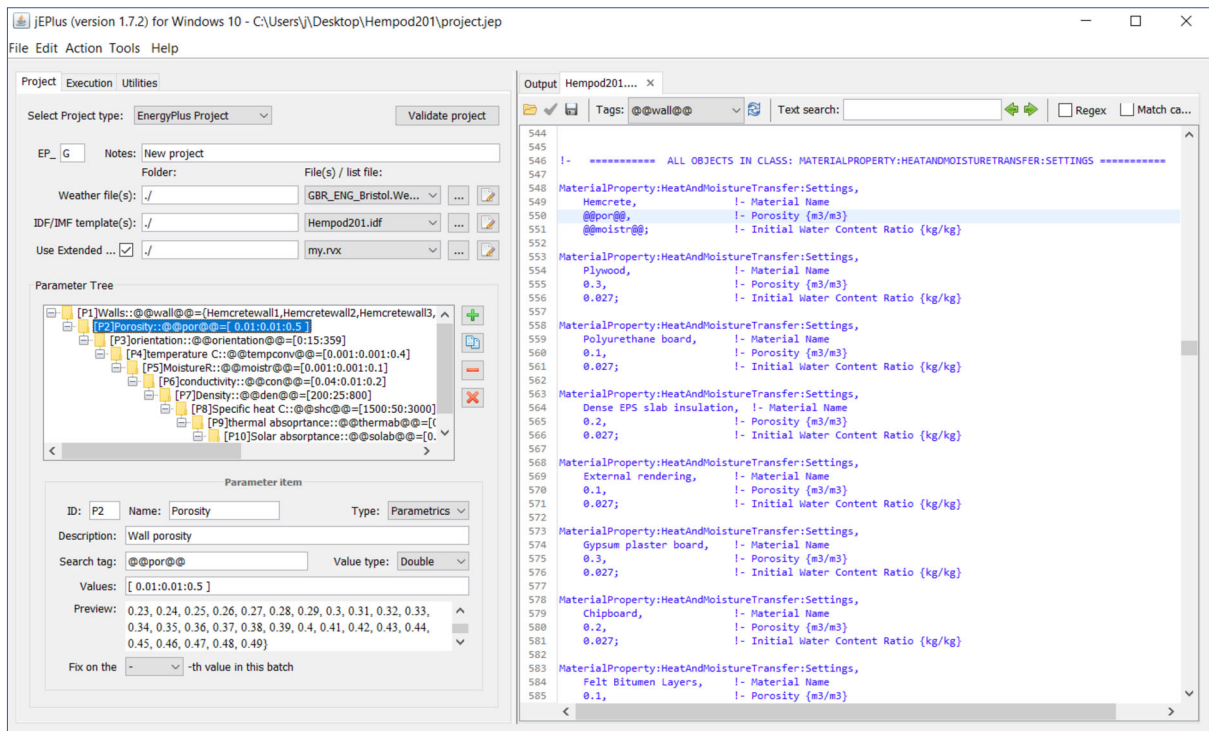


Figure B16: showing the porosity optimisation parameter specification

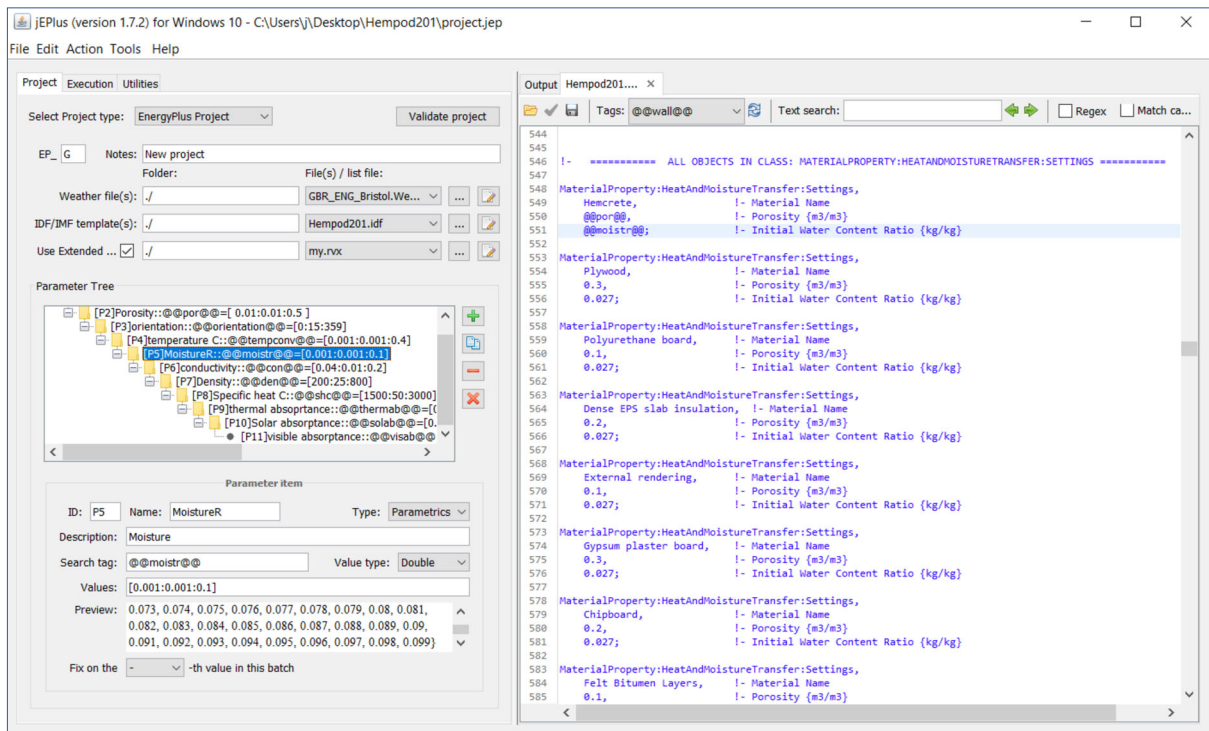


Figure B17: Showing the Initial water content ratio optimisation parameter specification

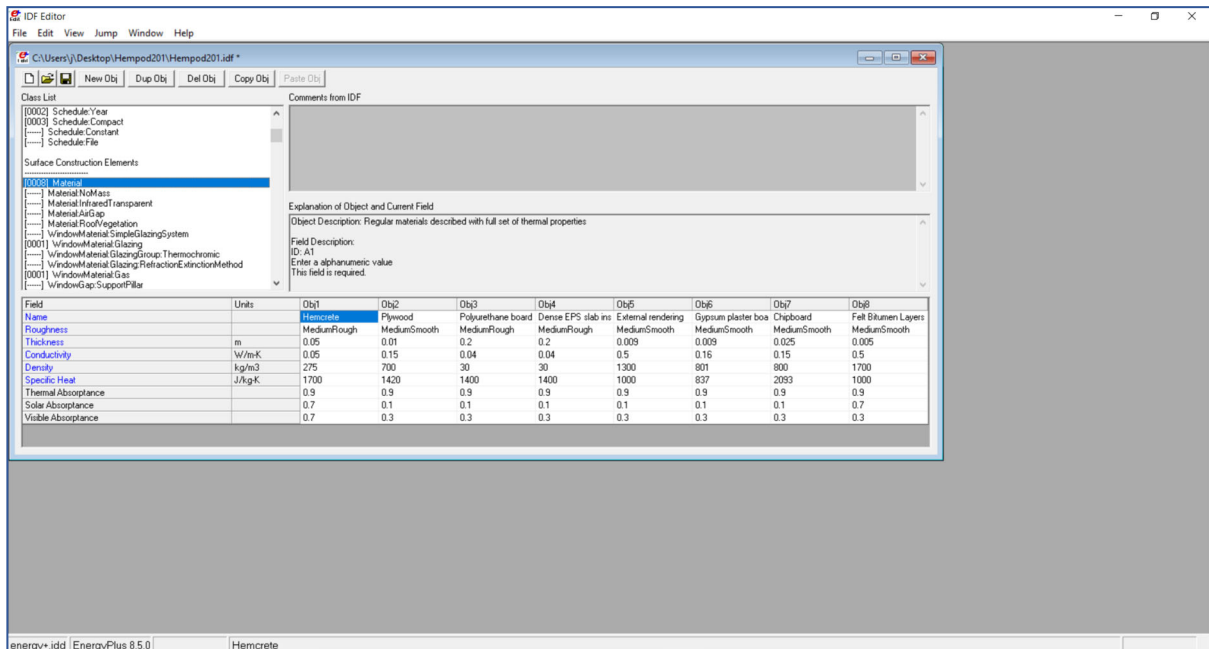


Figure B18: Showing the investigated field for Material property class list

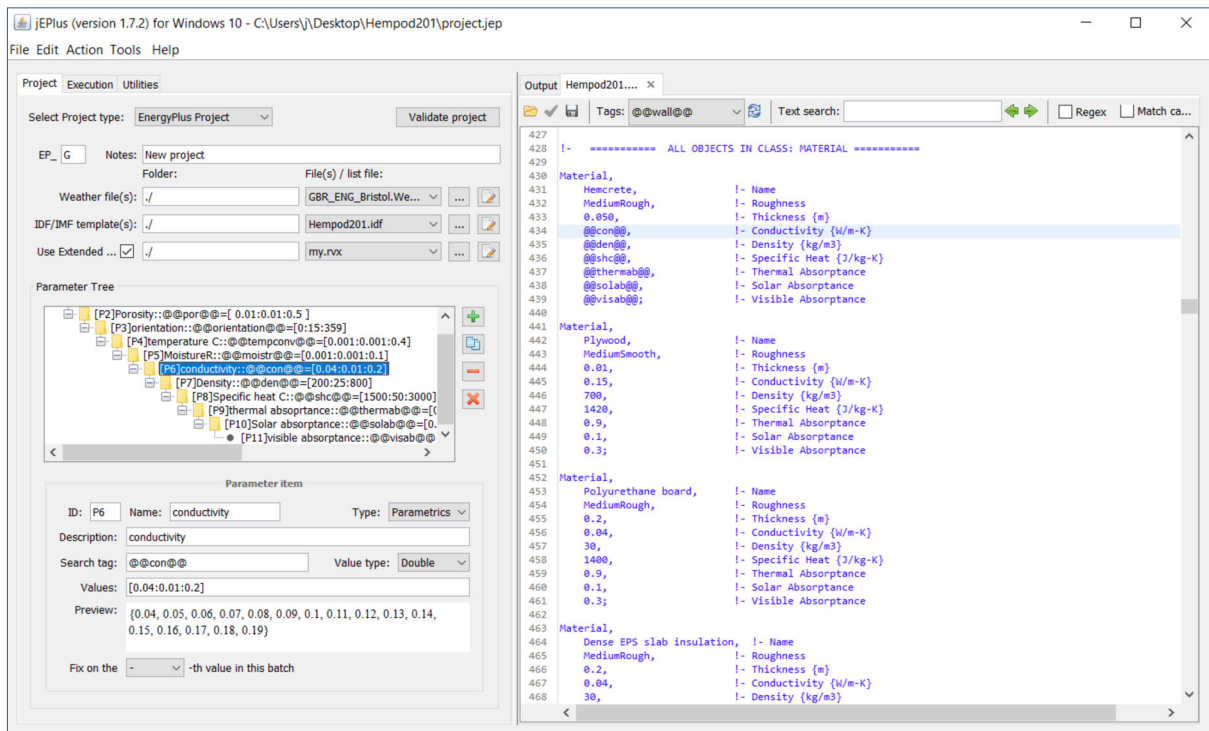


Figure B19: Showing the thermal conductivity optimisation parameter specification

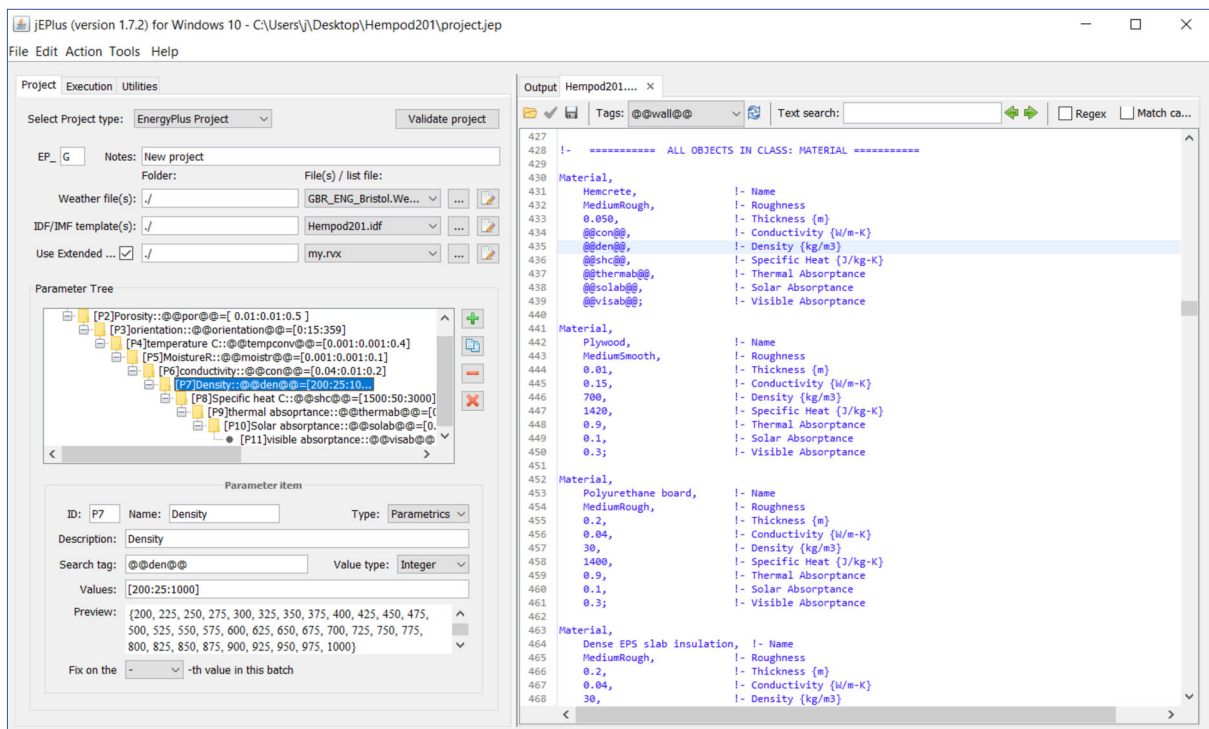


Figure B20: Showing the density optimisation parameter

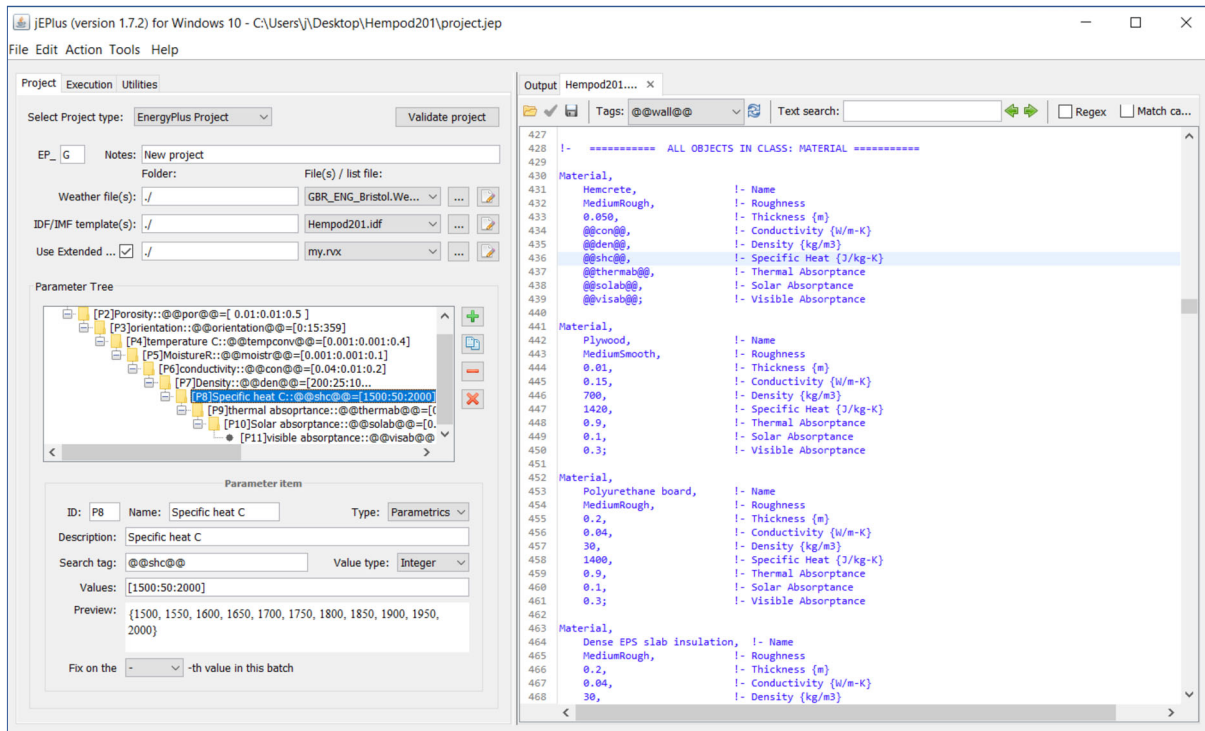


Figure B21: Showing specific heat capacity optimisation parameter specification

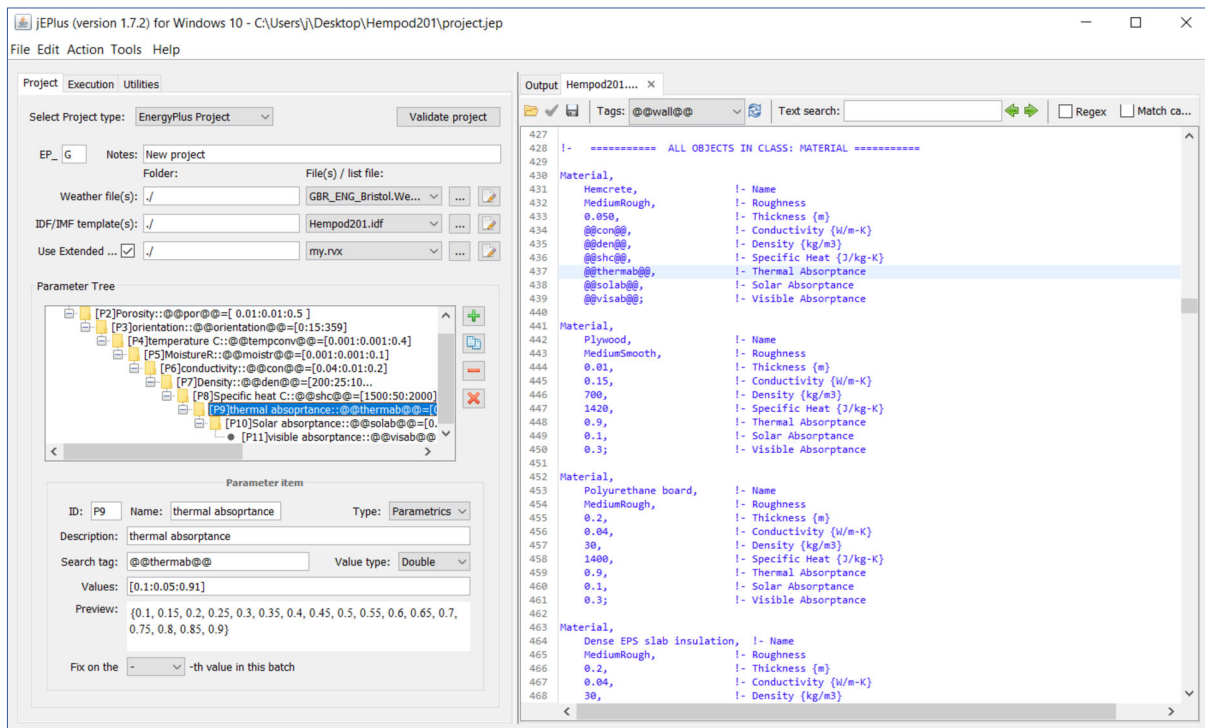


Figure B22: Showing thermal absorptance optimisation parameter – material property

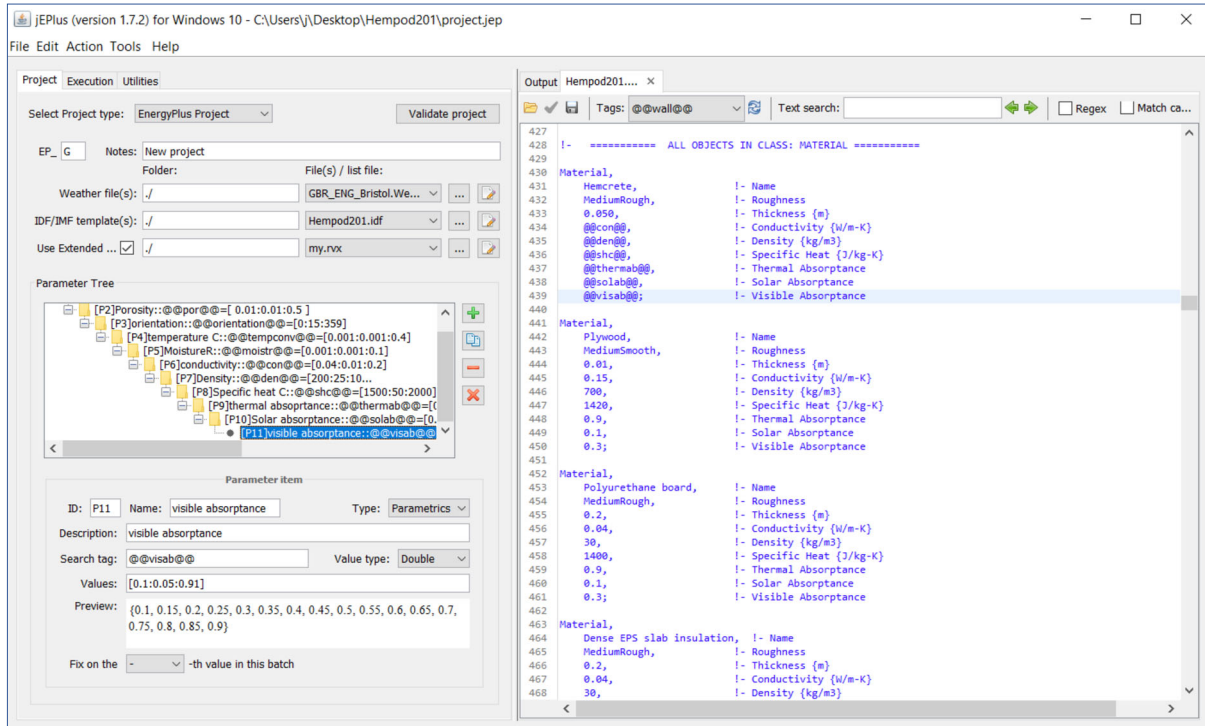


Figure B23: Showing visible absorbance optimisation parameter – material property

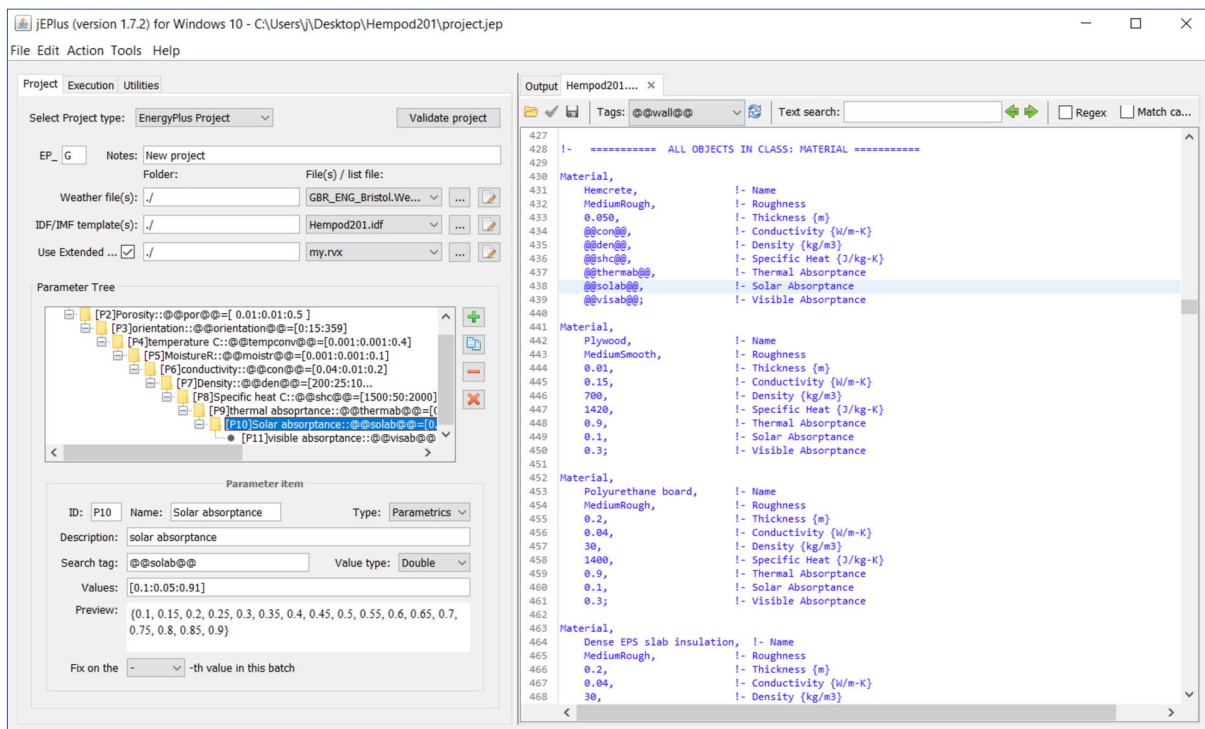


Figure B24: Showing solar absorbance optimisation parameter – material property

APPENDIX C: VALIDATION OF RESULTS WITH HEMPOD

This section contains all the diagrams referenced from section 6.1.1 as applicable.

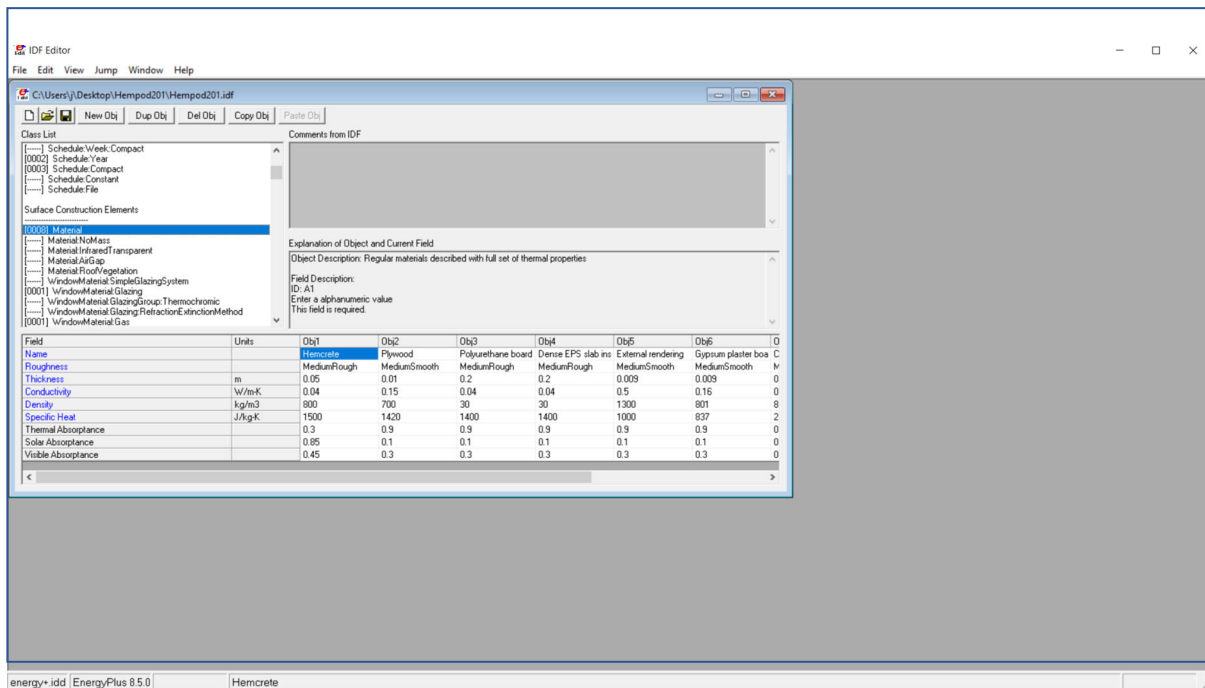


Figure C1: Showing material property for hemcrete simulation

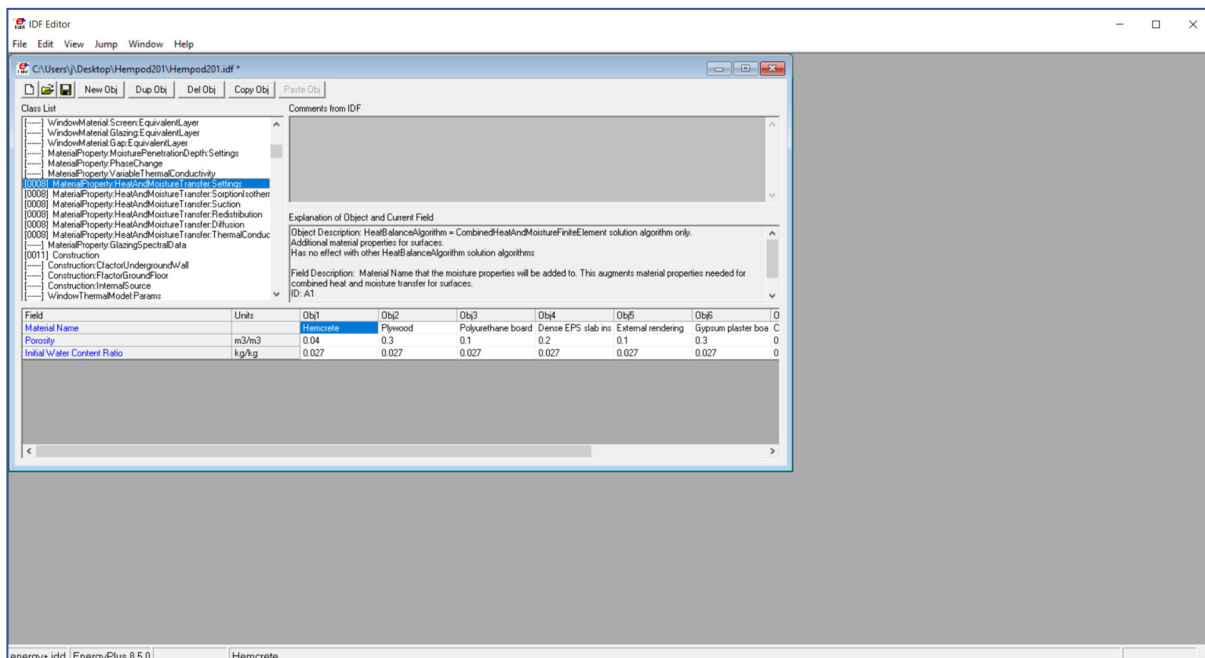


Figure C2: Showing HAMT- setting for hemcrete porosity and initial water content ratio

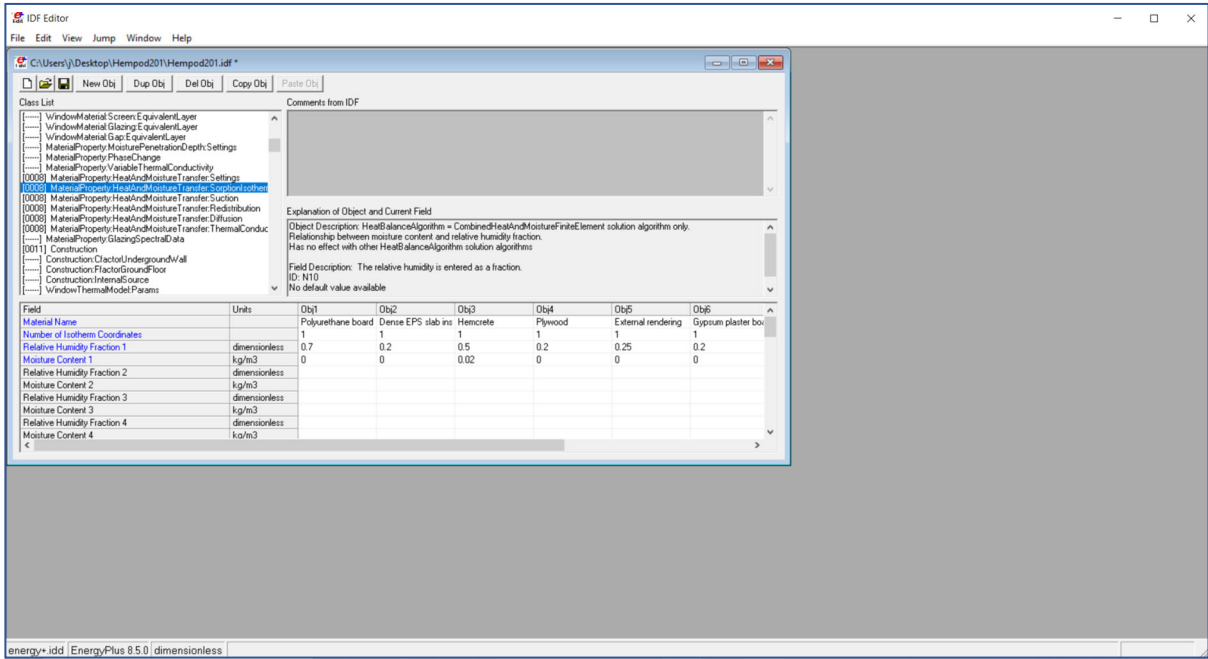


Figure C3: Showing HAMT – sorption isotherm for hempcrete relative humidity fraction and moisture content

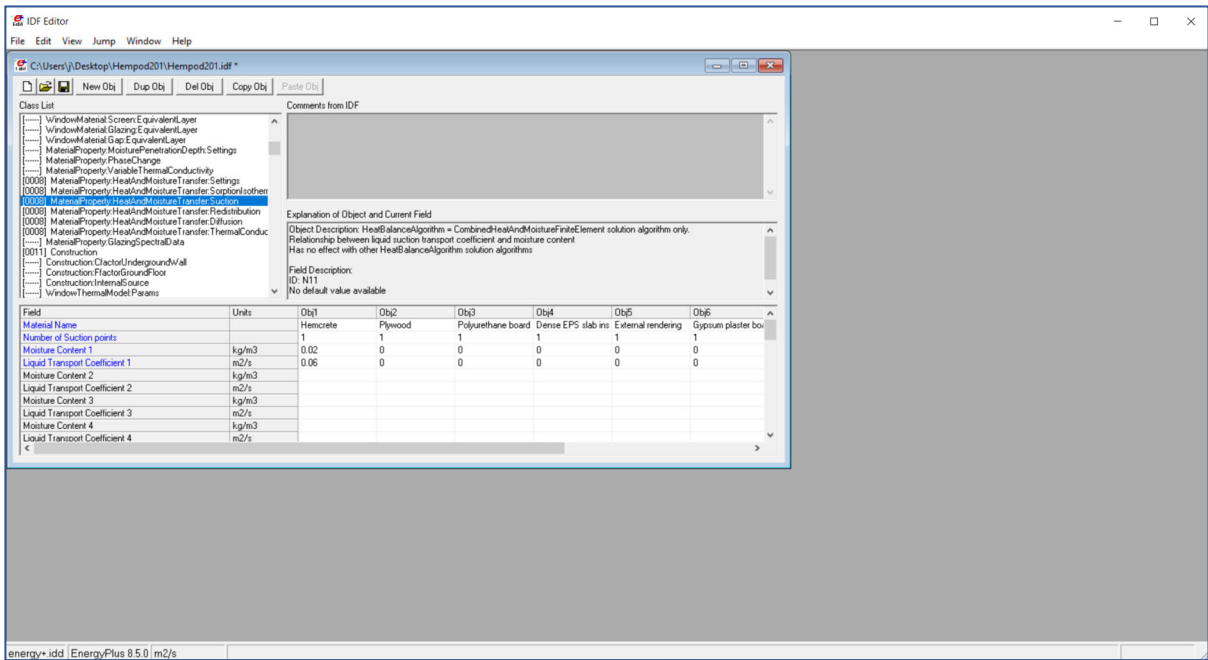


Figure C4: Showing HAMT – suction for hempcrete liquid transport coefficient and moisture content

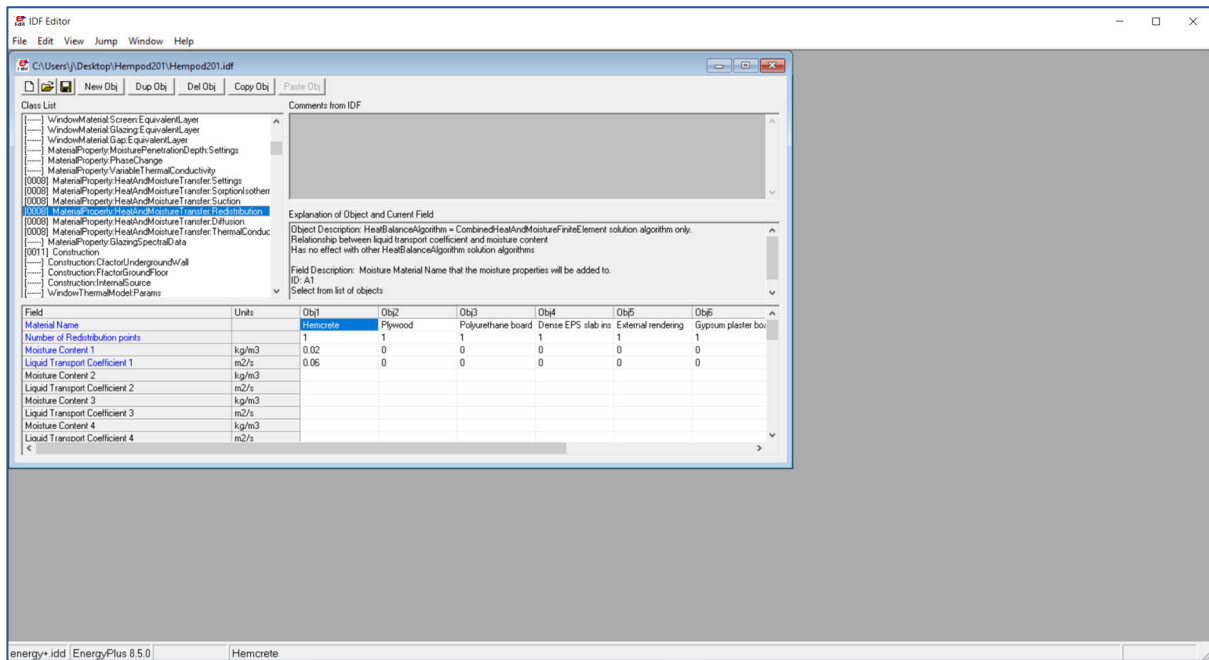


Figure C5: Showing HAMT – redistribution for hempcrete liquid transport coefficient and moisture content

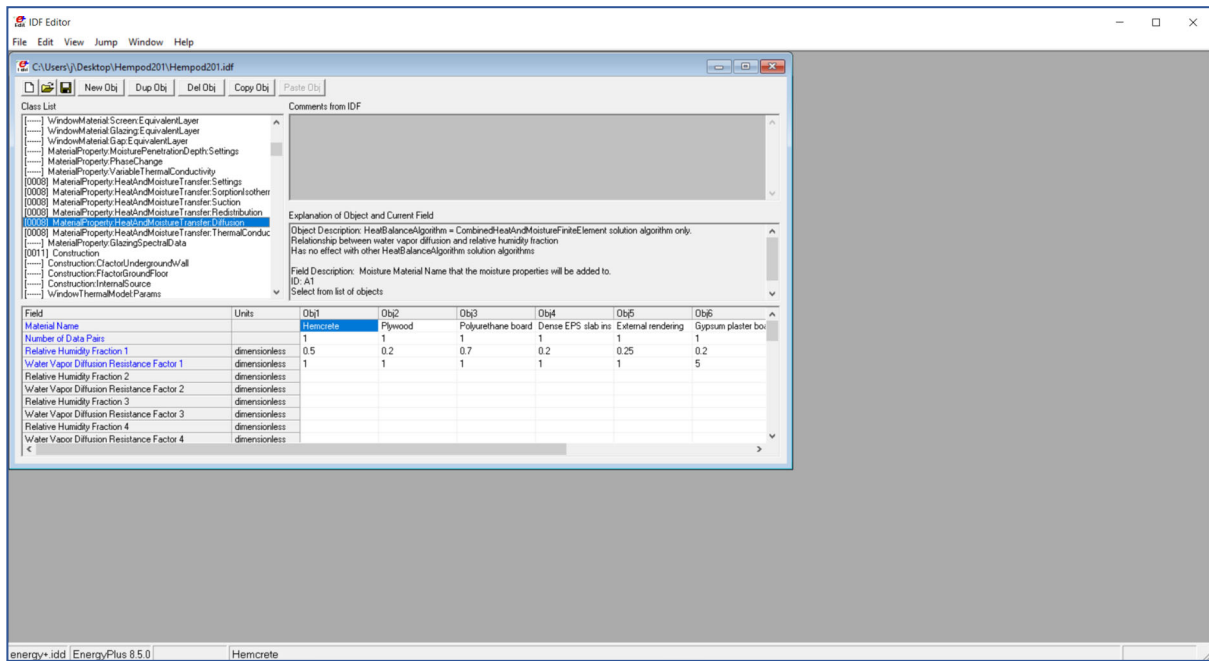


Figure C6: Showing HAMT – diffusion for hempcrete relative humidity fraction and water vapor diffusion

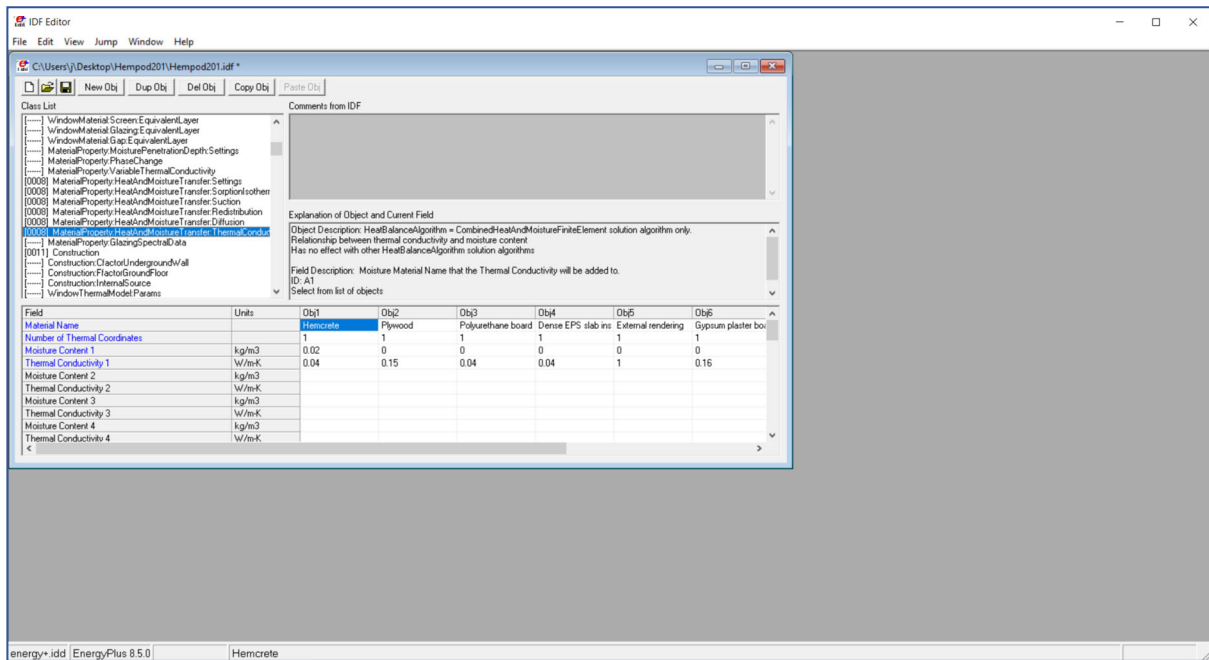


Figure C7: Showing HAMT – for hemcrete thermal conductivity and moisture content

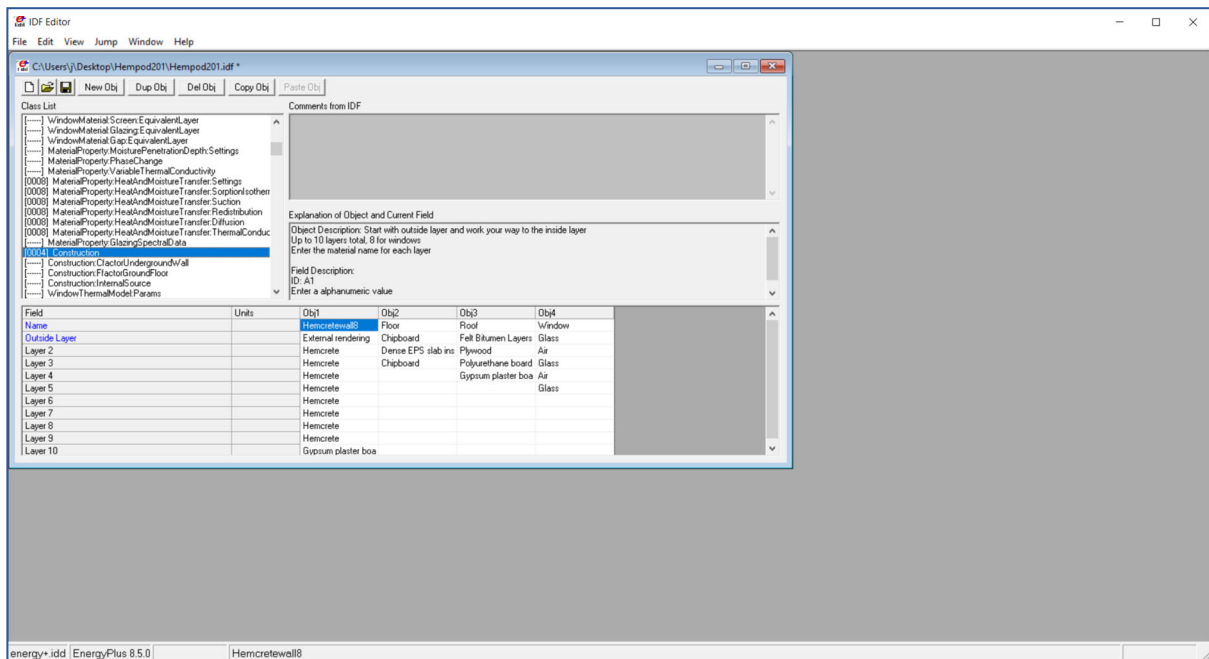


Figure C8: Showing Construction layers of hemcrete wall

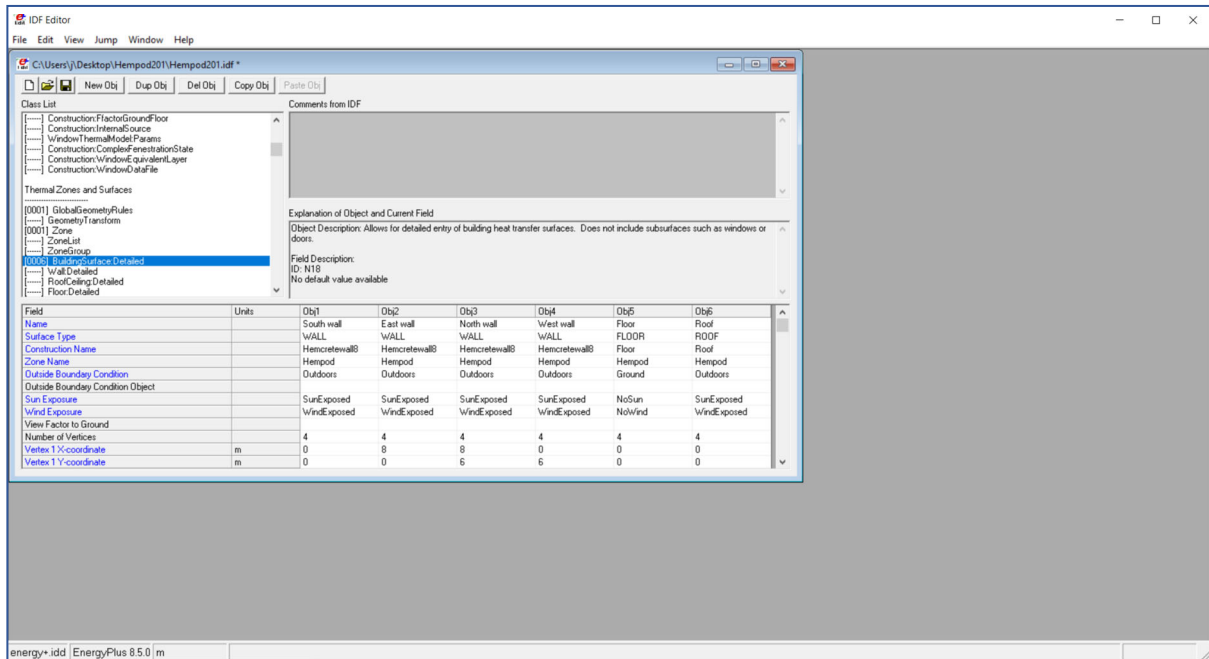


Figure C9: Showing Building surface detailed for Hempod wall construction

APPENDIX D: VALIDATION OF RESULTS WITH RESIDENTIAL BUILDING

This section contains all the diagrams referenced in section 6.1.2 as applicable.

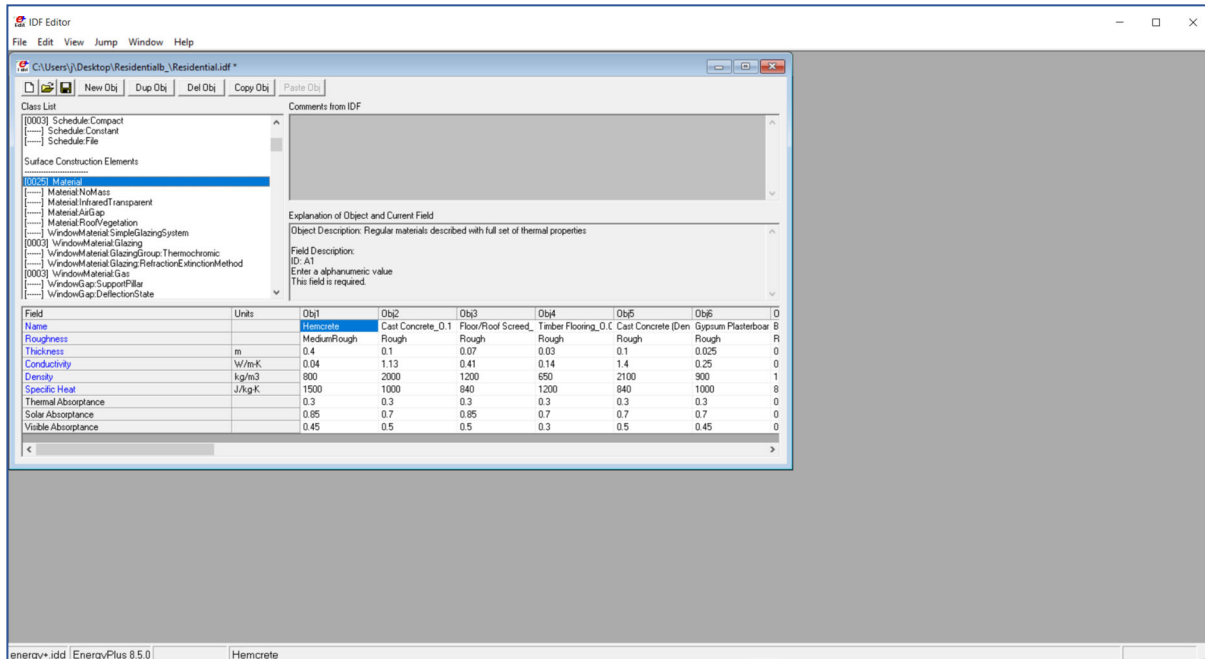


Figure D1: Showing the material property for hempcrete simulation applied to the residential building model

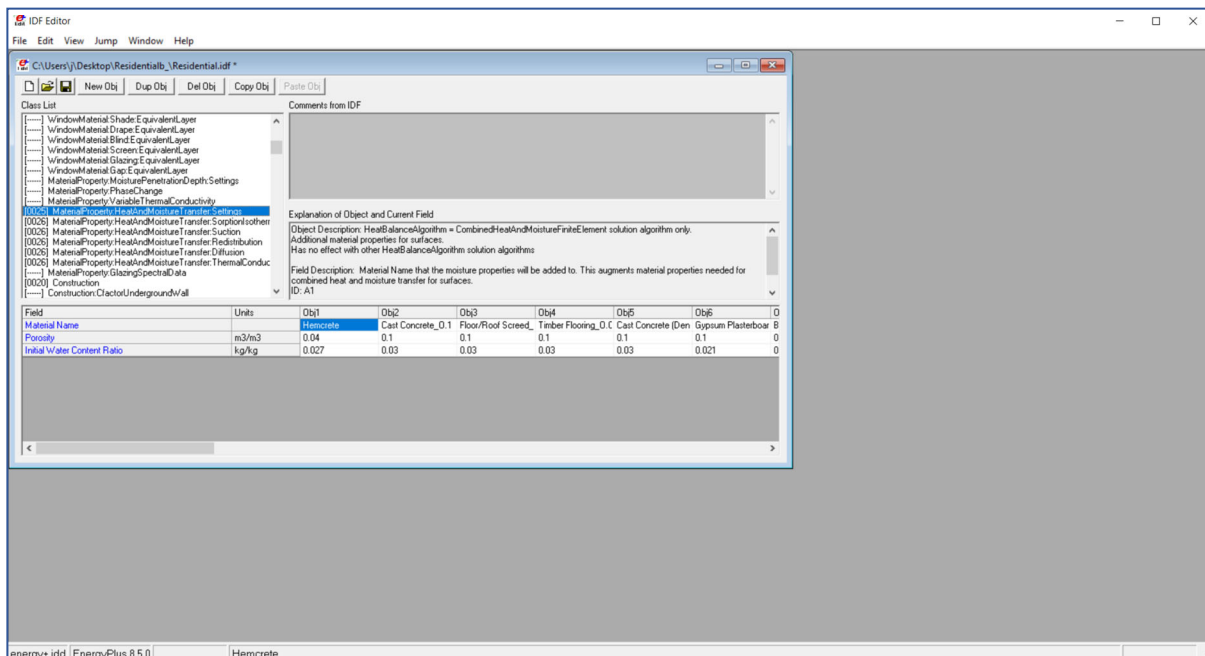


Figure D2: Showing HAMT- settings for hempcrete porosity and initial water content ratio

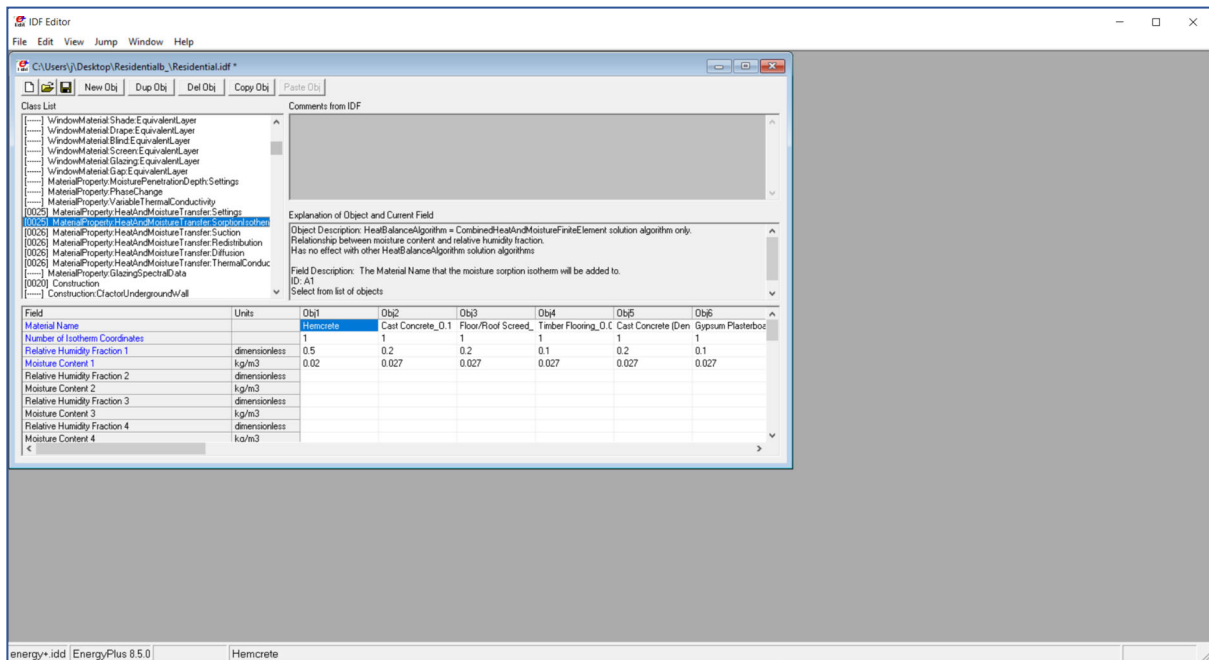


Figure D3: Showing HAMT – sorption isotherm for hempcrete relative humidity fraction and moisture content

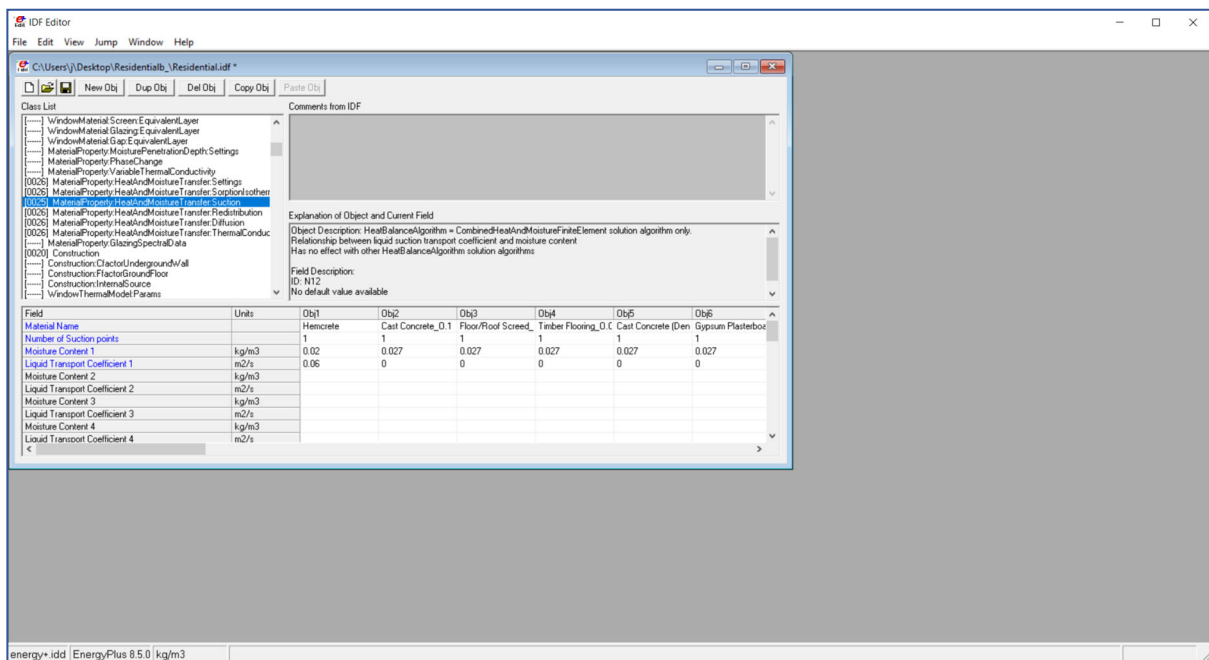


Figure D4: Showing HAMT – suction for hempcrete liquid transport coefficient and moisture content

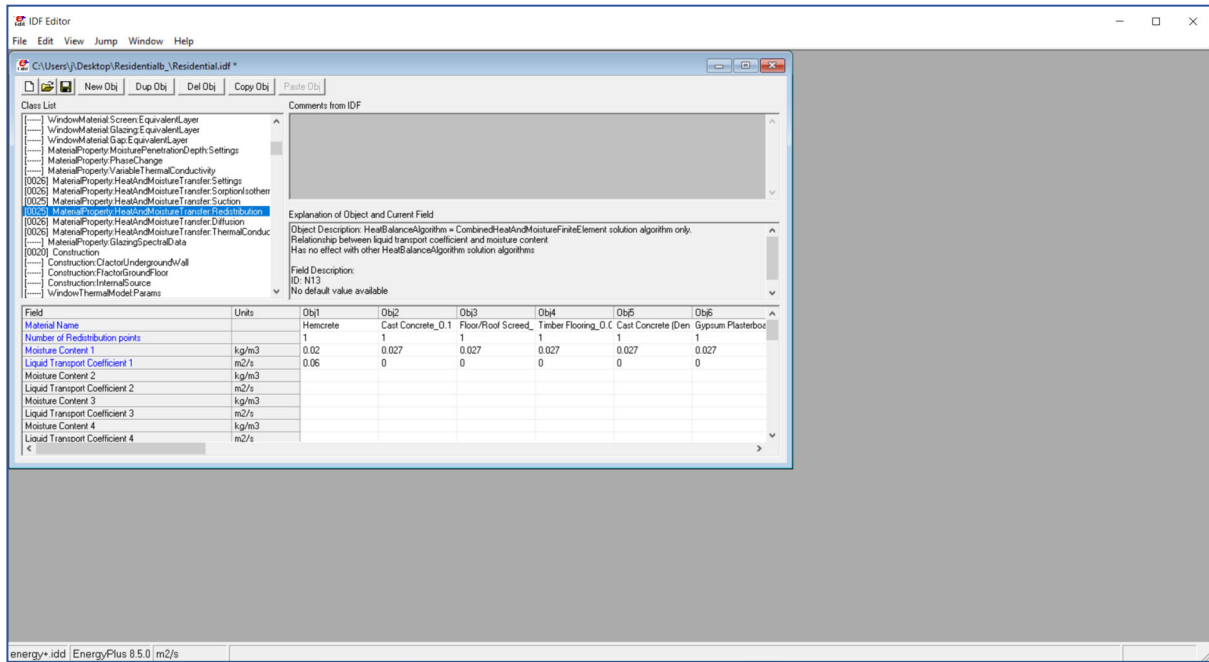


Figure D5: Showing HAMT – redistribution for hemcrete liquid transport coefficient and moisture content

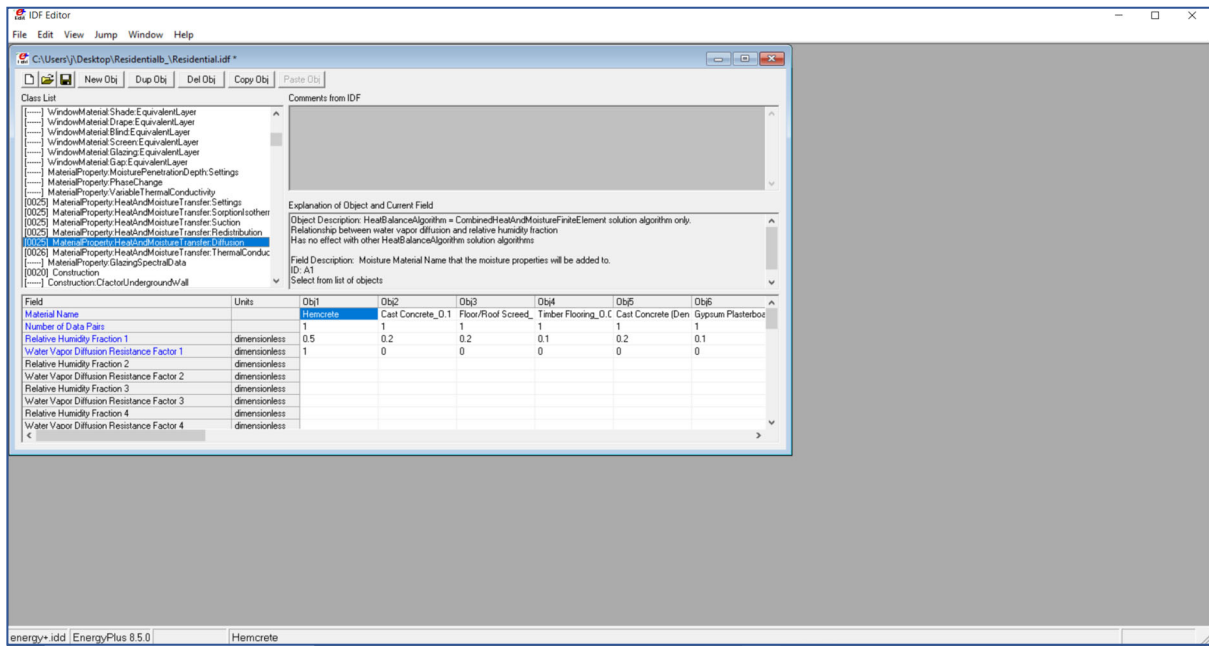


Figure D6: Showing HAMT – diffusion for hemcrete relative humidity fraction and water vapor diffusion

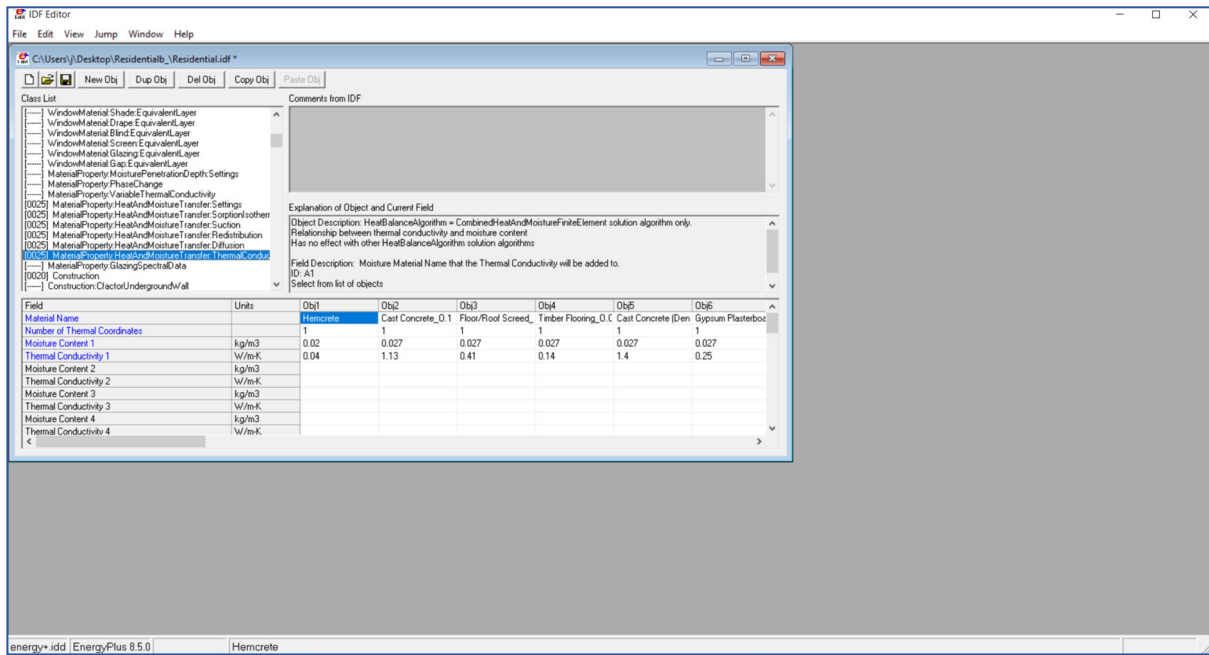


Figure D7: Showing HAMT – for hemcrete thermal conductivity and moisture content

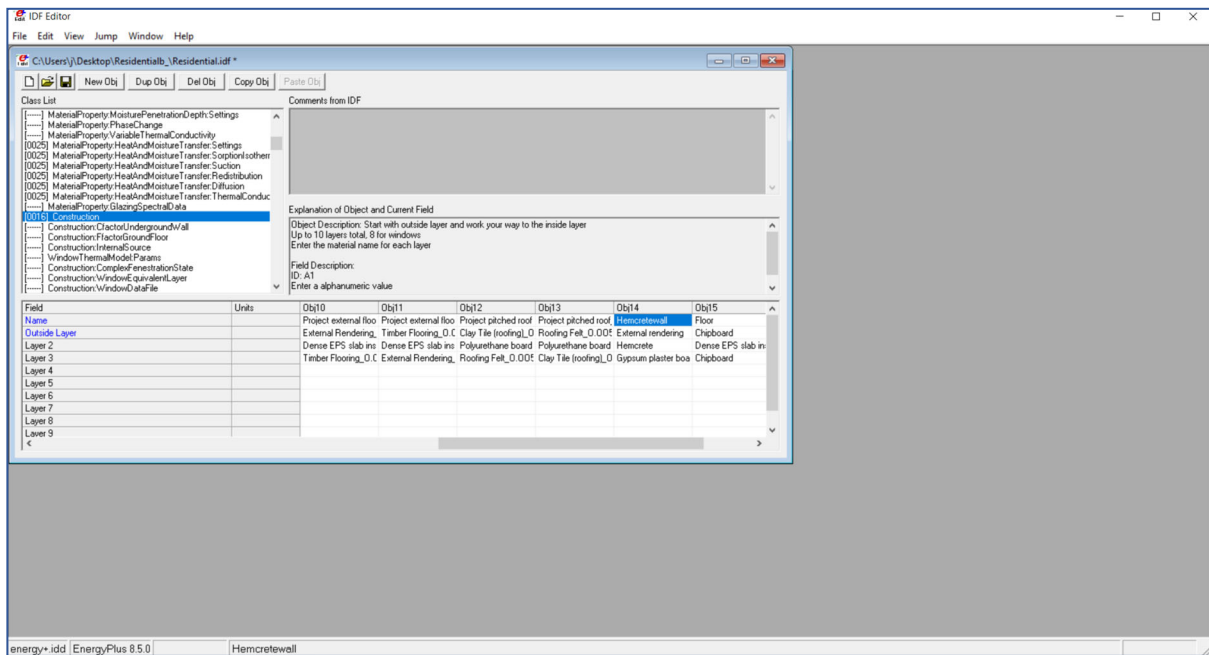


Figure D8: Showing Construction layers of hemcrete wall applied to the residential building model

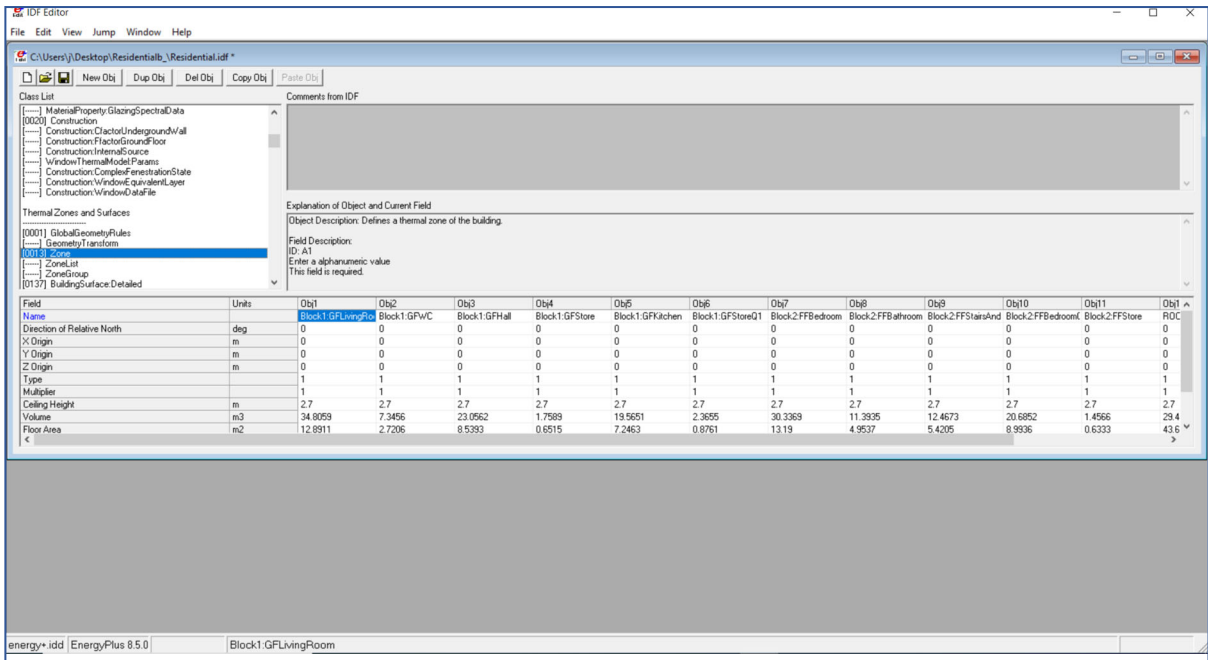


Figure D9: Showing the building model zone for HAMT Simulations of the residential building

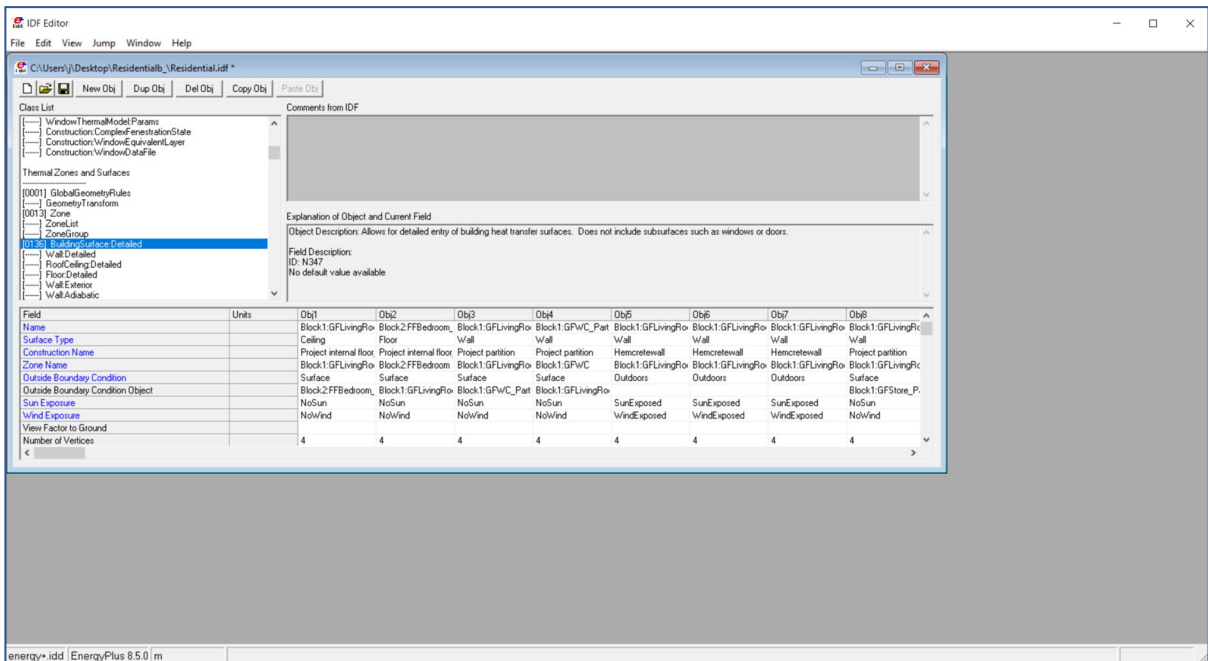


Figure D10: Showing Building surface detailed for the hempcrete wall construction applied to the living room, kitchen and bedroom of the residential building.

APPENDIX T: VALIDATION OF RESULTS WITH RESIDENTIAL BUILDING

Table T1: Residential building simulation experiment of combining conventional and natural material

S/NO	Construction composition (outside to inside)	Wall thickness	Living room RMSE air temperature (C)	Living room RMSE relative humidity (%)	Kitchen RMSE air temperature (C)	Kitchen RMSE relative humidity (%)	Bedroom RMSE air temperature (C)	Bedroom RMSE relative humidity (%)
1	External rendering (9mm), Chipboard (50mm), Rammed earth (50mm), Chipboard (50mm), Rammed earth (50mm), Gypsum plastering (9mm)	218mm	7.2	7.2	6.6	11.9	5.8	7.2
2	External rendering (9mm), Rammed earth (75mm), Chipboard (75mm), Rammed earth (75mm), Gypsum plastering (9mm)	243mm	7.4	7.6	6.8	12.0	6.0	7.5
3	External rendering (9mm), Chipboard (75mm), Rammed earth (75mm), Chipboard (75mm), Gypsum plastering (9mm)	243mm	6.9	6.5	6.3	11.7	5.5	6.5
4	External rendering (9mm), Chipboard (50mm), Rammed earth (50mm), Chipboard (50mm), Rammed earth (50mm), Chipboard (50mm), Gypsum plastering (9mm)	268mm	6.9	6.4	6.3	11.7	5.4	6.4
5	External rendering (9mm), Rammed earth (50mm), Chipboard (50mm), Rammed earth (50mm), Chipboard (50mm), Rammed earth (50mm), Chipboard (50mm), Rammed earth (50mm), Gypsum plastering (9mm)	268mm	7.2	7.1	6.6	11.9	5.8	7.1
6	External rendering (9mm), Rammed earth (75mm), Chipboard (75mm), Rammed earth (75mm), Chipboard (75mm), Gypsum plastering (9mm)	318mm	6.8	6.4	6.3	11.7	5.4	6.3
7	External rendering (9mm), Rammed earth (100mm), Chipboard (100mm), Rammed earth (100mm), Gypsum plastering (9mm)	318mm	6.8	6.4	6.3	11.7	5.4	6.3
8	External rendering (9mm), Chipboard (100mm), Rammed earth (100mm), Chipboard (100mm), Gypsum plastering (9mm)	318mm	6.7	6.1	6.1	11.7	5.4	6.3
9	External rendering (9mm), Rammed earth (100mm), Chipboard (100mm), Rammed earth (100mm), Chipboard (100mm), Gypsum plastering (9mm)	418mm	6.5	5.6	6.0	11.4	5.1	5.6

10	External rendering (9mm), Chipboard (50mm), Cast concrete (50mm), Chipboard (50mm), Cast concrete (50mm), Gypsum plastering (9mm)	218mm	7.2	7.3	6.6	11.9	5.8	7.2
11	External rendering (9mm), Cast concrete (75mm), Chipboard (75mm), Cast concrete (75mm), Gypsum plastering (9mm)	243mm	7.4	7.5	6.8	12.0	5.9	7.4
12	External rendering (9mm), Chipboard (75mm), Cast concrete (75mm), Gypsum plastering (9mm)	243mm	6.9	6.5	6.3	11.7	5.5	6.5
13	External rendering (9mm), Chipboard (50mm), Cast concrete (50mm), Chipboard (50mm), Cast concrete (50mm), Chipboard (50mm), Gypsum plastering (9mm)	268mm	6.8	6.4	6.2	11.6	5.3	6.4
14	External rendering (9mm), Cast concrete (50mm), Chipboard (50mm), Cast concrete (50mm), Chipboard (50mm), Gypsum plastering (9mm)	268mm	7.2	7.2	6.6	11.8	5.7	7.2
15	External rendering (9mm), Cast concrete (75mm), Chipboard (75mm), Cast concrete (75mm), Chipboard (75mm), Gypsum plastering (9mm)	318mm	6.5	5.6	6.0	11.2	5.1	6.8
16	External rendering (9mm), Cast concrete (100mm), Chipboard (100mm), Cast concrete (100mm), Gypsum plastering (9mm)	318mm	7.1	6.9	6.3	11.8	5.7	6.8
17	External rendering (9mm), Chipboard (100mm), Cast concrete (100mm), Gypsum plastering (9mm)	318mm	6.6	5.8	6.1	11.4	5.2	5.8
18	External rendering (9mm), Cast concrete (100mm), Chipboard (100mm), Cast concrete (100mm), Chipboard (100mm), Gypsum plastering (9mm)	418mm	6.5	5.6	6.0	11.4	5.1	5.6
19	External rendering (9mm), Cork board (50mm), Concrete block (50mm), Cork board (50mm), Concrete block (50mm), Gypsum plastering (9mm)	218mm	6.2	5.0	5.9	11.0	4.8	5.0
20	External rendering (9mm), Concrete block (75mm), Cork board (75mm), Concrete block (75mm), Gypsum plastering (9mm)	243mm	6.3	5.2	5.9	11.0	4.9	4.7
21	External rendering (9mm), Cork board (75mm), Concrete block (75mm), Cork board (75mm), Gypsum plastering (9mm)	243mm	6.1	4.4	5.7	10.8	4.6	4.4

22	External rendering (9mm), Cork board (50mm), Concrete block (50mm), Cork board (50mm), Concrete block (50mm), Gypsum plastering (9mm)	268mm	6.1	4.4	5.7	10.8	4.7	4.5
23	External rendering (9mm), Concrete block (50mm), Cork board (50mm), Concrete block (50mm), Cork board (50mm), Gypsum plastering (9mm)	268mm	6.2	4.8	5.9	11.0	4.9	4.5
24	External rendering (9mm), Concrete block (75mm), Cork board (75mm), Gypsum plastering (9mm)	318mm	6.1	4.4	5.7	10.8	4.7	4.3
25	External rendering (9mm), Concrete block (100mm), Cork board (100mm), Gypsum plastering (9mm)	318mm	6.1	4.7	5.7	11.0	4.8	4.7
26	External rendering (9mm), Cork board (100mm), Concrete block (100mm), Gypsum plastering (9mm)	318mm	6.0	4.0	5.7	10.6	4.6	4.0
27	External rendering (9mm), Concrete block (100mm), Cork board (100mm), Gypsum plastering (9mm)	418mm	6.0	4.0	5.7	10.6	4.6	3.9
28	External rendering (9mm), Timber (50mm), Straw bale (50mm), Gypsum plastering (9mm)	218mm	6.3	5.3	5.9	11.3	4.9	5.3
29	External rendering (9mm), Straw bale (75mm), Timber (75mm), Gypsum plastering (9mm)	243mm	6.2	5.0	5.7	11.1	4.7	4.9
30	External rendering (9mm), Timber (75mm), Straw bale (75mm), Gypsum plastering (9mm)	243mm	6.4	5.4	5.9	11.3	5.0	5.4
31	External rendering (9mm), Timber (50mm), Straw bale (50mm), Gypsum plastering (9mm)	268mm	6.4	5.5	5.9	11.4	5.0	5.5
32	External rendering (9mm), Straw bale (50mm), Timber (50mm), Gypsum plastering (9mm)	268mm	6.2	4.9	5.6	11.0	4.7	4.9
33	External rendering (9mm), Straw bale (75mm), Timber (75mm), Gypsum plastering (9mm)	318mm	6.1	4.6	5.4	10.9	4.4	4.7
34	External rendering (9mm), Straw bale (100mm), Timber (100mm), Gypsum plastering (9mm)	318mm	6.1	4.5	5.4	10.8	4.4	4.6

35	External rendering (9mm), Timber (100mm), Straw bale (100mm), Timber (100mm), Gypsum plastering (9mm)	318mm	6.2	4.9	5.7	11.0	4.7	4.9
36	External rendering (9mm), Straw bale (100mm), Timber (100mm), Straw bale (100mm), Timber (100mm), Gypsum plastering (9mm)	418mm	6.0	4.3	5.7	10.8	4.7	4.7
37	External rendering (9mm), Straw bale (50mm), Brickwork (50mm), Straw bale (50mm), Brickwork (50mm), Gypsum plastering (9mm)	218mm	6.5	5.7	5.9	11.7	5.3	5.7
38	External rendering (9mm), Straw bale (50mm), Brickwork (50mm), Straw bale (50mm), Brickwork (50mm), Straw bale (50mm), Gypsum plastering (9mm)	268mm	6.3	5.1	5.7	11.3	4.9	5.3
39	External rendering (9mm), Brickwork (50mm), Straw bale (50mm), Brickwork (50mm), Straw bale (50mm), Gypsum plastering (9mm)	268mm	6.5	5.6	6.0	11.5	5.1	5.5
40	External rendering (9mm), Brickwork (75mm), Straw bale (75mm), Brickwork (75mm), Straw bale (75mm), Gypsum plastering (9mm)	318mm	6.3	5.1	5.8	11.2	4.9	5.2
41	External rendering (9mm), Brickwork (100mm), Straw bale (100mm), Brickwork (100mm), Gypsum plastering (9mm)	318mm	6.4	5.4	5.9	11.3	5.0	5.4
42	External rendering (9mm), Straw bale (100mm), Brickwork (100mm), Straw bale (100mm), Gypsum plastering (9mm)	318mm	6.1	4.7	5.8	11.0	4.9	4.7
43	External rendering (9mm), Brickwork (100mm), Straw bale (100mm), Brickwork (100mm), Straw bale (100mm), Gypsum plastering (9mm)	418mm	6.1	4.6	5.7	10.9	4.7	4.6
44	External rendering (9mm), Straw bale (50mm), Cast concrete (50mm), Straw bale (50mm), Cast concrete (50mm), Gypsum plastering (9mm)	218mm	6.5	5.7	6.0	11.9	5.1	5.7
45	External rendering (9mm), Straw bale (50mm), Cast concrete (50mm), Straw bale (50mm), Cast concrete (50mm), Straw bale (50mm), Gypsum plastering (9mm)	268mm	6.3	5.1	5.8	11.2	4.9	5.1
46	External rendering (9mm), Cast concrete (50mm), Straw bale (50mm), Cast concrete (50mm), Straw bale (50mm), Gypsum plastering (9mm)	268mm	6.5	5.6	6.0	11.7	5.1	5.5
47	External rendering (9mm), Cast concrete (75mm), Straw bale (75mm), Cast concrete (75mm), Straw bale (75mm), Gypsum plastering (9mm)	318mm	6.3	5.1	5.9	11.2	4.7	5.3

48	External rendering (9mm), Cast concrete (100mm), Straw bale (100mm), Cast concrete (100mm), Gypsum plastering (9mm)	318mm	6.4	5.5	6.0	11.4	4.8	5.5
49	External rendering (9mm), Straw bale (100mm), Cast concrete (100mm), Straw bale (100mm), Gypsum plastering (9mm)	318mm	6.1	4.6	5.7	10.9	4.7	4.6
50	External rendering (9mm), Cast concrete (100mm), Straw bale (100mm), Cast concrete (100mm), Straw bale (100mm), Gypsum plastering (9mm)	418mm	6.0	4.3	5.6	10.7	4.4	4.2
51	External rendering (9mm), Adobe (50mm), Timber (50mm), Adobe (50mm), Timber (50mm), Gypsum plastering (9mm)	218mm	7.2	7.2	6.6	11.9	5.8	7.2
52	External rendering (9mm), Adobe (50mm), Timber (50mm), Adobe (50mm), Timber (50mm), Gypsum plastering (9mm)	268mm	7.1	6.9	6.5	11.6	5.7	7.0
53	External rendering (9mm), Timber (50mm), Adobe (50mm), Timber (50mm), Adobe (50mm), Gypsum plastering (9mm)	268mm	6.9	6.5	6.3	11.5	5.4	6.8
54	External rendering (9mm), Timber (75mm), Adobe (75mm), Timber (75mm), Adobe (75mm), Gypsum plastering (9mm)	318mm	6.8	6.2	6.1	11.7	5.2	6.2
55	External rendering (9mm), Timber (100mm), Adobe (100mm), Timber (100mm), Gypsum plastering (9mm)	318mm	6.6	6.0	6.0	11.5	5.0	6.0
56	External rendering (9mm), Adobe (100mm), Timber (100mm), Adobe (100mm), Gypsum plastering (9mm)	318mm	7.0	6.7	6.5	11.9	5.6	6.7
57	External rendering (9mm), Timber (100mm), Adobe (100mm), Timber (100mm), Adobe (100mm), Gypsum plastering (9mm)	418mm	6.5	5.7	6.0	11.4	5.1	5.7
58	External rendering (9mm), Adobe (50mm), Cast concrete (50mm), Adobe (50mm), Cast concrete (50mm), Gypsum plastering (9mm)	218mm	8.1	8.9	7.4	12.3	6.7	8.7
59	External rendering (9mm), Adobe (50mm), Cast concrete (50mm), Adobe (50mm), Cast concrete (50mm), Gypsum plastering (9mm)	268mm	7.9	8.5	7.2	12.2	6.5	8.6
60	External rendering (9mm), Cast concrete (50mm), Adobe (50mm), Cast concrete (50mm), Adobe (50mm), Gypsum plastering (9mm)	268mm	8.0	8.7	7.4	12.4	6.7	8.7

61	External rendering (9mm), Cast concrete (75mm), Adobe (75mm), Cast concrete (75mm), Adobe (75mm), Gypsum plastering (9mm)	318mm	7.8	8.3	7.2	12.2	6.4	8.1
62	External rendering (9mm), Cast concrete (100mm), Adobe (100mm), Cast concrete (100mm), Gypsum plastering (9mm)	318mm	7.9	8.5	7.3	12.2	6.5	8.3
63	External rendering (9mm), Adobe (100mm), Cast concrete (100mm), Adobe (100mm), Gypsum plastering (9mm)	318mm	7.7	8.1	7.1	12.0	6.3	8.1
64	External rendering (9mm), Cast concrete (100mm), Adobe (100mm), Cast concrete (100mm), Adobe (100mm), Gypsum plastering (9mm)	418mm	7.7	7.5	6.8	12.0	6.2	7.6
65	External rendering (9mm), Chipboard (50mm), Adobe (50mm), Chipboard (50mm), Adobe (50mm), Gypsum plastering (9mm)	218mm	7.1	7.0	6.9	11.9	5.7	6.7
66	External rendering (9mm), Chipboard (50mm), Adobe (50mm), Chipboard (50mm), Adobe (50mm), Gypsum plastering (9mm)	268mm	6.8	6.3	6.6	11.4	5.3	5.8
67	External rendering (9mm), Adobe (50mm), Chipboard (50mm), Adobe (50mm), Chipboard (50mm), Gypsum plastering (9mm)	268mm	7.0	6.7	6.7	11.5	5.5	6.0
68	External rendering (9mm), Adobe (75mm), Chipboard (75mm), Adobe (75mm), Chipboard (75mm), Gypsum plastering (9mm)	318mm	6.7	6.0	6.5	11.3	5.2	5.5
69	External rendering (9mm), Adobe (100mm), Chipboard (100mm), Adobe (100mm), Gypsum plastering (9mm)	318mm	6.9	6.5	6.7	11.7	5.5	5.9
70	External rendering (9mm), Chipboard (100mm), Adobe (100mm), Chipboard (100mm), Gypsum plastering (9mm)	318mm	6.5	5.7	6.1	11.5	5.1	5.7
71	External rendering (9mm), Adobe (100mm), Chipboard (100mm), Brick (100mm), Chipboard (100mm), Gypsum plastering (9mm)	418mm	6.4	5.4	5.9	11.3	5.0	5.4
72	External rendering (9mm), Bamboo (50mm), Cast concrete (50mm), Bamboo (50mm), Cast concrete (50mm), Gypsum plastering (9mm)	218mm	8.0	8.7	7.3	12.2	6.6	8.5
73	External rendering (9mm), Cast concrete (75mm), Bamboo (75mm), Cast concrete (75mm), Gypsum plastering (9mm)	243mm	8.0	8.8	7.3	12.3	6.6	8.6
74	External rendering (9mm), Bamboo (75mm), Cast concrete (75mm), Bamboo (75mm), Gypsum plastering (9mm)	243mm	7.8	8.4	7.1	12.2	6.4	8.5

75	External rendering (9mm), Bamboo (50mm), Cast concrete (50mm), Bamboo (50mm), Cast concrete (50mm), Gypsum plastering (9mm)	268mm	7.8	8.3	7.1	12.2	6.4	8.3
76	External rendering (9mm), Cast concrete (50mm), Bamboo (50mm), Cast concrete (50mm), Bamboo (50mm), Cast concrete (50mm), Gypsum plastering (9mm)	268mm	7.9	8.5	7.2	12.2	6.4	8.5
77	External rendering (9mm), Cast concrete (75mm), Bamboo (75mm), Cast concrete (75mm), Bamboo (75mm), Gypsum plastering (9mm)	318mm	7.7	8.1	7.0	12.1	6.2	8.0
78	External rendering (9mm), Cast concrete (100mm), Bamboo (100mm), Cast concrete (100mm), Gypsum plastering (9mm)	318mm	7.8	8.3	7.1	12.2	6.4	8.2
79	External rendering (9mm), Bamboo (100mm), Cast concrete (100mm), Bamboo (100mm), Gypsum plastering (9mm)	318mm	7.5	7.9	6.9	12.1	6.1	7.8
80	External rendering (9mm), Cast concrete (100mm), Bamboo (100mm), Cast concrete (100mm), Bamboo (100mm), Gypsum plastering (9mm)	418mm	7.4	7.4	6.7	12.0	5.9	7.4
81	External rendering (9mm), Bamboo (50mm), Rammed earth (50mm), Bamboo (50mm), Rammed earth (50mm), Gypsum plastering (9mm)	218mm	8.0	8.8	7.3	12.3	6.6	8.5
82	External rendering (9mm), Rammed earth (75mm), Bamboo (75mm), Rammed earth (75mm), Gypsum plastering (9mm)	243mm	8.1	8.9	7.4	12.4	6.7	8.6
83	External rendering (9mm), Bamboo (75mm), Rammed earth (75mm), Bamboo (75mm), Rammed earth (75mm), Gypsum plastering (9mm)	243mm	7.8	8.4	7.1	12.0	6.2	8.2
84	External rendering (9mm), Bamboo (50mm), Rammed earth (50mm), Bamboo (50mm), Rammed earth (50mm), Gypsum plastering (9mm)	268mm	7.8	8.3	7.0	11.9	6.0	8.1
85	External rendering (9mm), Rammed earth (50mm), Bamboo (50mm), Rammed earth (50mm), Bamboo (50mm), Rammed earth (50mm), Gypsum plastering (9mm)	268mm	7.9	8.6	7.1	12.1	6.3	8.4
86	External rendering (9mm), Rammed earth (75mm), Bamboo (75mm), Rammed earth (75mm), Bamboo (75mm), Gypsum plastering (9mm)	318mm	8.1	8.9	7.4	12.4	6.9	8.6
87	External rendering (9mm), Rammed earth (100mm), Bamboo (100mm), Rammed earth (100mm), Gypsum plastering (9mm)	318mm	7.8	8.4	7.1	12.2	6.4	8.4

88	External rendering (9mm), Bamboo (100mm), Rammed earth (100mm), Bamboo (100mm), Gypsum plastering (9mm)	318mm	7.6	8.3	6.9	12.1	6.3	8.3
89	External rendering (9mm), Rammed earth (100mm), Bamboo (100mm), Rammed earth (100mm), Bamboo (100mm), Gypsum plastering (9mm)	418mm	7.4	7.5	6.8	12.0	6.0	7.4
90	External rendering (9mm), Chipboard (50mm), Aerated concrete (50mm), Chipboard (50mm), Aerated concrete (50mm), Gypsum plastering (9mm)	218mm	6.9	6.6	6.5	11.8	5.7	6.6
91	External rendering (9mm), Chipboard (50mm), Aerated concrete (50mm), Chipboard (50mm), Aerated concrete (50mm), Chipboard (50mm), Gypsum plastering (9mm)	268mm	6.6	5.9	6.1	11.4	5.3	6.3
92	External rendering (9mm), Aerated concrete (50mm), Chipboard (50mm), Aerated concrete (50mm), Chipboard (50mm), Aerated concrete (50mm), Chipboard (50mm), Gypsum plastering (9mm)	268mm	6.7	6.2	6.3	11.5	5.4	6.5
93	External rendering (9mm), Aerated concrete (75mm), Chipboard (75mm), Aerated concrete (75mm), Chipboard (75mm), Gypsum plastering (9mm)	318mm	6.5	5.6	6.0	11.4	5.1	5.6
94	External rendering (9mm), Aerated concrete (100mm), Chipboard (100mm), Aerated concrete (100mm), Gypsum plastering (9mm)	318mm	6.6	5.8	5.9	11.6	5.3	5.7
95	External rendering (9mm), Chipboard (100mm), Aerated concrete (100mm), Chipboard (100mm), Gypsum plastering (9mm)	318mm	6.4	5.5	5.7	11.2	5.1	5.5
96	External rendering (9mm), Aerated concrete (100mm), Chipboard (100mm), Aerated concrete (100mm), Chipboard (100mm), Gypsum plastering (9mm)	418mm	6.3	5.5	5.7	11.0	5.0	5.4
97	External rendering (9mm), Bamboo (50mm), Aerated concrete (50mm), Bamboo (50mm), Aerated concrete (50mm), Gypsum plastering (9mm)	218mm	7.4	7.7	6.8	12.1	6.0	7.4
98	External rendering (9mm), Aerated concrete (75mm), Bamboo (75mm), Aerated concrete (75mm), Gypsum plastering (9mm)	243mm	7.2	7.2	6.6	11.9	5.7	7.0
99	External rendering (9mm), Bamboo (75mm), Aerated concrete (75mm), Bamboo (75mm), Gypsum plastering (9mm)	243mm	7.4	7.6	6.6	12.0	5.9	7.5

100	External rendering (9mm), Bamboo (50mm), Aerated concrete (50mm), Bamboo (50mm), Aerated concrete (50mm), Bamboo (50mm), Gypsum plastering (9mm)	268mm	7.3	7.3	6.7	12.1	5.9	7.3
101	External rendering (9mm), Aerated concrete (50mm), Bamboo (50mm), Aerated concrete (50mm), Bamboo (50mm), Aerated concrete (50mm), Gypsum plastering (9mm)	268mm	7.1	7.1	6.5	11.9	5.7	7.1
102	External rendering (9mm), Aerated concrete (75mm), Bamboo (75mm), Aerated concrete (75mm), Bamboo (75mm), Gypsum plastering (9mm)	318mm	7.0	6.8	6.5	11.9	5.7	6.8
103	External rendering (9mm), Aerated concrete (100mm), Bamboo (100mm), Aerated concrete (100mm), Gypsum plastering (9mm)	318mm	6.9	6.6	6.3	11.8	5.5	6.6
104	External rendering (9mm), Bamboo (100mm), Aerated concrete (100mm), Bamboo (100mm), Gypsum plastering (9mm)	318mm	7.1	7.0	6.5	11.9	5.7	7.0
105	External rendering (9mm), Aerated concrete (100mm), Bamboo (100mm), Aerated concrete (100mm), Bamboo (100mm), Gypsum plastering (9mm)	418mm	6.7	6.2	6.2	11.6	5.3	6.2
106	External rendering (9mm), Cob wall (50mm), Cast concrete (50mm), Cob wall (50mm), Cast concrete (50mm), Gypsum plastering (9mm)	218mm	8.2	9.0	7.4	12.2	7.0	8.6
107	External rendering (9mm), Cob wall (50mm), Cast concrete (50mm), Cob wall (50mm), Cast concrete (50mm), Cob wall (50mm), Gypsum plastering (9mm)	268mm	8.0	8.6	7.2	12.0	6.4	8.2
108	External rendering (9mm), Cast concrete (50mm), Cob wall (50mm), Cast concrete (50mm), Cob wall (50mm), Cast concrete (50mm), Gypsum plastering (9mm)	268mm	8.0	8.8	7.2	12.2	6.4	8.4
109	External rendering (9mm), Cast concrete (75mm), Cob wall (75mm), Cast concrete (75mm), Cob wall (75mm), Gypsum plastering (9mm)	318mm	7.8	8.4	7.0	12.0	6.2	8.0
110	External rendering (9mm), Cast concrete (100mm), Cob wall (100mm), Cast concrete (100mm), Gypsum plastering (9mm)	318mm	7.9	8.6	7.2	12.2	6.5	8.4
111	External rendering (9mm), Cob wall (100mm), Cast concrete (100mm), Cob wall (100mm), Gypsum plastering (9mm)	318mm	7.9	8.1	7.0	12.2	6.3	8.1

112	External rendering (9mm), Cast concrete (100mm), Cob wall (100mm), Cast concrete (100mm), Cob wall (100mm), Gypsum plastering (9mm)	418mm	7.6	7.9	6.9	12.1	6.2	7.8
113	External rendering (9mm), Chipboard (50mm), Cob wall (50mm), Chipboard (50mm), Cob wall (50mm), Gypsum plastering (9mm)	218mm	7.1	7.0	6.4	11.9	5.7	5.9
114	External rendering (9mm), Chipboard (50mm), Cob wall (50mm), Chipboard (50mm), Cob wall (50mm), Gypsum plastering (9mm)	268mm	6.8	6.3	6.2	11.7	5.4	5.7
115	External rendering (9mm), Cob wall (50mm), Chipboard (50mm), Cob wall (50mm), Cob wall (50mm), Chipboard (50mm), Cob wall (50mm), Gypsum plastering (9mm)	268mm	7.0	6.8	6.5	11.9	5.7	5.9
116	External rendering (9mm), Cob wall (75mm), Chipboard (75mm), Cob wall (75mm), Chipboard (75mm), Gypsum plastering (9mm)	318mm	6.7	6.1	6.2	11.6	5.4	5.7
117	External rendering (9mm), Cob wall (100mm), Chipboard (100mm), Cob wall (100mm), Gypsum plastering (9mm)	318mm	6.9	5.7	6.4	11.7	5.5	5.9
118	External rendering (9mm), Chipboard (100mm), Cob wall (100mm), Chipboard (100mm), Gypsum plastering (9mm)	318mm	6.6	5.5	6.1	11.4	5.2	5.7
119	External rendering (9mm), Cob wall (100mm), Chipboard (100mm), Cob wall (100mm), Chipboard (100mm), Gypsum plastering (9mm)	418mm	6.4	5.3	5.9	11.2	5.0	5.3
120	External rendering (9mm), Cob wall (50mm), Concrete block (50mm), Cob wall (50mm), Concrete block (50mm), Gypsum plastering (9mm)	218mm	7.9	8.6	7.2	12.4	6.5	8.2
121	External rendering (9mm), Cob wall (50mm), Concrete block (50mm), Cob wall (50mm), Concrete block (50mm), Cob wall (50mm), Gypsum plastering (9mm)	268mm	7.7	8.2	7.0	12.2	6.3	8.1
122	External rendering (9mm), Concrete block (50mm), Cob wall (50mm), Concrete block (50mm), Cob wall (50mm), Concrete block (50mm), Gypsum plastering (9mm)	268mm	7.7	8.2	7.0	12.1	6.3	8.0
123	External rendering (9mm), Concrete block (75mm), Cob wall (75mm), Concrete block (75mm), Cob wall (75mm), Gypsum plastering (9mm)	318mm	7.6	7.9	6.9	12.2	6.1	7.7
124	External rendering (9mm), Concrete block (100mm), Cob wall (100mm), Concrete block (100mm), Gypsum plastering (9mm)	318mm	7.5	7.8	6.9	12.1	6.0	7.6

125	External rendering (9mm), Cob wall (100mm), Concrete block (100mm), Cob wall (100mm), Gypsum plastering (9mm)	318mm	7.6	7.9	6.9	12.1	6.1	7.8
126	External rendering (9mm), Concrete block (100mm), Cob wall (100mm), Concrete block (100mm), Cob wall (100mm), Gypsum plastering (9mm)	418mm	7.2	7.2	6.6	11.9	5.8	7.1
127	External rendering (9mm), Brickwork (50mm), Rammed earth (50mm), Brickwork (50mm), Rammed earth (50mm), Gypsum plastering (9mm)	218mm	8.1	8.9	7.9	12.5	6.9	8.7
128	External rendering (9mm), Brickwork (50mm), Rammed earth (50mm), Brickwork (50mm), Rammed earth (50mm), Brickwork (50mm), Gypsum plastering (9mm)	268mm	8.0	8.7	7.3	12.2	6.6	8.5
129	External rendering (9mm), Rammed earth (50mm), Brickwork (50mm), Rammed earth (50mm), Gypsum plastering (9mm)	268mm	8.0	8.7	7.5	12.4	6.7	8.6
130	External rendering (9mm), Rammed earth (75mm), Brickwork (75mm), Rammed earth (75mm), Gypsum plastering (9mm)	318mm	7.8	8.5	7.1	12.0	6.5	8.3
131	External rendering (9mm), Rammed earth (100mm), Brickwork (100mm), Rammed earth (100mm), Gypsum plastering (9mm)	318mm	8.0	8.7	7.3	12.2	6.6	8.5
132	External rendering (9mm), Brickwork (100mm), Rammed earth (100mm), Gypsum plastering (9mm)	318mm	7.8	8.4	7.1	12.2	6.4	7.9
133	External rendering (9mm), Rammed earth (100mm), Brickwork (100mm), Rammed earth (100mm), Brickwork (100mm), Gypsum plastering (9mm)	418mm	7.6	8.0	7.0	12.1	6.2	7.9
134	External rendering (9mm), Chipboard (50mm), Brickwork (50mm), Chipboard (50mm), Brickwork (50mm), Gypsum plastering (9mm)	218mm	7.1	7.1	6.5	11.9	5.7	6.0
135	External rendering (9mm), Chipboard (50mm), Brickwork (50mm), Chipboard (50mm), Brickwork (50mm), Gypsum plastering (9mm)	268mm	6.8	6.3	6.2	11.4	5.4	5.7
136	External rendering (9mm), Brickwork (50mm), Chipboard (50mm), Brickwork (50mm), Chipboard (50mm), Gypsum plastering (9mm)	268mm	7.0	6.8	6.4	11.8	5.6	5.9

137	External rendering (9mm), Brickwork (75mm), Chipboard (75mm), Brickwork (75mm), Chipboard (75mm), Gypsum plastering (9mm)	318mm	6.7	6.2	6.0	11.3	5.1	5.4
138	External rendering (9mm), Brickwork (100mm), Chipboard (100mm), Brickwork (100mm), Gypsum plastering (9mm)	318mm	6.9	6.6	6.3	11.7	5.5	5.7
139	External rendering (9mm), Chipboard (100mm), Brickwork (100mm), Chipboard (100mm), Gypsum plastering (9mm)	318mm	6.6	5.7	6.0	11.4	5.1	5.5
140	External rendering (9mm), Brickwork (100mm), Chipboard (100mm), Brickwork (100mm), Chipboard (100mm), Gypsum plastering (9mm)	418mm	6.4	5.3	5.9	11.3	5.0	5.3
141	External rendering (9mm), glass-fibre quilt (50mm), Rammed earth (50mm), glass-fibre quilt (50mm), Rammed earth (50mm), Gypsum plastering (9mm)	218mm	6.5	5.5	6.1	11.4	5.3	5.1
142	External rendering (9mm), Rammed earth (75mm), glass-fibre quilt (75mm), Rammed earth (75mm), Gypsum plastering (9mm)	243mm	6.4	5.3	6.0	11.2	5.0	4.9
143	External rendering (9mm), glass-fibre quilt (75mm), Rammed earth (75mm), glass-fibre quilt (75mm), Gypsum plastering (9mm)	243mm	6.1	4.4	5.7	10.9	4.7	4.4
144	External rendering (9mm), glass-fibre quilt (50mm), Rammed earth (50mm), glass-fibre quilt (50mm), Rammed earth (50mm), glass-fibre quilt (50mm), Gypsum plastering (9mm)	268mm	6.1	4.7	5.7	10.8	4.9	4.7
145	External rendering (9mm), Rammed earth (50mm), glass-fibre quilt (50mm), Rammed earth (50mm), glass-fibre quilt (50mm), Rammed earth (50mm), Gypsum plastering (9mm)	268mm	6.2	4.9	5.9	11.0	4.9	4.7
146	External rendering (9mm), Rammed earth (75mm), glass-fibre quilt (75mm), Rammed earth (75mm), glass-fibre quilt (75mm), Gypsum plastering (9mm)	318mm	6.1	4.4	5.7	10.8	4.7	4.4
147	External rendering (9mm), Rammed earth (100mm), glass-fibre quilt (100mm), Rammed earth (100mm), Gypsum plastering (9mm)	318mm	6.2	4.7	5.8	11.0	4.8	4.7
148	External rendering (9mm), glass-fibre quilt (100mm), Rammed earth (100mm), glass-fibre quilt (100mm), Gypsum plastering (9mm)	318mm	6.0	4.0	5.7	10.6	4.6	4.0
149	External rendering (9mm), glass-fibre quilt (50mm), Cast concrete (50mm), glass-fibre quilt (50mm), Cast concrete (50mm), Gypsum plastering (9mm)	218mm	6.3	4.9	5.8	11.1	4.8	4.9

150	External rendering (9mm), glass-fibre quilt (50mm), Cast concrete (50mm), glass-fibre quilt (50mm), Cast concrete (50mm), glass-fibre quilt (50mm), Gypsum plastering (9mm)	268mm	6.0	4.6	5.6	10.8	4.5	4.7
151	External rendering (9mm), Cast concrete (50mm), glass-fibre quilt (50mm), Cast concrete (50mm), glass-fibre quilt (50mm), Cast concrete (50mm), Gypsum plastering (9mm)	268mm	6.2	4.8	5.8	11.0	4.7	4.8
152	External rendering (9mm), Cast concrete (75mm), glass-fibre quilt (75mm), Cast concrete (75mm), glass-fibre quilt (75mm), Gypsum plastering (9mm)	318mm	6.1	4.4	5.7	10.8	4.7	4.4
153	External rendering (9mm), Cast concrete (100mm), glass-fibre quilt (100mm), Cast concrete (100mm), Gypsum plastering (9mm)	318mm	6.2	4.7	5.9	11.0	4.9	4.7
154	External rendering (9mm), glass-fibre quilt (100mm), Cast concrete (100mm), glass-fibre quilt (100mm), Gypsum plastering (9mm)	318mm	6.0	4.0	5.4	10.6	4.4	4.4
155	External rendering (9mm), Phenolic foam (50mm), Rammed earth (50mm), Phenolic foam (50mm), Rammed earth (50mm), Gypsum plastering (9mm)	218mm	6.2	4.7	5.8	11.8	4.8	4.6
156	External rendering (9mm), Rammed earth (75mm), Phenolic foam (75mm), Rammed earth (75mm), Gypsum plastering (9mm)	243mm	6.6	6.0	6.1	11.6	5.2	6.0
157	External rendering (9mm), Phenolic foam (75mm), Rammed earth (75mm), Phenolic foam (75mm), Gypsum plastering (9mm)	243mm	6.1	4.1	5.7	10.7	4.7	4.1
158	External rendering (9mm), Phenolic foam (50mm), Rammed earth (50mm), Phenolic foam (50mm), Rammed earth (50mm), Phenolic foam (50mm), Gypsum plastering (9mm)	268mm	6.0	4.1	5.7	10.7	4.7	4.0
159	External rendering (9mm), Rammed earth (50mm), Phenolic foam (50mm), Rammed earth (50mm), Phenolic foam (50mm), Rammed earth (50mm), Gypsum plastering (9mm)	268mm	6.1	4.6	5.8	10.9	4.7	4.6
160	External rendering (9mm), Rammed earth (75mm), Phenolic foam (75mm), Rammed earth (75mm), Phenolic foam (75mm), Gypsum plastering (9mm)	318mm	6.0	3.9	5.7	10.5	4.6	3.8

161	External rendering (9mm), Rammed earth (100mm), Phenolic foam (100mm), Rammed earth (100mm), Gypsum plastering (9mm)	318mm	6.1	4.5	5.7	10.9	4.7	4.4
162	External rendering (9mm), Phenolic foam (100mm), Rammed earth (100mm), Phenolic foam (100mm), Gypsum plastering (9mm)	318mm	6.0	3.7	5.7	10.4	4.7	3.6
163	External rendering (9mm), Weather board (50mm), Brickwork (50mm), Weather board (50mm), Brickwork (50mm), Gypsum plastering (9mm)	218mm	7.2	7.1	6.5	12.0	5.7	6.7
164	External rendering (9mm), Weather board (50mm), Brickwork (50mm), Weather board (50mm), Brickwork (50mm), Weather board (50mm), Gypsum plastering (9mm)	268mm	6.8	6.6	6.1	11.7	5.4	6.2
165	External rendering (9mm), Brickwork (50mm), Weather board (50mm), Brickwork (50mm), Gypsum plastering (9mm)	268mm	7.0	6.8	6.3	11.9	5.5	6.5
166	External rendering (9mm), Brickwork (75mm), Weather board (75mm), Brickwork (75mm), Weather board (75mm), Gypsum plastering (9mm)	318mm	6.7	6.0	6.0	11.5	5.3	6.0
167	External rendering (9mm), Weather board (100mm), Brickwork (100mm), Weather board (100mm), Gypsum plastering (9mm)	318mm	6.5	5.7	6.1	11.4	5.1	5.5
168	External rendering (9mm), Brickwork (100mm), Weather board (100mm), Brickwork (100mm), Weather board (100mm), Gypsum plastering (9mm)	418mm	6.4	5.3	5.9	11.2	5.0	5.3
169	External rendering (9mm), Silicon (50mm), Concrete block (50mm), Silicon (50mm), Concrete block (50mm), Gypsum plastering (9mm)	218mm	7.2	7.3	6.9	12.0	5.8	7.3
170	External rendering (9mm), Silicon (50mm), Concrete block (50mm), Silicon (50mm), Concrete block (50mm), Silicon (50mm), Gypsum plastering (9mm)	268mm	6.9	6.7	6.5	11.5	5.6	6.0
171	External rendering (9mm), Concrete block (50mm), Silicon (50mm), Concrete block (50mm), Gypsum plastering (9mm)	268mm	7.1	7.0	6.7	12.0	5.7	6.3
172	External rendering (9mm), Concrete block (75mm), Silicon (75mm), Concrete block (75mm), Silicon (75mm), Gypsum plastering (9mm)	318mm	6.8	6.5	6.4	11.8	5.4	5.7

173	External rendering (9mm), Concrete block (100mm), Silicon (100mm), Concrete block (100mm), Gypsum plastering (9mm)	318mm	7.0	6.8	6.5	11.9	5.5	6.1
174	External rendering (9mm), Silicon (100mm), Concrete block (100mm), Gypsum plastering (9mm)	318mm	6.7	6.1	6.3	11.7	5.3	5.9
175	External rendering (9mm), Concrete block (100mm), Silicon (100mm), Concrete block (100mm), Silicon (100mm), Gypsum plastering (9mm)	418mm	6.5	5.7	6.0	11.4	5.1	5.7
176	External rendering (9mm), Cratherm board (50mm), Concrete block (50mm), Cratherm board (50mm), Concrete block (50mm), Gypsum plastering (9mm)	218mm	6.3	5.3	6.1	11.7	5.5	5.3
177	External rendering (9mm), Cratherm board (50mm), Concrete block (50mm), Cratherm board (50mm), Concrete block (50mm), Cratherm board (50mm), Gypsum plastering (9mm)	268mm	6.1	4.7	5.7	11.0	4.8	4.7
178	External rendering (9mm), Concrete block (50mm), Cratherm board (50mm), Concrete block (50mm), Cratherm board (50mm), Concrete block (50mm), Gypsum plastering (9mm)	268mm	6.3	5.1	6.0	11.4	5.3	5.0
179	External rendering (9mm), Concrete block (75mm), Cratherm board (75mm), Concrete block (75mm), Cratherm board (75mm), Gypsum plastering (9mm)	318mm	6.1	4.6	5.8	11.0	4.7	4.6
180	External rendering (9mm), Concrete block (100mm), Cratherm board (100mm), Concrete block (100mm), Gypsum plastering (9mm)	318mm	6.2	5.0	4.7	11.1	4.8	5.0
181	External rendering (9mm), Cratherm board (100mm), Concrete block (100mm), Cratherm board (100mm), Gypsum plastering (9mm)	318mm	6.0	4.3	5.7	10.8	4.7	4.3
182	External rendering (9mm), Timber board (50mm), Reinforced concrete (50mm), Timber board (50mm), Reinforced concrete (50mm), Gypsum plastering (9mm)	218mm	7.6	7.3	6.9	12.2	6.3	6.9
183	External rendering (9mm), Timber board (50mm), Reinforced concrete (50mm), Timber board (50mm), Reinforced concrete (50mm), Timber board (50mm), Gypsum plastering (9mm)	268mm	7.0	7.1	6.3	11.7	5.4	6.5
184	External rendering (9mm), Reinforced concrete (50mm), Timber board (50mm), Reinforced concrete (50mm)	268mm	7.3	7.4	6.5	12.0	5.9	6.7

196	External rendering (9mm), Aerated- concrete (100mm), Plywood (100mm), Aerated- concrete (100mm), Plywood (100mm), Gypsum plastering (9mm)	418mm	6.3	5.1	5.8	11.1	4.9	5.0
-----	---	-------	-----	-----	-----	------	-----	-----

Table T2: Simulation with hempcrete material

S/NO	Construction composition (outside to inside)	Wall thickness	Living room (C)	Living room (%)	Kitchen (C)	Kitchen (%)	Bedroom (C)	Bedroom (%)
1	External rendering (9mm), Hempcrete (50mm), Hempcrete (50mm), Hempcrete (50mm), Gypsum plastering (9mm)	218mm	4.1	4.9	5.1	10.7	4.2	4.7
2	External rendering (9mm), Hempcrete (75mm), Hempcrete (75mm), Hempcrete (75mm), Gypsum plastering (9mm)	243mm	4.0	4.7	5.0	10.6	4.0	4.0
3	External rendering (9mm), Hempcrete (50mm), Hempcrete (50mm), Hempcrete (50mm), Gypsum plastering (9mm)	268mm	4.0	4.5	5.0	10.6	4.0	3.9
4	External Rendering (9mm), Hempcrete (75mm), Hempcrete (75mm), Hempcrete (75mm), Gypsum plastering (9mm)	318mm	3.9	3.8	4.9	10.5	3.9	3.8
5	External rendering (9mm), Hempcrete (100mm), Hempcrete (100mm), Hempcrete (100mm), Gypsum plastering (9mm)	418mm	3.7	3.5	4.7	10.3	3.6	3.5

